# A taxonomic review of the vampire catfish genus *Paracanthopoma* Giltay, 1935 (Siluriformes, Trichomycteridae), with descriptions of nine new species and a revised diagnosis of the genus

**Mário de Pinna[1] & Fernando Cesar Paiva Dagosta[2]**

[1] Universidade de São Paulo (USP), Museu de Zoologia (MZUSP). São Paulo, SP, Brasil.
ORCID: https://orcid.org/0000-0003-1711-4816. E-mail: pinna@ib.usp.br (corresponding author)

[2] Universidade Federal da Grande Dourados (UFGD), Faculdade de Ciências Biológicas e Ambientais (FCBA). Dourados, MS, Brasil.
ORCID: https://orcid.org/0000-0001-7163-296X. E-mail: ferdagosta@gmail.com

**Abstract.** A taxonomic revision is presented of the genus *Paracanthopoma,* probably the least-known vandelliine genus at present. The work is based on most of the material available in museums worldwide and includes a major expansion in the knowledge about the genus. *Paracanthopoma* is circumscribed as a monophyletic group on the basis of nine putatively synapomorphic characters. Evidence is provided for *Paracanthopoma* and *Paravandellia* as sister groups and the two genera are comparatively diagnosed. A total of 13 species are recognized in *Paracanthopoma,* of which nine are new and one is transferred from *Paravandellia: Pc. ahriman,* new species, *Pc. alleynei* (Henschel *et al.,* 2021), *Pc. carrapata,* new species, *Pc. cangussu* Henschel *et al.,* 2021, *Pc. capeta,* new species, *Pc. daemon,* new species, *Pc. irritans,* new species, *Pc. malevola,* new species, *Pc. parva* Giltay, 1935, *Pc. saci* Dagosta & de Pinna, 2021, *Pc. satanica,* new species, *Pc. truculenta,* new species, and *Pc. vampyra,* new species. The holotype and paratype of *Pc. alleynei* are found to belong to two different species. The various taxa in *Paracanthopoma* display a high degree of phenotypic divergence and are diagnosed on the basis of traditional as well as new morphological characters of both external and internal anatomy. Geographical distributions are mapped for each species and an identification key is provided. Preliminary evidence suggests the existence of four main subclades within *Paracanthopoma.* The first one includes *Pc. ahriman, Pc. cangussu,* and *Pc. irritans.* A second subclade comprises *Pc. carrapata, Pc. daemon, Pc. parva,* and *Pc. truculenta.* A third clade includes *Pc. malevola* and *Pc. satanica* and a fourth comprises *Pc. alleynei* and *Pc. vampyra.* The last clade lacks some putative synapomorphies of all other members of *Paracanthopoma* and seems to be the sister group to the rest of the genus. Relationships of *Pc. capeta* and *Pc. saci* are not as clear, but some evidence exists for the former being related to the first subclade and the latter to the second subclade.

**Keywords.** Biodiversity; Evolution; Micropredation; Monophyly; Parasitism.

## INTRODUCTION

Hematophagous catfishes of the trichomycterid subfamily Vandelliinae are one of the emblematic subjects of natural history. Along with vampire bats, they are the only jawed vertebrates that feed exclusively on blood as adults. Vandelliine catfishes are most infamous for their occasional penetration of human (and other mammals') urethras, a fact that has generated immense folk and urban legend. They have been the subject of two popular books (Gudger, 1930; Spotte, 2002), tens of articles in newspapers and magazines and have also been featured in a number of television documentaries, to varying degrees of sensationalism.

In the Brazilian Amazon, vandelliine catfishes are popularly known as "candirus", a name also applying to their close relatives, the Stegophilinae and to some members of the unrelated Cetopsidae. Vandelliines are one of nine subfamilies of the neotropical family Trichomycteridae. Although vandelliines are not strictly parasitic under some definitions of the term (*e.g.,* Machado & Sazima, 1983) and most other trichomycterid species are actually generalized predators of aquatic invertebrates, the family as a whole is often referred to as "parasitic catfishes".

Despite obvious biological interest and inordinate degree of public attention, actual knowledge about vandelliines is scant in all aspects. The

latest revisionary study of the group was published over a century ago (Eigenmann, 1918), and is severely outdated. Because of that, it is often impossible to identify vandelliine specimens to species, and even generic limits are nebulous. Existing diagnoses and keys are useful only as very crude guides to the diversity in the group. Along with numerous undescribed forms, the taxonomy of vandelliines has been plagued with abundant synonymy, ineffective diagnoses, uninformative descriptions and various other nomenclatural and taxonomic problems.

Four genera comprised the Vandelliinae in Eigenmann (1918): *Branchioica* (today a synonym of *Paravandellia*), *Paravandellia, Urinophilus* (today a synonym of *Plectrochilus*), and *Vandellia*. The most relevant addition in the post-Eigenmann years was the genus *Paracanthopoma* Giltay, 1935 and its then single species *Pc. parva* Giltay, 1935. The taxon was markedly different from any vandelliines known until then, and the relevance of its distinguishing characters was well appreciated by Giltay. *Paracanthopoma parva* was described on the basis of two specimens collected by Carlos Lako from a relatively remote area in the Brazilian Amazon, the upper rio Catrimany, a tributary of the rio Branco, rio Negro System. Giltay's descriptions are accompanied by excellent illustrations, which perfectly depict the species and its distinguishing characters. The author did not go into much detail on the relationships or significance of the new taxon. He noted, however, that the united branchial membranes, free from the isthmus (the interpretation at the time), were similar to those in the stegophiline *Acanthopoma*. In his view, *Paracanthopoma* stood for vandelliines as *Acanthopoma* for stegophilines (Giltay, 1935: 3). That statement, incidentally, is the only indication of the subfamilial inclusion of the new taxon in the entire paper. For many years, both the species and the genus were rare in collections and *Paracanthopoma* remained an obscure, yet unanimously valid, taxon in trichomycterid taxonomy. Curiously, species of *Paracanthopoma* seem to include some of the most abundant vandelliines in the Amazon basin, and it is difficult to explain how they remained a rare item in collections for so long.

After almost 90 years without taxonomic novelties, two new species of *Paracanthopoma* were reported in 2021: *Pc. saci* Dagosta & de Pinna, 2021 and *Pc. cangussu* Henschel, Katz & Costa, 2021a. The former is the first, and so far only, record of the genus outside of the greater Amazonian drainages.

Vandelliines have a relatively restricted geographical distribution in South America, compared to some other freshwater fish groups of similar size. Their Cis-Andean distribution covers the Amazon, Orinoco, Essequibo, and Paraná-Paraguay basins. On the Trans-Andean side, a single vandelliine species occurs in the Magdalena basin, *Paravandellia phaneronema* (Miles, 1943). Their most conspicuous voids in distribution are the Atrato, Maracaibo, São Francisco, Parnaíba and Southeastern Brazilian coastal drainages (Wosiacki & de Pinna, 2007). Due to the highly conspicuous biology and aspect of vandelliines, it is unlikely that their absences in those basins are due

to incomplete sampling. Although collecting vandelliines sometimes requires directed sampling efforts, they are always well-known to local fishermen and are unlikely to go unnoticed by riverine folk. *Paracanthopoma* occupies a subset of the vandelliine range, with records in the same major basins except for the Magdalena.

Despite the overall unsatisfactory state of knowledge about their systematics, the Vandelliinae has been well-corroborated as a monophyletic group (Baskin, 1973; Schmidt, 1993; de Pinna, 1998, 2016; Fernández & Schaefer, 2009; Datovo & Bockmann, 2010; Ochoa *et al.,* 2020), something not surprising in view of their numerous unique specializations related to blood-feeding. Characters indicative of monophyly can be found since the earliest accounts on species of the group. Hypotheses have been proposed on the phylogenetic relationships among constituent vandelliine genera (Baskin, 1973; Schmidt, 1993), all of which admittedly based on rather limited character evidence and taxonomic representation. The sister group to the Vandeliinae is the Stegophilinae, also known for their parasitic habits, but in this case expressed as scale- and mucus-eating (lepidophagy and muciphagy). Together, the two subfamilies form the sister group to the Tridentinae, presumably non-parasitic. It has also been proposed that the Vandelliinae, Stegophilinae, Tridentinae, Sarcoglanidinae, Microcambevinae, and Glanapteryginae form a monophyletic group (Costa & Bockmann, 1994; de Pinna, 1998, Datovo & Bockmann, 2010; Ochoa *et al.,* 2020).

The advent of phylogenetics had a relatively early expression in trichomycterid systematics (including vandelliines) in the work of Baskin (1973; *see* de Pinna, 2016). Though available for many years only as a doctoral dissertation, Baskin's study paved the grounds for much subsequent work on Trichomycteridae, and influenced the systematics of the family for decades. It was also the first phylogenetic proposal for the larger clade of Loricarioidei, which includes also the families Nematogenyidae, Callichthyidae, Scoloplacidae (included in the work but then yet undescribed), Astroblepidae and Loricariidae. In fact, Baskin (1973) may well be the first study to explicitly apply Hennigian principles to any group of Neotropical fishes and its influence on the development of the field has been substantial despite its relatively limited availability (de Pinna, 2016). Baskin hypothesized Vandelliinae as a monophyletic group on the basis of several apomorphic traits, most of which are still valid today.

The molecular revolution in systematics has not yet had a large impact on our understanding of the the systematics of Vandelliinae, with all studies so far based on limited taxonomic representation and focused on broader questions about phylogenetic relationships of Trichomycteridae. Fernández & Schaefer (2009) conducted an analysis using mitochondrial (12S, 16S, ND4) and nuclear (histone H3) gene sequences, mostly of Stegophilinae and Vandelliinae. The two subfamilies are confirmed as monophyletic and each others' sister group, with the Vandelliinae having *Paravandellia* as sister group to *Vandellia* plus *Plectrochilus* (*Paracanthopoma* was not included). A subsequent analysis by Ochoa *et al.*

(2017) again reiterated vandelliine monophyly, but in this case including only representatives of *Vandellia* and *Paravandellia*. In that analysis, the Vandelliinae is curiously positioned as sister group to the sarcoglanidine genus *Stauroglanis.* More recently, Ochoa *et al.* (2020) revisited the phylogenetic relationships of trichomycterids using ultraconserved elements. Their results corroborate vandeliinae monophyly, but based on representatives of *Vandelia* and *Paracanthopoma* only. Ochoa *et al.* (2020) also support that Vandellinae and Stegophilinae are sister groups, with that clade being the sister group to Tridentinae. Such scheme agrees with previous proposals by Baskin (1973), de Pinna (1998) and even earlier views expressed in Eigenmann (1918).

Herein, we offer a taxonomic revision of the genus *Paracanthopoma* which exemplifies the degree to which vandelliines are poorly known, probably comprising one of the least-known groups of vertebrates. Results increase the number of *Paracanthopoma* species from three to 13, mostly due to previously undescribed forms. Diagnoses and descriptive data are provided for all of them, as well as information on their geographical distribution. Morphological data supporting the monophyly of *Paracanthopoma, Paravandellia,* and of the clade composed of the two genera, are also proposed.

## MATERIAL AND METHODS

### Anatomical and descriptive terminology

The profoundly modified anatomy of the taxa treated herein, in particular their buccal morphology, requires a new descriptive terminology. Many of the terms refer to anatomical features that have been noted and described by previous authors in informal prose, but which need to be expressed in technical terminology and defined precisely. Most of the new names refer to anatomical traits which are exclusive to Vandelliinae, but some refer to structures existing in some or most other Trichomycteridae. Because the present paper is the first extensive (in number of species) revisionary work on vandeliines in over a century, it is thought that this is the proper occasion to introduce the new terms. The terminology listed below is used repeatedly in the descriptive sections of this paper.

***Branchiostegal velum*** – A free continuous fold of integument across the branchiostegal region in *Paracanthopoma* (*cf.,* in Character Survey section). ***Dentary diastema*** – Medial region between dentary lobes. ***Dentary lobe*** – Modified region of lower lip that covers the ramus of each dentary, centered near the tooth-bearing mesial end (or homologous position when mandibular teeth are absent). ***Epiodontodeal velum*** – Retractible sheet of integument that covers the opercular and/or interopercular patches of odontodes in some Trichomycteridae. ***Hypodontal pad*** – Cushion of soft tissue underlying, and partly engulfing, median premaxillary dentition. ***Labial bursa*** – A pocket of soft tissue

in the posteromedial part of the upper lip, adjacent to the medial surface of the distal region of the premaxilla; within the labial bursa, the distal portions (caps) of scalpelloid teeth are generated and developed until a late calcification stage. In adults, these caps, which can be very numerous, represent replacement teeth. The basal plate portion of scalpelloid teeth only develops when the caps are already outside of the bursa. ***Odontodophore*** – Refers to the odontode-bearing complexes of the opercle and interopercle in trichomycterids, including both the odontodes themselves plus the associated modified soft tissues. This term is a shorcut for the "[inter-] opercular patch of odontodes" of previous authors. ***Periodontodal fold*** – Rim of elevated or folded integument commonly found around posterior, dorsal and ventral margins of opercular and interopercular odontodophores in most Trichomycteridae. Referred to by previous authors as "flap of skin". ***Scalpelloid teeth*** – The "claw-like" teeth of previous authors are here named scalpelloid teeth (from the Latin *scalpellum,* diminutive of *scalprum,* meaning a small knife or chisel; the name is adapted from Miranda-Ribeiro, 1917: 50). They are composed of a distal pungent portion attached obliquely to a roundish-elongate basal plate. They occur in the premaxilla of all Vandelliinae and, in somewhat attenuated form, also in both jaws of the stegophiline *Pareiodon*. A strikingly similar condition, yet certainly convergent, occurs in the gobiesocid genus *Flexor* and some close relatives (Briggs, 1955, fig. 51; Conway *et al.,* 2018, fig. 5). Scalpelloid teeth are the only adult premaxillary dentition in most species of *Paracanthopoma,* and all of *Plectrochilus* and *Vandellia.*

Nomenclature for bones and subdivisions of the braincase followed Patterson (1975). The lower jaw terminology was according to Nelson (1973), except that the compound angular + articular + retroarticular is referred to as anguloarticular. Caudal skeleton element names followed Lundberg & Baskin (1969), and Schultze & Arratia (1989). Nomenclature for structures associated with the hyoid bar were according to Arratia & Schultze (1990), except that the parurohyal is referred to as urohyal. Terminology for the suspensorium followed Arratia (1990) and Arratia & Schultze (1991), except that the autopalatine is referred to as palatine. Pelvic skeleton nomenclature was according to Shelden (1937). The controversial element at the temporal region of the skull in catfishes (*cf.,* Lundberg, 1975; Fink & Fink, 1981; Slobodian & Pastana, 2018; Kubicek, 2022) is referred to as the supracleithrum. Other osteological structures follow Weitzman (1962). Myological terminology followed Winterbottom (1974) and Datovo & Bockmann (2010). Exceptions to terminological suggestions of any of the above authors are noted and explained in the appropriate section.

The topographical indications such as "dorsal", "ventral", "lateral", etc. refer to the position of a structure relative to the whole body of the fish, unless otherwise noted. The term "mesial" is used in a relational sense, as opposed to "lateral". The term "median" refers to a location on a midsagittal plane of symmetry (of the whole fish, or of a structure).

## Species recognition and revisionary standards

The species concept adopted in this work is in accordance with the early inceptions of the phylogenetic species concept (Rosen, 1978, 1979; Nelson & Platnick, 1981; Nixon & Wheeler, 1990; but not its later versions; *cf.*, de Pinna, 1999). Accordingly, species are regarded as the smallest cluster of organisms diagnosable by a combination of character states. This concept minimizes reference to notions of processes to three factors only: ontogenetic variation, sexual dimorphism, and intraspecific variation. Species limits thus defined are hypothetical in the same sense as hypotheses of monophyly in phylogenetic analysis (de Pinna, 1999), although monophyly of recognized species is not required or implied. In practice, the delimitation of phylogenetic species limits began with the definition of diagnosable clusters of specimens (Reis & de Pinna, 2022). Once minimal diagnosable units are recognized, they are investigated as to whether they may represent biological phenomena other than taxonomic differentiation, such as sexual dimorphism, ontogenetic change, and intraspecific variation. The minimum degree of differentiation necessary to warrant recognition of species-level separation is not always clearly defined. In this study, two clusters are considered specifically differentiated when they display at least one trait in which 100% of examined specimens can be diagnosed. If all differential traits between two potential taxa show continuous variation, specific differentiation is not warranted. Species known from single or very few specimens obviously cannot be subject to any meaningful statistical treatment. Their recognition as a separate species is based on the presence of qualitative or quantitative differentiation equal or superior to that seen among the statistical ranges of other species recognized on the basis of more abundant samples. Geographic information is used as an ancillary principle when looking for divergent lineages. In freshwater fishes, river basin structure is not necessarily a reliable indicator of taxonomic identity (Dagosta & de Pinna, 2017, 2019) and is therefore used as a secondary parameter in detecting species differentiation. Because the species is here recognized as the smallest diagnosable taxonomic unit, the subspecific category is not employed.

Species accounts in the revisionary sections include all material examined for each taxon, listed according to country of origin (in alphabetical order), institutional acronym (in alphabetical order), and catalogue number (in numerical order). When entries for a single country are numerous, the list is further subdivided according to major river drainage. Localities include, in addition to country, any further political subdivisions available (usually state or its equivalent, then city, town or county), followed by additional locality information, including geographical coordinates. Examined museum specimens cover many decades of collection and associated data are expectedly extremely heterogeneous. The information provided is identical to that in files associated with the material. Any inferential data is explicitly indicated as such. The number of specimens provided (ex) is the total number in the lot at time of examination. The number of anatomical preparations (*e.g.,* c&s) is a subset of the total number.

## Meristics and morphometrics

Determining anal- and dorsal-fin ray counts in trichomycterids is more troublesome than in most other fish groups, because of the presence of a series of small accessory rays anterior to the fins, gradually merging with segmented rays and often not visible without dissection, plus the lack of a spine-locking mechanism. The multitude of methods of counting fin-rays in the family, often not stated explicitly, creates great difficulty in interpreting and comparing data in the literature (Tchernavin, 1944: 248). The procurrent fin rays can only be counted accurately in cleared and stained preparations. Procurrent rays are defined as all unsegmented raylike elements. The smallest anterior ones may escape detection even in fine radiographs. Because procurrent rays are usually observable only in a subset of examined specimens, herein they are not included in regular fin-ray counts, their number being provided separately. Pectoral, pelvic, dorsal, and anal fin-ray counts include a value for anterior unbranched segmented rays represented in Roman, and the branched segmented ones in Arabic numerals, separated by a plus sign. Procurrent-ray counts demand special attention because of the loose connection and distance between their bilateral halves, especially in the small anterior elements of the series, which are often detached from each other and easily mistaken for separate rays in cleared and stained preparations. Also, there are isolated ray halves sometimes interspersed in the caudal-fin procurrent series, which are counted only when occupying a position in the expected regular spacing of the series. In this paper, the dorsal and anal fin-ray counts include only segmented rays. The two posterior closely-set rays, when present, are counted separately. Principal caudal-fin rays include all branched elements plus one unbranched ray in each lobe, with counts for each lobe (dorsal first) separated by a plus sign. In the caudal fin, there may be a few rays which are neither principal nor procurrent, because they are segmented but located outside of the set of principal rays as normally defined. Such rays, which are usually one or two, are not counted. Vertebral counts do not include those in the compound Weberian centrum and the compound caudal centrum (PU1 + U1) is counted as one. Vertebral counts and position of pterygiophore insertion were based on radiographs and cleared and stained specimens. Branchiostegal rays were counted on cleared and stained preparations only.

Odontode count is a commonly-used but confusing meristics in trichomycterids. The problem derives mostly from the ubiquitous presence of numerous replacement odontodes in various stages of development in the odontodophore. Some are calcified only distally and immersed in soft tissue between remaining odontodes. Others are almost entirely formed, just with the basal portion still unattached. A replacement odontode may develop to an advanced condition, and remain in nearly fully-developed state, until its predecessor falls off, only then completing its development and attaching to the bone. The large and numerous replacement odon-

todes on the posterior margin of both the opercle and interopercle are particularly prone to confusion and can easily and erroneously be included in counts. The number of replacement odontodes is widely variable from specimen to specimen of the same species, likely as a result of different intensities of wear and tear, and sometimes equals that of attached odontodes. This provides ample margin for error in odontode counts. Once such errors are discounted, however, there is a very definite count of opercular and interopercular odontodes in trichomycterid genera and species, a value which includes those odontodes actually corresponding to a defined position on the bone. That count must include only odontodes that are attached to bone, or in the process of replacing an already detached odontode, or an obviously empty socket which happens to have lost both its occupant and replacement. In sum, the correct count represents the odontode-bearing capacity of the odontodophore. For species with numerous odontodes, such as a majority of taxa included in this paper, accurate figures can only be estimated from cleared and stained preparations. In unstained alcoholic specimens, attempts at odontode counting, though not impossible, are laborious and may incur in significant error.

Measurements were taken on the left side of specimens whenever possible. Large species *(e.g., Pc. carrapata, Pc. parva, Pc. truculenta)* were measured with digital calipers, point-to-point, and recorded to the nearest 0.1 mm. Small species were measured with ocular micrometers and are therefore projections. The unusual external morphology of the fishes treated in this study requires redefinition of many of the traditional landmarks used in catfish morphometrics, as detailed below. Figure 1 provides a visual aid to the location of homologous landmarks and derivative measurements.

***Standard length*** – from the anterior midpoint of snout to the posterior margin of the hypural plate (posterior margin of the hypural cartilage in small specimens where that portion may be relevant). ***Total length*** – from the anterior midpoint of snout to the tip of middle caudal-fin rays. This measurement is taken as "fork length" in species with forked caudal fins. ***Body depth*** – taken at vertical through origin of pelvic fins. ***Caudal peduncle length***
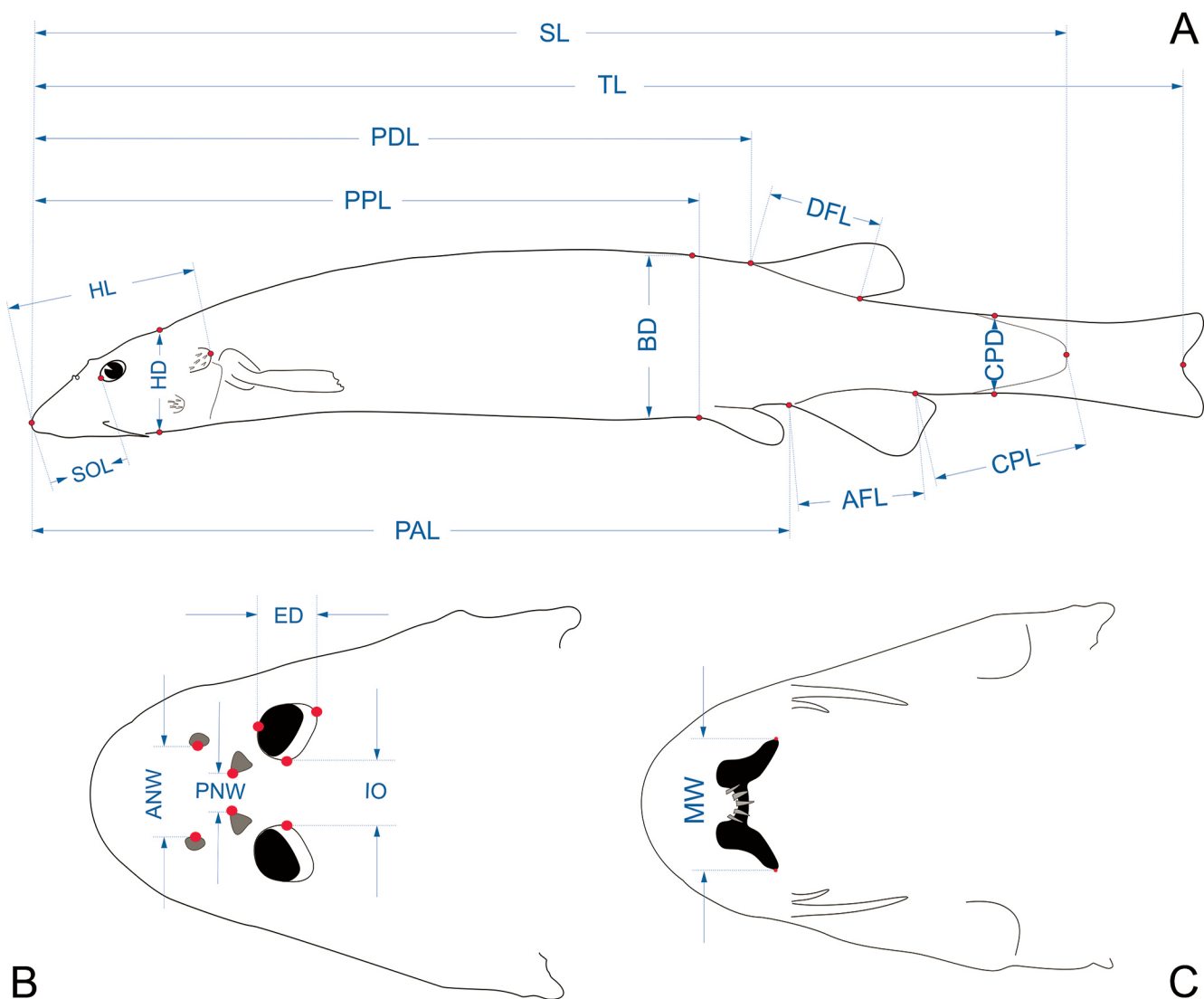


**Figure 1.** Schematic *Paracanthopoma* showing homologous landmarks and derivative measurements. (A) Left lateral view of body; (B) Dorsal head view; (C) Ventral head view.

– from the base of the last anal-fin ray to the posterior margin of the hypural plate. ***Caudal peduncle depth*** – taken at the midlength of caudal peduncle, including, when present, portion corresponding to procurrent rays. ***Predorsal length*** – from the anterior midpoint of snout to the base of the first segmented dorsal-fin ray. ***Preanal length*** – from the anterior midpoint of snout to the base of the first segmented anal-fin ray. ***Prepelvic length*** – from the anterior midpoint of snout to the base of the first (lateral) pelvic-fin ray. ***Dorsal-fin base length*** – from the base of the first segmented ray to the base of the last ray. ***Anal-fin base length*** – from the base of the first segmented ray to the base of the last ray. ***Head length (HL)*** – from the anterior midpoint of snout to the posterior margin of the opercular periodontodal fold. ***Head width*** – taken at its maximum width, at the ventral surface, excluding portions corresponding to opercular odontodophores (this is done in order to keep the variable position of the preserved opercle from biasing the measurement). ***Head depth*** – taken at the point where the branchiostegal membranes join the isthmus. ***Interorbital*** – between the mesial margins of the eyes, at their least distance. ***Eye diameter*** – taken along antero-posterior axis. ***Snout length*** – from the anterior midpoint of snout to the anterior margin of eye. ***Mouth width*** – between the clefts of the mouth. ***Anterior internarial width*** – between mesial margins of anterior nares (at their nearest point, in case of non-round narial opening). ***Posterior internarial width*** – as in preceding measurement, but between posterior nares.

### Preparation of material

Specimens were cleared and counterstained for bone and cartilage according to a modified version derived from Taylor & Van Dyke (1985) and Song & Parenti (1995). Specimens of small species were in some cases not bleached as part of the clearing and staining procedure to allow observation of internal chromatophores which become hidden by the post-mortem opacity of muscle tissue. Dissection of cleared and stained specimens follows in general the protocol of Weitzman (1974), with modifications to suit the peculiarities of vandelliine anatomy. In small specimens, most details of head osteology can be accessed in cleared and stained specimens by transparency, without the need of dissections. Branchial arches in vandelliinae are extremely delicate and poorly ossified, posing special challenges, especially with small specimens such as most species of *Paracanthopoma*. The ligaments which hold the branchial basket together are weaker than those connecting it to the surrounding structures. Thus, attempts to remove them by ordinary dissection methods often results in severely damaged branchial skeletons, In those cases, the branchial arches are best left in place and exposed by making an incision in the soft tissue along the anterior margin of the cleithra, extending all the way to the branchial orifice on both sides and leaving the hyoid arch intact. The cleithra are then carefully detached from the ventral branchial arches, then raised and flipped backwards to expose a ventral view of the full branchial basket.

Computerized tomographic (CT-Scan) images were done with a Phoenix v|tome|x M – General Electric Company, using voxel size X = 0.02370301 μm, number of images 5000, voltage 60 Kv, and current 220 mA. Images were processed using the software VG Studio Max, 2.2.3.69611 64 bit. Specimens intended for SEM examinations were cleaned of superficial mucus, when necessary, by *ca.* 30 min immersion in trypsin solution (prepared as for the clearing and staining procedure), then dehydrated in ethanol series (35%-70%-100%). Once in absolute ethanol, they were freed of superficial sand grains and other consolidated debris adhered to the integument by immersion in an ultrasound bath for 2 min. Specimens were subsequently critical-point dried, gold-coated and mounted on SEM stubs. Photographs of cleared and stained preparations were made with a multi-focus digital stereomicroscopic system.

Counts of vertebrae, pterygiophores and pleural ribs in alcoholic specimens were based on x-ray images made with a digital microradiographic system.

### Abbreviations

Institutional abbreviations follow Sabaj (2020).

**Anatomical abbreviations:** AA = angulo-articular; AC = anterior ceratohyal; BAS = basioccipital (fused with exoccipital but referable as general region); BB = basibranchial; BR = branchiostegal rays; CL = cleithrum; CPT = conical premaxillary teeth; DEN = dentary; E1-4 = epibranchials 1 to 4; EC = mesethmoid cornua; EPO = epioccipital; EXO = exoccipital (fused with basioccipital but referable as general region); F = frontal; HY = hyomandibula; HYP = hypohyal; INT = interopercle; LAT = lateral ethmoid; LJ = lower jaw; MAX = maxilla; ME = mesethmoid; MET = metapterygoid; MPR = median premaxilla; OP = opercle; ORB = orbitosphenoid; PAL = palatine; PAR = parasphenoid; PC = posterior ceratohyal; PMX = premaxilla; POP = preopercle; PTE = pterotic; QUA = quadrate; ST = scalpelloid tooth; SPP = sphenotic-prootic-pterosphenoid; SU = supracleithrum; SOC = supraoccipital; T = conical tooth; U = urohyal; WC = Weberian complex; VH = ventral hypohyal; V = vomer.

**Taxonomic abbreviations:** Pc = *Paracanthopoma;* Pl = *Plectrochilus;* Pv = *Paravandellia;* Vd = *Vandellia.*

**Other abbreviations:** c&s = cleared and stained preparation; SEM = material prepared for examination by scanning electron microscopy.

### Comparative material examined

Material examined of *Paracanthopoma* is listed in the respective species accounts. Comparative material of other vandelliines and other trichomycterids is listed below.

***Paravandellia oxyptera* Miranda-Ribeiro, 1912:** CAS 63840, 1 ex (♂, holotype of *Branchioica bertonii* Eigenmann, 1917), 19.0 mm SL, Paraguay, Assunción, from the gills of *Piaractus brachypomus,* col., A. de W. Bertoni, no date; CAS 77288, 1 ex (♂, paratype of *B. bertonii*), 22.0 mm SL (in poor state of preservation, head damaged or dissected, part of branchial region and lower jaw missing, abdomen cut), same data as CAS 63840; MCP 11812, 1 ex (♂), 22.0 mm SL, Brazil, rio Grande do Sul, São Borja, rio Uruguai, at Rancho da Amizade, col., J. Bertoletti *et al.,* 10 Nov 1987; MNRJ 790, holotype, *ca.* 15 mm SL (specimen in poor condition, with anterior portion of head degraded and some other parts missing), Brazil, Mato Grosso, rio Paraguai at Cáceres, col., A. Miranda-Ribeiro and Comissão Rondon, Oct 1908; MNRJ 15415, 8 ex (2♀, 6♂), 24.0-25.2 mm SL, Brazil, Paraná, Foz do Iguaçu, Bela Vista (*ca.* 2 km downstream from Itaipu dam), col., University of Maringá team, 12 Aug 1986; MZUSP 2214 (lectotype of *Pleurophysus hydrostaticus* Miranda-Ribeiro, 1918), Brazil, São Paulo, rio Claro; MZUSP 5252, 1 ex (paralectotype of *Pleurophysus. hydrostaticus*); MZUSP 48119, 2 ex (1♀, 1♂), 26.1-25.9 mm SL, Brazil, Paraná, Foz do Iguaçu, Bela Vista, *ca.* 2 km below Itaipu dam, col., joint team from Itaipu dam authority and Universidade Estadual de Maringá, 12 Aug 1986; MZUSP 83702, 2 ex (♂), 20.4-24.9 mm SL, Brazil, São Paulo, Iperó, rio Ipanema (trib. to rio Sorocaba, rio Tietê drainage), col., J.L. Birindelli *et al.,* Dec 2003; MZUSP 89973, 1 ex (♂), 27.3 mm SL, Brazil, Mato Grosso, Tangará da Serra, rio Sepotuba, below Salto das Nuvens (14°37'15"S, 57°44'20"W), col., H.A. Britski *et al.,* 09 Mar 2002; MZUSP 90600, 2 ex (♂), 17.6-21.4 mm SL, Brazil, Mato Grosso, Cáceres, rio Sepotuba (middle course) (rio Paraguai drainage) (15°24'37"S, 57°42'20"W), col., H.A. Britski *et al.,* 04 Mar 2002; MZUSP 95207, 5 ex (2 c&s), 17.1-20.0 mm SL, São Paulo, Iaras, rio Claro (rio Paranapanema drainage), near Rio Novo, between Águas de Santa Bárbara and Iaras (22°47'14"S, 49°06'05"W), col., C. Chalmon & A. Zeinad, 28 Aug 2007; MZUSP 102421, 32 ex (5 c&s), 17.5-21.0 mm SL, Mato Grosso do Sul, Coxim, rio Taquari at Cachoeira das Palmeiras, col., Centro de Estudos e Pesquisas do Pantanal Matogrossense, 07 Dec 1976; NUP 312, 17 ex (4♀, 13♂) (2 c&s), 23.3-29.4 mm SL, Brazil, Paraná, Município de Foz do Iguaçu, trib. to rio Paraná (upper Paraná drainage) at area of Itaipu Reservoir (approx. 25°24'S, 54°27'W), col., NUP team, 30 Jul 1988; UMMZ 207467, 1 ex (♂), 21.5 mm SL, Paraguay, Misiones, rio Parana, *ca.* 2 km east of Ayolas on property of Sr. Ed Borjesson (27°24'00"S, 56°46'12"W), col., J. Taylor *et al.,* 25 Aug 1979.

***Paravandellia phaneronema* (Miles, 1943):** All from Colombia. CZUT-IC 1290, 2 ex (♂) (1 c&s), 25.3-26.0 mm SL, Colombia, Tolima, Chaparral, río Saldaña (río Magdalena drainage) at mouth of río Amoyá (03°40'23"N, 75°23'18"W), col., L. García, F. Villa, N. Briñez, D. Castro, 08 feb 2005; ICN 16117, 1 ex (♂), 23.9 mm SL, Caldas, Norcasia, río Manso en La Punta (trib. to río La Miel, río Magdalena drainage), col., L. Mesa & P. Sánchez, 25 Mar 2006; ICN 16131, 47 ex (25♂, 22♀), 21.3-26.2 mm SL, Caldas, Norcasia, río Manso (trib. to río La Miel, río Magdalena drainage), at whirlpools,

col., L. Mesa & P. Sánchez, 25 Mar 2006; MCZ 35874, 1 ex (♂) (paratype of *Branchioica phaneronema*), 25.5 mm SL, La Virginia, Valle del Cauca, upper río Cauca, col., C. Miles, 14 Oct 1942; USNM 120141, 1 ex (♀) (paratype of *Branchioica phaneronema*), 25.6 mm SL, Virginia [= La Virginia], upper río Cauca, col., C. Miles, 14 Oct 1942; USNM 120142, 1 ex (paratype of *Branchioica magdalenae*), 20.6 mm SL, Honda, río Magdalena, Colombia, col., C. Miles, Feb 1943; MCP 20245, 1 c&s, 27.5 mm SL, Colombia, margin of río La Vieja, 300 m above mouth of río Roble, farm Playa Azul, upper río Cauca, col., C. Román-Valencia & J.L. Jiménez, 01 Jun 1996.

***Plectrochilus diabolicus* Myers, 1927:** MZUSP 57286, 1 ex (c&s), 67.5 mm SL, Amazonas, rio Amazonas, near mouth of rio Madeira, col., A. Zanata *et al.,* 1996; MZUSP 125621, 9 ex (3 c&s), 48.1-58.0 mm SL, Rondônia, Porto Velho, rio Sotério (11°36'38"S, 65°13'26"W), col., Naturae Expedition, 30 Oct 2011 (specimens damaged, squashed).

***Plectrochilus machadoi* Miranda-Ribeiro, 1917:** MZUSP 9608, 2 ex, 64.0 mm SL (1 c&s) Amazonas, rio Solimões, across from Codajás, mouth of Lago Pereira, col., EPA, 24 Sep 1968; MZUSP 57286, 1 ex (c&s), 67.5 mm SL, Amazonas, rio Amazonas, near mouth of rio Madeira, col., A. Zanata *et al.,* 1996.

***Vandellia cirrhosa* Valenciennes, 1846:** INPA 12419, 10 ex (3 c&s), 41.2-81.4 mm SL, Amazonas, rio Solimões, Ilha da Marchantaria, col., INPA team, 20 Mar 1976 (collected together with *V. sanguinea,* INPA 53199); MZUSP 63394, 12 ex (3 c&s), 40.3-113.4 mm SL, Amazonas, beach on Ilha Muratu, rio Solimões, in front of mouth of Lago Janauacá, col., Alpha Helix Expedition, 06-25 Jan 1977; MZUSP 63004, 11 ex (2 c&s), 47.5-63.4 mm SL, Mato Grosso, Barra do Garças, Ouro Fino, rio Araguaia, 30 km downsteam from Barra do Garças, col., W. Barrela *et al.,* 06-07 Oct 1997; MZUSP 30436, 11 ex (3 c&s), 46.7-131.9 mm SL, Rondônia, rio Madeira at Cachoeira do Teotônio (approx. 08°51'S, 64°03'W), col., M. Goulding, 05 May 1984; MZUSP 49781, 7 ex (2 c&s), 53.0-63.7 mm SL, Acre, rio Acre, between Seringal Paraíso and Lago Amapá, col., joint team from Instituto do Meio Ambiente do Acre and Universidade Federal do Acre, 30 Jun-01 Jul 1994.

***Vandellia sanguinea* Eigenmann, 1917:** MZUSP 29152, 27 ex (5 c&s), 42.6-58.1 mm SL, Rondônia, rio Machado, Paracaúba, col., M. Goulding, 04 Sep 1980; MZUSP 63395, 37 ex (5 c&s), 51.3-66.3 mm SL, Amazonas, rio Solimões, Ilha Muratu, across from mouth of Lago Janauacá, col., Alpha Helix Expedition, Jan 1977; MZUSP 63260, 6 ex (1 c&s), 69.5-92.1 mm SL, rio Tapajós, near Alter do Chão, col., M. Goulding, 25 Nov 1983.

## RESULTS

The taxonomic results are presented in this section. The character evidence for the monophyly of the various groupings recognized in this paper (including genera

*Paracanthopoma* and *Paravandellia*) is discussed in subsequent sections (*see* "Character evidence for recognized taxa"), where relevant illustrations are cross-referenced.

## Taxonomic accounts

### *Paracanthopoma* Giltay

*Paracanthopoma* Giltay, 1935: 1 [type species: *Paracanthopoma parva* Giltay, 1935, by original designation] – Myers, 1944: 598 [key] – Gosline, 1945: 66 [catalogue] – Burgess, 1989: 324 [checklist] – Eschmeyer, 1990: 292 [catalog] – Eschmeyer, 1998: 2057 [catalog] – Spotte, 2002: 97 [historical account; summary of previously published information] – de Pinna & Wosiacki, 2003: 276 [checklist] – Ferraris, 2007: 410 [checklist].

**Diagnosis:** *Paracanthopoma* is distinguished from all other genera of Vandelliinae by the following putative synapomorphies: 1 = presence of a branchiostegal velum across the isthmus ("free branchial membrane" of previous authors); 2 = median premaxilla with dorsal bilateral flanges bracing lateral margins of mesethmoid neck; 3 = median premaxilla with narrow, well-defined posterior median recess; 4 = maxilla distally bifurcated (incipient in *Pc. daemon*); 5 = posterior articular process of palatine directed straight posteriorly, parallel to neurocranium; 6 = anterior margin of palatine at articulation with premaxilla with deep indentation where a corresponding process of the premaxilla inserts; 7 = coronoid process formed mostly or exclusively by the dentary, with anguloarticular portion reduced or absent; 8 = upper pharyngeal toothplate absent; 9 = articulation between neural arch of complex vertebra and supraoccipital limited to a small dorsomedial portion. Further distinguished from *Vandellia* and *Plectrochilus* by the scalpelloid teeth restricted to the distal tip of the premaxilla (vs. distributed along a long portion of the bone); by the post-articular process of anguloarticular large, pointed, directed straight laterally and projecting beyond lateral limits of anterior portion of suspensorium and jaw skeleton (vs. process inconspicuous, not projecting laterally); by the mesethmoid cornua lacking ventral bilateral processes at contact with premaxilla (vs. well-defined ventral process articulating with anterior process of premaxilla); by the skull roof mostly unossified (vs. skull roof entirely ossified); by the lack of a process on the ventral portion of the metapterygoid (vs. process present proximal to articulation with quadrate); by the presence of three or four branchiostegal rays (vs. five). Further distinguished from *Paravandellia* by the conical premaxillary teeth absent or few (one or two) (vs. conical teeth always present and four to nine in number); by the eyes located entirely dorsally on the head (vs. eyes located near the lateral margin of the head).

**Geographic distribution:** Species of *Paracanthopoma* are broadly distributed in the northern cis-Andean South American drainages, namely Amazon, Orinoco,
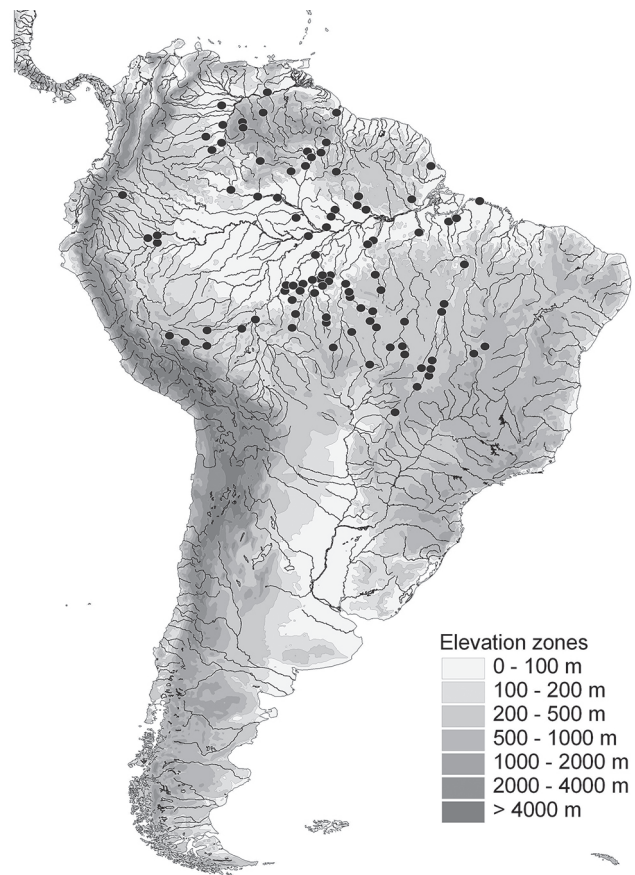


**Figure 2.** Map of South America showing geographical distribution of *Paracanthopoma*.

and Essequibo, with a single locality also in the Upper Paraguay (Fig. 2). They have not yet been recorded from large lowland Amazonian tributaries west of the mouth of the rio Negro, including the Japurá, Putumayo, Purus, and Juruá. Other notable absence include the rivers of the Guyana region between the Essequibo and the mouth of the Amazon (except for a single occurrence at rio Amapá Grande in Brazil).

## Key to species of *Paracanthopoma*

Although the various species of *Paracanthopoma* are very different from each other, often by decisive diagnostic traits, perceiving some of those differences can be challenging at first. Their generally white skin lacks contrast, thus rendering superficial details difficult to visualize. What little dark pigment there is, fades rather quickly under normal preservation conditions. Also, the integument is often preserved in folded or deformed positions in critical areas of the body, masking otherwise striking distinctions in shape and proportions. Odontodes and teeth may be deeply sunk in integument, making counts prone to errors. Those difficulties are aggravated in very small specimens and those with a long history of preservation, when normal shrinkage further deforms external morphological traits. Access to cleared and stained specimens, CT and SEM images greatly facilitates identifications, but such resources are not always available.
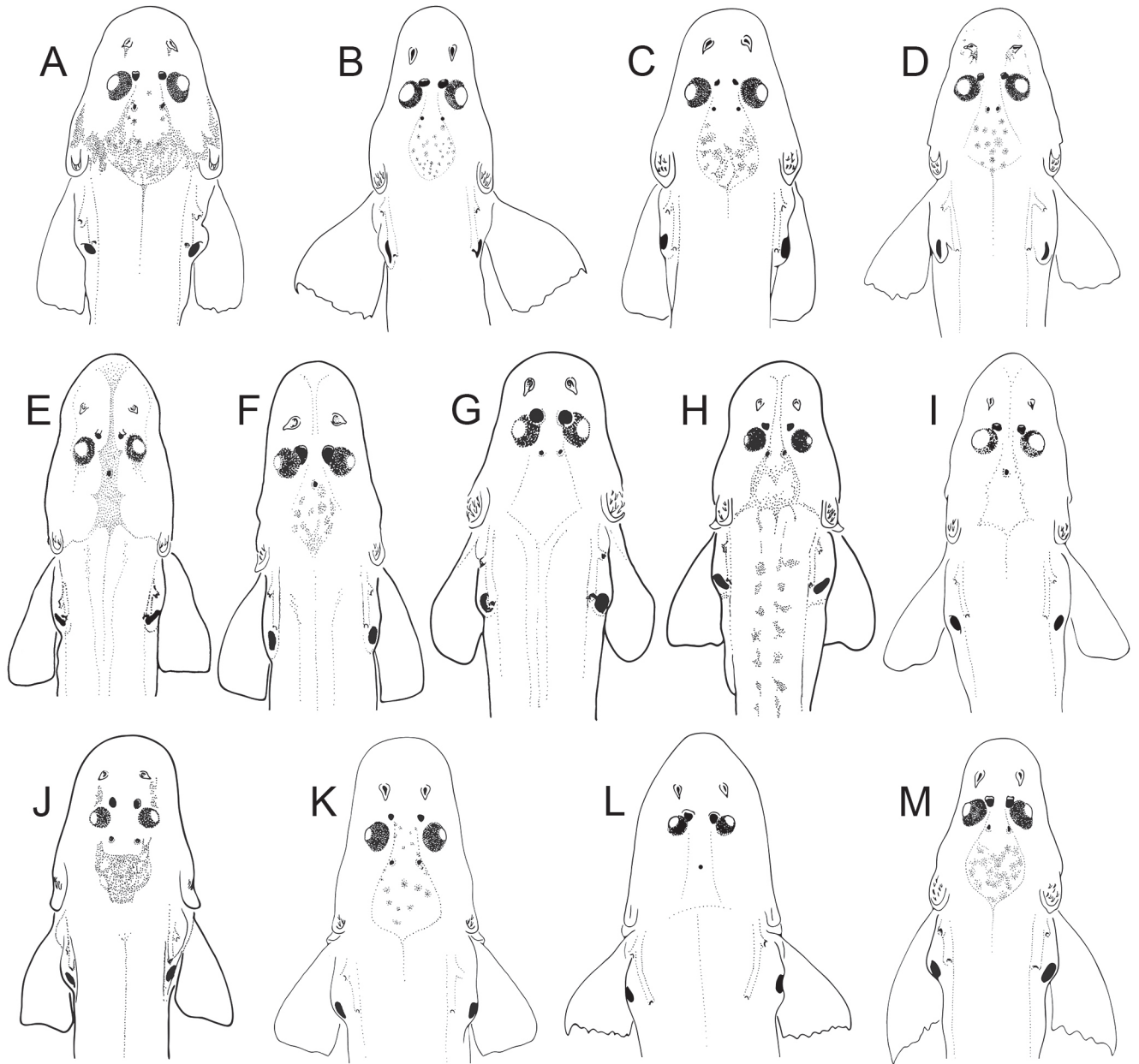
**Figure 3.** Schematic representations of the head of species of *Paracanthopoma* in dorsal view. (A) *Pc. ahriman;* (B) *Pc. alleynei;* (C) *Pc. cangussu;* (D) *Pc. capeta;* (E) *Pc. carrapata;* (F) *Pc. daemon;* (G) *Pc. irritans;* (H) *Pc. malevola;* (I) *Pc. parva;* (J) *Pc. saci;* (K) *Pc. satanica;* (L) *Pc. truculenta;* (M) *Pc. vampyra.*

The key below attempts to circumvent such difficulties to some degree, by placing emphasis on easily observable traits that are less prone to deformation during fixation or long preservation, with less accessible traits (*e.g.,* vertebral number and other osteological data) given as a means of confirmation when necessary. Still, reliance on some meristic data and other minute details is unavoidable in certain cases, and cleared and stained preparations or x-rays are necessary to reliably obtain such information. Procurrent fin rays, teeth and odontodes can rarely be accurately counted on alcoholic specimens of *Paracanthopoma,* even when well-preserved. Fortunately, the general habitus of the body and, especially, the head of most species are largely diagnostic, provided availability of well-preserved specimens and some degree of familiarity with their range of variation. Although differences of this sort are unappealling when expressed in words, they are fully apprehended visually. Thus, comparative illustrations are offered as aids to identification (Figs. 3, 4).

1a.    Maxillary barbel extending for less than half of distance between its base and anterior limit of interopercular odontodophore; distance between interopercular odontodophore and eye at least 2.5 times distance between two odontodophores; epiphyseal canals joining medially, opening as single median pore on top of skull ................................................................................................................................................................................................................ 2

1b.    Maxillary barbel extending for more than half of distance between its base and anterior limit of interopercular odontodophore; distance between opercular and interopercular odontodophore approximately equal or only slightly smaller than that between latter and eye; epiphyseal canals not conjoined medially, opening as two separate pores behind eyes ................................................................................................................................................. 5
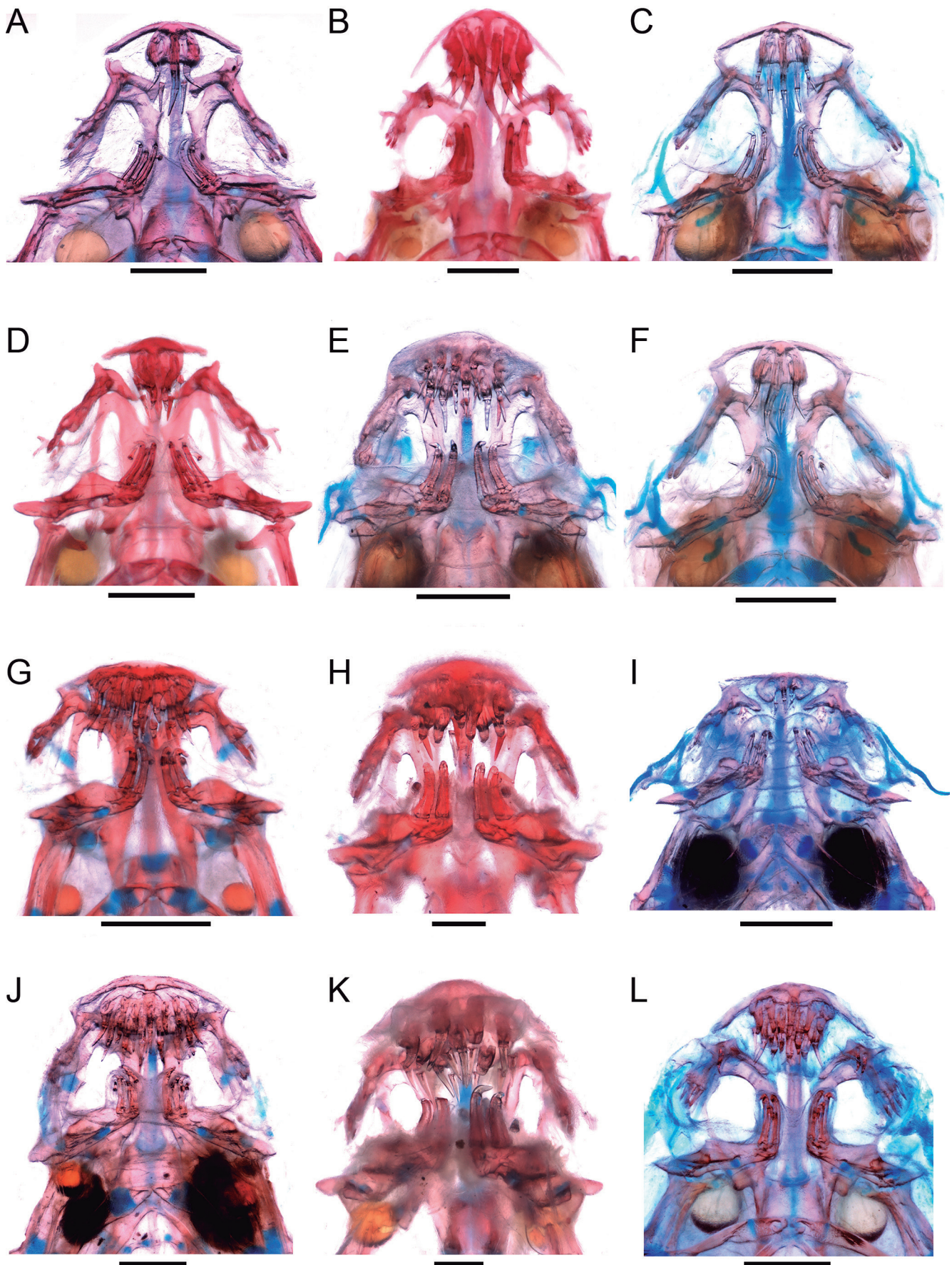
**Figure 4.** Comparative chart of jaws and anterior portion of head of *Paracanthopoma* species, cleared and stained specimens, ventral views: (A) *Pc. ahriman* FMNH 105525; (B) *Pc. alleynei* MZUSP 103052; (C) *Pc. cangussu* MZUSP 86250; (D) *Pc. capeta* MZUSP 29154; (E) *Pc. daemon* MZUSP 95597; (F) *Pc. irritans* INPA 20529; (G) *Pc. malevola* MCP 36217; (H) *Pc. parva* MZUSP 30400; (I) *Pc. saci* MZUSP 125626; (J) *Pc. satanica* MZUSP 100149; (K) *Pc. truculenta* MZUSP 30404; (L) *Pc. vampyra* MZUSP 100138. Scale bars = 500 μm. *Pc. carrapata* not shown.

2a. Origin of anal fin at same vertical through origin of dorsal fin, or only slightly posterior to it; caudal fin truncate or only slightly concave; procurrent caudal-fin rays 19 or 20 dorsally and 20 or 21 ventrally, the latter series extending anteriorly to vertical through posterior end of anal fin .........................*Pc. daemon*

2b. Origin of anal fin well posterior to that of dorsal fin (at vertical through middle of base of dorsal fin or further posteriorly); caudal fin clearly bilobed or strongly concave; procurrent caudal-fin rays 14 to 19 dorsally and 14 to 18 ventrally, the latter series not reaching anteriorly to vertical through posterior end of anal fin............................................................................................................................................................. 3

3a. Opercular and interopercular odontodophores extremely reduced in size and number of odontodes, inconspicuous on surface of head, opercular odontodophore with one or two odontodes sunk in narrow slit of skin; lateral line strongly angled dorsoposteriorly, its distal pore distant from axillary gland pore, and located posterior to vertical through posterior margin of latter ............................................................................................................ *Pc. truculenta*

3b. Opercular and interopercular odontodophores clearly visible on surface of head, with four or more odontodes exposed; lateral line parallel to longitudinal axis of body or only gently curved dorsoposteriorly, its distal opening adjacent to axillary gland pore, and located anterior to vertical through posterior margin of latter ............................................................................................................................................................................................................... 4

4a. Dorsal surface of skull largely covered with muscle, so that in dorsal aspect the exposed portion of the braincase is equivalent maximally to interorbital; opercular and interopercular odontodophore far smaller than eye.......................................................................................................................... *Pc. carrapata*

4b. Head musculature not covering extensively the dorsal surface of skull, exposed portion of the braincase larger than interorbital; opercular and interopercular odontodophore approximately as large as eye, or only slightly smaller .................................................................................................. *Pc. parva*

5a. Median premaxillary teeth 13 or more, forming a rectangular arrangement occupying most or all surface of visible upper jaw ................................................ 6

5b. Median premaxillary teeth 11 or fewer forming a small semicircular or triangular arrangement occupying only middle portion of visible upper jaw ............ 7

6a. Odontodophores relatively large, with 11 or 12 opercular and 7 or 8 interopercular odontodes; presence of a bilateral series of irregular dark spots along each side of dorsal midline; vertebrae 40; procurrent caudal-fin rays 19 to 21 dorsally and 18 to 20 ventrally; median premaxillary teeth 18 or 19; principal caudal-fin rays 6 + 7 ..........................................................................................................................................................*Pc. malevola*

6b. Odontodophores small, with 5 or 6 opercular and 4 or 5 interopercular odontodes; dorsum lacking dark pigment; vertebrae 42 or 43; procurrent caudal-fin rays 32 dorsally and 30 to 32 ventrally; median premaxillary teeth 13; principal caudal-fin rays 6 + 6 ...................................................... *Pc. satanica*

7a. Three pelvic-fin rays; opercular odontodophore minuscule, at middle of large roundish area of thickened integument and periodontodal fold vestigial or absent; prepelvic length 56.0-61.1% SL; caudal peduncle length 24.0-26.6% SL ...................................................... *Pc. saci*

7b. Five pelvic-fin rays; opercular odontodophore well-developed, surrounded by well-defined, narrow periodontodal fold; prepelvic length 62.1-67.8% SL; caudal peduncle length 17.9-24.0% SL ................................................................................................................................................................ 8

8a. Median premaxilla and associated dentition small, with 5 or fewer teeth occupying less than half of exposed upper jaw; maxillary barbel short, its tip reaching maximally 75% of distance to interopercular odontodophore; premaxilla lacking any conical teeth; opercular odontodes 6-9 ........................................... 9

8b. Median premaxilla and associated dentition large, with 11 teeth occupying more than half of exposed upper jaw; maxillary barbel long, its tip reaching interopercular odontodophore or 95% of distance to it; premaxilla with one or two conical teeth near corner of mouth; opercular odontodes 10-13 ....... 12

9a. Width of opercular periodontodal fold approximately uniform around its perimeter, encircling opercular odontodes only, not extended anteriorly as horizontal ridge of integument; base of maxillary barbel anterior to vertical through anterior margin of eye in lateral view ................................................*Pc. capeta*

9b. Ventral portion of opercular periodontodal fold hypertrophied, extending anteriorly in straight line to dorsal margin of interopercular odontodophore, forming prominent horizontal ridge of integument between odontodophores; base of maxillary barbel at or posterior to vertical through eye in lateral view .................................................................................................................................................................................................................. 10

10a. Intense dark pigment on head, in stark contrast to white body, formed by combination of brain pigment over posterior and lateral parts of neurocranium, plus integumentary pigmentation extending laterally onto area of opercular odontodophore and between opercular and interopercular odontodophores; vertebrae 45; median premaxillary teeth 2 to 4 .........................................................................................................................................................*Pc. ahriman*

10b. Dark pigment on head faint, reduced to few spots of dark brain pigment; vertebrae 39 to 44; median premaxillary teeth 5................................................. 11

11a. Principal caudal-fin rays 5 + 5; caudal peduncle depth 10.8-13.0% SL; posterior internarial width 8.1-10.0% HL; procurrent caudal-fin rays 28-30 dorsally and 27-29 ventrally; deepest portion of the caudal peduncle (corresponding to longest procurrent caudal-fin rays) approximately at its half-length; dorsal and ventral profiles of caudal peduncle posteriorly strongly converging towards base of caudal fin, forming pronounced concave regions clearly delimiting beginning of caudal fin; interorbital larger than eye diameter .........................................................................................................................*Pc. cangussu*

11b. Principal caudal-fin rays 6 + 6; caudal peduncle depth 8.3-10.6% SL; posterior internarial width 3.3-5.5% HL; procurrent caudal-fin rays 19-25 dorsally and 21-25 ventrally; caudal peduncle progressively deeper to base of caudal fin; dorsal and ventral profiles of caudal peduncle gently continuous with caudal fin, with only slight depression in some specimens; interorbital smaller than eye diameter .................................................................................*Pc. irritans*

12a. Interorbital smaller than eye diameter; caudal fin gently convex or truncate; interopercular odontodes 8 or 9; vertebrae 40 to 42; procurrent caudal-fin rays 22 to 27 dorsally and 21 to 25 ventrally; caudal-fin rays 5 + 6 or 6 + 6.......................................................................................................................................*Pc. vampyra*

12b. Interorbital equal or larger than eye diameter; caudal fin gently concave or bilobed; interopercular odontodes 12-14; vertebrae 38 or 39; procurrent caudal-fin rays 14 to 19 dorsally and ventrally; caudal-fin rays 6 + 7 ........................................................................................................................................... *Pc. alleynei*

## *Paracanthopoma ahriman,* new species
### (Fig. 5)

**Holotype:** FMNH 105525, 19.9 mm SL, Venezuela, T.F. Amazonas, río Autana at Playa Cucurito in front of caño Cucurito (approx. 05°14′N, 66°10′W), col., B. Chernoff, A. Machado & J. Wheeler, 09 Feb 1992.

**Paratypes:** All collected with holotype. FMNH 147290, 10 ex (2 c&s, 1 SEM), 17.5-20.4 mm SL; MZUSP 126890, 3 ex (1 c&s), 17.2-19.6 mm SL.

**Non-type specimens:** MHNLS 18018, 8 ex, 15.0-17.4 mm SL, Venezuela, Amazonas, Caño Guachapana (trib. to Río Orinoco) (03°21′17,6″N,

69°02'25,0"W), col., C. Lasso, O. Lasso-Alcala, O. Leon Mata, D. Rodriguez Olarte, 28 Nov 2003; MHNLS 24334, 1 ex, 21.82 mm SL, Colombia, Vichada, Rio Guaviare (Río Orinoco drainage), Laguna El Gusano, margen derecha (03°57'36,6"N, 67°57'56,6"W), col., C. Lasso, M. Sierra, M. Patiño, F. Villa, A. Ortega, 16 Feb 2008.

**Diagnosis:** Unique among *Paracanthopoma* in having 45 vertebrae (vs. 44 or fewer). Distinguished form all congeners except *Pc. cangussu, Pc. capeta,* and *Pc. irritans* by the presence of five median premaxillary teeth (with one or two often in replacement) (vs. either three or 9 to19 in total). The species is further distinguished from all congeners, except *Pc. cangussu* and *Pc. irritans,* by the broad and horizontally long ventral portion of the opercular periodontodal fold, forming a lateral ridge of integument extending anteriorly to the dorsal margin of the interopercular odontodophore (vs. ventral part of fold not anteriorly extended, independent from interopercular odontodophore). Distinguished from *Pc. cangussu* by the shorter caudal peduncle (19.2-21.5% SL, vs. 21.8-24.0), by the longer predorsal length (71.8-76.7% SL; vs. 66.7-71.3); by the wider anterior internarial width (17.6-20.2% HL; vs. 13.3-17.1); by the wider posterior internarial width (10.1-11.4% HL; vs. 8.1-10.0). Distinguished from *Pc. capeta* by the broader head (head width 80.7-87.6% HL; vs. 68.0-72.0); by the mouth cleft directed more strongly posteriorly than laterally (vs. opposite); by the roundish median premaxilla (vs. trapezoidal with nearly straight anterior margin). Distinguished from *Pc. irritans* by the broader head (head width 80.7-87.6% HL; vs. 73.3-76.9); by the broader interorbital (14.8-17.9% HL; vs. 11.0-12.8); by the wider anterior internarial width (17.6-20.2% HL; vs. 13.4-16.5); by the larger posterior internarial width (10.1-11.4% HL; vs. 3.3-5.5). The heavy dark pigmentation of the head, forming striking contrast with its mostly white body, distinguishes *Pc. ahriman* from all other vandelliines. The peculiar dark pattern is composed of brain pigment, seen by transparency, in combination with integumentary chromatophores disposed in specific areas. Brain pigment covers the posterior part of the neurocranium, extending anteriorly alongside lateral margins of skull as narrow dark fields. Integumentary pigment covers the opercular odontodophore and region immediately surrounding it, with a dark band extending along the ventral margin of opercular odontodophore anteriorly to alongside dorsal margin of interopercular odontodophore, and slightly beyond. The intensity of such dark cephalic pigmentation is unique to the species, but is now faded in available specimens, so it can only be useful for identification in freshly-preserved specimens.

**Description:** Morphometric data for the holotype and paratypes are provided in Table 1. Body relatively short (HL 17.0-18.3%SL). Cross-section of body depressed at pectoral-fin insertion, becoming round at approximately midlength of pectoral fin, and increasingly compressed posterior to that point. Caudal peduncle tapering gradually to caudal fin as seen in dorsal view. Dorsal profile of body gently convex from head to origin of dorsal fin (Fig. 5), with translucent middorsal keel along posterior two-thirds of that trajectory. Dorsal profile of head continuous with that of dorsum, anterior portion of which flattened. Caudal peduncle paddle-shaped, its dorsal and ventral profiles convex, strongly expanded immediately posterior to tips of dorsal and anal fins, due to well-developed procurrent caudal-fin ray series (Fig. 5). Ventral profile of body and head straight until tip of pectoral fin, then gently convex or straight to origin of pelvic fin. Ventral profile of body posterior to anus straight to region of ventral accessory caudal-fin rays. Myotomes visible along whole body, progressively narrower and more sloped posteriorly. Region of longitudinal skeletogenous septum visible along nearly whole body. Integument thin, not heavily covering bases of fins. Axillary gland large, involving most of pectoral-fin base, except anteriorly, and extending posteriory to beyond limit of pectoral fin for variable distance, maximally for distance equivalent to fin length. Gland tapering posteriorly, with its posterior part more or less visible according to volume of secretion in lumen at time of fixation. Axillary gland pore hypertrophied, located at vertical through midlength of pectoral fin, directed dorsoposteriorly and widely open in most specimens.

Dorsal profile of head continuous with that of dorsum (Fig. 5). Head longer than broad, (head width 80.7-87.6% HL) snout round and broad, slightly differentiated from rest of head (Fig. 5). Muscles not significantly covering dorsal part of head, neurocranium entirely exposed. Head depressed, its depth 34.0-45.9% HL, with dorsal profile straight and horizontal in lateral view until anterior nostrils, then angled ventrally and straight to tip. Eye large, (15.0-17.6% HL) without free orbital rim, located dorsolaterally on head and directed anterodorsolaterally. Integument over eye thin, whole eyeball visible in preserved specimens. Eyes mostly on anterior half of HL, interorbital width approximately equal to longitudinal diameter of eye. Eyelens occupying much of lateral surface of eye and constricted by round iris only marginally. Anterior nostril small (Fig. 6), located in small depression of integument and surrounded by short tubule of integument produced posteriorly into small round or slightly pointed process, with double elastin cores. Anterior internarial width equal or slightly larger than interorbital. Posterior naris roundish and slightly smaller than anterior ones, with short flap of integument anteriorly, not occluding opening (Fig. 6). Posterior naris positioned mesially to eye, their anterior margin posterior to transverse line through anterior margin of eyes. Posterior internarial width narrower than interorbital.

Opercular odontodophore large, larger than eye when periodontodal fold included, dorsolaterally located on head, at middepth of head in lateral aspect (Fig. 5). Periodontodal fold very large, especially ventrally, encircling dorsal, posterior and ventral sides of odontodophore and maximally over 50% of depth of toothed portion. Ventral portion of periodontodal fold extending anteriorly as broad straight or slightly convex ridge to dorsal margin of interopercular periodontodal fold, forming horizontal keel between two odontodophores.

**Figure 5.** *Paracanthopoma ahriman,* FMNH 105525, holotype, 19.9 mm SL, Venezuela, T.F. Amazonas, Río Autana. (A) Lateral view of body; (B) Dorsal view of head; (C) Ventral view of head.
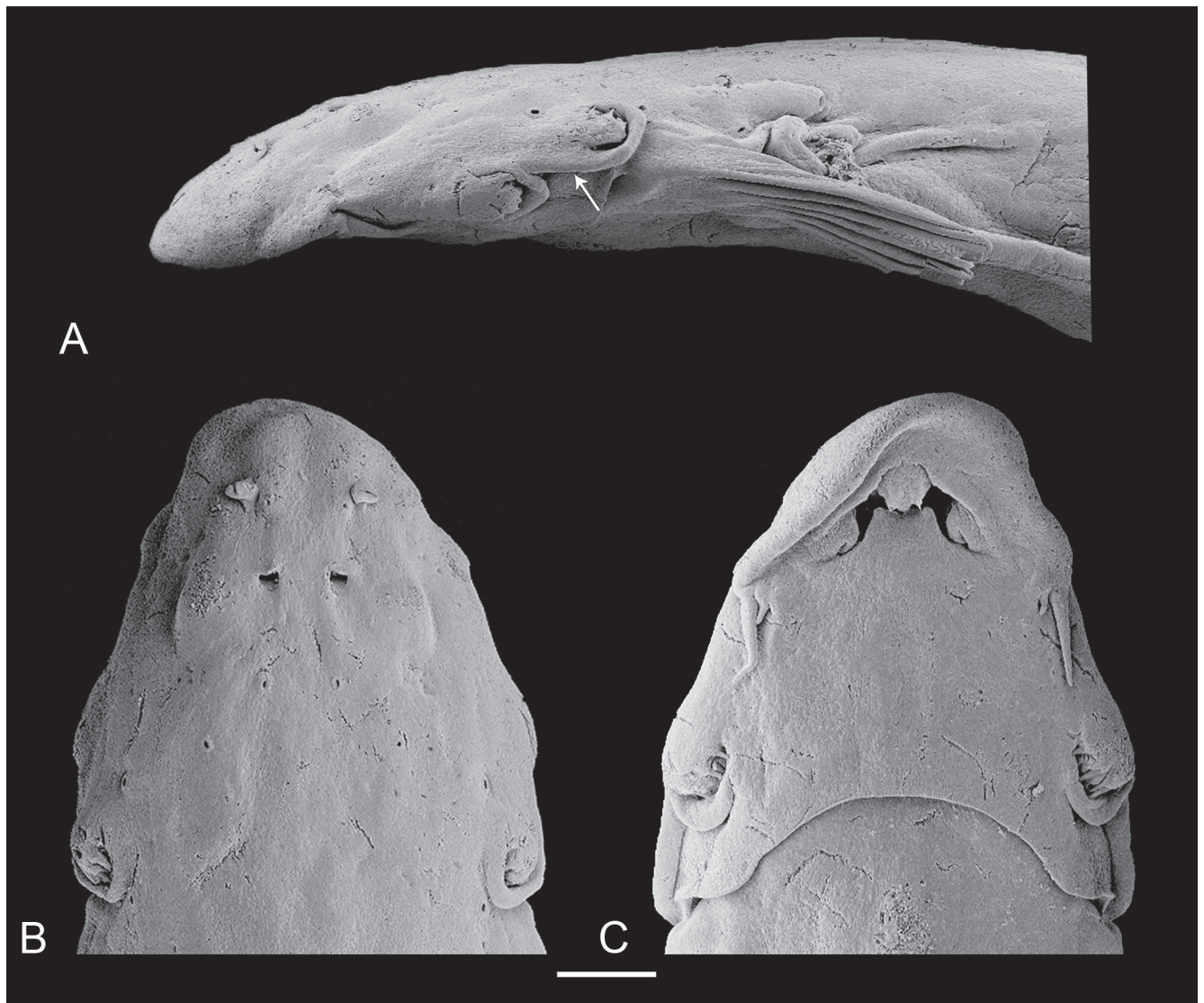


**Figure 6.** *Paracanthopoma ahriman,* FMNH 147290, SEM images of head. (A) Lateral; (B) Dorsal; (C) Ventral. Arrow indicates extended periodontodal fold between opercular and interopercular odontodophores. Scale bar = 500 μm.

**Table 1.** Morphometric data of *Paracanthopoma ahriman*. Ranges, mean and SD include holotype. Head subunits were obtained with an ocular micrometer and therefore as projections. **Abbreviations:** min = minimum value; max = maximum value; n = number of specimens; SD = standard deviation.

| | n | holotype | min | max | mean | SD |
|---|---|---|---|---|---|---|
| Standard length (mm) | 6 | 19.9 | 17.7 | 20.1 | 19.0 | |
| **Percentages of SL** | | | | | | |
| Total length | 6 | 1.1 | 1.1 | 1.1 | 1.1 | 0.0 |
| Body depth | 6 | 13.7 | 12.6 | 14.7 | 13.6 | 0.7 |
| Caudal peduncle length | 6 | 19.2 | 19.2 | 21.5 | 20.0 | 0.9 |
| Caudal peduncle depth | 6 | 10.3 | 8.1 | 10.6 | 9.8 | 0.9 |
| Predorsal length | 6 | 76.7 | 71.8 | 76.7 | 74.4 | 2.0 |
| Preanal length | 6 | 74.7 | 70.4 | 74.7 | 72.2 | 1.4 |
| Prepelvic length | 6 | 67.1 | 63.4 | 67.8 | 65.9 | 1.6 |
| Dorsal-fin base length | 6 | 8.2 | 6.7 | 8.5 | 7.6 | 0.6 |
| Anal-fin base length | 6 | 8.2 | 7.4 | 8.2 | 7.9 | 0.3 |
| Pectoral-fin length | 6 | 12.3 | 12.1 | 14.0 | 12.9 | 0.8 |
| Head length | 6 | 17.1 | 17.0 | 18.3 | 17.6 | 0.5 |
| **Percentages of HL** | | | | | | |
| Head width | 6 | 87.6 | 80.7 | 87.6 | 84.0 | 2.4 |
| Head depth | 6 | 40.0 | 34.0 | 45.9 | 40.3 | 4.4 |
| Pectoral-fin length | 6 | 76.2 | 69.2 | 78.4 | 73.7 | 3.8 |
| Interorbital | 6 | 16.2 | 14.8 | 17.9 | 16.1 | 1.0 |
| Eye diameter | 6 | 16.2 | 15.0 | 17.6 | 16.1 | 1.0 |
| Snout length | 6 | 37.1 | 37.0 | 37.6 | 37.3 | 0.2 |
| Mouth width | 6 | 24.8 | 22.9 | 25.9 | 24.4 | 1.1 |
| Anterior internarial width | 6 | 19.0 | 17.6 | 20.2 | 19.0 | 1.1 |
| Posterior internarial width | 6 | 11.4 | 10.1 | 11.4 | 10.7 | 0.6 |

Opercular odontodes 6, closely positioned in roughly circular arrangement, with three smaller anterior and three posterior larger ones. Main axis of opercular odontodes oriented horizontally in lateral view, with distal portions of larger posterior ones curved strongly mesially (with top and bottom odontodes of that series with some dorsal and ventral components, respectively). Curvature less intense in smaller three odontodes of anterior series. Few caps of replacement odontodes interspersed with mature ones. Interopercular odontodophore similar in size to opercular one, located ventrolaterally on head, immediately ventral to horizontal through origin of pectoral fin, with 7 odontodes closely positioned in two irregular rows, with larger ones in posterior row. Interopercular odontodophore closer to opercular one than to eye. Two or three replacement tooth caps located posteromesially to mature ones. Interopercular periodontodal fold of integument well-developed, oval and extending well-beyond tips of odontodes, especially posterolaterally. Epiodontodeal velum thin and transparent, covering more than half of length of odontodes.

Mouth inferior (ventral), strongly flattened (Fig. 5). Each premaxilla with single scalpelloid teeth attached to its distal tip (visible only in skeletal preparations; Figs. 4A, 7), but actually two adjacent tooth sockets, one of which normally vacant, corresponding to half-formed replacement tooth adjacent to mature one. Three additional initial-stage replacement caps suspended in soft tissue directly dorsal to mature one and its incomplete neighbor. Mature scalpelloid tooth with distal portion disproportionately reduced and very strongly curved over rest of teeth, with tiny pungent tip nearly adpressed to margin of basal plate. Scalpelloid tooth deeply hidden in labial tissue and impossible to expose in preserved specimens without damaging soft tissue. Conical teeth absent in premaxilla (Figs. 4A, 7). Paralabial sac apparently reduced to space immediately mesial to distal portion of premaxilla, entirely inside of mouth and difficult to locate externally. Upper lip very thick, obliterating much of mouth opening. Median premaxilla small, with 5 teeth disposed in single row, with one central largest tooth and two smaller ones on each side (Figs. 4A, 7). In most specimens, one or two teeth in process of replacement, but total count of five obvious by tooth sockets and relative position of attached teeth. Tooth bases disposed at approximately same transverse line, with median tooth slightly more anterior. All teeth posteriorly oblique to ventral surface of median premaxilla at base, at approximately 45° angle, and curved further posteriorly at distal pungent portion. All median premaxillary teeth strongly laterally compressed basally, with the central one extremely broad longitudinally- and flat-based. Three to five replacement tooth caps posterodorsally to mature dentition. Median premaxillary velum thick, covering all teeth when extended. Hypodontal pad of median premaxilla narrow, following profile of median premaxilla. Lower jaw narrow, composed mostly of narrow and pointed, triangular dentary lobes, continuous with mental region posteriorly (Figs. 5, 6). Jaw cleft short and strongly directed laterally, its lateral portion almost transverse to longitudinal axis and leaving little or no space separating lower jaw from inner margin of upper jaw. Dentary diastema small, strongly concavely or angulate, fitting snugly onto posterior margin of median premaxilla. Rami of mandible very close together at midline. Dentary teeth 3 or 4, closely packed at mesial end of dentary and disposed as two ventral teeth and one or two dorsal ones (Figs. 4A, 7). Axis of dentary teeth anteromesially-directed at base, but curved anterolaterally at distal third. Branchiostegal velum forming large, continuous, round and posteriorly concave curve across whole of mental region. Dorsal portion of branchial membrane approaching but not covering anterior margin of pectoral-fin base. Branchial openings small, spanning approximately area between ventral margin of opercular odontodophore and dorsal margin of interopercular periodontodeal fold. Maxillary barbel very short and proximally broad, its base flap-like, only distal portion filamentous (Figs. 5 and 6). Posterior point of its base at, or slightly anterior to, vertical through anterior margin of eye, its tip extending posteriorly maximally to base of interopercular odontodes, but often shorter than that. Mesial (or ventral) part of maxillary-barbel base inserting directly onto corner of mouth without major intervening membranous outgrowth. Rictal barbel (Fig. 6) located mesially to base of maxillary one and varying in size (sometimes between sides of specimen), ranging from nearly absent externally to approximately one-fifth of maxillary barbel length. Nasal barbel vestigially represented by posterior elongated portion of fold around anterior naris described above, with double internal elastin core.
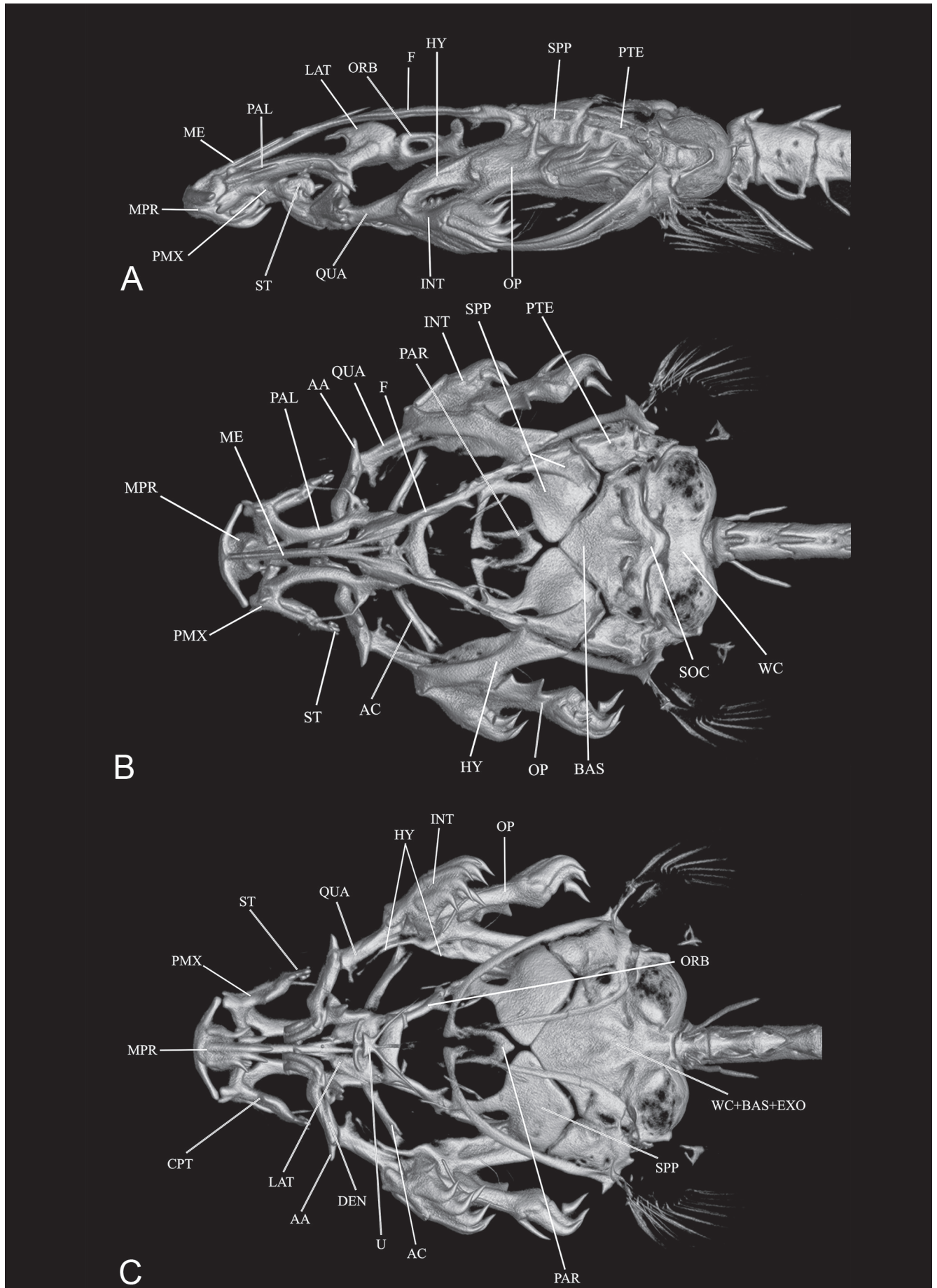
**Figure 7.** *Paracanthopoma ahriman,* holotype FMNH 105525, CT scan images of head skeleton, (A) Lateral; (B) Dorsal; (C) Ventral. Specimen poorly calcified, some structures not properly shown.

Lateral line short and mostly straight, surrounded by thickened tissue similar to that of axillary gland, making its profile extremely thick on surface of body. Terminal lateral-line pore approximately at vertical through mid-length of pectoral-fin, near dorsal margin of axillary pore, slightly produced laterally from surface of body. Short secondary branch splitting off ventrally from anterior portion of canal, with corresponding pore opening approximately at midlength of main canal. Single short lateral-line tubule curved and irregularly calcified, extending approximately for middle one-third of main canal.

Pectoral fin short (69.2-78.4% HL), with i + 5 rays, truncate or gently convex, its distal margin irregular at close range, its base on ventral side of body. Pelvic fins small, well-separated from each other at base, with i + 4 rays. Pelvic splint present. Origin of pelvics well anterior to vertical through origin of dorsal-fin, entirely covering anus and extending posteriorly well beyond origin of anal fin. Posterior margin of pelvic fin round. Dorsal fin small, with approximately same area as caudal fin in lateral aspect, broadly triangular with round apex or roughly rectangular, with gently convex distal margin and ii + 5 (only one specimen) or ii + 6 fin rays, plus 5 procurrent ones. Anal fin small, approximately with same size as dorsal fin and slightly more elongate and rectangular in shape than latter, with gently convex distal margin and ii + 5 fin rays, plus 5 procurrent ones. Origin of anal fin at vertical through origin of dorsal-fin. Anal fin with same size, slightly smaller or slightly larger than dorsal one. Caudal fin truncate with round edges, slightly convex in some specimens, less deep than maximum depth of caudal peduncle. Principal caudal-fin rays 5 + 6, 6 + 6 or 6 + 7 (modally 6 + 6), with variation apparently due mostly to differences in branching patterns. Procurrent caudal-fin rays 26 dorsally and 25 ventrally (values based on one specimen only).

Vertebrae 45 (n = 10). One specimen with 46, but due to one deformed duplicated vertebra. First dorsal-fin pterygiophore subsequent to neural spine of vertebra 23 (n = 3). First anal-fin pterygiophore subsequent to haemal spine of vertebra 23 (n = 2) or 24 (n = 1). Dorsal-fin pterygiophores 7 (n = 3). Anal-fin pterygiophores 6 (n = 3). Branchiostegal rays 3 or 4, with number bilaterally asymmetrical in two specimens.

**Pigmentation in preservative:** Specimens nearly entirely white at present, due to postmortem fading. Description below based on condition prior to fading. Body mostly white. Irregular row of internal dark chromatophores along vertebral column in caudal peduncle, irregularly outlining individual vertebrae. Large dark dots irregularly spaced along dorsal and ventral profiles of caudal peduncle, extending along bases of dorsal and anal fins and sometimes also along dorsum. Series of peritoneal dark chromatophores on dorsal limit of abdominal cavity, near border of hypaxial series, especially pronounced on posterior half of abdomen. Head with intense dark pigmentation (Fig. 3A) contrasting with mostly white body. Main dark field on head formed by brain pigment visible by transparency on posterior part of neurocranium, with two narrow convergent fields extending anteriorly and meeting between eyes. Integumentary pigment covering opercular odontodophore and region immediately surrounding it, with very dark narrow band along ventral margin of opercular periodontodal fold extending anteriorly alongside dorsal margin of interopercular periodontodal fold, and further anteriorly to approximately vertical through middle of eye. Separate irregular dark field anteroventral to eye. Few dark spots on anterior portion of dorsal surface of pectoral-fin base.

**Etymology:** The name is from Zoroastrian religion, the oldest monotheism, and refers to Angra Mainyu (Ahriman in Persian), enemy of Ahura Mazda, creator of the universe. Ahriman is the maker of snakes, demons and all things evil from a human standpoint (thus, presumably also candirus) and is approximately equivalent to, and probably historical ancestor of, the devil in Abrahamic mythology.

**Geographical distribution:** *Paracanthopoma ahriman,* is known from the upper río Orinoco in Venezuela (Fig. 20).

**Remarks:** This species shows the most constant vertebral number in *Paracanthopoma,* with 10 examined specimens all with 45 vertebrae.

### *Paracanthopoma alleynei*
### (Henschel, Bernt, Baskin, Schmidt, Lujan, 2021)
### (Fig. 8)

*Paracanthopoma* sp. 2 – Wosiacki & de Pinna, 2007: 73 [catalog].
*Paracanthopoma parva* [*non* Giltay 1935] – Schmidt, 1993 [in part, only specimen AMNH 72898, later designated as holotype of *Paravandellia alleynei;* occurrence in Essequibo drainage, Guyana; photograph of live specimen (Fig. 2)].
*Paravandellia alleynei* Henschel, Bernt, Baskin, Schmidt, Lujan, 2021b: 7, figs. [holotype: AMNH 72898, 26.0 mm SL; Guyana: Region 7 (Cuyuni-Mazaruni): Confluence of Mazaruni and Cuyuni rivers at Kartabo Point, Essequibo River basin, 06°22′56″N, 58°41′36″W, col., K. Schmidt, R. Schmidt and A. Pappantoniou, 10 Jul 1983; paratype: AMNH 72899 SW, 1 ex (c&s), 22.0 mm SL; collected with holotype; actually represents *Pc. parva*].

**Material examined**

**Type material:** AMNH 72898, 1 ex, holotype of *Paravandellia alleynei,* 26.0 mm SL, Guyana, Region 7 (Cuyuni-Mazaruni), Confluence of Mazaruni and Cuyuni rivers at Kartabo Point, Essequibo River basin (06°22′56″N, 58°41′36″W), col., K. Schmidt, R. Schmidt and A. Pappantoniou, 10 Jul 1983.

**Non-type material (all from Brazil):** INPA 16555 (mixed with 2 ex of *Pc. parva*), 6 ex, 18.9-23.1 mm SL, Brazil, Roraima, Boa Vista, Maracá, rio Branco, col.,

O. Bitar, May 1988; MZUSP 103052, 5 ex (3 c&s), 18.6-22.6 mm SL, collected with INPA 16555; LIRP 7399, 13 ex, 10.1-17.8 mm SL, Roraima, Boa Vista, rio Uraricoera at Localidade de Alagadiço (rio Branco drainage) (03°22′30″N, 60°35′43″W), col., A. Datovo, 16 Feb 2007; LIRP 7412, 1 ex, 10.1 mm SL, Roraima, Boa Vista, rio Uraricoera at Localidade de Alagadiço (rio Branco drainage) (03°22′30″N, 60°35′43″W), col., M. Carvalho & A. Datovo, 16 Feb 2007; LIRP 12697, 14 ex, 11.4-19.1 mm SL, Roraima, Boa Vista, rio Uraricoera at Localidade de Alagadiço (rio Branco drainage) (03°22′30″N, 60°35′43″W), col., A. Datovo & M. Carvalho 16 Feb 2007; LIRP 12698, 1 ex, 16.7 mm SL, Pará, Jacareacanga, rio Teles Pires [= rio São Manuel] (08°51′28″S, 57°25′10″W), col., M. Carvalho & A. Datovo, 04 Dec 2005 (mixed with 2 ex of *Pc. irritans*); LIRP 12699, 1 ex, 17.6 mm SL, Mato Grosso, Apiacás, rio Teles Pires [= rio São Manuel] close to Santa Rosa lodge (08°51′49″S, 57°24′38″W), rio Tapajós drainage, col., M. Carvalho, 03 Dec 2005 (mixed with 2 ex of *Pc. irritans*); NUP 7525, 1 ex, 23.6 mm SL, Mato Grosso, Aripuanã, Serra do Expedito, unnamed creek tributary to rio Praia Grande (rio Madeira basin) (10°02′51″S, 59°23′21″W).

**Diagnosis:** Distinguished form all congeners except *Pc. vampyra* by the presence of eleven median premaxillary teeth (vs. either three to nine or 13 and more); by four to six scalpelloid teeth (decreasing in size laterally) stacked in parallel at the distal end of the premaxilla (vs. scalpeloid teeth one or two, equal in size when two); by the presence of one or two conical teeth on the premaxilla (inserted basally relative to distal scalpelloid teeth) (vs. no conical teeth on premaxilla); by the long and ventrally-flat, almost spatulate, snout (vs. snout not pronouncedly spatulate). Distinguished from *Pc. vampyra* by the bilobed or concave caudal fin (vs. truncate or convex); the fewer procurrent caudal-fin rays (14 to 19 dorsally and ventrally) not forming prominent expansions on caudal peduncle (vs. 22 to 27 dorsal and 21 to 25 ventral, forming large expansions along most of caudal peduncle, which as a consequence is spatulate in shape); the pectoral fin broadly triangular in shape, with rays not markedly differing in length (vs. fin pointedly triangular in specimens 15 mm SL or larger, with rays steeply decreasing in size posteriorly); the presence of scattered dark spots on lateral surface of abdominal wall (vs. absence of dark pigmentation on abdomen); the mostly round mesethmoid cornua (vs. strongly angulate); the long and slender premaxilla (vs. short and thick); the longer snout (39.3-43.1; vs. 35.3-37.6% HL); the short broad parasphenoid, its length less than twice its maximum width (vs. parasphenoid elongate, its length 2.5-3.5 times its maximum width), and the concave anterior margin of the supraoccipital, not extending anteriorly beyond transverse line through articulation with sphenotic (vs. anterior margin of supraoccipital irregularly straight, extending well anteriorly to transverse line through articulation with sphenotic).

**Description:** Morphometric data for the holotype and paratypes are provided in Table 2. Body moderately elongate (HL 16.9-18.8% SL). Cross-section of body slightly broader than deep at pectoral-fin insertion and increasingly compressed posterior to that point, tapering to caudal fin. Dorsal profile of body gently convex from head to origin of dorsal fin. (Fig. 8) Dorsal and ventral profiles of caudal peduncle straight and converging towards midline along anterior half and straight or slightly convex and diverging along posterior half, corresponding to area of procurrent caudal-fin rays, with overal effect of gently concave dorsal and ventral margins (Fig. 8). Caudal peduncle narrow, not markedly expanded by procurrent rays. Ventral profile of body straight at pectoral-fin origin and then gently convex until pelvic-fin origin. Myotomes and longitudinal skeletogenous septum clearly visible through thin integument along whole body. Axillary gland small and narrow, elongate in shape, its anterior end adpressed to dorsoposterior margin of muscular pectoral-fin base, extending posteriorly to beyond margin of adpressed pectoral fin (but no specimens with full gland, making its profile difficult to determine precisely). Large, round or oval, axillary-gland pore located approximately at vertical through anterior third of pectoral fin, sometimes immediately posterior to vertical through end of pectoral-fin base.

Dorsal profile of head continuous with that of dorsum (Fig. 8), its origin sometimes indicated by slight constriction of anterior end of epaxial musculature. Head much longer than broad (head width 60.5-63.9% HL), snout broad and very long, parabolic with continuous round anterior margin. Head muscles not entering skull roof. Head strongly depressed (Figs. 8, 9) (head depth 32.7-35.7% HL) with dorsal profile gently convex, nearly straight, to tip of snout. Ventral profile of head straight, flattened. Eye large (12.4-14.9% HL), without free orbital rim, located dorsolaterally on head and directed dorsolaterally, with pronounced dorsal component (Fig. 8). Integument over eye thin and transparent. Middle of eye almost exactly at middle of HL, interorbital width approximately 75% of longitudinal diameter of eye. Eyelens occupying most of lateral surface of eye and either entirely unconstricted by iris or constricted only marginally, with large round pupil, in specimens examined. Anterior nostril small, surrounded by short tubule of integument produced posteriorly into small pointed process (Fig. 9), with double elastin cores. Anterior internarial width slightly larger than interorbital. Posterior naris slightly larger than anterior one, round or triangular in shape, adjacent ot mesial margin of eye and partly occluded by anterior flap of integument. Posterior naris positioned anteromesially to eye, their middle posterior to transverse line through anterior margin of eyes. Posterior internarial width narrower than interorbital nd approximately equal to diameter of one nostril.

Opercular odontodophore large and elongate, dorsolaterally located on head, on dorsal half of head depth in lateral view, anterodorsally to pectoral-fin base (Figs. 8, 9). Opercular odontodes 12 or 13, arranged in four irregular vertical rows of three or four. Main axis of opercular odontodes oriented horizontally in lateral view, with distal portion of larger ones curved dorsoposteriorly. Few caps

of replacement odontodes interspersed with mature ones. Opercular periodontodal fold well-differentiated but small, extending only shortly beyond tips of odontodes. Interopercular odontodophore slightly larger than opercular one, located ventrolaterally on head, immediately ventral to horizontal through origin of pectoral fin, with 12 to 14 odontodes closely positioned in single row or two partly imbricated rows. Interopercular odontodo-



**Figure 8.** *Paracanthopoma alleynei,* MZUSP 103052, 21.6 mm SL, Brazil, Roraima, Boa Vista, Maracá, Rio Branco. (A) Lateral view of body; (B) Dorsal view of head; (C) ventral view of head.
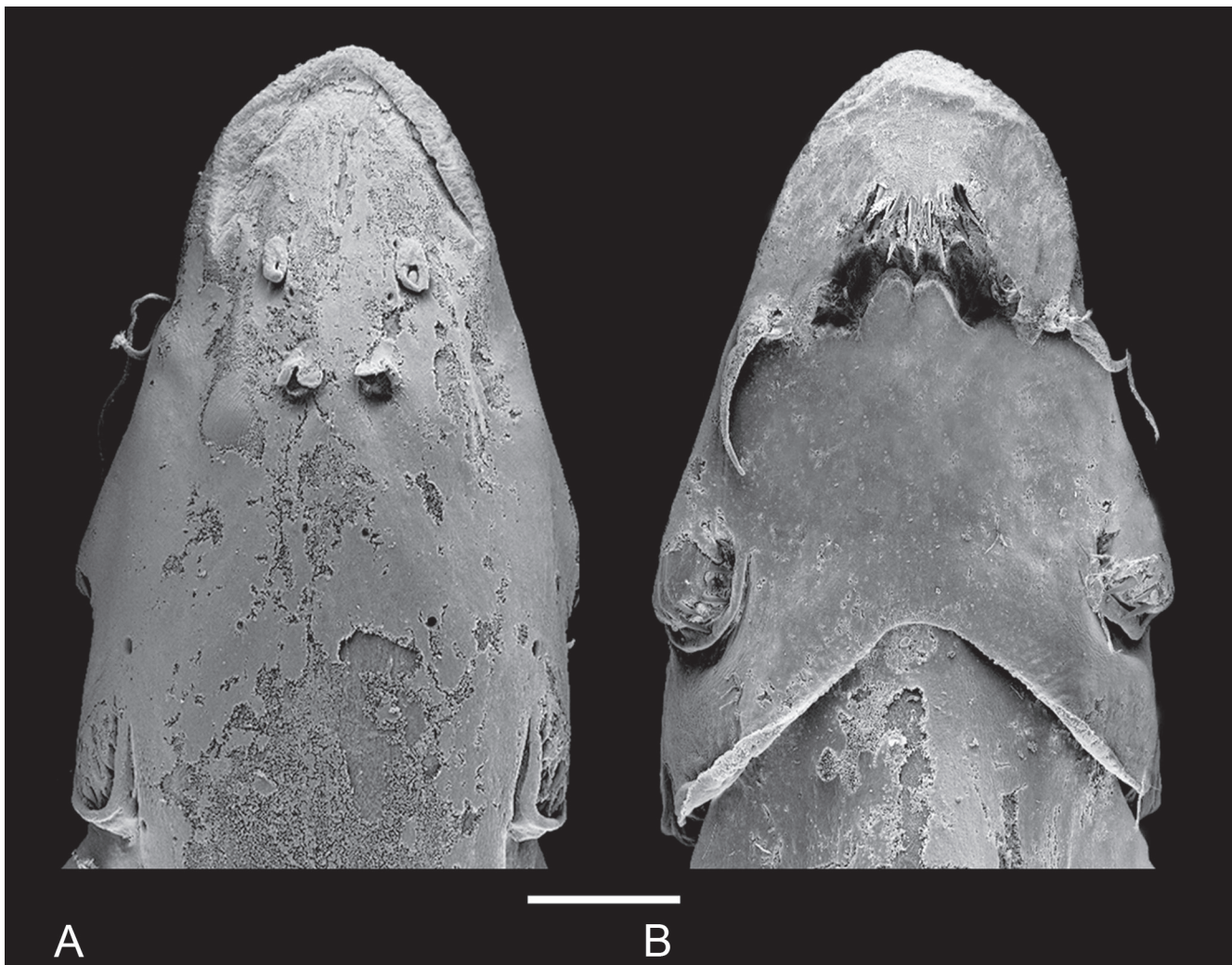


**Figure 9.** *Paracanthopoma alleynei,* INPA 16555, SEM images of head. (A) Dorsal; (B) Ventral. Scale bar = 500 μm.

**Table 2.** Morphometric data of *Paracanthopoma alleynei*. Head subunits were obtained with an ocular micrometer and therefore as projections. **Abbreviations:** min = minimum value; max = maximum value; n = number of specimens; SD = standard deviation.

|  | n | min | max | Mean | SD |
|---|---|---|---|---|---|
| Standard length (mm) | 5 | 20.0 | 21.2 | 20.7 |  |
| **Percentages of SL** |  |  |  |  |  |
| Total length | 5 | 1.1 | 1.1 | 1.1 | 0.0 |
| Body depth | 5 | 10.0 | 12.5 | 11.4 | 0.9 |
| Caudal peduncle length | 5 | 17.9 | 20.0 | 19.0 | 1.0 |
| Caudal peduncle depth | 5 | 5.8 | 6.9 | 6.4 | 0.4 |
| Predorsal length | 5 | 70.0 | 73.8 | 72.2 | 1.4 |
| Preanal length | 5 | 70.6 | 74.4 | 73.0 | 1.4 |
| Prepelvic length | 5 | 64.4 | 67.3 | 66.1 | 1.2 |
| Dorsal-fin base length | 5 | 6.4 | 9.4 | 7.7 | 1.1 |
| Anal-fin base length | 5 | 6.1 | 6.9 | 6.4 | 0.3 |
| Pectoral-fin length | 5 | 10.6 | 12.8 | 11.6 | 1.0 |
| Head length | 5 | 16.9 | 18.8 | 17.7 | 0.8 |
| **Percentages of HL** |  |  |  |  |  |
| Head width | 5 | 60.5 | 63.9 | 62.0 | 1.4 |
| Head depth | 5 | 32.7 | 35.7 | 34.4 | 1.1 |
| Pectoral-fin length | 5 | 61.4 | 67.2 | 64.7 | 2.4 |
| Interorbital | 5 | 10.5 | 13.0 | 11.7 | 0.9 |
| Eye diameter | 5 | 12.4 | 14.9 | 14.3 | 1.1 |
| Snout length | 5 | 39.3 | 43.1 | 41.0 | 1.4 |
| Mouth width | 5 | 17.1 | 18.6 | 17.9 | 0.6 |
| Anterior internarial width | 5 | 15.0 | 19.1 | 16.8 | 1.6 |
| Posterior internarial width | 5 | 4.1 | 6.1 | 5.1 | 0.8 |

phore approximately equidistant between opercular one and eye. Interopercular periodontodal fold well-differentiated, roundish and extending only shortly beyond tips of odontodes. Epiodontodeal velum thin, covering entire length of odontodes.

Mouth inferior (ventral), strongly flattened ventrally (Figs. 8, 9). Each premaxilla with 4 to 6 small scalpelloid teeth attached to its distal tip and disposed in peculiar parallel and aligned arrangement (Figs. 4B, 10). Scalpelloid teeth progressively larger mesially, deeply hidden in labial tissue and difficult to expose in preserved specimens without damage to soft tissue. Single large conical tooth at anteriormost point of premaxilla (Figs. 4B, 10), corresponding to angle at midlength of bone, its axis mostly straight, directed ventrally, with tip gently curved posteriorly. Upper lip broad, continuous with ventral surface of snout. Median premaxilla large, with 11 teeth disposed in two irregular curved rows (Figs. 4B, 10), anterior one with three teeth on each side (separated by median gap) and posterior one with two teeth on each side and one in middle. All teeth posteriorly oblique to ventral surface of median premaxilla at base and curved further posteriorly at distal pungent portion, those on lateral regions of median premaxilla also with lateral component. All median premaxillary teeth strongly laterally compressed basally. Three to five replacement tooth caps posterodorsally to mature dentition. Median premaxillary velum absent or very reduced. Hypodontal pad of median premaxilla broad, occupying entire upper jaw. Lower jaw narrow, composed mostly of narrow and elongated dentary lobes, anteriorly round and continuous with mental

region posteriorly (Fig. 8). Jaw cleft short and strongly directed posteriorly, its lateral portion almost parallel to longitudinal axis. Dentary diastema narrow and well-defined, angulate. Dentary teeth 4, closely packed at mesial end of dentary and disposed as two ventral and two dorsal ones, not exactly aligned (Figs. 4B, 10). Dentary teeth long, their axis anteriorly-directed at base, but strongly curved dorsally at distal third.

Branchiostegal velum forming large, continuous, hyperbolic and posteriorly concave, free fold across whole of mental region (Figs. 8, 9). Dorsal portion of velum reaching, but not covering, anterior margin of pectoral-fin base. Branchial openings small, spanning approximately area between ventral margin of opercular odontodophore and mid-depth of interopercular oontodophore. Maxillary barbel long and thin, reaching slightly beyond base of anteriormost interopercular odontodes. Posterior point of its base anterior to vertical through anterior margin of eye in lateral view. Mesial (or ventral) part of maxillary-barbel base inserting directly onto corner of mouth without intervening membranous outgrowth. Rictal barbel small but well-differentiated, located mesially to base of maxillary one and approximately one-fifth of its length. Nasal barbel vestigially represented by posterior elongated portion of fold around anterior naris described above, with double internal elastin core.

Lateral line short and straight, extending alongside dorsal margin of anterior portion of axillary gland. Terminal lateral-line pore immediately dorsal to axillary gland opening. Very short secondary branch splitting off ventrally from proximal portion of canal, with corresponding pore opening anterior to midlength of main canal. Single long lateral-line tubule, straight in shape, extending for approximately 70% of main canal posterior to bifurcation.

Pectoral fin short (61.4-67.2% HL), triangular in shape and with truncate or gently convex margin, its base on ventral side of body. Pectoral-fin rays i + 5, not differing markedly in length. Pelvic fins small, rectangular with convex margin, closely positioned at base, with i + 4 rays. Pelvic splint present. Origin of pelvics well anterior to vertical through origin of dorsal-fin, entirely covering anus and urogenital openings and ending just short of anal-fin origin. Dorsal fin triangular with round apex, with gently convex or straight distal margin and ii + 7 rays, plus 5 procurrent ones. Anal fin smaller than dorsal one, roughly rectangular in shape, with distal margin gently convex anteriorly and concave posteriorly and ii + 5 fin rays, plus 4 or 5 procurrent ones. Origin of anal fin posterior to vertical through origin of dorsal-fin. Caudal fin bilobed or concave, deeper than maximum depth of caudal peduncle when spread. Principal caudal-fin rays 6 + 7. Procurrent caudal-fin rays 14 to 19 both dorsally and ventrally.

Vertebrae 38 (n = 3) or 39 (n = 8; holotype). First dorsal-fin pterygiophore subsequent to neural spine of vertebra 21 (n = 3). First anal-fin pterygiophore subsequent to haemal spine of vertebra 22 (n = 1) or 23 (n = 2). Dorsal-fin pterygiophores 8 (n = 3). Anal-fin pterygiophores 6 (n = 3). Branchiostegal rays 3.
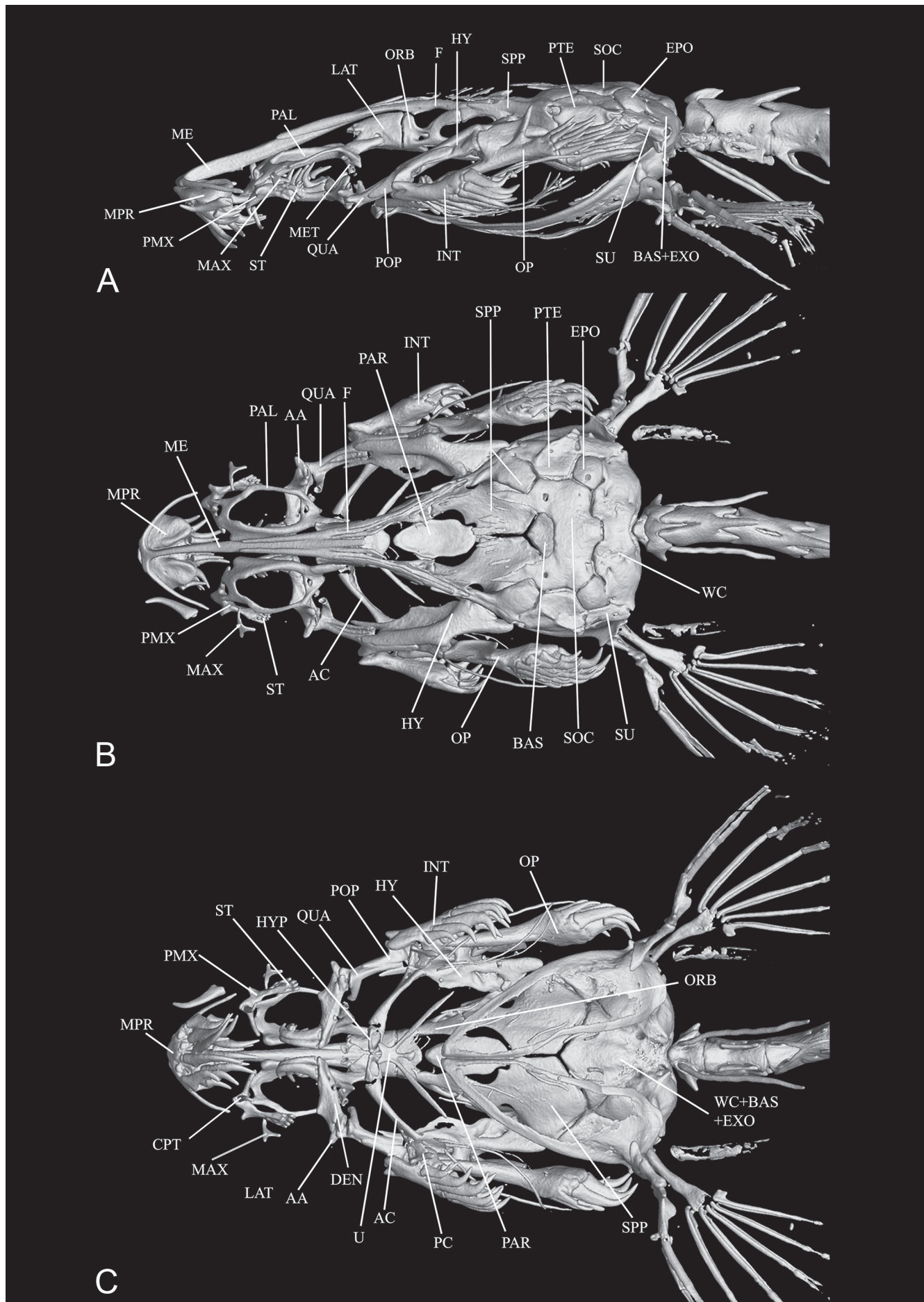
**Figure 10.** *Paracanthopoma alleynei,* MZUSP 103052, CT scan images of head skeleton, (A) Lateral; (B) Dorsal; (C) Ventral.

**Pigmentation in preservative:** Body almost entirely white. Scattered dark spots over lateral surface of abdominal wall, not extending dorsally onto myotomal region. Posterior half of neurocranium with irregular dark brain pigment seen by transparency. Sparse fields of chromatophores between eyes and nostrils, anterolaterally to eyes and dorsal to maxillary barbel base. Isolated spots near base of dorsal fin and on basal portion of caudal fin and hypural plate.

**Geographical distribution:** *Paracanthopoma alleynei* has been recorded from uplands in both Brazilian and Guiana shields, in the rio Essequibo, upper rio Branco, rio Teles Pires and rio Aripuanã basins (Fig. 20).

**Remarks:** The paratype of *Pc. alleynei* (AMNH 72899SW) belongs to a species different from the holotype. Examination of that specimen reveals that it has an epiphyseal comissure of the latero-sensory canal opening as a single median s6 pore; an anteriorly-produced supraoccipital extending approximately to the epiphyseal comissure; nine median premaxillary teeth (three of which currently fallen off but indicated by sockets); one or two scalpelloid teeth on the premaxilla (inferred by sockets), no conical premaxillary teeth; the interopercle closer to the opercle than to the lower jaw articulation; a very small ascending process of the opercle; a thick-walled palatine, with a relatively narrow central fenestra; the palatine cartilage for the articulation of the maxilla at the midlength of the lateral margin of the bone; and the mesial margin of the palatine produced mesially at its midlength. All those characteristics contrast with conditions in the holotype and remaining specimens of *Pc. alleynei* (no epiphyseal commissure and double s6 pores; anteriorly concave supraoccipital; 11 median premaxillary teeth; four to six scalpelloid teeth; one or two conical premaxillary teeth; interopercle closer to lower-jaw articulation than to opercle; large ascending process of the opercle; thin-walled palatine with a central fenestra occupying nearly the entire area of the bone; the palatine cartilage for the articulation of the maxilla at the anterior half of the lateral margin of the bone; and the mesial margin of the palatine continuous, not produced mesially). Those characters show that the paratype is a very different species from the holotype, and also that it belongs to a disjunct subgroup of the genus, the *parva*-clade (*see* Discussion below). The paratype specimen was first reported in Schmidt (1993, then bearing the number AMNH 72898SW) and was cleared and stained on the occasion of that publication. As then, the specimen is today well-stained for cartilage but not for bone. It has lost the external portions of all fins, caudal- and pelvic-fin supports, part of the mesethmoid cornua, most odontodes, all scalpelloid teeth and some median premaxillary teeth. Nonetheless, the skeletal features mentioned above can still be clearly confirmed. Although the condition of the specimen does not allow examination of all relevant details, it most likely belongs to *Pc. parva*, or a very similar form. Illustrations of the specimen and accompanying text in Schmidt (1993, figs. 1, 2) are suf-

ficient to show that it is a taxon different from the holotype, such as the epiphyseal comissure opening as a single median pore. The description of *Pc. alleynei* (Henschel *et al.,* 2021: 10) mentions the latter condition as typical for the species, an observation presumably based on the paratype only because it does not correspond to the holotype (with double pores). Both the holotype and paratype of *Pc. alleynei* have been collected in the same locality and date, but from different hosts (the former from *Brachyplatystoma vaillantii* and the latter probably from *Doras micropoeus*). Co-occurrence of *Pc. alleynei* and *Pc. parva* is previously recorded in at least one other sample (INPA 16555, from the rio Branco).

## *Paracanthopoma cangussu* Henschel, Katz & Costa, 2021 (Fig. 11)

*Paracanthopoma cangussu* Henschel, Katz & Costa, 2021a: 3, figs. 1-2 [holotype: UFRJ 12696, 11.8 mm SL; type locality: Brazil: Tocantins State: Pium Municipality: sandbank at a beach in the Bananal Island, Javaés River drainage, Araguaia River basin, 09°59′52″S, 50°06′49″W].

### Material examined

**All from Brazil:** INPA 16558, 3 ex, 14.4-16.2 mm SL, no data; MZUSP 94982, 15 ex, 14.2-17.5 mm SL, Brazil, Parque Estadual do Cantão, rock pool in rio Araguaia, col., unknown, Jan 2006; MZUSP 86236, 39 ex (7 mol), 12.2-14.6 mm SL, Mato Grosso, Cocalinho, Corixo da Saudade (= Corixinho, trib. to rio Araguaia), 25 km NW of Cocalinho by road MT-326 (14°17′20.6″S, 51°09′12.1″W), col., O. Oyakawa, 13 Oct 2004; MZUSP 86250, 8 ex (2 c&s), 12.5-17.3 mm SL, Mato Grosso, Cocalinho, rio Cristalino (trib. to rio Araguaia), 47 km from Cocalinho by road MT-326 (14°12′45″S, 51°18′21″W), col., J.L. Birindelli *et al.,* 14 Oct 2004; MZUSP 86257, 6 ex, 12.4-14.1 mm SL, Mato Grosso, Cocalinho, Ribeirão Água Preta (trib. to rio Cristalino, rio Araguaia drainage), approx. 79 km NW of Cocalinho by road MT-326 (14°08′57″S, 51°32′21″W), col., C. Moreira, 14 Oct 2004; MZUSP 86271, 40 ex (4 c&s), 12.0-15.3 mm SL, Mato Grosso, Cocalinho, Corixão do Meio (trib. to rio Cristalino; rio Araguaia drainage), approx. 12 km NW of Cocalinho, at road MT-326 (14°11′14″S, 51°14′58″W), col., MZUSP team, 14 Oct 2004; MZUSP 105899, 1 ex, 13.0 mm SL, from MZUSP 86271.

**Diagnosis:** Distinguished form all congeners except *Pc. ahriman, Pc. capeta,* and *Pc. irritans* by the presence of five median premaxillary teeth (some of which often in replacement) (vs. either three or 9 to19 in total). The species is further distinguished from all congeners, except *Pc. ahriman* and *Pc. irritans,* by the broad and long ventral portion of the opercular periodontodal fold, forming a lateral ridge of integument extending anteriorly to the dorsal margin of the interopercular odontodophore (vs. ventral part of fold not anteriorly extend-

**Figure 11.** *Paracanthopoma cangussu,* MZUSP 105899, 13.0 mm SL, Brazil, Mato Grosso, Cocalinho, Corixão do Meio. (A) Lateral view of body; (B) Dorsal view of head; (C) ventral view of head.

ed, independent from interopercular odontodophore). Distinguished from *Pc. ahriman* by the longer caudal peduncle (21.8-24.0% SL, vs. 19.2-21.5); by the shorter predorsal length (66.7-71.3% SL; vs. 71.8-76.7); by the narrower anterior internarial width (13.3-17.1% HL; vs. 17.6-20.2); by the narrowersmaller posterior internarial width (8.1-10.0% HL; vs. 10.1-11.4). Distinguished from *Pc. capeta* by the longer caudal peduncle (21.8-24.0% SL; vs. 18.0-20.4); by the deeper caudal peduncle (10.8-13.0% SL; vs. 7.0-8.8); by the longer predorsal and preanal lengths (66.7-71.3 and 68.6-70.3% SL; vs. 72.2-74.1 and 71.8-75.9, respectively); by the wider head (75.7-83.3% SL; vs. 68.0-72.0); by the smaller eye (14.7-16.2% SL; vs. 16.7-21.7); by the mouth cleft directed more strongly posteriorly than laterally (vs. opposite); by the roundish median premaxilla (vs. trapezoidal with nearly straight anterior margin). Distinguished from *Pc. irritans* by having 5 + 5 principal caudal-fin rays (vs. 6 + 6); by the deeper caudal peduncle (10.8-13.0% SL; vs. 8.3-10.6); by the wider posterior internarial width (8.1-10.0% HL; vs. 3.3-5.5); by more numerous procurrent caudal-fin rays (28-30 dorsally and 27-29 ventrally, vs. 19-25 dorsally and 21-25 ventrally); by the deepest portion of the caudal peduncle (corresponding to longest procurrent caudal-fin rays) approximately at its half-length (vs. caudal peduncle progressively deeper to base of caudal fin); by the dorsal and ventral profiles of caudal peduncle posteriorly strongly converging towards base of caudal fin, forming pronounced concave regions clearly delimiting beginning of caudal fin (vs. dorsal and ventral profiles of caudal peduncle gently continuous with caudal fin, with only slight depression in some specimens); by the interorbital larger than eye diameter (vs. smaller).

**Description:** Morphometric data for the holotype and paratypes are provided in Table 3. Body moderately elongate (HL 16.7-18.0% SL). Cross-section of body slightly broader than deep at pectoral-fin insertion and increasingly compressed posterior to that point, tapering to caudal fin. Dorsal profile of body gently convex, nearly straight, from head to origin of dorsal fin (Fig. 11). Dorsal and ventral profiles of caudal peduncle strongly convex posterior to ends of dorsal and anal fins, spatulate, expanded by procurrent caudal-fin rays (Fig. 11). Dorsal and ventral profiles of caudal peduncle strongly converging towards base of caudal fin, forming pronounced concave regions clearly delimiting beginning of caudal fin. Ventral profile of body straight to pectoral-fin base and then gently convex until pelvic-fin origin, with some specimens with distented abdomens due to gut contents. Myotomes and longitudinal skeletogenous septum clearly visible through thin integument along whole body. In few specimens, axillary gland full with secretion, very large and protruding markedly on surface of body. In majority of specimens, gland empty, much smaller and less conspicuous. When full, anterior end of gland surrounding dorsoposterior, ventral and posterior margins of muscular pectoral-fin base, as thick corselet, extending posteriorly beyond margin of adpressed pectoral fin for distance equivalent to fin length. Gland narrowing to blunt posterior end, extending along limit between hypaxial musculature and abdominal cavity, its large round or oval pore located at middle of pectoral-fin length or slightly anterior to that, in dorsal view. Condition of gland posterior to pore evidently related to amount of secretion stored at time of preservation.

Dorsal profile of head continuous with that of dorsum (Fig. 11), its origin indicated by slight constriction of anterior end of epaxial musculature. Head longer than broad (head width 75.7-83.3% HL), snout broad, parabolic with a continuous round anterior margin. Head muscles not entering skull roof. Head moderately depressed (head depth 33.3-41.7% HL) with dorsal profile gently convex, nearly straight, with curvature accentuated close to tip of snout. Ventral profile of head straight, flat. Eye small (14.7-16.2% HL), without free orbital rim, located dorsolaterally on head and directed dorsolaterally, with

**Table 3.** Morphometric data of *Paracanthopoma cangussu.* Head subunits were obtained with an ocular micrometer and therefore as projections. **Abbreviations:** min = minimum value; max = maximum value; n = number of specimens; SD = standard deviation.

| | n | min | max | Mean | SD |
|---|---|---|---|---|---|
| Standard length (mm) | 6 | 13.0 | 13.8 | 13.3 | |
| **Percentages of SL** | | | | | |
| Total length | 6 | 1.1 | 1.1 | 1.1 | 0.0 |
| Body depth | 6 | 12.7 | 15.2 | 13.9 | 1.0 |
| Caudal peduncle length | 6 | 21.8 | 24.0 | 22.9 | 0.7 |
| Caudal peduncle depth | 6 | 10.8 | 13.0 | 11.8 | 0.9 |
| Predorsal length | 6 | 66.7 | 71.3 | 69.1 | 1.7 |
| Preanal length | 6 | 68.6 | 70.3 | 69.4 | 0.6 |
| Prepelvic length | 6 | 62.7 | 64.4 | 63.6 | 0.7 |
| Dorsal-fin base length | 6 | 6.7 | 7.0 | 6.9 | 0.1 |
| Anal-fin base length | 6 | 6.8 | 7.9 | 7.2 | 0.5 |
| Pectoral-fin length | 6 | 9.7 | 12.0 | 11.1 | 0.8 |
| Head length | 6 | 16.7 | 18.0 | 17.2 | 0.5 |
| **Percentages of HL** | | | | | |
| Head width | 6 | 75.7 | 83.3 | 79.6 | 2.6 |
| Head depth | 6 | 33.3 | 41.7 | 37.6 | 2.9 |
| Pectoral-fin length | 6 | 62.5 | 70.0 | 66.4 | 2.8 |
| Interorbital | 6 | 14.3 | 16.7 | 15.5 | 0.8 |
| Eye diameter | 6 | 14.7 | 16.2 | 15.6 | 0.5 |
| Snout length | 6 | 34.7 | 38.6 | 36.4 | 1.7 |
| Mouth width | 6 | 21.3 | 26.4 | 24.6 | 1.8 |
| Anterior internarial width | 6 | 13.3 | 17.1 | 15.6 | 1.4 |
| Posterior internarial width | 6 | 8.1 | 10.0 | 9.5 | 0.7 |

pronounced lateral component (Fig. 11). Integument over eye thin and transparent. Middle of eye slightly anterior to middle of HL. Interorbital larger than eye diameter. Eyelens unconstricted by iris in specimens examined. Anterior nostril small, surrounded by short tubule of integument produced posteriorly into well-defined pointed nasal barbel, with double elastin cores. Anterior internarial width approximately equal to interorbital. Posterior naris as large as anterior one, adjacent to anteromesial margin of eye and partly occluded by anterior flap of integument. Anterior margin of posterior naris leveled or slightly anterior to transverse line through anterior margin of eyes. Posterior internarial width narrower than interorbital and larger than diameter of one nostril.

Opercular odontodophore well exposed on dorsolateral surface of head, on dorsal half of head depth in lateral view, anterodorsally to pectoral-fin base. Opercular odontodes 6 to 9, closely positioned in more or less irregular roundish disposition, with two largest ones posteriorly. Main axis of opercular odontodes oriented horizontally in lateral view, with distal portions of larger posterior ones curved dorsoposteriorly. Opercular periodontodal fold well-differentiated but short, extending shortly beyond tips of odontodes, its ventral side extending anteriorly as broad straight or slightly convex ridge to dorsal margin of interopercular periodontodal fold. Interopercular odontodophore slightly smaller than opercular one, located ventrolaterally on head, immediately ventral to horizontal through origin of pectoral fin, with 8 or 9 odontodes closely positioned in two irregular, partly imbricating, rows. Interopercular odontodes larg-

er posteriorly, dorsal ones curved dorsoposteriorly and ventral ones curved ventroposteriorly. Interopercular odontodophore slightly closer to opercular one than to eye. Interopercular periodontodal fold of integument well-developed, roundish, extending well beyond tips of odontodes. Epiodontodeal velum thin and transparent, covering most of odontodes.

Mouth inferior (ventral). Each premaxilla with 1 or 2 scalpelloid teeth attached (in parallel when 2) to its distal tip (Figs. 4C, 12). Two tooth sockets always present, but one of them usually in process of replacement. Scalpelloid teeth deeply hidden in labial tissue and impossible to expose in preserved specimens without damaging soft tissue. No conical teeth on premaxilla. Upper lip very broad, continuous with ventral surface of snout (Fig. 11). Median premaxilla small, restricted to middle of upper jaw, with 5 teeth closely disposed in one row, with central tooth largest and two smaller ones on each side (Figs. 4C, 12). In most specimens, one or two teeth in process of replacement, but total count of five obvious by tooth sockets and relative position of attached teeth. Tooth bases disposed at approximately same transverse line, with lateral-most teeth slightly anterior to others. All teeth posteriorly oblique to ventral surface of median premaxilla at base and curved further posteriorly at distal pungent portion. Basal portion of all median premaxillary teeth strongly compressed laterally. Median premaxillary velum well-defined, semicircular, covering whole dentition when intact. Hypodontal pad of median premaxilla small, forming round mound following tooth distribution. Lower jaw narrow, composed mostly of short pointed dentary lobes, mostly confluent at midline, continuous with mental region posteriorly (Fig. 11). Jaw cleft short, oblique relative to longitudinal axis. Dentary diastema small and angulate. Dentary teeth 4 (when 3, replacement one in formation), closely packed at mesial end of dentary and disposed as two ventral and two dorsal ones, not exactly aligned (Figs. 4C, 12). Dentary teeth long and strongly curved, with ventral ones longer and with curvature positioned distally and dorsal ones shorter and with curvature approximately at midlength. All dentary teeth with their axis anteromesially-directed at base, but strongly curved dorsally at distally.

Branchiostegal velum forming large free fold, in continuous posteriorly concave arc across whole of mental region (Fig. 11). Dorsal portion of fold reaching, but not covering, anterior margin of pectoral-fin base. Branchial openings small, spanning part of area between ventral margin of opercular odontodophore and mid-depth of interopercular odontodophore, anteroventrally to pectoral-fin base. Maxillary barbel very thin, especially distally, reaching to midlength of interopercular odontodophore. Posterior point of its base at, or slightly anterior to, vertical through anterior margin of eye in lateral view. Mesial (or ventral) part of maxillary-barbel base inserting directly onto corner of mouth without intervening membranous outgrowth. Rictal barbel small to vestigial, attached mesially to base of maxillary. Nasal barbel small but well differentiated, continuous with posterior portion of integument fold around anterior naris described above,
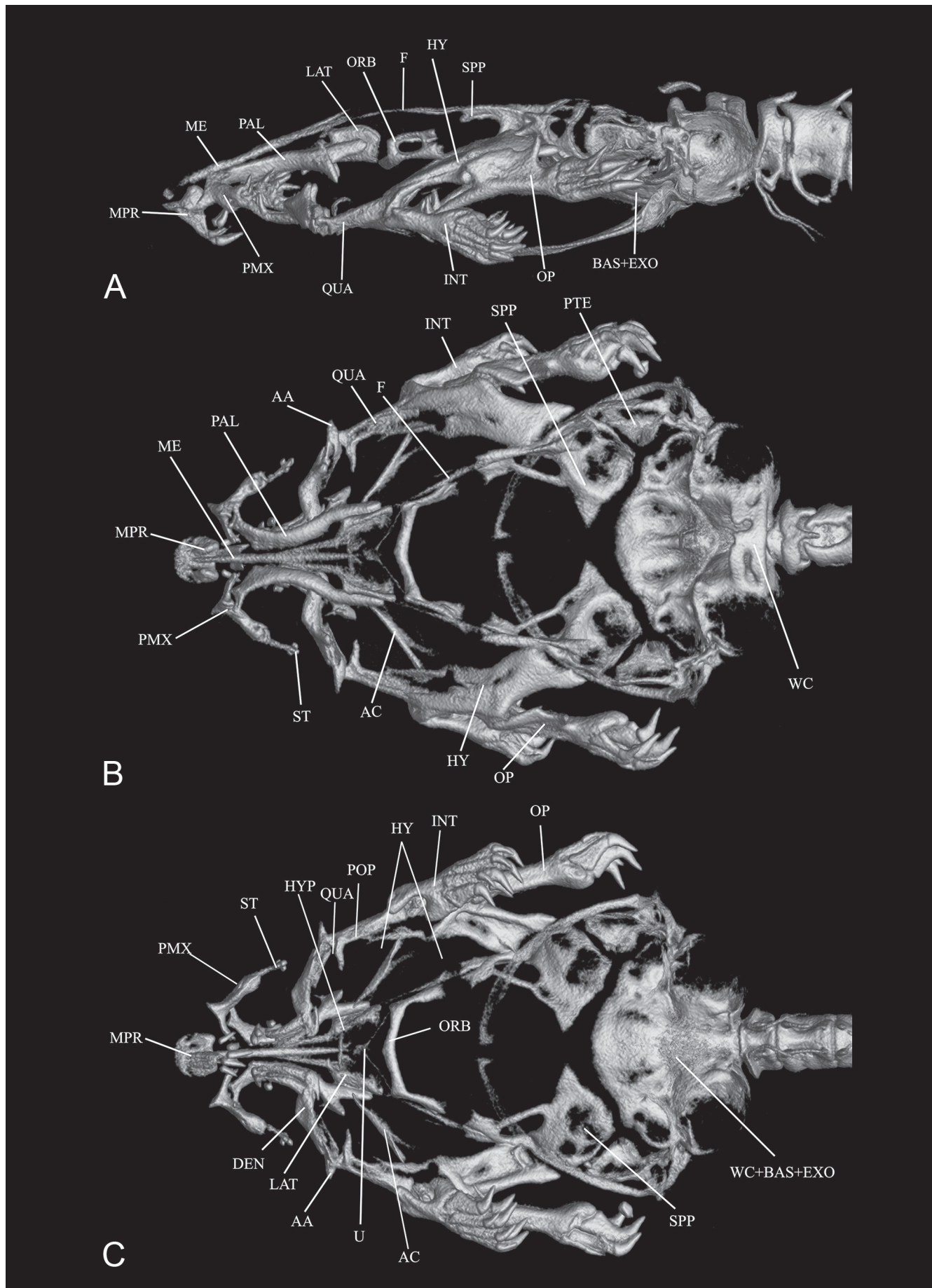
**Figure 12.** *Paracanthopoma cangussu,* MZUSP 105899, CT scan images of head skeleton. (A) Lateral; (B) Dorsal; (C) Ventral. Specimen poorly calcified, some structures not properly shown.

with double internal elastin core visible in cleared and stained specimens.

Lateral line very short, slightly curved dorsally distally, extending alongside dorsal margin of anterior portion of axillary gland. Terminal lateral-line pore dorsal to axillary gland opening. Very short secondary branch splitting off ventrally from proximal portion of main canal, with corresponding pore opening at approximately basal third of main canal. Single lateral-line tubule very poorly calcified, extending for most of main canal posterior to bifurcation.

Pectoral fin short (62.5-70.0% HL), with convex-truncate margin, its base on ventral side of body. Pectoral-fin rays i + 5 (i + 6 on one side of one specimen). Pelvic fin very small, close to each other at base, modally with i + 4 rays, (a few specimens with i + 3 or i + 5), with variable branching pattern ranging from all rays unbranched to maximum of four branched. Pelvic splint present. Origin of pelvics close to origin of anal fin, slightly anterior to vertical through origin of dorsal-fin, entirely covering anus and urogenital papilla and extending posteriorly to origin of anal fin. Posterior margin of pelvic fin round. Dorsal fin roughly rectangular-roundish, with gently convex distal margin. Dorsal-fin rays ii + 5 plus 3 or 4 procurrent ones. Anal fin similar in size and shape to dorsal fin but more roundish, modally with ii + 5 rays, plus 4 or 5 procurrent ones. Origin of anal fin at vertical through origin of dorsal fin. Caudal fin truncate with round corners, less deep than maximum depth of caudal peduncle. Principal caudal-fin rays 5 + 5. Procurrent caudal-fin rays 28 (n = 2), 29 (n = 3) or 30 (n = 1) dorsally and 27 (n = 2), 28 (n = 2) or 29 (n = 2) ventrally.

Vertebrae 42 (n = 1), 43 (n = 2) or 44 (n = 3). First dorsal-fin pterygiophore subsequent to neural spine of vertebra 21 (n = 3) or 22 (n = 3). First anal-fin pterygiophore subsequent to haemal spine of vertebra 21 (n = 1), 22 (n = 2) or 23 (n = 3). Dorsal-fin pterygiophores 6 (n = 1) or 7 (n = 5). Anal-fin pterygiophores 6 (n = 6). Branchiostegal rays 3.

**Pigmentation in preservative:** Body almost entirely white. Faint series of irregular dark spots along dorsal midline to origin of dorsal fin, bilaterally arranged in few specimens. Posterior part of caudal peduncle with irregular longitudinal stripe formed by internal chromatophores along vertebral column, with some dark spots also over hypural plate in some specimens. Dorsal half of abdomen with isolated dark chromatophores, especially visible in specimens with distended abdomens. Posterior half of neurocranium with irregular dark brain pigment seen by transparency, forming anteriorly concave rough pattern, extending anteriorly along edges of neurocranium as two lines sometimes extending as series of spots between eyes and nostrils and along mesethmoid. Intense irregular dark fields anteriorly to eyes, also extending ventrolaterally towards maxillary barbel base. Some specimens with few isolated chromatophores at base of opercular odontodophore. Internal pigmentation intense, with nearly entire vertebral column covered with dark chromatophores, especially concentrated on

bases of neural spines of trunk. Internal chromatophores also on dorsal surface of peritoneum and lateral surface of cardiac region.

**Geographical distribution:** Known so far from the rio Araguaia basin (Fig. 20).

## *Paracanthopoma capeta,* new species
### (Fig. 13)

**Holotype:** MZUSP 29154, 14.5 mm SL, Brazil, Amazonas, rio Negro, praia Mari-Mari, upstream from Barcelos and slightly above mouth of rio Cuiuni (approximately 00°32'S, 63°24'W), col., M. Goulding, 30 May 1979.

**Paratypes:** MZUSP 100144, 6 ex (2 c&s), 14.1-15.6 mm SL, collected with holotype.

**Diagnosis:** Distinguished from all congeners by the supraoccipital well-developed, its anterior margin extending transversely across the skull (vs. supraoccipital receded into deep concavity or produced anteriorly as median spike); by the extremely long, thread-like maxilla (vs. maxilla not thread-like); and by the single-row dentition disposed in a v-shape, with lateral teeth gradually more anteriorly and the central tooth inserted most posteriorly (vs. row or rows of teeth approximately aligned transversely). Distinguished from all congeners except *Pc. ahriman, Pc. cangussu,* and *Pc. irritans* by the presence of five median premaxillary teeth (one or two often in replacement) (vs. either three or 9 to19 in total). Distinguished from *Pc. ahriman* by the narrower head (head width 68.0-72.0% HL; vs. 80.7-87.6). Distinguished from *Pc. cangussu* by the shorter caudal peduncle (18.0-20.4% SL; vs. 21.8-24.0); by the less deep caudal peduncle (7.0-8.8% SL; vs. 10.8-13.0); by the longer predorsal and preanal lengths (72.2-74.1 and 71.8-75.9% SL; vs. 66.7-71.3 and 68.6-70.3, respectively); by the narrower head (68.0-72.0% SL; vs. 75.7-83.3); by the larger eye (16.7-21.7% SL; vs. 14.7-16.2). Distinguished from *Pc. irritans* by the narrower head (68.0-72.0% HL; vs. 73.3-76.9); by the mouth cleft directed more strongly laterally than posteriorly (vs. opposite); and by the median premaxilla trapezoidal with nearly straight anterior margin (vs. roundish).

**Description:** Morphometric data for the holotype and paratypes are provided in Table 4. Body short (HL 16.5-21.1% SL). Cross-section of body approximately as deep as broad at pectoral-fin insertion and increasingly compressed posterior to that point, tapering to caudal fin. Dorsal profile of body gently convex or straight from head to origin of dorsal fin (Fig. 13). Dorsal and ventral profiles of caudal peduncle gently convex posterior to dorsal and anal fins, moderately spatulate, expanded by procurrent caudal-fin rays (Fig. 13). Ventral profile of body straight at pectoral-fin base and then gently convex until pelvic-fin origin, with some specimens with greatly distended abdomens. Myotomes and longitudi-

nal skeletogenous septum clearly visible through thin integument along whole body. Axillary gland very large, elongate in shape, protruding markedly on surface of body when full with secretion, extending along limit between hypaxial musculature and abdominal cavity. Anterior end of gland surrounding dorsal, ventral and posterior margins of muscular pectoral-fin base, as thick corselet, extending posteriorly to beyond margin of ad-pressed pectoral fin. Posterior end of gland blunt and round, its large round or oval pore opening dorsally at its middle portion, approximately at vertical through half of pectoral- fin length. Condition of gland posterior to pore evidently related to amount of secretion stored.

Dorsal profile of head continuous with that of dor-sum (Fig. 13), its origin sometimes indicated by slight constriction of anterior end of epaxial musculature. Head longer than broad (head width 68.0-72.0% HL), snout broad, parabolic with a continuous round anteri-or margin. Head muscles not entering skull roof. Head moderately depressed (head depth 41.2-63.9% HL), with dorsal profile in lateral view straight until eye, then bend-ing ventrally and straight again to tip of snout. Ventral profile of head straight or slightly convex. Eye large (16.7-21.7% HL), without free orbital rim, located dorso-laterally on head and directed dorsolaterally, with pro-nounced lateral component (Fig. 13). Integument over eye thin and transparent. Middle of eye approximately at middle of HL, interorbital width almost equal to longi-tudinal diameter of eye. Eyelens constricted by iris only marginally, with large round or oval pupil in specimens examined. Anterior nostril small, surrounded by short

tubule of integument produced posteriorly into small pointed process (Figs. 13, 14), with double elastin cores. Conspicuous recess-like elongate depression immediate-ly posterior to base of anterior nostril, with plicate inner surfaces. Anterior internarial width slightly larger than interorbital. Posterior naris small, slightly larger than an-terior ones, roundish or triangular in shape, adjacent to mesial margin of eye and partly occluded by anterior flap of integument (Figs. 13, 14). Anterior margin of posterior naris posterior to transverse line through anterior margin of eye. Posterior internarial width narrower than interor-bital and 2-2.5 times diameter of one nostril.

Opercular odontodophore medium-sized and elon-gate, dorsolaterally located on head, on dorsal half of head depth in lateral view, anterodorsally to pectoral-fin base. Opercular odontodes 6 or 7, irregularly positioned with larger ones posteriorly. Main axis of opercular odontodes oriented horizontally in lateral view, with distal portions of larger posterior ones curved medi-odorsally. Two or three caps of replacement odontodes interspersed with mature ones. Opercular periodontodal fold well-differentiated, extending well beyond tips of odontodes. Interopercular odontodophore larger than, or as large as, opercular one, located ventrolaterally on head, at horizontal through origin of pectoral fin, with 6 or 7 odontodes closely positioned in one main pos-terior row with five odontodes, plus one or two smaler ones anteriorly. Interopercular odontodes progressiely larger posteriorly, with largest ones strongly compressed at base. Interopercular odontodophore slightly closer to opercular one than to eye. Interopercular periodon-todal fold of integument well-developed but narrow, roundish, extending shortly beyond tips of odontodes. Epiodontodeal velum poorly-differentiated, thin and transparent, irregularly covering most of odontodes.

Mouth inferior (ventral), flattened ventrally (Fig. 13). Each premaxilla with 1 or 2 large scalpelloid teeth (al-ways two tooth sockets) attached to its distal tip dis-posed in parallel (Figs. 4D, 15). Scalpelloid teeth deeply hidden in labial tissue and difficult to expose in pre-served specimens without damage to soft tissue. No conical teeth on premaxilla. Upper lip very broad, con-tinuous with ventral surface of snout. Median premaxilla small, occupying only central portion of upper jaw, with 5 teeth with insertions disposed in single v-shaped row (Figs. 4D, 15). Bases of teeth strongly off-set, with those of lateral-most teeth most anterior, with following teeth in-serted half-way to posterior margin of median premaxilla and central (largest) tooth posterior-most, inserted close to posterior margin of bone. All teeth posteriorly oblique to ventral surface of median premaxilla, with anterior one on each side also strongly inclined mesially. Distal pungent portion of lateral teeth curved posterolaterally, and of median one curved posteriorly. Basal portion of all median premaxillary teeth strongly compressed laterally. Two or three replacement tooth caps interspersed with mature dentition. Median premaxillary velum small, but covering most of tooth surace. Hypodontal pad of medi-an premaxilla small, roundish, occupying small area pro-portional to small median premaxillary dentition. Lower

**Table 4.** Morphometric data of *Paracanthopoma capeta*. Ranges, mean and SD include holotype. Head subunits were obtained with an ocular micrometer and therefore as projections. **Abbreviations:** min = minimum value; max = maximum value; n = number of specimens; SD = standard deviation.

| | n | holotype | min | max | mean | SD |
|---|---|---|---|---|---|---|
| Standard length (mm) | 5 | 14.5 | 14.0 | 18.3 | 15.6 | |
| **Percentages of SL** | | | | | | |
| Total length | 5 | 1.1 | 1.1 | 1.1 | 1.1 | 0.0 |
| Body depth | 5 | 15.8 | 13.5 | 15.8 | 15.1 | 1.0 |
| Caudal peduncle length | 5 | 19.3 | 18.0 | 20.4 | 19.3 | 0.8 |
| Caudal peduncle depth | 5 | 8.8 | 7.0 | 8.8 | 8.0 | 0.7 |
| Predorsal length | 5 | 72.8 | 72.2 | 74.1 | 73.0 | 0.7 |
| Preanal length | 5 | 72.8 | 71.8 | 75.9 | 73.8 | 1.7 |
| Prepelvic length | 5 | 63.2 | 63.2 | 66.9 | 65.2 | 1.6 |
| Dorsal-fin base length | 5 | 9.6 | 6.4 | 9.6 | 7.6 | 1.4 |
| Anal-fin base length | 5 | 7.9 | 6.3 | 8.3 | 7.5 | 0.7 |
| Pectoral-fin length | 5 | 14.9 | 11.9 | 14.9 | 13.2 | 1.1 |
| Head length | 5 | 21.1 | 16.5 | 21.1 | 18.6 | 2.0 |
| **Percentages of HL** | | | | | | |
| Head width | 5 | 72.0 | 68.0 | 72.0 | 69.8 | 1.8 |
| Head depth | 5 | 48.2 | 41.2 | 63.9 | 50.8 | 8.2 |
| Pectoral-fin length | 5 | 70.8 | 63.6 | 81.8 | 71.3 | 6.7 |
| Interorbital | 5 | 15.7 | 14.0 | 19.3 | 15.6 | 2.2 |
| Eye diameter | 5 | 16.9 | 16.7 | 21.7 | 18.6 | 2.1 |
| Snout length | 5 | 34.9 | 34.9 | 50.6 | 41.2 | 6.5 |
| Mouth width | 5 | 28.9 | 26.3 | 37.3 | 30.6 | 4.1 |
| Anterior internarial width | 5 | 19.3 | 16.7 | 24.1 | 19.7 | 2.9 |
| Posterior internarial width | 5 | 12.0 | 9.6 | 12.0 | 11.2 | 1.1 |

jaw narrow, composed mostly of small knob-like dentary lobes, largely confluent basally, round anteriorly and, continuous with mental region posteriorly (Fig. 13). Jaw cleft short and oriented obliquely to longitudinal axis. Dentary diastema angulate. Dentary teeth 3 or 4 (when three, one obviously missing, in process of replacement), closely set at mesial end of dentary and disposed as two ventral and two dorsal ones, not exactly aligned (Figs. 4D, 15). Dentary teeth very long, their main axis sloped medially in ventral view, and their distal portions strongly curved dorsally, hooked.

Branchiostegal velum forming large, continuous, hyperbolic and posteriorly concave, free fold across whole of mental region, its lateral portion plicate near margin (Figs. 13, 14). Dorsal portion of velum reaching, but not covering, anterior margin of pectoral-fin base. Branchial openings medium-sized, spanning approximately area between ventral margin of opercular odontodophore
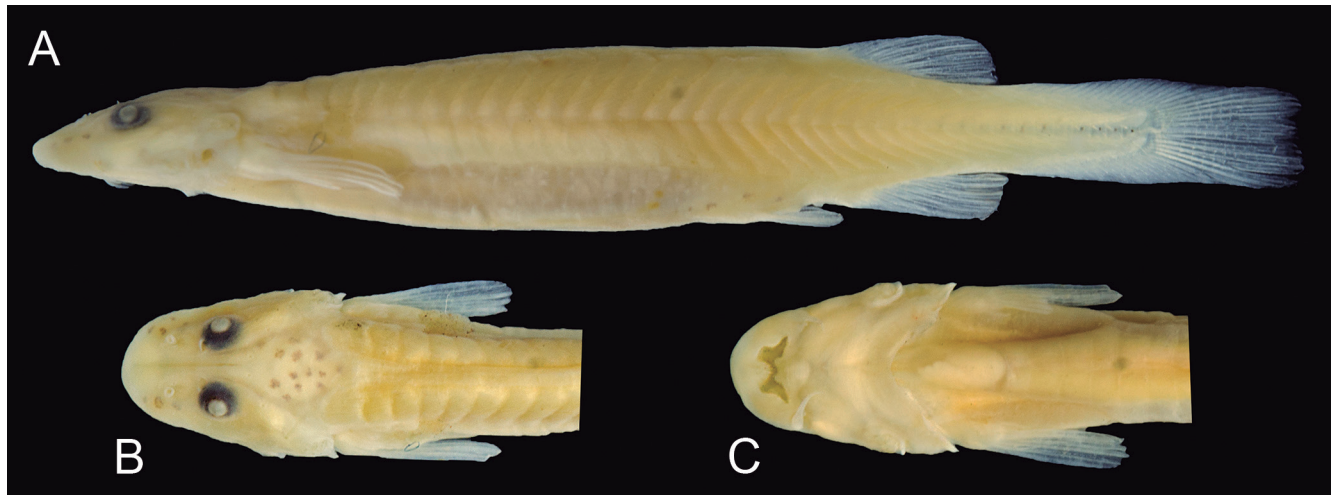


**Figure 13.** *Paracanthopoma capeta,* holotype, MZUSP 29154, 14.5 mm SL, Brazil, Amazonas, Rio Negro. (A) Lateral view of body; (B) Dorsal view of head; (C) ventral view of head.
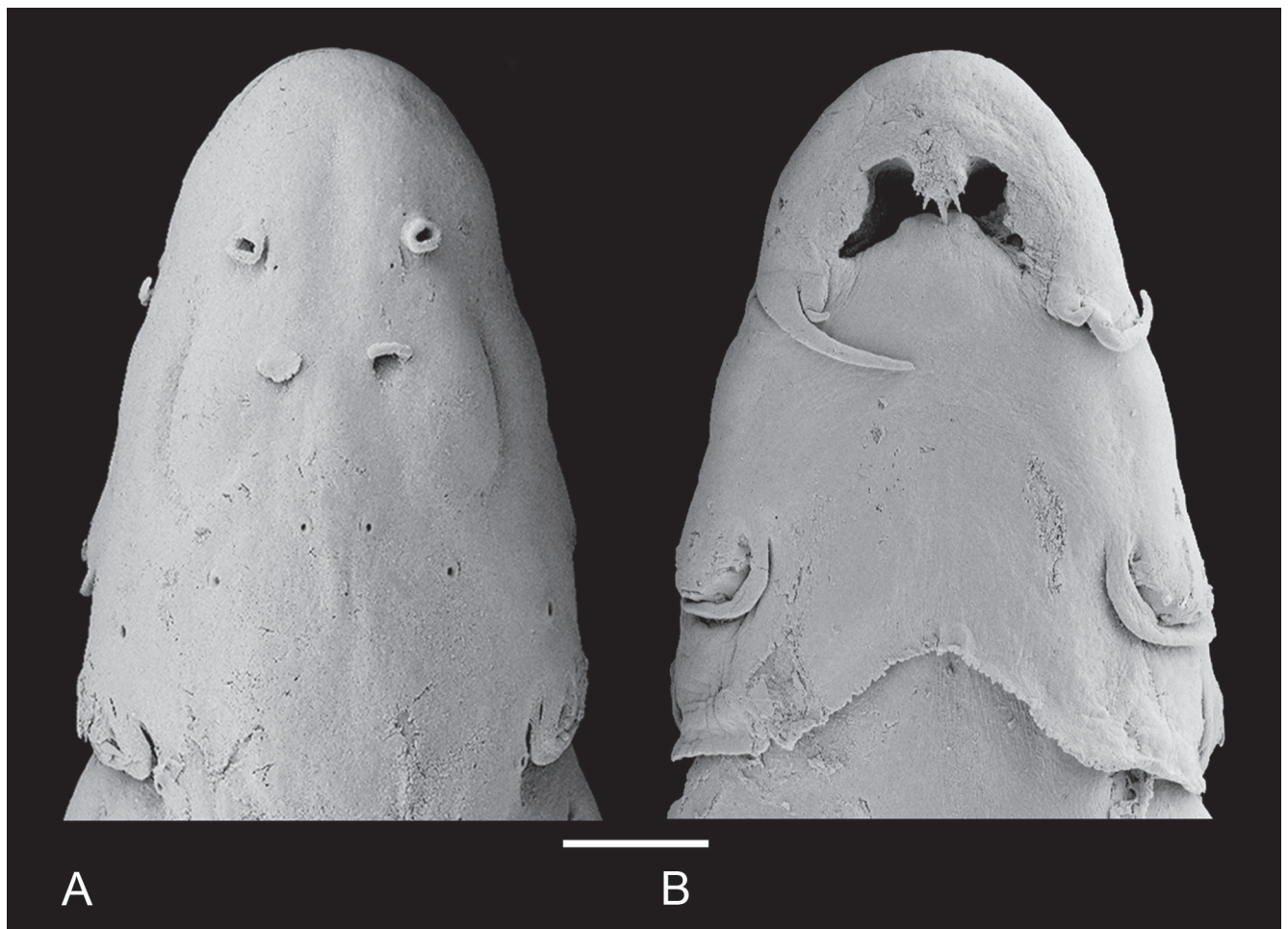


**Figure 14.** *Paracanthopoma capeta,* paratype, MZUSP 100144, SEM images of head. (A) Dorsal; (B) Ventral. Scale bar = 500 μm.
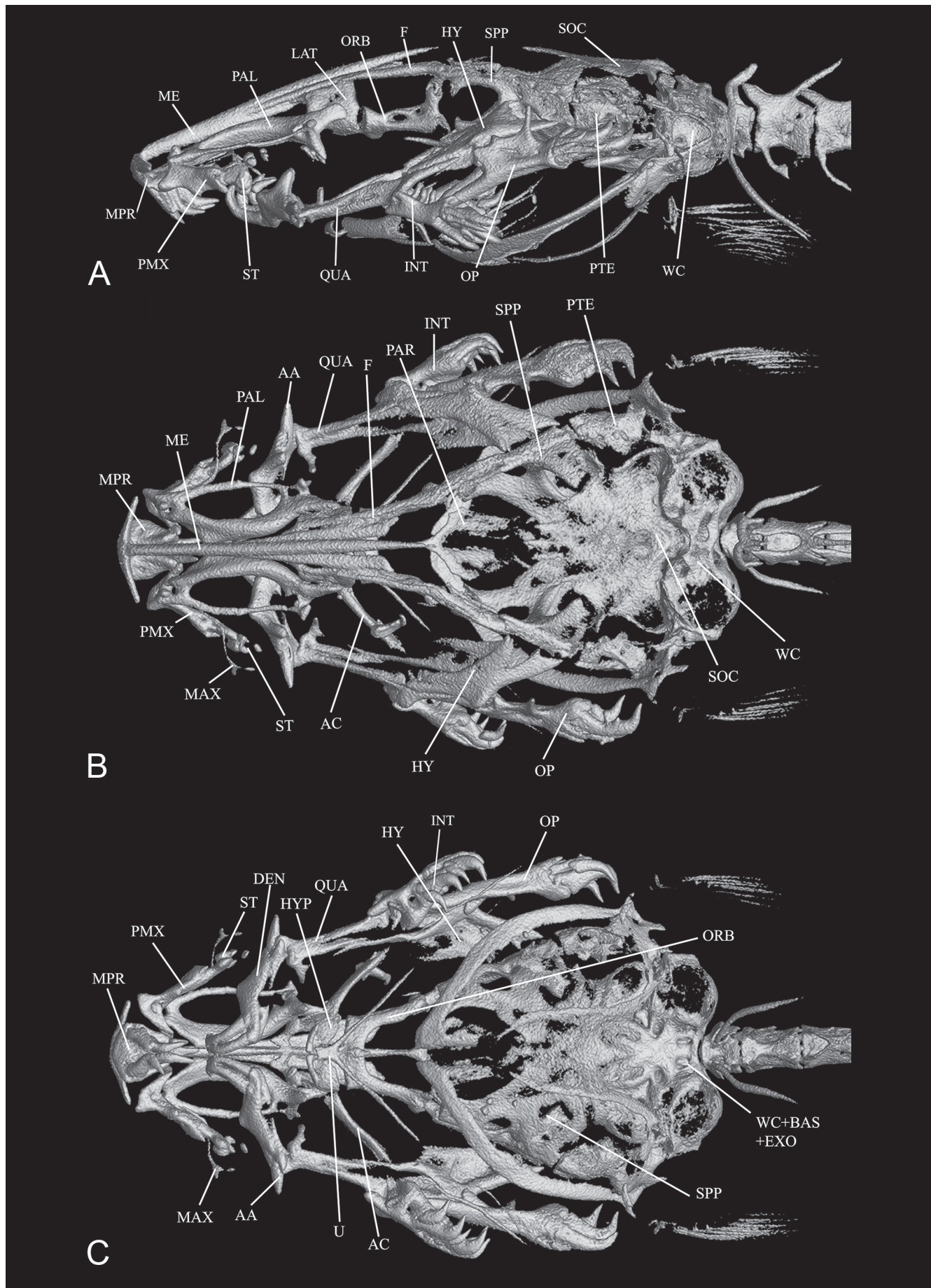
**Figure 15.** *Paracanthopoma capeta,* holotype MZUSP 29154, CT scan images of head skeleton, (A) Lateral; (B) Dorsal; (C) Ventral. Specimen poorly calcified, some structures not properly shown.

and ventral margin of interopercular odontodophore, anteriorly to base of pectoral fin. Maxillary barbel long and thin, not reaching base of interopercular odontodophore (extending approximatelly three-fourths of distance to it). Posterior point of its base anterior to vertical through anterior margin of eye in lateral view. Mesial (or ventral) part of maxillary-barbel base inserting directly onto corner of mouth without intervening membranous outgrowth. Rictal barbel small but well-differentiated, attached mesially to base of maxillary one and approximately one-fifth of its length. Nasal barbel vestigially represented by posterior elongated portion of fold around anterior naris described above (Figs. 13, 14), with double internal elastin core.

Lateral line short and straight, extending alongside dorsal margin of anterior portion of axillary gland. Terminal lateral-line pore immediately dorsal to axillary gland opening. Very short secondary branch splitting off ventrally (or laterally and immediately curving ventrally) from proximal portion of main canal, with corresponding pore opening anteriorly to midlength of main canal. Single lateral-line tubule straight, extending for half of main canal posterior to bifurcation.

Pectoral fin short (62.5-70.0% HL), elongate with gently convex or truncate margin. Margin of fin irregular at close range. Pectoral-fin rays i + 5, its base on ventral side of body. Pelvic fin small, well-separated at base, with i + 4 rays. Pelvic splint present. Origin of pelvics close to origin of anal fin, well anterior to vertical through origin of dorsal-fin, entirely covering anus and urogenital papilla and extending posteriorly to origin of anal fin. Posterior margin of pelvic fin gently convex or truncate. Dorsal fin elongate, roughly rectangular, with roundish edge and gently convex distal margin. Dorsal-fin rays ii + 5 or i + 6, plus 3 to 6 procurrent ones. Anal fin similar in shape to dorsal fin, with ii + 5 rays, plus 3 or 4 procurrent ones. Origin of anal fin at or slightly posterior to vertical through origin of dorsal-fin. Anal fin with same size, slightly smaller or slightly larger than dorsal one. Caudal fin truncate or slightly concave, its maximum depth when expanded deeper than maximum depth of caudal peduncle. Principal caudal-fin rays 6 + 6. Procurrent caudal-fin rays 16 to 21 dorsally and 19 or 20 ventrally.

Vertebrae 36 (n = 1) or 37 (n = 1). First dorsal-fin pterygiophore subsequent to neural spine of vertebra 20 (n = 1). First anal-fin pterygiophore subsequent to haemal spine of vertebra 20 (n = 1) or 21 (n = 1). Dorsal-fin pterygiophores 7 (n = 2). Anal-fin pterygiophores 6 (n = 2). Branchiostegal rays 3.

**Pigmentation in preservative:** Body almost entirely white. Few scattered dark chromatophores on posterior part of sides of abdominal wall, more evident in specimens with distended abdomens. Small black dot at middle of each vertebra along posterior part of caudal peduncle, formed by internal chromatophores. Posterior half of neurocranium with irregular dark brain pigment seen by transparency. Field of dark chromatophores anteriorly to eyes, at lateral part of snout.

**Etymology:** From the Portuguese vernacular term capeta (probably from a combination of capa, meaning cape, and -eta, diminutive suffix), meaning the devil.

**Geographical distribution:** *Paracanthopoma capeta* has been recorded from a single locality in the middle rio Negro, Northern Brazil (Fig. 20).

**Biology:** The type series was collected from the gill chamber of a specimen of *Phractocephalus hemioliopterus* (Pimelodidae), 1.08 m in length (label does not specify if SL or TL) and 22 kg. Three paratypes have distended abdomens, apparently full with discolored blood.

### *Paracanthopoma carrapata,* new species
### (Fig. 16)

**Holotype:** MZUSP 100145, 23.3 mm SL, Brazil, Rondônia, rio Madeira at Calama (08°01′42″S, 62°52′34″W), col M. Goulding, Feb-Apr 1980.

**Paratypes:** All collected with holotype. MZUSP 100142, 2 ex, 17.3-22.8 mm SL; MZUSP 100143, 3 ex (1 c&s), 22.2-22.7 mm SL.

**Diagnosis:** Distinguished from all congeners by extremely large median premaxillary dentition, with the distal (post-bend) portion larger than the basal portion (vs. two portions approximately the same length or the basal longer than the distal). Distinguished from all congeners except *Pc. daemon, Pc. parva,* and *Pc. truculenta* by the presence of nine teeth on the median premaxilla (vs. 3 to 5 or 11 and more; sometimes 10 in *Pc. daemon*); by the presence of a single median s6 pore, visible on the middle of skull posterior to eyes (vs. paired s6 pores, distant from midline of skull), and by the supraoccipital anteriorly produced into large pointed spike (vs. either anteriorly concave or straight across skull roof). Distinguished from all other *Paracanthopoma* except *Pc. parva* and *Pc. truculenta* by the posterior margin of the anal fin well posterior to vertical through that of the dorsal fin (vs. margins of two fins approximately at same vertical or that of anal fin only slightly posterior to that of dorsal fin); and by the deeply emarginate caudal fin (vs. truncate with round corners or slightly concave). Distinguished from *Pc. daemon* and *Pc. truculenta* by the robust structure of the palatine, especially of the lateral strut, wider than the central fenestra (vs. lateral strut less wide than the central fenestra). Distinguished from *Pc. daemon* and *Pc. parva* by the extensive invasion of the skull roof by head musculature, with widest exposed part of neurocranium approximately equivalent to, or less than, interorbital (vs. exposed part of neurocranium larger than interorbital). Distinguished from *Pc. truculenta* by the proportionally larger eye (13.9-14.4% HL; vs. 9.9-13.3); the longer head (20.9-22.2% HL; vs. 16.5-20.0); the more numerous opercular odontodes (four; vs. one or two) exposed on the surface of skin (vs. mostly hidden in integument); the continuous anterodorsal margin of the hyomandibula
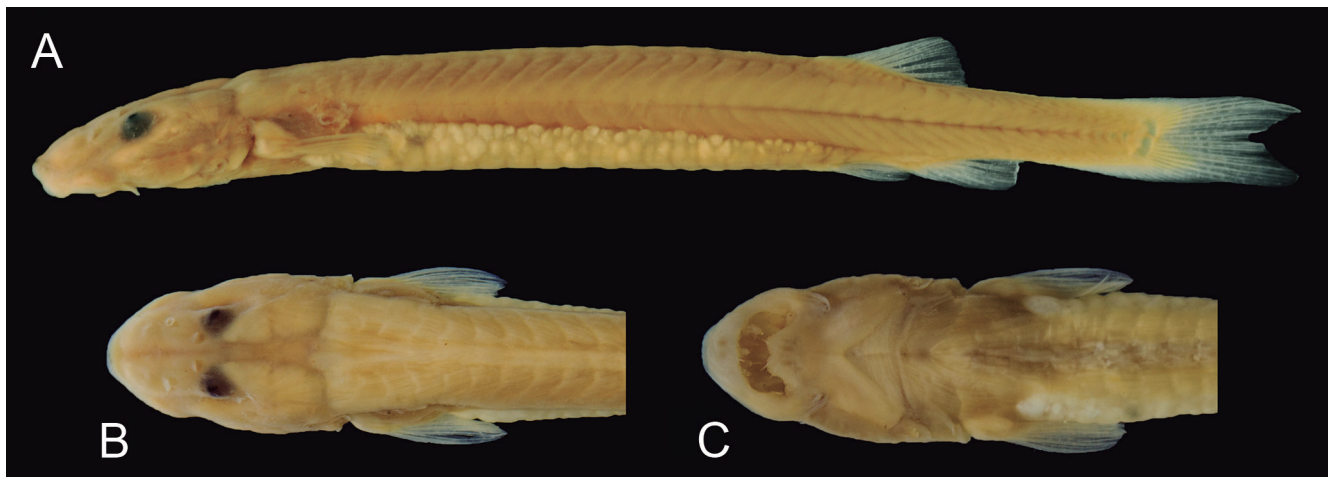
**Figure 16.** *Paracanthopoma carrapata,* holotype, MZUSP 100145, 23.3 mm SL, Brazil, Rondônia, Rio Madeira at Calama. (A) Lateral view of body; (B) Dorsal view of head; (C) ventral view of head.

(vs. with a well-defined semicircular recess at its anterior half). Further distinguished from *Pc. parva* by the smaller interopercular odontododes, where the largest odontode is smaller than the long axis of the interopercle (vs. largest interopercular odontode longer than long axis of the bone) and by the interopercular odontodes being clustered at the distal end of the bone, with their insertions at approximately the same plane (vs. odontodes inserted partly towards the ventral margin of the interopercle, with their insertions tile-like at that area).

**Description:** Morphometric data for the holotype and paratypes are provided in Table 5. Body moderately elongate (HL 20.9-22.2% SL). Cross-section of body as deep as wide at pectoral-fin insertion, increasingly compressed posterior to that point, tapering to caudal fin. Dorsal profile of body gently convex, nearly straight, from head to origin of dorsal fin (Fig. 16). Dorsal and ventral profiles of caudal peduncle straight anteriorly, then gently convex at region of procurrent caudal-fin rays. Caudal peduncle low, slightly expanded by procurrent rays along posterior third or half. Ventral profile of body mostly straight, slightly convex near pelvic-fin origin (Fig. 16), distended in specimen with full gut. Myotomes clearly visible along whole body. Longitudinal skeletogenous septum also evident along whole of body. Axillary gland small, not protruding markedly on surface of body and not reaching posterior margin of pectoral fin, covering only posterior half of pectoral-fin base. Its pore opening at vertical through midlength of pectoral fin.

Dorsal profile of head separated from that of dorsum by muscle limit. Head longer than broad (head width 59.8-69.3% HL). Snout broad, parabolic with a roundish-pointed tip, separated from rest of head by small constriction in dorsal view (Fig. 16). Muscles covering most of dorsal part of head, with head width approximately 4.5 times the maximum width of exposed skull roof in dorsal view. Exposed area proportionally larger in small specimen (MZUSP 100142, 17.3 mm SL). Head deep for *Paracanthopoma* (head depth 39.3-51.5% HL), with convex dorsal profile, strongly curved ventrally anteriorly to eyes. Eye medium-sized (13.9-14.4% HL), without free

orbital rim, located dorsolaterally on head and directed dorsolaterally (Fig. 16). Integument over eye thin, entire eyeball visible through skin. Middle of eye slightly anterior to middle of HL, interorbital width approximately equal to longitudinal diameter of eye. Eyelens very large, taking most of lateral surface of eye and either entirely unconstricted by iris or constricted only marginally, with large round pupil in specimens examined. Anterior nostril small, surrounded by short tubule of integument produced posteriorly into small pointed process (Fig. 16), with double elastin cores. Anterior internarial width slightly larger than interorbital. Posterior naris slightly larger than anterior ones, roundish or triangular, but sometimes with semilunar aspect because of partial occlusion by anterior

**Table 5.** Morphometric data of *Paracanthopoma carrapata*. Ranges, mean and SD include holotype. **Abbreviations:** min = minimum value; max = maximum value; n = number of specimens; SD = standard deviation.

| | n | min | max | Mean | SD |
|---|---|---|---|---|---|
| Standard length (mm) | 5 | 17.2 | 23.3 | 21.3 | |
| **Percentages of SL** | | | | | |
| Total length | 5 | 1.1 | 1.1 | 1.1 | 0.0 |
| Body depth | 5 | 8.6 | 12.7 | 11.1 | 1.7 |
| Caudal peduncle length | 5 | 14.7 | 16.7 | 15.5 | 1.0 |
| Caudal peduncle depth | 5 | 5.9 | 6.8 | 6.3 | 0.4 |
| Predorsal length | 5 | 73.4 | 75.6 | 74.0 | 0.9 |
| Preanal length | 5 | 78.1 | 80.2 | 79.0 | 0.8 |
| Prepelvic length | 5 | 69.5 | 74.4 | 71.3 | 2.0 |
| Dorsal-fin base length | 5 | 6.5 | 8.0 | 7.0 | 0.6 |
| Anal-fin base length | 5 | 4.3 | 6.7 | 5.4 | 0.9 |
| Pectoral-fin length | 5 | 9.7 | 12.1 | 10.8 | 0.9 |
| Head length | 5 | 20.9 | 22.2 | 21.5 | 0.5 |
| **Percentages of HL** | | | | | |
| Head width | 5 | 59.8 | 69.3 | 63.9 | 4.1 |
| Head depth | 5 | 39.3 | 51.5 | 46.5 | 4.4 |
| Pectoral-fin length | 5 | 49.5 | 61.4 | 55.6 | 5.0 |
| Interorbital | 5 | 10.7 | 12.4 | 11.7 | 0.7 |
| Eye diameter | 5 | 13.9 | 14.4 | 14.1 | 0.2 |
| Snout length | 5 | 39.2 | 41.8 | 40.5 | 1.1 |
| Mouth width | 5 | 28.7 | 34.0 | 31.5 | 2.5 |
| Anterior internarial width | 5 | 17.5 | 20.4 | 19.2 | 1.1 |
| Posterior internarial width | 5 | 5.7 | 7.2 | 6.7 | 0.6 |

flap of integument. Posterior naris positioned anteromesially to eye, their middle slightly posterior to transverse line through anterior margin of eyes (Fig. 16). Posterior internarial width narrower than interorbital.

Opercular odontodophore very small, laterally located on head, approximately at, or slightly dorsal to, middepth of head. Odontodophore externally inconspicuous on general view of head, identifiable mostly by its proportionally small, elongate periodontodeal fold. Opercular odontodes 4, with 2 large posterior ones (one of which often in process of replacement), closely positioned and with tips strongly curved dorsally. Two anterior odontodes much smaller than posterior ones, only slightly curved dorsally. Interopercular odontodophore very small, located ventrolaterally on head, at or immediately ventral to horizontal through origin of pectoral fin, with 3 odontodes closely positioned in single row, much closer to opercular odontodophore than to eye. Interopercular periodontodal fold of integument small, oval in shape. Epiodontodeal velum thick, very small but proportional to size of odontodophore, entirely covering odontodes when extended.

Mouth inferior (ventral) and very large, occupying most of anterior part of head ventrally (Fig. 16). Each premaxilla with single scalpelloid teeth attached to its distal tip (visible only in skeletal preparations), but actually two tooth sockets adjacently-positioned, one of which normally vacant, corresponding to half-formed replacement tooth adjacent to mature one. Two additional initial-stage replacement caps positioned nearby. Mature scalpelloid tooth with distal portion disproportionately reduced and very strongly curved over rest of teeth, with pungent tip nearly adpressed to margin of basal plate. Scalpelloid teeth deeply hidden in labial tissue, only exposed when premaxilla forcibly abducted. Conical teeth absent in premaxilla (Fig. 17). Upper lip thick, sucker-like. Median premaxilla very large, with 9 teeth disposed in one anterior row of four (convex anteriorly), one posterior row of four (convex posteriorly), plus single middle tooth (Fig. 17). Teeth on anterior row more or less evenly spaced, those on posterior row more widely spaced medially than laterally. All nine teeth perpendicular to median premaxilla at base, but strongly curved posteriorly at distal pungent portion, those of anterior row taller than those of posterior row. All median premaxillary teeth strongly laterally compressed basally. Numerous replacement tooth caps posterodorsally to mature dentition, creating crowded aspect at posterior limit of median premaxillary dentition. Median premaxillary teeth occupying almost all of upper jaw and most of interior of mouth (Figs. 16, 17). Median premaxillary velum absent. Hypodontal pad of median premaxilla thin or absent, not cushioning teeth. Lower jaw wide, with long dentary lobes mostly fused to each other at midline, continuous with mental region posteriorly. Lower jaw cleft deep and strongly directed posterolaterally, not reaching parallel to longitudinal axis and with broad space separating it laterally from inner margin of upper jaw (Fig. 16). Dentary diastema poorly differentiated, represented by small concave, sometimes angulate area at midline (Fig. 16).

Rami of mandible very close together at midline. Dentary teeth 4, closely packed at mesial end of dentary, disposed in two pairs, one dorsal and one ventral (Fig. 17). Axis of dentary teeth anteroventrally-directed at base, with distal portions curved dorsally or anterodorsally. Branchiostegal velum forming large, continuous, round and posteriorly concave, free fold across whole of mental region (Fig. 16). Dorsal portion of branchial membrane partly covering anterior margin of pectoral-fin base. Branchial openings small, located anteroventrally to pectoral-fin base, spanning approximately for area between ventral margin of opercular odontodophore and ventral margin of interopercular odontodophore. Maxillary barbel very short and broad at base (Fig. 16). Posterior point of is base at or slightly anterior to vertical through anterior margin of eye in lateral view, its tip extending posteriorly approximately to vertical through middle of eyes in lateral view. Mesial (or ventral) part of maxillary-barbel base adjacent to membranous outgrowth extending posteriorly from corner of mouth. Rictal barbel vestigial, located mesially to base of maxillary one and represented by triangular flap of integument, its base immersed in membranous expansion at corner of mouth (Fig. 16). Rictal barbel sometimes difficult to identify among irregularities of surrounding integument flap, but homology with trichomycterid rictal barbel evident by well-developed internal core. Nasal barbel vestigially represented by posterior elongated portion of fold around anterior naris described above, with double internal elastin core.

Lateral line short, straight along most of its length and gently bent or curved dorsally at posterior portion. Its terminal pore approximately at vertical through midlength of pectoral-fin, at horizontal through center of eye in lateral view, at or slightly posterior to vertical through anterior margin of axillary pore. Short secondary branch splitting off ventrally from anterior portion of canal and running nearly in parallel to ventral margin of main canal, with corresponding pore opening approximately at midlength of main canal or slighly anterior to that point. Poorly-ossified lateral-line tubule extending for section of main canal between bifurcation and dorsal bending.

Pectoral fin very short (49.5-61.4% HL), with i + 5 rays, first one (unbranched) not longer than remaining rays. Distal margin of pectoral fin gently convex, its base near ventral margin of body in lateral view, when abdomen not distended by gut contents. Pelvic fins small, well-separated from each other at base, with i + 4 rays. Pelvic splint present. Origin of pelvics located approximately at vertical through origin of dorsal-fin, covering anus and extending posteriorly to origin of anal fin. Posterior margin of pelvic fin round. Dorsal fin small, broadly triangular with roundish apex, with gently convex distal margin and ii + 6 fin rays (ii + 5 in one specimen), plus 5 procurrent ones. Anal fin small, slightly more elongate than dorsal one, with gently convex distal margin and ii + 5 fin rays, plus 4 procurrent ones. Origin of anal fin posterior to vertical through middle of dorsal-fin base. Caudal fin strongly concave, with concavity more pronounced with growth. Principal caudal-fin rays 6 + 7. Procurrent caudal-fin rays 15 dorsally and ventrally.

**Figure 17.** *Paracanthopoma carrapata,* holotype MZUSP 100145, CT scan images of head skeleton, (A) Lateral; (B) Dorsal; (C) Ventral.

Vertebrae 39 (n = 1). First dorsal-fin pterygiophore subsequent to neural spine of vertebra 20 (n = 1). First anal-fin pterygiophore subsequent to haemal spine of vertebra 23 (n = 1). Dorsal-fin pterygiophores 7 (n = 1). Anal-fin pterygiophores 6 (n = 1, but malformed in single c&s specimen). Branchiostegal rays 3 (n = 1).

**Pigmentation in preservative:** Body almost entirely white or uniform dark tan, with little or no dark chromatophores on surface of body. Narrow fields or spots of brain pigment seen by transparency along edges of posterior part of braincase. Some specimens with internal dark chromatophores visible along vertebrae of caudal peduncle.

**Etymology:** The specific epithet comes from carrapato (feminin declension, carrapata), which in Portuguese is a collective name for blood sucking ticks in general.

**Geographical distribution:** *Paracanthopoma carrapata* is known from a single locality in the middle rio Madeira in the Brazilian Amazon (Fig. 20).

**Biology:** One specimen in MZUSP 100142 has the abdomen distended with coagulated blood.

**Remarks:** Few specimens of this species are known and it more material and data are needed. All specimens so far were collected sympatrically with *Pc. truculenta,* but in much lower frequencies. In the material examined, all individuals of *Pc. carrapata* were initially found in lots composed mostly of *Pc. truculenta.* The two species are obviously different and can be distinguished at a glance when mixed in a sample. Also occurring sympatrically and abundantly is *Pc. parva,* a species more difficult to distinguish from *Pc. carrapata.* The question arises as to whether *Pc. carrapata* may be based on a rare hybrid between *Pc. parva* and *Pc. truculenta.* Indeed, part of the character combination diagnostic of *Pc. aparavalhada* is intermediate between those two species. The shorter body, exposed opercular odontodophore and relatively larger eye approach conditions in *Pc. parva,* while the extensive invasion of the skull roof by head musculature resembles the situation in *Pc. truculenta.* The number of opercular odontodes in *Pc. carrapata* is also intermediate between the counts in the other two species. Against such interpretation is the fact that *Pc. carrapata* has at least one exclusively derived condition which is not phenotypically intermediate or paralleled in either *Pc. parva* or *Pc. truculenta:* the uniquely large size of the median premaxillary teeth, which have their distal portion (postbend) larger than the basal portion. The presence of an autapomorphic condition is taken as evidence that the taxon is an independent lineage.

### *Paracanthopoma daemon,* new species
### (Fig. 18)

**Holotype:** MZUSP 103047, 20.4 mm SL, Brazil, Mato Grosso, Gaúcha do Norte, rio Coronel Vanick (rio Xingu drainage), *ca.* 20 km from Vila do Culuene (13°31'34"S, 52°43'52"W), col., F.C.T. Lima, C.R. Moreira, A.C. Ribeiro & C.M.C. Leite, 08 Oct 2007.

**Paratypes:** MZUSP 95597, 5 ex (2 c&s), 14.7-18.6 mm SL, collected with holotype.

**Diagnosis:** Distinguished from all congeners except *Pc. carrapata, Pc. parva,* and *Pc. truculenta* by the presence of 9 or 10 teeth on the median premaxilla (vs. 3 to 5 or 11 and more); by the presence of a single median s6 pore, visible on the middle of skull posterior to transverse line through posterior margin of eyes (vs. paired s6 pores, posterior to posterior margin of eye, distant from midline of skull), and by the supraoccipital anteriorly produced into large pointed spike (vs. either anteriorly concave or straight across skull roof). Distinguished from *Pc. carrapata, Pc. parva,* and *Pc. truculenta* by the caudal fin truncate with round corners or only slightly concave (vs. deeply emarginate, bilobed); by the expanded caudal peduncle having an even depth along its length (vs. peduncle less deep anteriorly and expanding close to caudal fin); by the more numerous ventral caudal-fin procurrent rays (20 or 21; vs. 14-18); by the origin of the anal fin anterior to the vertical through the middle of dorsal-fin base (vs. origin of anal fin posterior to that point); and by the fewer vertebrae (35 or 36; vs. 37-40).

**Description:** Morphometric data for the holotype and paratypes are provided in Table 6. Body moderately elongate (HL 16.9-20.4% SL). Cross-section of body as deep as broad or slightly deeper than broad at pectoral-fin insertion and increasingly compressed posterior to that point, tapering to caudal fin. Dorsal profile of body gently convex from head to origin of dorsal fin (Fig. 18). Dorsal and ventral profiles of caudal peduncle straight or gently convex. Caudal peduncle spatulate, expanded by procurrent rays along nearly its entire length (Fig. 18). Ventral profile of body straight or gently convex until pelvic-fin origin (Fig. 18), with some specimens with distended abdomens due to full ovaries. Myotomes and longitudinal skeletogenous septum clearly visible along whole body. Axillary gland comparatively small, elongate in shape, not protruding markedly on surface of body and extending maximally to end of adpressed pectoral fin. Gland tapering to fine posterior tip, its large round pore located approximately at vertical through midlength of pectoral fin. Condition of gland posterior to pore evidently related to amount of secretion stored. In some specimens, post-pore part of gland appearing as nearly absent, clearly due to empty condition of its lumen.

Dorsal profile of head continuous with that of dorsum, sometimes broken by slight muscle constriction or change in angle (Fig. 18). Head longer than broad (head width 61.0-64.0% HL), snout broad, semicircular in dorsal view. Muscles covering only lateral portion of dorsal aspect of head, with skull roof mostly exposed. Head deep for *Paracanthopoma* (head depth 42.6-53.0% HL), with dorsal profile straight and sloped dorsally until eye in lateral view, then angled to horizontal and straight to

**Figure 18.** *Paracanthopoma daemon,* holotype, MZUSP 103047, 20.4 mm SL, Brazil, Mato Grosso, Gaúcha do Norte, Rio Coronel Vanick. (A) Lateral view of body; (B) Dorsal view of head; (C) ventral view of head.

trunk. Eye large (14.8-17.0% HL), without free orbital rim, located dorsolaterally on head and directed dorsolaterally, covered by thin and transparent integument (Fig. 18). Middle of eye slightly anterior to middle of HL, interorbital width approximately equal to or slightly shorter than longitudinal diameter of eye. Eyelens occupying central portion of lateral surface of eye and constricted by iris marginally, with large round pupil in specimens examined. Anterior nostril small, located in narrow teardrop-shaped slit on surface of skin and surrounded by short tubule of integument produced posteriorly into small pointed process, with double elastin cores. Anterior internarial width slightly larger than interorbital. Posterior naris larger than anterior one, partly occluded

**Table 6.** Morphometric data of *Paracanthopoma daemon.* Ranges, mean and SD include holotype. Head subunits were obtained with an ocular micrometer and therefore as projections. **Abbreviations:** min = minimum value; max = maximum value; n = number of specimens; SD = standard deviation.

| | n | holotype | min | max | mean | SD |
|---|---|---|---|---|---|---|
| Standard length (mm) | 4 | 20.4 | 14.7 | 20.4 | 17.8 | |
| **Percentages of SL** | | | | | | |
| Total length | 4 | 1.1 | 1.1 | 1.1 | 1.1 | 0.0 |
| Body depth | 4 | 15.4 | 12.3 | 15.5 | 14.3 | 1.5 |
| Caudal peduncle length | 4 | 20.5 | 18.6 | 21.1 | 19.9 | 1.2 |
| Caudal peduncle depth | 4 | 8.3 | 7.9 | 9.7 | 8.6 | 0.8 |
| Predorsal length | 4 | 69.9 | 69.9 | 71.8 | 70.4 | 0.9 |
| Preanal length | 4 | 72.4 | 71.8 | 74.6 | 72.8 | 1.2 |
| Prepelvic length | 4 | 66.0 | 64.8 | 66.7 | 66.0 | 0.8 |
| Dorsal-fin base length | 4 | 8.3 | 7.7 | 9.7 | 8.4 | 0.9 |
| Anal-fin base length | 4 | 6.4 | 6.4 | 8.0 | 7.5 | 0.7 |
| Pectoral-fin length | 4 | 11.5 | 11.5 | 14.2 | 13.3 | 1.2 |
| Head length | 4 | 18.6 | 16.9 | 20.4 | 18.8 | 1.5 |
| **Percentages of HL** | | | | | | |
| Head width | 4 | 61.0 | 61.0 | 64.0 | 62.3 | 1.5 |
| Head depth | 4 | 42.6 | 42.6 | 53.0 | 45.5 | 5.0 |
| Pectoral-fin length | 4 | 72.1 | 67.3 | 85.0 | 74.5 | 7.5 |
| Interorbital | 4 | 13.1 | 11.7 | 14.0 | 12.8 | 1.0 |
| Eye diameter | 4 | 14.8 | 14.8 | 17.0 | 15.8 | 1.0 |
| Snout length | 4 | 40.2 | 39.4 | 45.0 | 41.1 | 2.6 |
| Mouth width | 4 | 28.7 | 20.4 | 32.0 | 25.9 | 5.4 |
| Anterior internarial width | 4 | 17.2 | 16.0 | 20.0 | 17.9 | 1.7 |
| Posterior internarial width | 4 | 9.0 | 6.4 | 9.0 | 8.1 | 1.2 |

by anterior flap of integument. Posterior naris positioned anteromesially and adjacent to eye, their middle at transverse line through anterior margin of eye. Posterior internarial width narrower than interorbital.

Opercular odontodophore medium-sized, laterally located on head, on dorsal half of head depth in lateral view. Opercular odontodes 5, closely positioned as two very large ones juxtaposed posteriorly and three smaller anterior ones. Main axis of opercular odontodes oriented horizontally in lateral view, with their distal portion curved dorsomedially. One or two caps of replacement odontodes posteriorly to mature ones. Interopercular odontodophore either similar-sized, or slightly larger than opercular one, located ventrolaterally on head, immediately ventral to horizontal through origin of pectoral fin, with 4 or 5 odontodes closely positioned in single row of four near posterior edge of interopercle, plus single smaller one anteriorly (when 5). Odontodes of posterior row strongly angled medially. Interopercular odontodophore much closer to opercular one than to eye. One or two replacement tooth caps located posteromesially to mature ones. Opercular and interopercular periodontodal folds thin and transparent. Epiodontodeal velum not visible in specimens available.

Mouth inferior (ventral). Each premaxilla with single scalpelloid teeth attached to its distal tip (Figs. 4E, 19), but actually two adjacent tooth sockets, one of which vacant, corresponding to half-formed replacement tooth adjacent to mature one. Vacant socket position varying among specimens and between sides of same specimen, being either lateral or mesial one. One or two additional initial-stage replacement caps suspended in soft tissue dorsally to mature one and its incomplete neighbor. Mature scalpelloid tooth with distal portion disproportionately reduced and very strongly curved over rest of teeth, with pungent tip nearly adpressed to margin of basal plate. Scalpelloid tooth deeply hidden in labial tissue, but its distal surface easily emerging when premaxilla forcibly abducted. Conical teeth absent in premaxilla. Upper lip thick, ventral surface not plicate. Median premaxilla very large, with 9 or 10 teeth disposed in one anterior row (convex anteriorly) of four or five, one posterior row (convex posteriorly) of four plus single middle tooth

(Figs. 4E, 19). All teeth perpendicular to ventral surface of median premaxilla basally, but strongly curved posteriorly at distal pungent portion, those on anterior row taller than on posterior one. All median premaxillary teeth strongly laterally compressed basally. Median premaxillary dentition occupying most of exposed upper jaw and most of interior of mouth. Many replacement tooth caps posterodorsally to mature dentition, creating confusing aspect to posterior limit of median premaxillary dentition. Median premaxillary velum irregular. Hypodontal pad of median premaxilla thickly cushioning teeth. Lower jaw wide, occupied mostly by large dentary lobes largely continuous with each other and continuous with mental region posteriorly. Dentary diastema well differentiated, represented by small concave or angulate area at midline. Rami of mandible very close together at midline. Jaw cleft deep and strongly directed posteriorly, approaching parallel to longitudinal axis and forming broad space separating lower jaw laterally from inner margin of upper jaw. Dentary teeth 4, closely packed at mesial end of dentary and disposed in two aligned pairs, one dorsal and one ventral, with only latter visible in ventral view (Figs. 4E, 19). Axis of dentary teeth anteroventrally-directed at base, but strongly curved dorsally distally. Branchiostegal velum forming large, continuous, round and posteriorly concave, free fold across whole of mental region (Fig. 18). Dorsal portion of branchial membrane reaching anterior margin of pectoral-fin base. Branchial openings small, located anteriorly to pectoral-fin base, spanning approximately for area between ventral margin of opercular odontodophore and dorsal margin of interopercular odontodophore. Maxillary barbel very short and proximally broad, its base flap-like, only distal portion filamentous. Posterior point of is base anterior to vertical through anterior margin of eye, its tip extending posteriorly approximately to vertical through posterior margin of eyes, or slightly anterior to that, in lateral view. Mesial (or ventral) part of maxillary-barbel base continuous with membranous outgrowth extending posteriorly from corner of mouth. Rictal barbel vestigial, located mesially to base of maxillary one, its base immersed in membranous expansion at corner of mouth. Rictal barbel sometimes difficult to identify among irregularities of surrounding integument folds, but its homology with trichomycterid rictal barbel evident by well-developed internal core in cleared and stained specimens. In some specimens, no clear external component of rictal barbel. Nasal barbel vestigially represented by posterior elongated portion of fold around anterior naris described above.

Lateral line short and straight, curved dorsally near posterior end in some populations its terminal pore slightly anterior to vertical through midlength of pectoral-fin, near dorsal margin of axillary pore. Short secondary branch splitting off ventrally from anterior portion of canal, with corresponding pore opening approximately at anterior third of main canal. Single lateral-line tubule extending for more than half of sector of canal posterior to bifurcation.

Pectoral fin short (67.3-85.0% HL), with i + 5 rays. Distal margin of pectoral fin gently convex, nearly straight, its base immediately ventral to midline of body in lateral view. Pelvic fins small, well-separated from each other at base, with i + 4 rays. Pelvic splint present. Origin of pelvics located well anterior to vertical through origin of dorsal-fin, entirely covering anus and extending posteriorly to origin of anal fin or beyond. Posterior margin of pelvic fin round. Dorsal fin small, triangular with broadly round apex, gently convex distal margin and i + 6 (holotype) or ii + 6 fin rays, plus 4 or 5 procurrent ones. Anal fin small, slightly more elongate in shape than dorsal one, with gently convex distal margin and i + 5 (holotype) or ii + 5 fin rays, plus 4 procurrent ones. Origin of anal fin slightly posterior to vertical through origin of dorsal-fin. Caudal fin truncate or slightly concave. Principal caudal-fin rays 5 + 7, 6 + 6 (holotype) or 6 + 7. Procurrent caudal-fin rays 19 or 20 dorsally and 20 or 21 ventrally.

Vertebrae 35 (n = 3) or 36 (n = 3, holotype). First dorsal-fin pterygiophore subsequent to neural spine of vertebra 17 (n = 1) or 18 (n = 1). First anal-fin pterygiophore subsequent to haemal spine of vertebra 19 (n = 1) or 20 (n = 1). Dorsal-fin pterygiophores 7 (n = 2). Anal-fin pterygiophores 6 (n = 2). Branchiostegal rays 3.

**Pigmentation in preservative:** Body almost entirely white. Neurocranium dark with brain pigment seen by transparency. Faint dark field along lateral and middle regions of snout, anterodorsally to maxillary barbel base. Dark spots on bases of opercular and interopercular odontodophores. Sparse dark spots along dorsum, more concentrated near dorsal fin. Dark spots on hypural plate and adjacent region of caudal-fin base. Irregular series of dark spots along dorsal part of abdomen, particularly visible in specimens with abdominal distention.

**Etymology:** Daemon is a latinized form of the Greek daimon, referring to the supernatural entities hierarchically between gods and mortals, including inferior divinities and ghosts of some dead men. The word was incorporated into the Judean-Christian tradition by its usage in Greek translations of sacred texts.
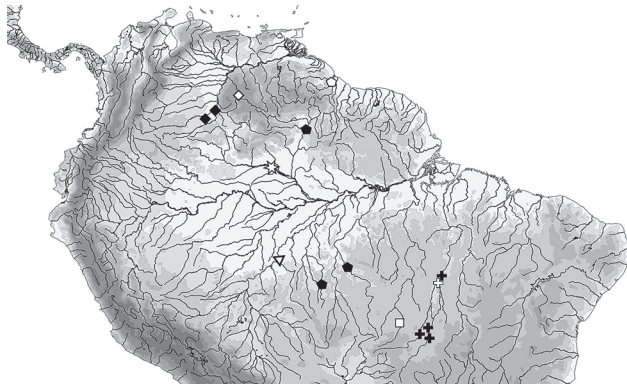
**Geographical distribution:** *Paracanthopoma daemon* is known to occur in a single locality in the rio Coronel Vanick, tributary to the upper rio Xingu in central Brazil (Fig. 20).

**Notes on ecology:** *Paracanthopoma daemon* seems to be a small inhabitant of psammic environments. One of the collectors of the type series (C. Moreira) informs that the specimens were captured during daytime at a river sector with mild current, in a small fine-sand bank close to the margin of the river, surrounded by fields of mud on one side and coarse gravel on the other. It occurred syntopically with *Mastiglanis asopos* (Heptapteridae). Other vandelliines caught in the same site, but on muddy substrate, included two undescribed species of *Vandellia*.

**Remarks:** The holotype and the largest paratype of this species (20.4 and 18.6 mm SL, respectively) are mature females with large eggs, indicating that *Pc. daemon* ma-
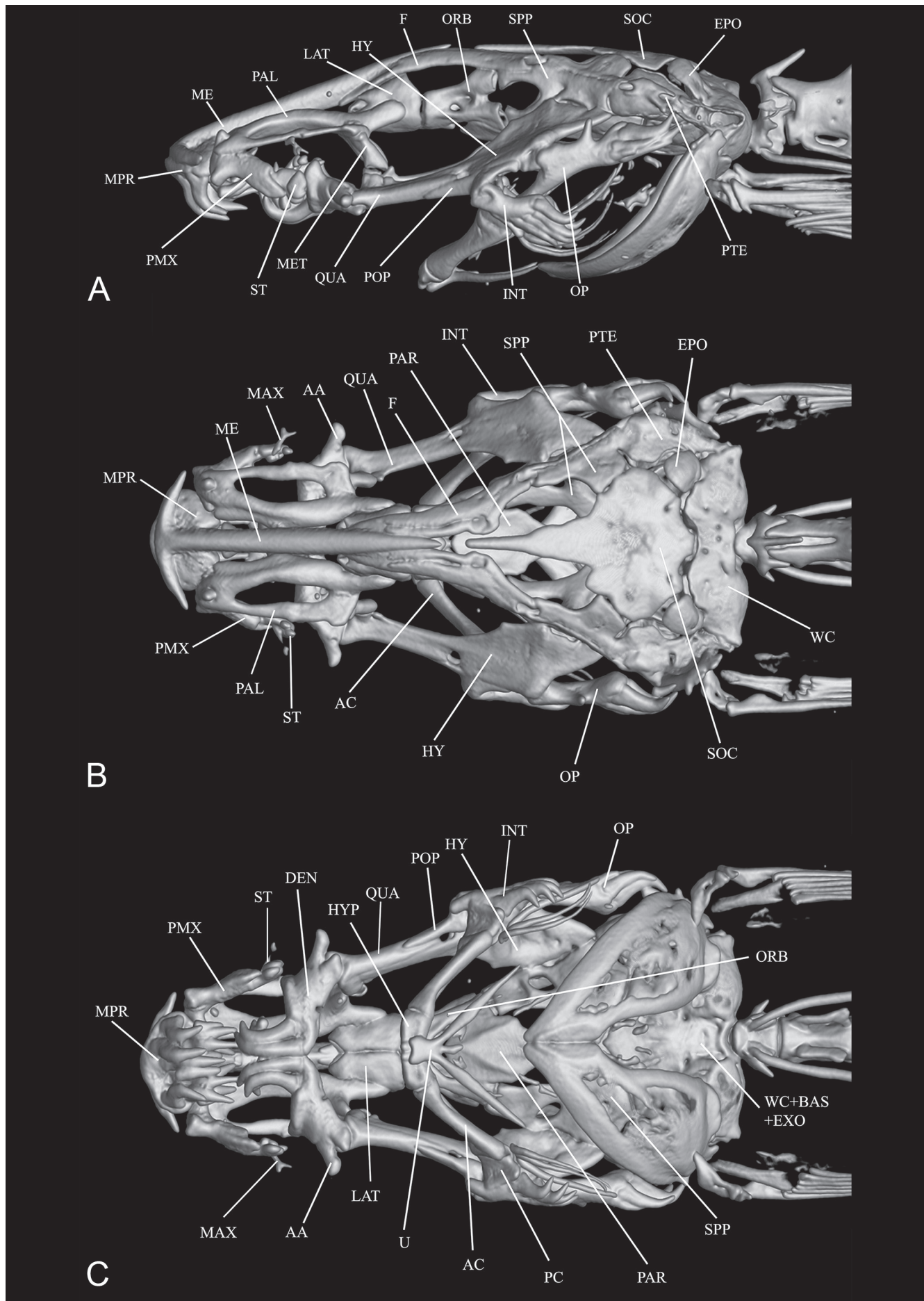
**Figure 19.** *Paracanthopoma daemon,* holotype, MZUSP 103047, CT scan images of head skeleton, (A) Lateral; (B) Dorsal; (C) Ventral.

**Figure 20.** Map of northern South America showing geographical distribution of *Paracanthopoma ahriman,* (losenge); *Pc. alleynei* (pentagon), *Pc. cangussu* (cross); *Pc. capeta* (6-tip star); *Pc. carrapata* (inverted triangle), *Pc. daemon* (square). Open symbols represent type localities. Some symbols may represent more than a single locality or lot of specimens.

tures at a considerably smaller size than its closest relatives *Pc. carrapata*, *Pc. parva* and *Pc. truculenta*. The distinctive characteristics of *Pc. daemon* are unambiguous at all comparable sizes.

### *Paracanthopoma irritans,* new species
### (Fig. 21)

*Paracanthopoma* sp. 4 – Wosiacki & de Pinna, 2007: 73 [catalog].

**Holotype:** MZUSP 126815 (split from MZUSP 100136) 16.5 mm SL, Brazil, Pará, rio Trombetas, approx. 70 km upstream from Oriximiná (approx. 01°32′S, 56°14′W), col A.C. Lima 21 Jan 2001.

**Paratypes: BRAZIL:** INPA 12430, 2 ex, 10.4 mm SL (smaller specimen; larger one damaged), Brazil, Amazonas, rio Capucapu (trib. to rio Jatapu, rio Uatumã drainage), col., J. Porto, 27 Nov 1988; INPA 20529, 23 ex (2 c&s), 15.4-20.1 mm SL, Amapá, rio Amapá Grande at Cachoeira Grande, col., M. Jégu, 25 Aug 1992; LIRP 12689, 21 ex, 12.5-18.6 mm SL, Pará, Jacareacanga, rio Cururu (rio Teles-Pires drainage), (08°49′36″S, 57°14′03″W), col., M. Carvalho & A. Datovo, 06 Dec 2005; LIRP 12690, 21 ex, 11.8-16.8 mm SL, Pará, Jacareacanga, rio Teles-Pires, (08°53′04″S, 57°23′02″W), col., M. Carvalho & A. Datovo, 05 Dec 2005; LIRP 12691, 6 ex, 12.7-17.3 mm SL, Pará, Jacareacanga, sand bank on right margin of rio Cururu (rio Teles-Pires drainage) (08°53′42″S, 57°14′27″W), col., M. Carvalho & A. Datovo, 06 Dec 2005; LIRP 12692, 2 ex, 15.8-16.2 mm SL, Pará, Jacareacanga, rio Cururu (rio Teles-Pires drainage), (08°52′27″S, 57°15′09″W), col., M. Carvalho & A. Datovo, 06 Dec 2005; LIRP 12695, 11 ex, 9.3-15.5 mm SL, Mato Grosso, Apiacás, rio Tapajós drainage (08°50′52.72″S, 57°25′14.21″W), col., M. Carvalho, 02 Dec 2005; LIRP 12698, 2 ex, 11.6-13.8 mm SL, Pará, Jacareacanga, rio Teles Pires (08°51′28″S, 57°25′10″W), col., M. Carvalho & A. Datovo, 04 Dec 2005 (mixed with 1 ex of *Pc. alleynei*); LIRP 12699, 2 ex, 11.9-12.6 mm SL, Mato Grosso, Apiacás, rio Tapajós drainage (08°51′58.89″S,

57°24′41.85″W), col., M. Carvalho, 03 Dec 2005 (mixed with 1 ex of *Pc. alleynei*); MZUSP 87049, 4 ex, 8.4-11.8 mm SL, Mato Grosso, Gaúcha do Norte, rio Curisevo (trib. to rio Xingu), Porto do Vitório, near Ribeirão Kevuaieli (13°02′05″S, 53°25′19″W), col., C. Moreira, I. Landim & A. Datovo, 19 Oct 2004 (collected together with *Pc. parva* MZUSP 87048); MZUSP 87099, 1 ex, 15.3 mm SL, Mato Grosso, Paranatinga, rio Jatobá (trib. to rio Ronuro, rio Xingu drainage), at bridge on road from Salto da Alegria to Nova Ubiratã (12°49′19″S, 54°09′24″W), col., J.L. Birindelli *et al.* team, 22 Oct 2004; MZUSP 94977, 2 ex, 9.8 and 14.3 mm SL, Brazil, Amazonas, rio Jaú, Lago do Miratucu (rio Negro drainage), col., A.L. Kirovsky, 10 Jun 1996; MZUSP 94981, 4 ex, 10.7-14.8 mm SL, Brazil, rio Xingu, col., unknown, 17 Sep 2001; MZUSP 95675, 1 ex, 13.4 mm SL, Mato Grosso, Gaúcha do Norte, Ribeirão da Anta and flood lake, at mouth on rio Culuene (rio Xingu drainage) (13°30′53″S, 53°05′34″W), col., F.C.T. Lima *et al.,* 12 Oct 2007; MZUSP 96052, 27 ex (3 c&s), 10.2-16.3 mm SL, Pará, Jacareacanga, rio Teles Pires immediately below Sete Quedas rapids, rio Tapajós drainage (09°19′01″S, 56°46′47″W), col., L.M. Sousa & A.L. Netto-Ferreira, 26 Sep 2007; MZUSP 99803, 5 ex, 15.0-17.6 mm SL, Pará, Jacareacanga, rio Teles Pires (rio Tapajós drainage), downstream from Sete Quedas (09°19′56″S, 56°46′33″W), col., L.M. Sousa & A.L. Netto-Ferreira, 09 Jun 2008; MZUSP 99942, 1 ex, 13.6 mm SL, Pará, Jacareacanga, rio Teles Pires (rio Tapajós drainage), downstream from Sete Quedas (09°20′38″S, 56°46′42″W), col., L.M. Sousa & A.L. Netto-Ferreira, 10 Jun 2008; MZUSP 100136, 16 ex (3 c&s), 12.5-17.0 mm SL, collected with holotype; MZUSP 100233, 10 ex (2 c&s), 12.8-16.8 mm SL, Amapá/Pará, rio Jari, above Cachoeira de Santo Antônio, between Porto Sabão and 5 km above mouth of rio Uiratapuru (00°37′02″S, 52°31′35″W), col., C.R. Moreira and F.A. Bockmann, 20-24 Feb 2008; MZUSP 100235, 201 ex (15 c&s), 10.6-15.5 mm SL, Amapá, rio Jari, near left margin, downstream from Laranjal do Jari, col., C.R. Moreira & F.A. Bockmann, 08 Oct 2007; MZUSP 103511, 14 ex, 9.1-13.4 mm SL, Amapá, Laranjal do Jari, Igapó on left margin of rio Jari, upstream from Iratapuru, upstream from Cachoeira de Santo Antônio (00°35′05″S, 52°36′59″W), col., J. Birindelli *et al.,* 22 Feb 2009 (collected with *Pc. parva,* MZUSP 126876); MZUSP 111690, 1 ex, 14.4 mm SL, Pará, Altamira, rio Xingu at Praia do Pajé, at mouth of Igarapé Panela (03°14′12″S, 52°13′21″W), col., O. Oyakawa *et al.,* 08 Nov 2011; MZUSP 118136, 1 ex, 15.4 mm SL, Mato Grosso, Apiacás, rio Teles Pires (rio Tapajós drainage) (07°53′55.86″S, 57°50′36.32″W), col., W. Ohara, 31 Aug 2015; MZUSP 119685, 2 ex [mixed with 6 ex of *Pv. oxyptera*], 15.4-17.2 mm SL, Pará, Altamira, rio Curuá, at Curuá Beach t Castelo dos Sonhos district (08°20′53.94″S, 55°04′58.55″W), col., O. Oyakawa *et al.,* 07 Aug 2015; MZUSP 120574, 6 ex, 11.8-13.7 mm SL, Pará, Tracuateua, Igarapé Açaiteua (rio Quatipuru drainage) (01°08′39.09″S, 46°59′14.56″W), col., R. Reis *et al.,* 21 Aug 2014; MZUSP 120575, 6 ex, 10.9-13.6 mm SL, Pará, Tracuateua, Igarapé Açaiteua (rio Quatipuru drainage), col., R. Reis *et al.,* 05 Jun 2015; MZUSP 120576, 1 ex, 12.2 mm SL, Pará, Tailândia, Agropalma, rio Acará drain-

age (02°30'10.8"S, 48°53.0'W), col., Renan Reis, 2016. **PERU:** INHS 42756, 3 ex, 13.6-15.5 mm SL, Loreto, río Nanay (río Amazonas drainage) at Pampa Chica, N edge of Iquitos, col., M.H. Sabaj *et al.,* 27 Jul 1997. **VENEZUELA:** MBUCV-V 14057, 1 ex, 18.1 mm SL, Cataniapo, Las Pavas, Caño Las Pavas, tributary of río Cataniapo (río Orinoco drainage) (05°34'00"N, 67°30'36"W), col., R. Royero, 25 Jul 1982; MBUCV-V 17853, 11 ex, 13.2-14.8 mm SL (mixed with additional specimens of *Paravandellia* sp.), Amazonas, Mavaca, río Mavaca (río Orinoco drainage), beaches upstream from Campamento Base, Expedición Tapirapecó, col., R. Royero *et al.,* 22 Mar 1988; MBUCV-V 19816, 20 ex, 12.2-14.9 mm SL, Apure, Capanaparo, La Pica, Caño La Pica, tributary of río Capanaparo (río Orinoco drainage) at road San Fernando de Apure-Puerto Páez, col., O. Castillo, 20 May 1989; MBUCV-V 29078, 1 ex, 17.7 mm SL, Amazonas, Cataniapo, Las Pavas, río Cataniapo (río Orinoco drainage), port at Comunidad Las Pavas (05°36'00"N, 67°30'37"W), col., R. Royero, 16 Aug 1984; MZUSP 87065, 1 ex, 17.3 mm SL, Bolívar, río Aro (río Orinoco drainage), Hato Las Mayitas, south of Moitaco (07°58'25"N, 64°11'17"W), col., F. Provenzano & A. Rojas, 16 Apr 2004; MZUSP 106060, 2 ex, 15.9-16.5 mm SL, Amazonas, río Mavaca, beach upstream from base-camp of Tapirapecó Expedition, col., R. Royero *et al.,* 22 Mar 1988; USNM 272286, 1 ex, 14.7 mm SL, Amazonas, Ature, río Orinoco, raudales de Ature, eastern shore, (approx. 05°36'N, 67°37'W), col., R.P. Vari *et al.,* 02 Dec 1984.

**Diagnosis:** Distinguished form all congeners except *Pc. ahriman, Pc. cangussu,* and *Pc. capeta,* by the presence of five median premaxillary teeth (two or three often in replacement) (vs. either three or 9 to19 in total). The species is further distinguished from all congeners, except *Pc. ahriman* and *Pc. cangussu,* by the broad and long ventral portion of the opercular periodontodal fold, forming a lateral ridge of integument extending anteriorly to the dorsal margin of the interopercular odontodophore (vs. ventral part of fold not anteriorly extended, independent from interopercular odontodophore). Distinguished from *Pc. ahriman* by the sparse dark pigmentation on the head (vs. heavy dark pigmentation on head, faded in long-preserved specimens); by the narrower head (head width 73.3-76.9% HL; vs. 80.7-87.6); by the narrower interorbital (11.0-12.8% HL; vs. 14.8-17.9); by the narrower anterior internarial width (13.4-16.5% HL; vs. 17.6-20.2); by the narrower posterior internarial width (3.3-5.5% HL; vs. 10.1-11.4). Distinguished from *Pc. cangussu* by having 6 + 6 principal caudal-fin rays (vs. 5 + 5); by the less deep caudal peduncle (8.3-10.6% SL; vs. 10.8-13.0); by the narrower posterior internarial width (3.3-5.5% HL; vs. 8.1-10.0); by the fewer procurrent caudal-fin rays (19-25 dorsally and 21-25 ventrally, vs. 28-30 dorsally and 27-29 ventrally); by the caudal peduncle progressively deeper to base of caudal fin (vs. deepest portion of caudal peduncle approximately at its half-length); by the dorsal and ventral profiles of caudal peduncle gently continuous with caudal fin, with only slight depression in some specimens (vs. profiles of caudal peduncle posteriorly

strongly converging towards base of caudal fin, forming pronounced concave regions clearly delimiting beginning of caudal fin); by the interorbital smaller than eye diameter (vs. larger). Further distinguished from *Pc. capeta* by the broader head (73.3-76.9% HL; vs. 68.0-72.0); by the mouth cleft directed more strongly posteriorly than laterally (vs. opposite); and by the roundish median premaxilla (vs. trapezoidal with nearly straight anterior margin).

**Description:** Morphometric data for the holotype and paratypes are provided in Table 7. Body moderately elongate (HL 16.7-18.6% SL). Cross-section of body slightly broader than deep at pectoral-fin insertion and increasingly compressed posterior to that point, tapering to caudal fin. Dorsal profile of body gently convex, nearly straight, from head to origin of dorsal fin (Fig. 21). Dorsal and ventral profiles of caudal peduncle strongly convex posterior to ends of dorsal and anal fins, spatulate, expanded by procurrent caudal-fin rays. Dorsal and ventral profiles of caudal peduncle gently continuous with caudal fin, with only slight depression in some specimens. Ventral profile of body straight to pectoral-fin base and then gently convex until pelvic-fin origin, with some specimens with distented abdomen due to gut content. Myotomes and longitudinal skeletogenous septum clearly visible through thin integument along whole body. In few specimens, axillary gland full with secretion, very large and protruding markedly on surface of body. In majority of specimens, gland empty, much smaller and less conspicuous. When full, anterior end of gland surrounding dorsoposterior, ventral and posterior margins of muscular pectoral-fin base, as thick corselet, extending posteriorly beyond margin of adpressed pectoral fin for distance equivalent to fin length. Gland narrowing to blunt posterior end, extending along limit between hypaxial musculature and abdominal cavity, its large round or oval pore located slightly posterior to middle of pectoral-fin length, in dorsal view. Condition of gland posterior to pore evidently related to amount of secretion stored at time of preservation.

Dorsal profile of head continuous with that of dorsum, its origin indicated by slight constriction of anterior end of epaxial musculature. Head longer than broad (head width 73.3-76.9% HL), snout broad, parabolic with a continuous round anterior margin (Fig. 21). Head muscles not entering skull roof. Head moderately depressed (head depth 34.9-45.1% HL) with dorsal profile gently convex, nearly straight, with curvature accentuated close to tip of snout. Ventral profile of head straight, flat. Eye large (14.0-18.7% HL), without free orbital rim, located dorsolaterally on head and directed dorsolaterally, with pronounced lateral component. Integument over eye thin and transparent. Middle of eye slightly anterior to middle of HL, interorbital smaller than eye diameter. Eyelens large and unconstricted by iris in specimens examined. Anterior nostril small, surrounded by short tubule of integument only slightly produced posteriorly into very small nasal barbel (Fig. 22). Anterior internarial width approximately equal to interorbital. Posterior naris

**Table 7.** Morphometric data of *Paracanthopoma irritans*. Ranges, mean and SD include holotype. Head subunits were obtained with an ocular micrometer and therefore as projections. **Abbreviations:** min = minimum value; max = maximum value; n = number of specimens; SD = standard deviation.

|  | n | holotype | min | max | mean | SD |
|---|---|---|---|---|---|---|
| Standard length (mm) | 5 | 16.7 | 14.0 | 17.2 | 15.8 |  |
| **Percentages of SL** | | | | | | |
| Total length | 5 | 1.1 | 1.1 | 1.1 | 1.1 | 0.0 |
| Body depth | 5 | 14.4 | 13.6 | 16.0 | 14.6 | 1.0 |
| Caudal peduncle length | 5 | 21.6 | 21.6 | 23.5 | 22.6 | 0.7 |
| Caudal peduncle depth | 5 | 9.6 | 8.3 | 10.6 | 9.5 | 1.1 |
| Predorsal length | 5 | 72.0 | 69.7 | 72.6 | 71.2 | 1.2 |
| Preanal length | 5 | 70.4 | 68.1 | 70.4 | 69.1 | 1.0 |
| Prepelvic length | 5 | 64.8 | 62.1 | 64.8 | 63.5 | 1.2 |
| Dorsal-fin base length | 5 | 8.0 | 7.7 | 8.8 | 8.3 | 0.4 |
| Anal-fin base length | 5 | 8.0 | 7.6 | 8.5 | 8.1 | 0.4 |
| Pectoral-fin length | 5 | 12.0 | 10.6 | 12.4 | 11.6 | 0.9 |
| Head length | 5 | 17.6 | 16.7 | 18.6 | 17.5 | 0.8 |
| **Percentages of HL** | | | | | | |
| Head width | 5 | 76.9 | 73.3 | 76.9 | 75.5 | 1.6 |
| Head depth | 5 | 40.7 | 34.9 | 45.1 | 40.4 | 3.7 |
| Pectoral-fin length | 5 | 67.0 | 60.4 | 68.6 | 64.0 | 3.7 |
| Interorbital | 5 | 11.0 | 11.0 | 12.8 | 11.6 | 0.9 |
| Eye diameter | 5 | 17.6 | 14.0 | 18.7 | 17.0 | 1.9 |
| Snout length | 5 | 36.3 | 34.1 | 39.6 | 37.0 | 2.5 |
| Mouth width | 5 | 26.4 | 23.3 | 26.4 | 25.4 | 1.3 |
| Anterior internarial width | 5 | 15.4 | 13.4 | 16.5 | 15.6 | 1.3 |
| Posterior internarial width | 5 | 5.5 | 3.3 | 5.5 | 4.5 | 1.0 |

large and widely open twice as large as anterior ones, adjacent to anteromesial margin of eye and partly occluded by anterior flap of integument (Fig. 22). Anterior margins of posterior nares leveled or slightly anterior to transverse line through anterior margins of eyes. Posterior internarial width narrower than interorbital and narrower than diameter of one nostril.

Opercular odontodophore medium-sized and nearly round, dorsolaterally located on head, on dorsal half of head depth in lateral view, anterodorsally to pectoral-fin base. Opercular odontodes 6 to 9, closely positioned in more or less irregular roundish disposition, with two largest ones posteriorly. Main axis of opercular odontodes oriented horizontally in lateral view, with distal portions of larger posterior ones curved dorsoposteriorly. Opercular periodontodal fold well-differentiated but short, extending shortly beyond tips of odontodes, its ventral side extending anteriorly as broad straight or slightly convex edge to dorsal margin of interopercular periodontodal fold. Interopercular odontodophore slightly larger than opercular one, located ventrolaterally on head, immediately ventral to horizontal through origin of pectoral fin, with 8 or 9 odontodes closely positioned in two irregular, partly imbricating, rows. Interopercular odontodes larger posteriorly, dorsal ones curved dorsomedioposteriorly and ventral ones curved ventroposteriorly. Interopercular odontodophore slightly closer to opercular one than to eye. Interopercular periodontodal fold of integument well-developed, roundish, extending well beyond tips of odontodes. Epiodontodal velum thin and transparent, covering most of odontodes.

Mouth inferior (ventral). Each premaxilla with 1 or 2 scalpelloid teeth attached (in parallel when 2) to its distal tip. Two tooth sockets always present, but one of them usually in process of replacement. Scalpelloid teeth deeply hidden in labial tissue and impossible to expose in preserved specimens without damaging soft tissue. No conical teeth on premaxilla (Figs. 4F, 23). Upper lip very broad, with ventral surface of snout. Median premaxilla small, restricted to middle of upper jaw, with 5 teeth disposed in single row, with one central largest tooth and two smaller ones on each side. In most specimens, one or two teeth in process of replacement, but total count of five obvious by tooth sockets and relative position of attached teeth. Tooth bases disposed at approximately same transverse line, with central one slightly anterior to others (Figs. 4F, 23). All teeth posteriorly oblique to ventral surface of median premaxilla at base and curved further posteriorly at distal pungent portion, those on lateral regions of median premaxilla also with lateral component. Basal portion of all median premaxillary teeth strongly compressed laterally. Median premaxillary velum well-defined, semicircular, covering whole dentition when intact. Hypodontal pad of median premaxilla small, forming round mound following tooth distribution. Lower jaw narrow, composed mostly of short pointed dentary lobes, mostly confluent at midline, continuous with mental region posteriorly. Jaw cleft short, oblique relative to longitudinal axis. Dentary diastema small and angulate. Dentary teeth 4 (when 3, replacement one in formation), closely packed at mesial end of dentary and disposed as two ventral and two dorsal ones, not exactly aligned (Figs. 4F, 23). Dentary teeth long and strongly curved, with ventral ones longer and with curvature positioned distally and dorsal ones shorter and with curvature approximately at midlength. All dentary teeth with their axis anteromesially-directed at base, but strongly curved dorsally at distally.

Branchiostegal velum forming large free fold, in continuous posteriorly concave arc across whole of mental region (Fig. 22). Dorsal portion of fold reaching, but not covering, anterior margin of pectoral-fin base. Branchial openings small, spanning part of area between ventral margin of opercular odontodophore and mid-depth of interopercular odontodophore, anteroventrally to pectoral-fin base. Maxillary barbel very thin, especially distally, in most populations not reaching, or barely reaching, interopercular odontodophore (Fig. 22; but some with longer berbels reaching to middle of interopercular odontodophore, *e.g.*, MZUSP 120575). Posterior point of maxillary barbel base at, or slightly anterior to, vertical through anterior margin of eye in lateral view. Mesial (or ventral) part of maxillary-barbel base inserting directly onto corner of mouth without intervening membranous outgrowth. Rictal barbel small to vestigial, attached mesially to base of maxillary barbel. Nasal barbel very small, represented by posterior elongated portion of integument fold around anterior naris, with double internal elastin core visible in cleared and stained specimens.

Lateral line very short, slightly curved dorsally distally, extending alongside dorsal margin of anterior portion of

axillary gland. Terminal lateral-line pore dorsal to axillary gland opening. Very short secondary branch splitting off ventrally from proximal portion of main canal, with corresponding pore opening at approximately basal third of main canal. Single lateral-line tubule very poorly calcified, extending for most of main canal posterior to bifurcation.

Pectoral fin short (60.4-68.6% HL), with convex-truncate margin, its base on ventral side of body. Pectoral-fin rays i + 5 (i + 6 on one side of one specimen). Pelvic fin very small, close to each other at base, modally with i + 4 rays, (a few specimens with i + 3 or i + 5), with variable branching pattern ranging from all rays unbranched to
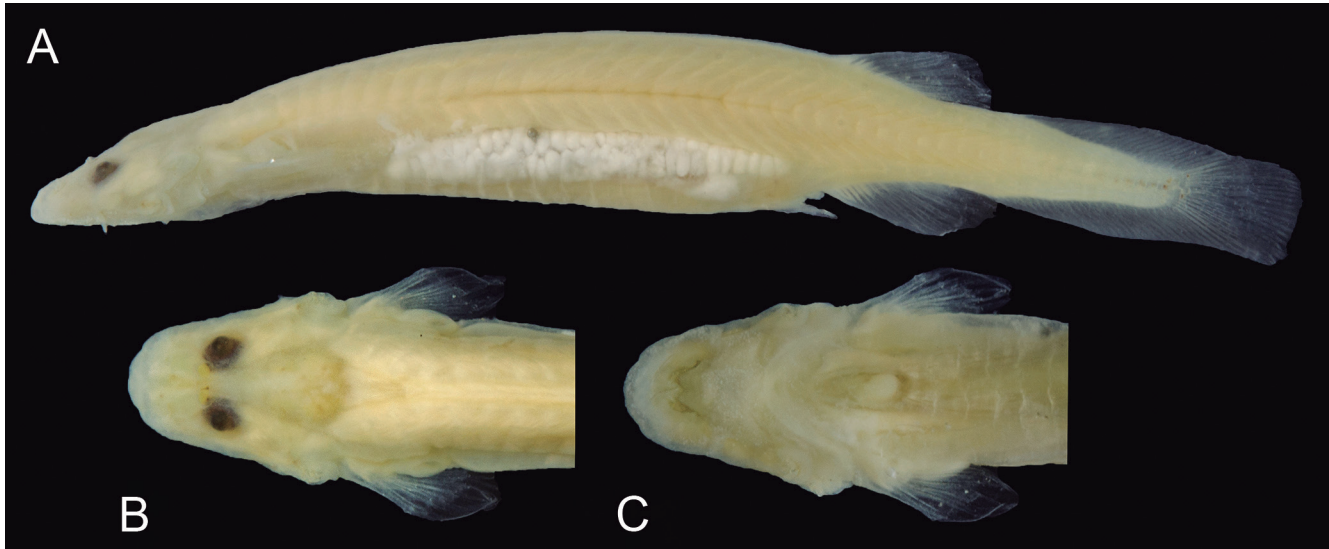


**Figure 21.** *Paracanthopoma irritans,* holotype, MZUSP 126815, 16.5 mm SL, Brazil, Pará, Rio Trombetas, (A) Lateral view of body; (B) Dorsal view of head; (C) ventral view of head.
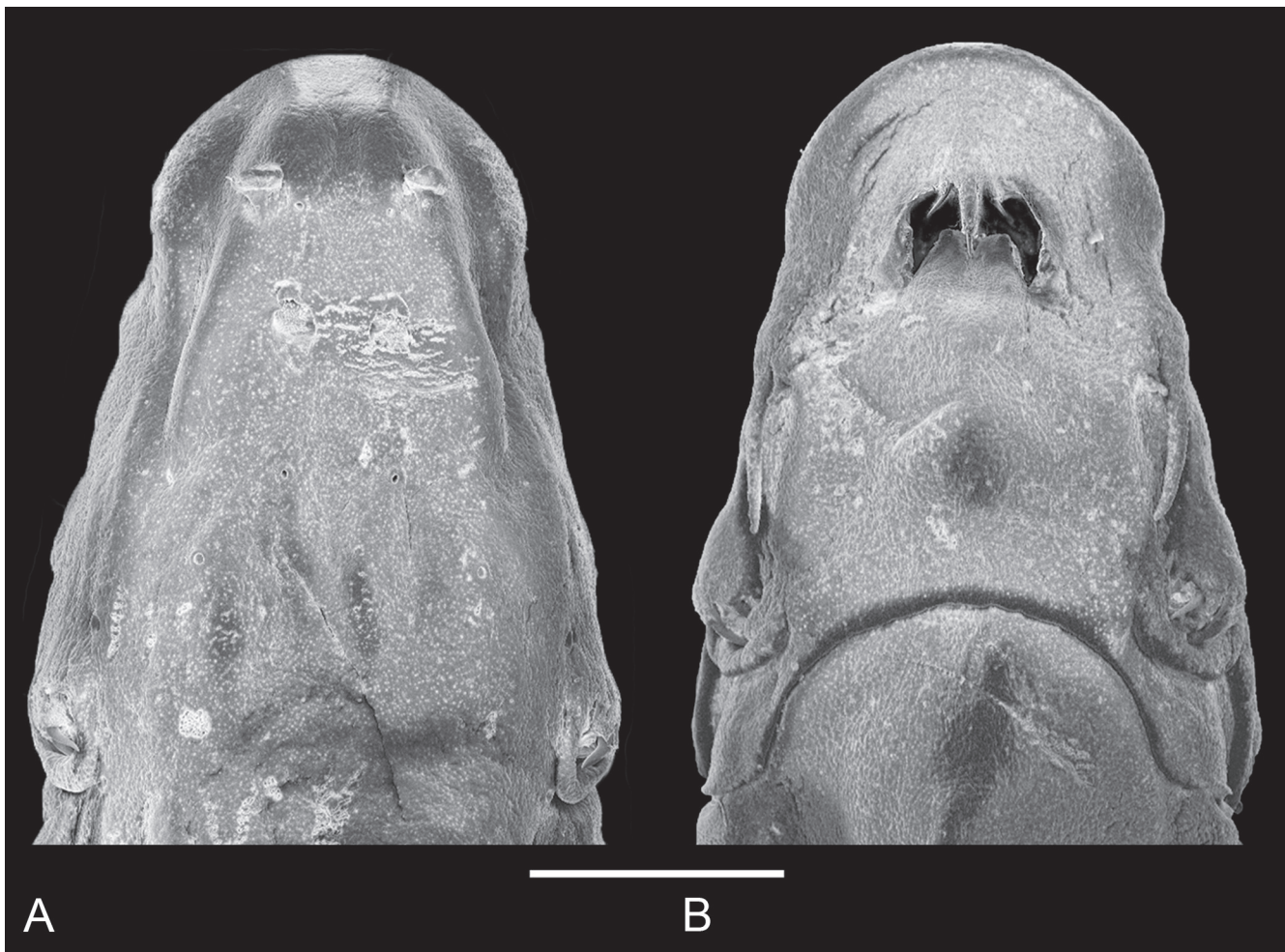


**Figure 22.** *Paracanthopoma irritans,* paratype, MZUSP 96052, SEM images of head. (A) Dorsal; (B) Ventral. Scale bar = 500 µm.

**Figure 23.** *Paracanthopoma irritans,* holotype, MZUSP 126815, CT scan images of head skeleton, (A) Lateral; (B) Dorsal; (C) Ventral. Specimen poorly calcified, some structures not properly shown.

maximum of four branched. Pelvic splint usually present, absent in few specimens. Origin of pelvics close to origin of anal fin, slightly anterior to vertical through origin of dorsal-fin, entirely covering anus and urogenital papilla and extending posteriorly to origin of anal fin. Posterior margin of pelvic fin round. Dorsal fin small, roughly rectangular-roundish, with gently convex distal margin. Dorsal-fin rays i + 6 or ii + 6, a single specimen with ii + 5, plus 4-6 procurrent ones. Anal fin small, similar in size and shape to dorsal fin but more roundish, modally with ii + 5 rays (one specimen i + 5), plus 4-6 procurrent ones. Origin of anal fin at vertical through origin of dorsal fin. Caudal fin truncate with round corners, less deep than maximum depth of caudal peduncle. Principal caudal-fin rays 6 + 6 (n = 16) with an anomalous specimen in MZUSP 100136 with 5 + 5. Procurrent caudal-fin rays 19 (n = 4), 20 (n = 1), 21 (n = 3), 22 (n = 2), 23 (n = 4), 24 (n = 2) or 25 (n = 1) dorsally and 21 (n = 1), 22 (n = 1), 23 (n = 4), 24 (n = 6) or 25 (n = 5) ventrally.

Vertebrae 39 (n = 3), 41 (n = 4), 42 (n = 4), 43 (n = 5) or 44 (n = 1). First dorsal-fin pterygiophore subsequent to neural spine of vertebra 21 (n = 6), 22 (n = 9), 23 (n = 2). First anal-fin pterygiophore subsequent to haemal spine of vertebra 20 (n = 1), 21 (n = 3), 22 (n = 8), 23 (n = 4) or 24 (n = 1). Dorsal-fin pterygiophores 6 (n = 17). Anal-fin pterygiophores 6 (n = 17). Branchiostegal rays 3.

**Pigmentation in preservative:** Body almost entirely white. Dorsum lacking dark pigment. Posterior part of caudal peduncle with irregular longitudinal stripe formed by internal chromatophores along vertebral column, with some dark spots also over hypural plate in some specimens. Dorsal half of abdomen with few sparse dark chromatophores. Posterior half of neurocranium with irregular dark brain pigment seen by transparency, forming irregular bilateral patterns, often delimiting dark protrusion at midline. Brain pigment faintly extending anteriorly along edges of neurocranium. Some specimens with dark fields over *epirostralis* muscle, anterolaterally to eyes, and a spot on opercular odontodophore.

**Etymology:** From the Latin *irritans,* irritating, taken from the name of the human flea, *Pulex irritans.*

**Geographical distribution:** *Paracanthopoma irritans* has a widespread but patchy distribution in the tributaries of the Amazon basin in Brazil and Peru, and río Orinoco in Venezuela (Fig. 27). Except for a record in the río Nanay (rio Amazonas drainage in Peru), all other lots are from Amazonian tributaries east of the mouth of the rio Negro. It is absent in the Araguaia system, where it is apparently replaced by *Pc. cangussu*. It has not yet been recorded in the southwestern Amazon. This is the only species of *Paracanthopoma* that occurs in any of the isolated drainages north of the mouth of the Amazon (rio Amapá Grande).

**Biology:** An 8.4 mm SL specimen of *Pc. irritans* in MZUSP 87049 is the smallest vandelliine yet found with evidence of ingested blood. The species also seems to mature at relatively small sizes. The lot MZUSP 96052 includes six female specimens with large mature eggs visible externally, the smallest of which is 13.0 mm SL and the largest 15.0 mm SL.

**Remarks:** This species is one of the most variable in *Paracanthopoma,* with much geographically-correlated morphological variation. A few of those variations stand out as possibly relevant taxonomicaly. Specimens in MZUSP 100235 (rio Jari) differ from usual *Pc. irritans* in having a visually much narrower caudal peduncle, which results in a distinct body shape. Since this difference is not reflected in additional characters, it is here considered as a populational variant. Specimens in MZUSP 94981 (rio Xingu) differ from the type series in a number of details. Their head is proportionally shorter and narrower, their caudal peduncle is more strongly spatulate, and their anterior nostril is more anteriorly located (in lateral aspect approximately at middistance between posterior nostrils and tip of snout rather than closer to former). They possibly represent a distinct species, though certainly close to *Pc. irritans* and *Pc. cangussu*. Given the few specimens available and the relatively imprecise locality information, their description at this time seems unwarranted. Finally, specimens in MZUSP 120575 are different from a majority of other samples of *Pc. irritans* in having obviously longer maxillary and rictal barbels. In view of the wide geographical distribution and phenotypic variation, it is possible that *Pc. irritans* actually comprises additional species not yet recognized.

### *Paracanthopoma malevola,* new species
### (Fig. 24)

**Holotype:** INPA 59836, 20.0 mm SL, Brazil, Amazonas, Apuí, Igarapé das Araras (trib. to rio Guariba; rio Aripuanã drainage) (08°46'10"S, 60°26'40"W), col., W. Pedroza *et al.,* 05 Nov 2008.

**Paratypes: All from Brazil:** INPA 31566, 6 ex (1 SEM), 15.7-19.0 mm SL (collected with holotype); LIRP 11893, 2 ex, 17.5-19.7 mm SL, Rondônia, Machadinho D'Oeste, Igarapé Preto (trib. to rio Ji-Paraná), upstream from rapids sector, at Tabajara village (08°52'49.94"S, 62°05'17.20"W), col., F. Bastos *et al.,* 14 Sep 2013; LIRP 14342, 2 ex, 19.8-25.6 mm SL, Mato Grosso, Sapezal, rio Juruena (12°54'15"S, 58°54'33"W), col., R. Ilário, 01 Apr 2008; MCP 36217, 32 ex, 14.3-20.7 mm SL, Rondônia, Igarapé Bananeiras (rio Madeira drainage), at road BR-425, North of Guajará-Mirim, *ca.* 110 km S of road BR-364 (10°38'28"S, 65°17'34"W), col., P. Buckup *et al.,* 25 Jul 2004; MCP 36224, 14 ex, 14.4-22.5 mm SL, Amazonas, unnamed Igarapé, *ca.* 43 km E of rio Madeira, by Transamazônica road (07°37'11"S, 62°40'57"W), col., R. Reis *et al.,* 27 Jul 2004; MZUSP 121845, 1 ex, 19.9 mm SL, Amazonas, Manicoré, rio Macaco (trib. to rio Branco) in Parque Nacional Campos Amazônicos (08°27'20.88"S, 61°42'01.08"W), col., O. Oyakawa *et al.,* 02 Oct 2016; MZUSP 122042, 3 ex, 18.6-23.4 mm SL,

Amazonas, Manicoré, igarapé tributary to rio Manicoré (07°52′53.40″S, 61°18′23.17″W), col., O. Oyakawa *et al.,* 04 Oct 2016; MZUSP 122109, 1 ex, 21.9 mm SL, Amazonas, Manicoré, rio Manicorezinho, (rio Branco drainage) at side road 15 km south of Transamazônica road (BR-230) at District of Santo Antônio do Matupi (07°59′57.33″S, 61°22′53.52″W), col., O. Oyakawa *et al.,* 04 Oct 2016; MZUSP 122492, 19 ex, 17.1-20.1 mm SL, Amazonas, Apuí, Igarapé II at side Road Dom Pedro (06°50′22.34″S, 59°42′26.89″W), col., O. Oyakawa *et al.,* 09 Oct 2016; MZUSP 122699, 1 ex, 18.3 mm SL, Amazonas, Apuí, igarapé tributary to rio Apuí, *ca.* 30 km from Apuí towards Vila de Sucunduri (07°08′45.38″S, 59°37′12.00″W), col., O. Oyakawa *et al.,* 10 Oct 2016; MZUSP 122705, 9 ex, 16.1-18.3 mm SL, Amazonas, Apuí, Camaiú, rio Camaiú near bridge at Transamazônica road (BR-230) (06°55′59.81″S, 59°19′48.36″W), col., O. Oyakawa *et al.,* 11 Oct 2016; MZUSP 122770, 7 ex, 14.5-20.7 mm SL, Amazonas, Apuí, igarapé at side road of Transamazônica road (BR-230), 40 km south of Apuí from Rua Bahia (07°27′50.94″S, 59°51′22.18″W), col., O. Oyakawa *et al.,* 13 Oct 2016; MZUSP 122793, 2 ex, 18.2-20.3 mm SL, Amazonas, Apuí, igarape at side road starting at Transamazônica road (BR-230), 9 km before ferry-boat across rio Sucunduri (06°50′05.28″S, 59°07′42.60″W), col., O. Oyakawa *et al.,* 11 Oct 2016; MZUSP 126816, 4 ex (2 c&s), 16.4-19.2 mm SL, collected with holotype.

**Non-type specimens:** MZUSP 122243, 7 ex, 15.3-16.4 mm SL, Brazil, Amazonas, Apuí, rio Roosevelt drainage (trib. to rio Aripuanã, rio Madeira system), small igarapé at side road joining Transamazônica road (BR-230) to Amazon Roosevelt Lodge (07°33′05.40″S, 60°41′39.62″W), col., Oyakawa *et al.,* 06 Oct 2016.

**Diagnosis:** *Paracanthopoma malevola* is distinguished from all congeners by the presence of 18 or 19 median premaxillary teeth (the most numerous in *Paracanthopoma,* which otherwise have 3 to 13 median premaxillary teeth). The rectangular, broader than long, shape of the median premaxillary tooth patch (vs. roughly squarish, triangular or roundish) also distinguishes the species from all congeners except *Pc. satanica*. Distinguished from the latter species also by the more numerous opercular (11 or 12; vs. 5 or 6) and interopercular (7 or 8; vs. 4 or 5) odontodes; by the fewer vertebrae (40; vs. 42 or 43); by the fewer caudal-fin procurrent rays (19-21 dorsally and 18-20 ventrally; vs. 32 dorsally and 30-32 ventrally); by one additional ventral principal caudal-fin ray (6 + 7; vs. 6 + 6); and by the presence of dark pigment on dorsum forming a series of irregular spots along each side of dorsal midline (vs. no dark pigment on dorsum or only few sparse dark dots not forming any pattern).

**Description:** Morphometric data for the holotype and paratypes are provided in Table 8. Body elongate (HL 15.5-18.4% SL). Cross-section of body as broad as deep, or broader than deep (the latter when axillary gland tumescent) at pectoral-fin insertion and increasingly compressed posterior to that point, tapering to cau-

dal fin. Dorsal profile of body nearly straight from head to origin of dorsal fin (Fig. 24). Dorsal and ventral profiles of caudal peduncle straight or gently convex posterior to ends of dorsal and anal fins, spatulate, expanded by procurrent caudal-fin rays. Ventral profile of body nearly straight until pelvic-fin origin, but greatly distented in some specimens due to gut contents. Myotomes and longitudinal skeletogenous septum clearly visible through thin integument along whole body. Axillary gland very large, elongate in shape, extending along limit between hypaxial musculature and abdominal cavity and protruding markedly on surface of body when full with secretion. Anterior end of gland surrounding dorsoposterior, ventral and posterior margins of muscular pectoral-fin base, as thick corselet, extending posteriorly to beyond margin of adpressed pectoral fin (maximally to *ca.* 50% of fin length beyond its margin). Gland tapering to fine posterior tip, its large round or oval pore (sometimes collapsed as slit) located at its anterior portion, approximately at vertical through middle of pectoral-fin length. Posterior portion of gland extending posteriorly from region ventral to pore, and its size apparently related to amount of secretion stored, nearly invisible in some specimens.

Dorsal profile of head continuous with that of dorsum (Fig. 24). Head longer than broad (head width 72.3-83.0% HL), snout very broad, semicircular with a continuous round anterior margin. Head muscles not entering skull roof. Head depressed (head depth 34.1-42.0% HL) with dorsal profile straight and horizontal until eye, then bending ventrally, straight or gently con-

**Table 8.** Morphometric data of *Paracanthopoma malevola*. Ranges, mean and SD include holotype. Head subunits were obtained with an ocular micrometer and therefore as projections. **Abbreviations:** min = minimum value; max = maximum value; n = number of specimens; SD = standard deviation.

| | n | holotype | min | max | mean | SD |
|---|---|---|---|---|---|---|
| Standard length (mm) | 6 | 20 | 15.7 | 20.0 | 18.2 | |
| **Percentages of SL** | | | | | | |
| Total length | 6 | 1.1 | 1.1 | 1.2 | 1.1 | 0.0 |
| Body depth | 6 | 11.0 | 10.1 | 16.0 | 12.1 | 2.1 |
| Caudal peduncle length | 6 | 19.5 | 17.6 | 20.6 | 19.6 | 1.1 |
| Caudal peduncle depth | 6 | 7.8 | 7.3 | 8.8 | 8.0 | 0.6 |
| Predorsal length | 6 | 70.8 | 70.8 | 74.0 | 72.0 | 1.5 |
| Preanal length | 6 | 72.1 | 70.4 | 74.0 | 72.1 | 1.3 |
| Prepelvic length | 6 | 64.3 | 61.6 | 66.2 | 64.4 | 1.6 |
| Dorsal-fin base length | 6 | 7.8 | 7.4 | 10.4 | 8.4 | 1.1 |
| Anal-fin base length | 6 | 6.5 | 6.5 | 8.9 | 7.9 | 0.9 |
| Pectoral-fin length | 6 | 11.7 | 11.7 | 12.7 | 12.1 | 0.3 |
| Head length | 6 | 16.9 | 15.5 | 18.4 | 17.0 | 1.0 |
| **Percentages of HL** | | | | | | |
| Head width | 6 | 72.3 | 72.3 | 83.0 | 78.4 | 3.8 |
| Head depth | 6 | 42.0 | 34.1 | 42.0 | 37.5 | 3.2 |
| Pectoral-fin length | 6 | 68.8 | 68.8 | 75.8 | 73.3 | 2.7 |
| Interorbital | 6 | 14.3 | 13.6 | 15.9 | 14.7 | 0.8 |
| Eye diameter | 6 | 12.5 | 12.5 | 14.3 | 13.5 | 0.6 |
| Snout length | 6 | 40.2 | 36.3 | 40.2 | 38.4 | 1.5 |
| Mouth width | 6 | 30.4 | 28.4 | 33.3 | 31.0 | 1.9 |
| Anterior internarial width | 6 | 16.1 | 16.1 | 18.2 | 17.3 | 0.9 |
| Posterior internarial width | 6 | 9.8 | 8.0 | 11.0 | 9.7 | 1.0 |

vex, to tip of snout. Ventral profile of head straight, flattened. Eye medium-sized (12.5-14.3% HL), without free orbital rim, located dorsolaterally on head and directed dorsolaterally. Integument over eye thin and transparent. Eye located at middle of HL, interorbital width larger than longitudinal diameter of eye. Eyelens largely constricted by iris, with oval pupil in specimens examined. Anterior nostril small, surrounded by short tubule of in-

tegument produced posteriorly into small pointed process, with double elastin cores. Anterior internarial width approximately equal to interorbital. Posterior naris slightly larger than anterior one, roundish or roughly triangular in shape, located close to anteromesial margin of eye and provided with anterior flap of integument (Fig. 25). Center of posterior nares approximately at transverse line through anterior margin of eyes. Posterior internarial



**Figure 24.** *Paracanthopoma malevola,* holotype, INPA 59836, 20.0 mm SL, Amazonas, Apuí, Igarapé das Araras. (A) Lateral view of body; (B) Dorsal view of head; (C) ventral view of head.



**Figure 25.** *Paracanthopoma malevola,* paratype, INPA 31566, SEM images of head. (A) Dorsal; (B) Ventral. Scale bar = 500 μm.

width narrower than interorbital and 2-2.5 times as wide as diameter of one nostril.

Opercular odontodophore small and oval, dorsolaterally located on head, on dorsal half of head depth in lateral view, anterodorsally to pectoral-fin base (Fig. 25). Opercular odontodes 11 or 12 in number, disposed in two irregular rows. Odontode bases compressed, and their main axis oriented dorsoposteriorly in lateral view, with distal portions curved medially, especially those of inner row. Two or three caps of replacement odontodes interspersed with mature ones. Opercular periodontodal fold well-differentiated. Interopercular odontodophore more elongate in shape than opercular one, located ventrolaterally on head, slightly ventral to horizontal through origin of pectoral fin. Interopercular odontodes 7 or 8, directed posteroventrally, with tips curved dorsoposteriorly. Odontode bases strongly compressed, mostly positioned in single rows, with short second row posteriorly. Interopercular odontodophore closer to opercular one than to eye. Interopercular periodontodal fold of integument narrow but well-differentiated. Epiodontodeal velum thick, covering most of odontodes.

Mouth inferior (ventral), strongly flattened ventrally (Figs. 24, 25). Each premaxilla with one scalpelloid teeth attached to its distal tip, and one additional tooth socket with partly-formed tooth in parallel (Fig. 4G). Scalpelloid teeth deeply hidden in labial tissue and difficult to expose in preserved specimens without damaging soft tissue. Conical teeth absent on premaxilla (Figs. 4G, 26). Upper lip very broad but poorly-differentiated, continuous with ventral surface of snout. Median premaxilla broad, with 18 or 19 teeth quite irregularly disposed in two poorly-defined rows (Figs. 4G, 26). General shape of median premaxillary tooth patch (but not of underlying bone) rectangular in ventral view in alcoholic specimens. All teeth posteriorly oblique to ventral surface of median premaxilla at base and curved further posteriorly at distal pungent portion, those on lateral edge of median premaxilla also with some lateral curvature. Basal portion of all median premaxillary teeth somewhat compressed laterally. Some replacement tooth caps interspersed with mature dentition. Median premaxillary velum poorly-differentiated. Hypodontal pad of median premaxilla broad and rectangular, its posterior margin mostly straight, perpendicular to longitudinal head axis and occupying most of surface of upper jaw. Lower jaw narrow, composed mostly of roundish and mostly confluent dentary lobes, continuous with mental region posteriorly. Jaw cleft short directed posterolaterally, curved laterally at posterior end. Dentary diastema reduced to small median concavity between dentary lobes. Dentary teeth 4, loosely disposed at mesial end of dentary, arranged in two ventral and two dorsal ones, not aligned so that in ventral view three or four teeth simultaneously visible (Figs. 4G, 26). Dentary teeth long, their axis anteriorly-directed at base, but curved dorsally or dorsolaterally at distal half. Median tooth of ventral row longer than others.

Branchiostegal velum forming large, continuous, round and posteriorly concave, free fold across whole of mental region (Fig. 25). Dorsal portion of branchial membrane reaching and slightly overlapping anterior margin of pectoral-fin base. Branchial opening small, located anteriorly to pectoral-fin base, approximately equal to space between opercular and interopercular odontodophores. Maxillary barbel very short, extending maximally for half distance between its base and base of interopercular odontodophore; slightly longer in smaller specimens. Posterior point of its base anterior to vertical through anterior margin of eye in lateral view. Rictal barbel tiny, vestigial, undifferentiated externally in some specimens, located mesially to base of maxillary one. Nasal barbel vestigially represented by posterior elongated portion of fold around anterior naris described above, with double internal elastin core.

Lateral line short and straight, extending alongside dorsal margin of anterior portion of axillary gland. Terminal lateral-line pore immediately dorsal to axillary gland opening. Very short secondary branch splitting off ventrally from proximal portion of main canal, with corresponding pore opening anteriorly to midlength of main canal. Single lateral-line tubule poorly calcified, extending over part of main canal posterior to bifurcation.

Pectoral fin short (68.8-75.8% HL), roughly triangular in shape when expanded and gently convex anterior and posterior margins, its base on ventral half of body in lateral view. Pectoral-fin rays i + 5, with first ray not longer than other rays. Pelvic fins well separated from each other at base, with i + 4 rays. Pelvic splint present. Origin of pelvics close to origin of anal fin, well anterior to vertical through origin of dorsal-fin, entirely covering anus and urogenital papilla and extending posteriorly to origin of anal fin. Posterior margin of pelvic fin gently convex. Dorsal fin elongate, roughly triangular with roundish edge and gently convex distal margin. Dorsal-fin rays ii + 6, plus 5 or 6 procurrent ones. Anal fin similar in shape to dorsal fin, with ii + 5 rays, plus 6 or seven procurrent ones. Origin of anal fin at or slightly posterior to vertical through origin of dorsal-fin. Caudal fin roughly rectangular, truncate with round edges and gently convex margin, as deep or deeper than maximum depth of caudal peduncle. Principal caudal-fin rays 6 + 7 in all specimens. Procurrent caudal-fin rays 19-21 dorsally and 18-20 ventrally.

Vertebrae 40 (n = 2). First dorsal-fin pterygiophore subsequent to neural spine of vertebra 21 (n = 1) or 22 (n = 1). First anal-fin pterygiophore subsequent to haemal spine of vertebra 22 (n = 2). Dorsal-fin pterygiophores 7 (n = 2). Anal-fin pterygiophores 6 (n = 2). Branchiostegal rays 4.

**Pigmentation in preservative:** Body mostly white. Two irregular rows of dark chromatophores on dorsum, extending along both sides of dorsal midline to base of dorsal fin. Isolated dark chromatophores spread over dorsal sides of abdominal wall, exposed in specimens with distended abdomens, otherwise retracted as inconspicuous dark line along dorsal limit of abdominal cavity. Short row of dark chromatophores along dorsal margin of lateral line. Some specimens with isolated small spots along longitudinal skeletogenous septum. Posterior part of neurocranium with dark brain pigment seen by transparency,
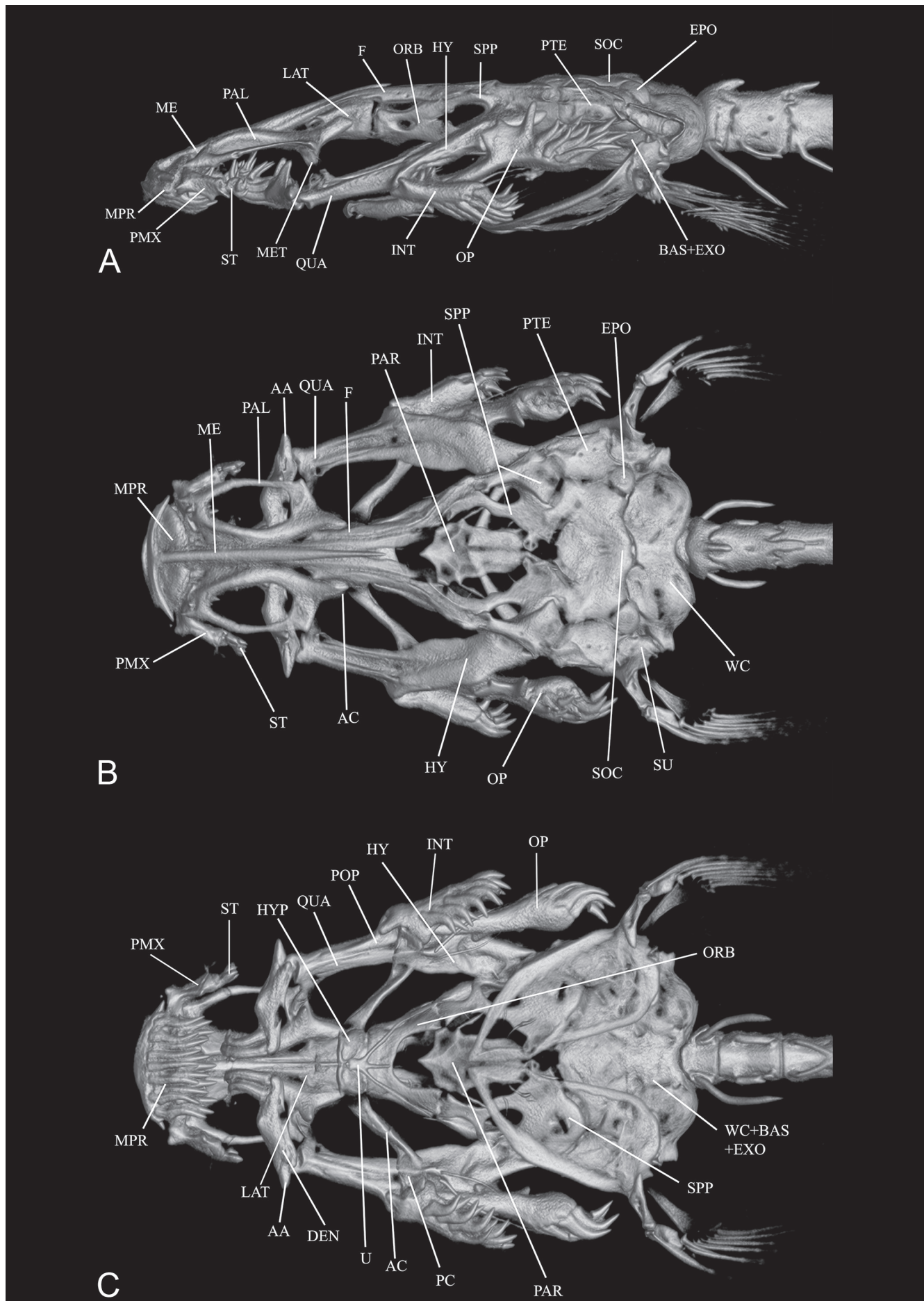
**Figure 26.** *Paracanthopoma malevola,* holotype, INPA 59836, CT scan images of head skeleton, (A) Lateral; (B) Dorsal; (C) Ventral.
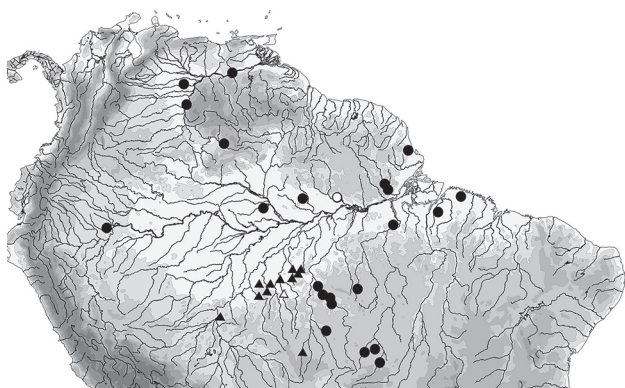
**Figure 27.** Map of northern South America showing geographical distribution of *Paracanthopoma irritans* (dot) and *Pc. malevola* (triangle). Open symbols represent type localities. Some symbols may represent more than a single locality or lot of specimens.

forming irregular spots or uniform dark covering with anterior white recess. Integumentary chromatophores around margin of neurocranium, extending anteriorly between eyes. Dense dark fields anteriorly to eyes, adjacent and sometimes continuous with dark ring outlining nasal capsule. Margin of snout white. Dark spots around dorsal and anterior margins of opercular odontodophore. Dark line along dorsal, anterior or medial margins of interopercular odontodophore in some specimens. Most specimens with narrow dark markings along anterior margin of median premaxilla in ventral view. Regular series of spots, one per vertebra, along caudal peduncle, formed by internal chromatophores and gradually fading anteriorly. Few scattered spots on base of caudal-fin rays.

**Etymology:** From the Latin malevolus, meaning ill-disposed, inimical. An adjective.

**Geographical distribution:** *Paracanthopoma malevola* has been recorded from tributaries of the rio Madeira basin draining the Brazilian shield such as the rio Aripuanã, Machado, and Sucunduri. It is also found in the upper rio Madeira, in a tributary of the rio Mamoré, and in the upper rio Juruena (rio Tapajós basin) (Fig. 27).

**Remarks:** Specimens in MZUSP 122243 differ from other samples of the species in having a much broader head, which expands abruptly at approximately the transverse line through the middle of the eyes. In typical *Paracanthopoma malevola,* the head is not only narrower but also widens gently and evenly along its length. While such differences result in striking visual distinctiveness in head shape, we found no additional corroborative evidence indicative of separate specific status and thus consider the rio Roosevelt sample as a populational variation of *Pc. malevola.*

### *Paracanthopoma parva* Giltay, 1935
### (Fig. 28)

*Paracanthopoma parva* Giltay, 1935: 1, figs. 1-3 [type locality: Brésil, Rio Catrymany supérieur, type: IRSNB 43,

cotype: IRSNB 602 (1)] – Gosline, 1945: 66 [catalogue] – Walschaerts, 1987: 16-17 [type catalog] – Burgess, 1989: 324 [checklist] – Schmidt, 1993 [in part, only c&s specimen AMNH 72898SW, later designated as paratype of *Paravandellia alleynei* Henschel *et al.,* 2021b and recatalogued as AMNH 72899SW; occurrence in Essequibo drainage, Guyana; figs. 1, 3 (cephalic latero-sensory canals; jaws; dentition)]. – Eschmeyer *et al.,* 1998: 1292 [catalog] – Spotte, 2002: 97 [historical account; summary of previously published information] – de Pinna & Wosiacki, 2003: 276 [checklist; geographical distribution] – Zuanon & Sazima, 2005 [feeding behavior; phoresis on body of host] – Ferreira *et al.,* 2007: 190 [list, occurrence in rio Branco] – Ferraris, 2007: 410 [checklist] – Wosiacki & de Pinna, 2007: 73 [catalog]; Henschel *et al.,* 2021b [redescription and data on type specimens; anatomy; comparisons;; CT-scan images of head skeleton; invalid lectotype designation].

### Material examined

**Type material:** IRSNB 43, 1 ex, holotype of *Paracanthopoma parva* Giltay, 1935, 24.3 mm SL, Brazil, Roraima, upper rio Catrimani (trib. to rio Branco), col., C. Lako and G. Salathé; IRSNB 602, 1 ex, paratype of *Paracanthopoma parva* Giltay, 1935, 25.2 mm SL, collected with holotype; AMNH 72899SW (originally AMNH 72899SW), 1 ex (c&s), 22.0 mm SL, paratype of *Paravandellia alleynei.*

**Non-type material: BRAZIL: rio Araguaia:** MZUSP 53594, 1 ex, 20.7 mm SL, Mato Grosso, rio Araguaia, near Araguaiana, col., unknown, Jul 1997; MZUSP 53824, 19 ex (4 c&s), 20.4-29.7 mm SL, Mato Grosso, rio Araguaia near Araguaiana (from the branchial chamber of *Rhaphiodon* sp.), col., unknown, Jul 1997; MZUSP 89181, 5 ex 14.0-17.5 mm SL, Mato Grosso, Cocalinho, rio Araguaia, col., unknown, 25 Jul 2005; MZUSP 104095, 5 ex, 24.5-26.4 mm SL, Tocantins, Ananás, rio Araguaia, near border of São Geraldo do Araguaia (06°08'24"S, 48°19'47"W), col., G. Baumgartner *et al.,* May 2009; **rio Branco:** CAS 118205, 1 ex, 24.1 mm SL, Amazonas, upper rio Catrimani, col., S. Lako; INPA 8158, 2 ex, 14.9-15.7 mm SL, Roraima, rio Tacutu (= Itacutu), next to the market, col., J.A.A. Gomes and J. Zuanon, 26 Mar 1992; INPA 16555 (mixed with 6 ex of *Pc. alleynei*), 2 ex (1 c&s), 21.2-22.4 mm SL, Roraima, Boa Vista, Maracá, rio Branco, col., O. Bitar, May 1988; **rio Jari:** MZUSP 100234, 1 ex, 19.1 mm SL, Amapá/Pará, rio Jari, above Cachoeira de Santo Antônio, between Porto Sabão and 5 km above mouth of rio Uiratapuru (00°37'02"S, 52°31'35"W), col., C.R. Moreira & F.A. Bockmann, 20-24 Feb 2008; MZUSP 126876, 2 ex, 17.4-17.7 mm SL, Amapá, Laranjal do Jari, Igapó on left margin of rio Jari, upstream from mouth of rio Iratapuru, upstream from Cachoeira de Santo Antônio (00°35'05"S, 52°36'59"W), col., J. Birindelli *et al.,* 22 Feb 2009 (collected with *Pc. irritans,* MZUSP 103511); MZUSP 104874, 2 ex, 21.3-21.6 mm SL, Pará, Monte Dourado, rio Jari, right margin, in front of

mouth of Igarapé Carrapatinho, upstream from Cachoeira de Santo Antônio (00°35'39"S, 52°38'36"W), col., M.C. Soares & M.R. Carvalho, 02 May 2009; **rio Madeira:** MNRJ 15422, 11 ex, 20.7-25.0 mm SL, Rondônia, Nova União, rio Urupá (trib. to rio Machado), col., unknown, 13 Jul 1986; MZUSP 13994, 5 ex, 26.2-29.0 mm SL, Rondônia, Paraíso, channel of rio Machado (from body of *Brachyplatystoma filamentosum*), col., M. Goulding, 06 May 1978; MZUSP 30397, 1 ex, 26.8 mm SL, Rondônia, Paraíso, rio Machado (from dorsal fin of *Brachyplatystoma filamentosum*), col., M. Goulding, 20 May 1978; MZUSP 30400, 10 ex (3 c&s, 1 head removed for SEM), 26.6-30.4 mm SL, Rondônia, Independência, rio Machado (main channel) (from body of *Brachyplatystoma filamentosum,* 39 kg), col., M. Goulding, 06 May 1978; MZUSP 30407, 1 ex, approx. 9 mm SL (specimen damaged), Mato Grosso, Aripuanã, rio Madeira (probably rio Aripuanã) (from *Brachyplatystoma filamentosum*), col., M. Goulding, 31 Dec 1979; **rio Negro:** MPEG 3329, 1 ex, 31.7 mm SL, Amazonas, Santa Isabel do rio Negro, rio Negro at Ilha de Tamaquaré, col., M. Goulding, 10 Oct 1979; MZUSP 29793, 2 ex, 20.3-25.2 mm SL, Amazonas, rio Negro at Cachoeira de São Gabriel (from body of "surubim", 40 cm), col., M. Goulding, 18 May 1979, MZUSP 100230, 2 ex, 19.2-25.0 mm SL, rio Negro at Cachoeira de São Gabriel, col., M. Goulding, 18 May 1979; **rio Tapajós:** LIRP 7668, 10 ex, 13.7-22.1 mm SL, Mato Grosso, Sapezal, rio Juruena (12°54'22.00"S, 58°55'01.00"W), col., R, Ilário, 21 Jan 2009; LIRP 12696, 3 ex 19.0-24.8 mm SL, Pará, Jacareacanga, rio Teles Pires (08°51'28"S, 57°25'10"W), col., M. Carvalho & A. Datovo, 04 Dec 2005; MZUSP 24277, 1 ex 12.6 mm SL, Pará, São Luis, rio Tapajós, col., EPA, 05 Nov 1970; MZUSP 63076, 25 ex (4 c&s), 15.5-32.6 mm SL, Mato Grosso, Nova
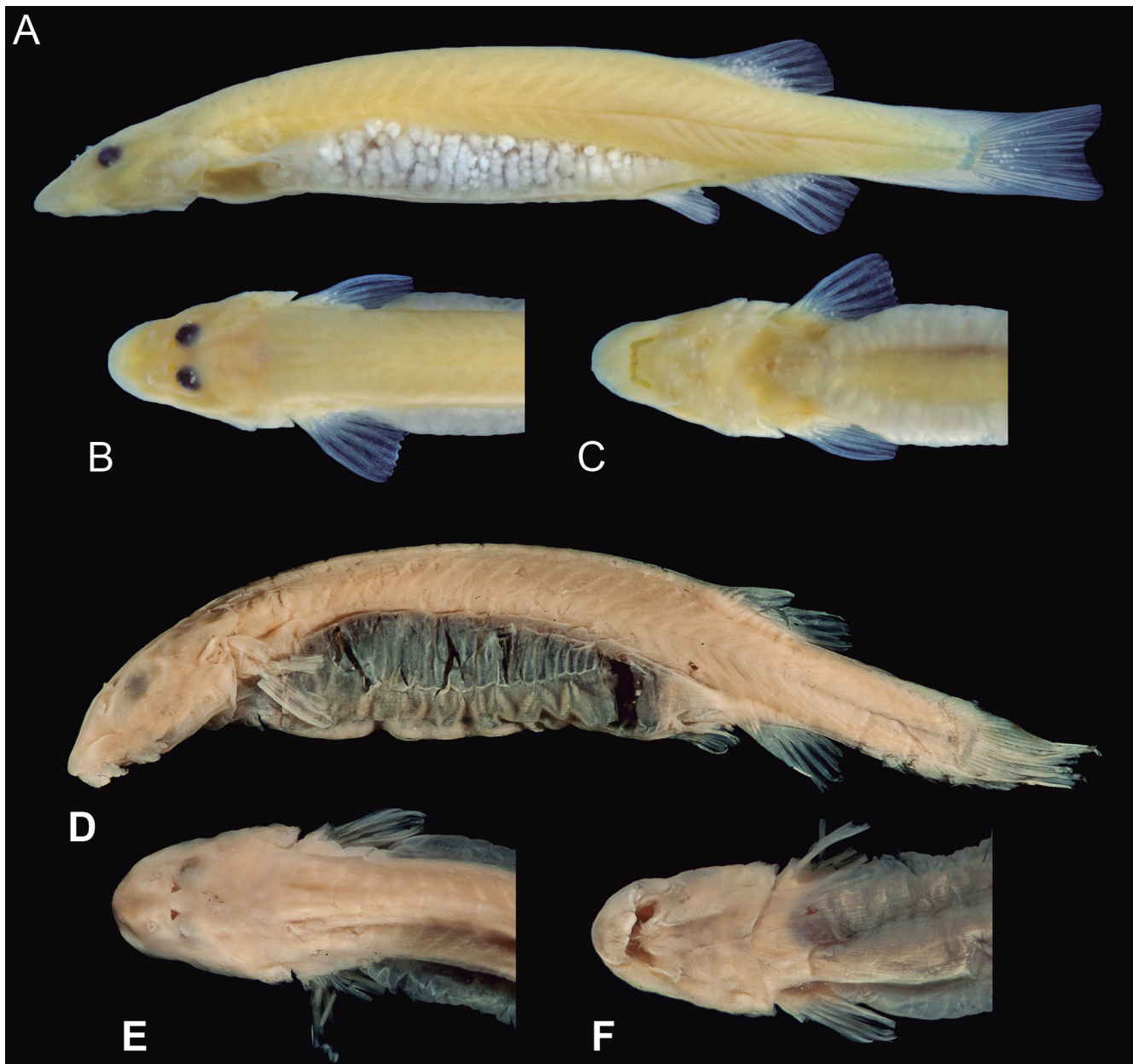


**Figure 28.** *Paracanthopoma parva,* MNRJ 15422, 22.7 mm SL, Brazil, Rondônia, Nova União, Rio Urupá. (A) Lateral view of body; (B) Dorsal view of head; (C) ventral view of head. CAS 118205, 24.1 mm SL, Brazil, Amazonas, upper Rio Catrimani. (D) Lateral view of body; (E) Dorsal view of head; (F) Ventral view of head.

Mutum, rio Arinos, col., H.F. Mendes, 16 Jan 1998; MZUSP 64923, 1 ex, 12.3 mm SL, Pará, Monte Cristo, rio Tapajós, lake on island in front of Monte Cristo, col., EPA, 08 Dec 1970; MZUSP 95662, 6 ex, 13.4-27.4 mm SL, Mato Grosso, Paranaíta, rio Teles Pires near ferryboat dock at road MT-416 (09°27′07″S, 56°30′46″W), col., L.M. Sousa & A.L. Netto-Ferreira, 27 Sep 2007; MZUSP 95934, 1 ex, 27.8 mm SL, Mato Grosso, Itauba, rio Teles Pires (10°58′30″S, 55°44′03″W), col., J.L.O. Birindelli & P. Hollanda-Carvalho, 01 Oct 2007; MZUSP 96148, 1 ex, 15.5 mm SL, Mato Grosso, Paranaíta, submerged rocks at middle of rio Teles Pires (09°26′58″S, 56°29′19″W), col., L.M. Sousa & A.L. Netto-Ferreira, 28 Sep 2007; MZUSP 99703, 17 ex (2 mol), 21.3-27.4 mm SL, Mato Grosso, Itauba, rio Teles Pires, near Pousada Ana Lima (a local lodge) (11°00′40″S, 55°23′47″W), col., R.A.G. Fuentes, 23 Mar 2008; MZUSP 101366, 8 ex (1 SEM), 23.7-32.0 mm SL, Mato Grosso, rio Arinos (from *Brycon* sp. and *Pseudoplatystoma* sp.), col., H.F. Mendes, 14 Jan 2000; MZUSP 109848, 2 ex, 23.5-25.5 mm SL, Mato Grosso, Sapezal, rio Juruena at PCH (pequena central hidrelétrica) telegráfica (12°51′01″S, 58°55′38″W), col., R. Ilário, 31 Jan 2009; MZUSP 116411, 1 ex, 35.2 mm SL, Mato Grosso, Paranaíta, rio Apiacás (trib. to rio Teles Pires) (09°11′42.39″S, 57°05′05.31″W), col., W. Ohara, 19 Nov 2014; MZUSP 119276, 2 ex, 26.9-29.8 mm SL, Pará, Novo Progresso, rio Jamanxizinho (trib. to rio Jamanxin) (07°02′28.50″S, 55°41′20.72″W), col., O. Oyakawa *et al.,* 10 Aug 2015; MZUSP 126271, 8 ex, 22.1-26.3 mm SL, Mato Grosso, Novo Mundo, rio Rochedo (trib. to rio Teles Pires), under bridge on dirt road from Vila Cinco Mil and Vila do Rochedo (09°44′02.31″S, 55°42′02.70″W), col., O. Oyakawa *et al.,* 18 Oct 2017. **rio Tocantins:** MZUSP 40585, 29 ex (5 c&s), 18.2-27.2 mm SL, Goiás, Monte Alegre de Goiás, rio Paranã above the mouth of rio Bezerra, col., J.C. de Oliveira & W.J.E.M. da Costa, 10 Jan 1989; MZUSP 114443, 1 ex, 16.1 mm SL, Tocantins, Aurora do Tocantins, rio Palmas, at encounter with rio Sombra, at Balneário Douradas (12°48′11.3″S, 46°22′08.4″W), col., Oyakawa *et al.,* 01 Dec 2012; **rio Trombetas:** INPA 12420, 1 ex, 23.5 mm SL, Igarapé Caxipacoré, col., E. Ferreira, M. Jegú, 20 Apr 1985; MZUSP 15715-23, 6 ex (2 c&s), 19.6-27.2 mm SL, Pará, Trapiche da Sede da Reserva Biológica de Trombetas (from body of *Brachyplatystoma filamentosum,* 130 cm SL), col., R.M.C. Castro, 11 Jul 1979; **rio Xingu:** MZUSP 74624, 13 ex (1 head prepared for SEM), 17.2-25.4 mm SL, Mato Grosso, rio Xingu, Parque Indígena do Xingu, Posto Diauarum, col., G.R. Kloss, 08 Dec 1973; MZUSP 74650, 5 ex, 18.1-22.6 mm SL, same locality and collector as MZUSP 74624, 12 Dec 1973; MZUSP 87048, 1 ex, 27.4 mm SL, Mato Grosso, Gaúcha do Norte, rio Curisevo, Porto do Vitório, near Ribeirão Kevuaieli (13°02′05″S, 53°25′19″W), col., C. Moreira *et al.,* 19 Oct 2004 (collected together with *Pc. irritans* MZUSP 87049); MZUSP 91959, 3 ex, 22.1-29.4 mm SL, Mato Grosso, Paranatinga, rio Culuene, at the planned site of upcoming hydroelectric dam Paranatinga II (approx. 13°49′S, 53°15′W), col., J. Birindelli *et al.,* 21 Aug 2006; MZUSP 94143, 1 ex, 23.5 mm SL, Mato Grosso, Gaúcha do Norte, rio Culuene, Fazenda do Sr. Zezé (*ca.* 2 km above

bridge) (13°30′53″S, 53°05′40″W), col., F.C.T. Lima *et al.,* 21-26 May 2007; MZUSP 97190, 2 ex, 26.8-28.5 mm SL, Pará, Altamira, rio Curuá (trib. to rio Iriri), at village of Castelo dos Sonhos (08°19′07″S, 55°05′23″W), col., J.L. Birindelli *et al.,* 22 Oct 2007; MZUSP 111769, 1 ex, 14.9 mm SL, Pará, Altamira, rio Xingu, island beach immediately downstream from Vila de Belo Monte (03°05′52″S, 05°44′12″W), col., O. Oyakawa *et al.,* 13 Nov 2011. **COLOMBIA:** FMNH 94767, 1 ex, 29.6 mm SL, Vichada, río Tomo near Puerto Borracho (río Orinoco drainage), col., W.W. Lamar, 17 Feb 1979. **ECUADOR:** FMNH 99519, 2 ex, 20.2-25.2 mm SL, río Aguarico, near Destacamiento Militar Cuyabeno and confluence of río Cuyabeno and río Aguarico (río Napo drainage), col., D. Stewart *et al.,* 21 Oct 1983. **GUYANA:** ANSP 179207, 2 ex, 24.0-29.7 mm SL, Rupununi (Region 9), Ireng River, 6.9 km WSW of village of Karasabai (04°01′10″N, 59°36′06″W), col., M.H. Sabaj *et al.,* 01 Nov 2002; ANSP 180020, 3 ex, 10.5-13.3 mm SL, Rupununi (Region 9), Takutu River, 3.77 km SSW of Lethem (03°21′18″N, 59°49′51″W), col., M. Sabaj *et al.,* 16 Nov 2003; MHNLS 21614, 1 ex, 14.3 mm SL, Essequibo River at Akuthopono Rocks (01°39′02,4″N, 58°37′40,5″), col., C. Lasso, J. Señaris, A. Eustace, 25-26 Oct 2006 (Mixed with 1 ex of *Ochmacanthus* cf. *flabelliferus*). **PERU:** ANSP 180483, 1 ex, 22.8 mm SL, Madre de Dios, río Manuripe (Orton-Madre de Dios drainage), road crossing at town of Mavila (11°55′44″S, 69°07′15″W), col., M. Sabaj *et al.,* 31 Jul 2004; MUSM 4562, 3 ex 22.9-25.4 mm SL, Madre de Dios, Parque Nacional Manu, Manu, Pakitza, río Manu, col., H. Ortega, 22 Jun 1993 (collected together with *Paravandellia* sp. MUSM 20672); MUSM 20674, 1 ex 24.3 mm SL, Madre de Dios, Manu, Parque Nacional Manu, Panagua, rio Manu, col., W. Valle, 06 May 1991; INHS 42780, 1 ex 24.0 mm SL, Loreto, río Nanay, Sabolla Cocha, near Sabolla (río Amazonas drainage), col., C. Chuquipiondo Guardia, 28 Jul 1997; USNM 357993, 2 ex, 22.4-24.8 mm SL, Madre de Dios, Manu, Parque Nacional Manu, Pakitza, río Manu close to mouth of río Panahua, col., W. Valle, 06 May 1991 (collected together with *Paravandellia* sp. USNM 317775). **VENEZUELA:** MCNG 22882, 1 ex, 25.1 mm SL, Amazonas, Atabapo, Ventuari, río Paru, 10 km upstream from confluence with río Asisa (04°40.00′N, 65°58.00′W), col., L. Nico, E. Guayamore, 02 Oct 1989.

**Diagnosis:** Distinguished from all congeners except *Pc. carrapata, Pc. daemon,* and *Pc. truculenta* by the presence of nine (*Pc. daemon* occasionally with 10) teeth on the median premaxilla (vs. 3 to 5 or 11 and more); by the presence of a single median s6 pore, visible on the middle of skull posterior to eyes (vs. paired s6 pores, distant from midline of skull), and by the supraoccipital anteriorly produced into large pointed spike (vs. either anteriorly concave or straight across skull roof). Distinguished from all congeners except *Pc. carrapata* and *Pc. truculenta* by the posterior margin of the anal fin well posterior to vertical through that of the dorsal fin (vs. margins of two fins approximately at same vertical or that of anal fin only slightly posterior to that of dorsal fin); and by the

deeply emarginate, bilobed caudal fin (vs. truncate with round corners or only slightly concave). Distinguished from *Pc. carrapata* and *Pc. truculenta* by lacking an extensive invasion of the skull roof by head musculature, with widest exposed part of neurocranium wider than interorbital (vs. exposed part of neurocranium reduced, approximately equivalent to interorbital); and by the larger opercular and interopercular odontodophores, approximately as large as eye (vs. odontodophores smaller than eye). Distinguished from *Pc. carrapata* by having smaller median premaxillary teeth, with the distal (post-bend) portion as large as the basal portion (vs. distal portion larger than basal one); by the longer interopercular odontododes, where the largest odontode is longer than the long axis of the interopercle (vs. largest odontode smaller than the long axis of the bone); and by the interopercular odontodes inserted partly towards the ventral margin of the interopercle, with their insertions tile-like at that area (vs. odontodes clustered at the distal end of the bone, with their insertions at approximately the same plane). Distinguished from *Pc. truculenta* by having four or five opercular odontodes, clearly visible on surface of skin (vs. opercular odontodophore very reduced, bearing only one or two odontodes not protruding from surface of head, sunk in small slit of integument).

**Description:** Morphometric data for the holotype and paratypes are provided in Table 9. Body short (HL 18.0-22.1% SL) (Fig. 28). Cross-section of body slightly broader than deep at pectoral-fin insertion and increasingly compressed posterior to that point, tapering to caudal fin. Dorsal profile of body straight from head to origin of dorsal fin (Fig. 28), except in specimens preserved with curved vertebral column, often those with full guts, where it is convex. Dorsal and ventral profiles of caudal peduncle straight and converging towards midline along anterior half and straight or slightly convex and diverging along posterior half, sometimes angulate at beginning of procurrent caudal-fin rays. Caudal peduncle narrow, but expanded by procurrent rays along posterior third or half. Proportion of expansion greater in smaller individuals, with most of peduncle expanded, paddle-shaped, in very small specimens, *ca.* 11-14 mm SL (*e.g.,* ANSP 180020). Ventral profile of body gently convex until pelvic-fin origin (Fig. 28), with some specimens with greatly distended abdomens due to gut contents. Myotomes and longitudinal skeletogenous septum clearly visible along whole body. Axillary gland very large, elongate in shape, protruding markedly on surface of body and making anterior pat of trunk widest part of fish (except in those with distended abdomens). Anterior end of gland surrounding dorsal, ventral and posterior surfaces of muscular pectoral-fin, as thick corselet, extending posteriorly to beyond margin of adpressed pectoral fin (for at least 50% of fin length, sometimes 100%). Gland tapering to fine posterior tip, its large round or oval pore located at is midlength, approximately at vertical through beginning of last third of pectoral fin. Condition of gland posterior to pore evidently related to amount of secretion stored. In some specimens, post-

**Table 9.** Morphometric data of *Paracanthopoma parva*. Ranges, mean and SD include types. Head subunits were obtained with an ocular micrometer and therefore as projections. **Abbreviations:** hol = holotype; par = paratype; min = minimum value; max = maximum value; n = number of specimens; SD = standard deviation.

| | n | hol | par | min | max | Mean | SD |
|---|---|---|---|---|---|---|---|
| Standard length (mm) | 17 | 24.3 | 25.2 | 22.7 | 29.5 | 26.0 | |
| **Percentages of SL** | | | | | | | |
| Total length | 17 | 1.1 | 1.1 | 1.1 | 1.1 | 1.1 | 0.0 |
| Body depth | 17 | 12.6 | 15.3 | 10.2 | 15.4 | 12.1 | 1.7 |
| Caudal peduncle length | 17 | 17.8 | 17.0 | 15.0 | 19.6 | 17.3 | 1.3 |
| Caudal peduncle depth | 17 | 8.3 | 8.2 | 5.9 | 8.4 | 7.1 | 0.8 |
| Predorsal length | 17 | 72.5 | 71.6 | 68.4 | 74.6 | 71.2 | 1.7 |
| Preanal length | 17 | 73.6 | 72.0 | 71.8 | 78.9 | 76.1 | 2.5 |
| Prepelvic length | 17 | 65.0 | 66.7 | 62.9 | 70.5 | 67.1 | 2.3 |
| Dorsal-fin base length | 17 | 6.7 | 8.2 | 5.2 | 8.2 | 6.6 | 0.9 |
| Anal-fin base length | 17 | 4.8 | 6.2 | 4.4 | 6.2 | 5.3 | 0.6 |
| Pectoral-fin length | 17 | 13.3 | 12.8 | 10.8 | 14.4 | 12.8 | 0.8 |
| Head length | 17 | 20.2 | 21.3 | 18.0 | 22.1 | 20.0 | 1.3 |
| **Percentages of HL** | | | | | | | |
| Head width | 17 | 67.1 | 68.3 | 57.1 | 68.3 | 64.1 | 3.4 |
| Head depth | 17 | 41.8 | 39.5 | 32.3 | 42.9 | 38.2 | 3.0 |
| Pectoral-fin length | 17 | 65.9 | 60.0 | 56.1 | 70.2 | 64.0 | 4.8 |
| Interorbital | 17 | 12.9 | 14.9 | 10.2 | 17.6 | 12.6 | 1.9 |
| Eye diameter | 17 | 16.1 | 14.9 | 11.5 | 18.6 | 15.1 | 1.6 |
| Snout length | 17 | 44.1 | 44.5 | 39.8 | 46.9 | 42.8 | 2.5 |
| Mouth width | 17 | 19.6 | 25.7 | 19.6 | 31.6 | 27.5 | 2.9 |
| Anterior internarial width | 17 | 22.2 | 20.9 | 16.6 | 22.2 | 18.9 | 1.8 |
| Posterior internarial width | 17 | 9.4 | 11.4 | 5.5 | 11.5 | 8.3 | 1.6 |

pore part of gland appearing as nearly absent, clearly due to empty condition of its lumen.

Dorsal profile of head continuous with that of dorsum, sometimes indicated by slight muscle constriction. Head longer than broad (head width 57.1-68.3% HL), snout broad, parabolic with a round tip, sometimes with central portion of snout slightly differentiated (Figs. 28, 29). Muscles covering most of dorsal part of head, with head width varying between 3 to 4 times the width of exposed skull roof in dorsal view. Exposed area proportionall larger in small specimens. Head deep for *Paracanthopoma* (head depth 32.3-42.9% HL), with dorsal profile straight and horizontal until eye in lateral view, then angled ventrally an straight to tip. Eye large (11.5-18.6% HL), without free orbital rim, located dorsolaterally on head and directed dorsolaterally, with pronounced dorsal component (Fig. 28). Integument over eye thin at middle, thick and opaque at margin. Middle of eye almost exactly at middle of HL, interorbital width approximately 75% of longitudinal diameter of eye. Eyelens very large, occupying most of lateral surface of eye and either entirely unconstricted by iris or constricted only marginally, with large round pupil, in specimens examined. Anterior nostril small, located in narrow teardrop-shaped slit on surface of skin and surrounded by short tubule of integument produced posteriorly into small pointed process (Fig. 29), with double elastin cores. Anterior internarial width slightly larger than interorbital. Posterior naris slightly larger than anterior ones, round or triangular in shape, partly occluded by anterior flap of integument.

Posterior naris positioned anteromesially to eye, their middle at, or posterior to, transverse line through anterior margin of eyes. Posterior internarial width narrower than interorbital.

Opercular odontodophore medium-sized, dorsolaterally located on head, on dorsal half of head depth in lateral view. Opercular odontodes 4 or 5, closely positioned as two very large ones juxtaposed posteriorly and two or three smaller anterior ones. Main axis of opercular odontodes oriented horizontally in lateral view, with their distal portion curved dorsoposteriorly. Two or three caps of replacement odontodes posteriorly to mature ones. Interopercular odontodophore either similar-sized, slightly larger or slightly smaller than opercular one, located ventrolaterally on head, immediately ventral to horizontal through origin of pectoral fin, with 3 (rarely) to 5 (modally 4) odontodes closely positioned in single row of three or four near posterior edge of interopercle, plus single smaller one anteriorly (when 5). Interopercular odontodophore much closer to opercular one than to eye. Two or three replacement tooth caps located posteromesially to mature ones. Interopercular periodontodal fold of integument well-developed, nearly round and extending well-beyond tips of odontodes. Epiodontodeal velum thick, covering odontodes almost or quite to internal rim of periodontodal fold.

Mouth inferior (ventral), often filled with tightly bitten chunks of meat, supposedly from host fish, often entirely hiding internal mouth morphology. Each premaxilla with single scalpelloid teeth attached to its distal tip (visible only in skeletal preparations), but actually two adjacent tooth sockets, one of which normally vacant, corresponding to half-formed replacement tooth adjacent to mature one (**Figs. 4H, 30**). Vacant socket position varying among specimens, being either lateral or mesial one. Normally two additional initial-stage replacement caps suspended in soft tissue dorsally to mature one and its incomplete neighbor. Mature scalpelloid tooth with distal portion disproportionately reduced and very strongly curved over rest of teeth, with pungent tip nearly adpressed to margin of basal plate. Scalpelloid tooth deeply hidden in labial tissue, but its distal surface easily emerging when premaxilla forcibly abducted. Conical teeth absent in premaxilla. Upper lip thick, ventral surface of its anterior region deeply plicate longitudinally (Fig. 29). Lateral portions of upper lip with less numerous oblique plicae, only on its parabucal surface. Median premaxilla very large, with 9 teeth disposed in one anterior row of four (convex anteriorly), one posterior row of four (convex posteriorly) plus single middle tooth (**Figs. 4H, 30**). All teeth perpendicular to ventral surface of median premaxilla basally, but strongly curved posteriorly at distal pungent portion, those on anterior row taller than on posterior one. All median premaxillary teeth strongly laterally compressed basally. Median premaxillary dentition occupying almost all of upper jaw and most of interior of mouth. Many replacement tooth caps posterodorsally to mature dentition, creating confusing aspect to posterior limit of median premaxillary dentition. Median premaxillary velum absent. Hypodontal pad of median premaxilla thickly cushioning teeth. Lower jaw wide, occupied mostly with large den-
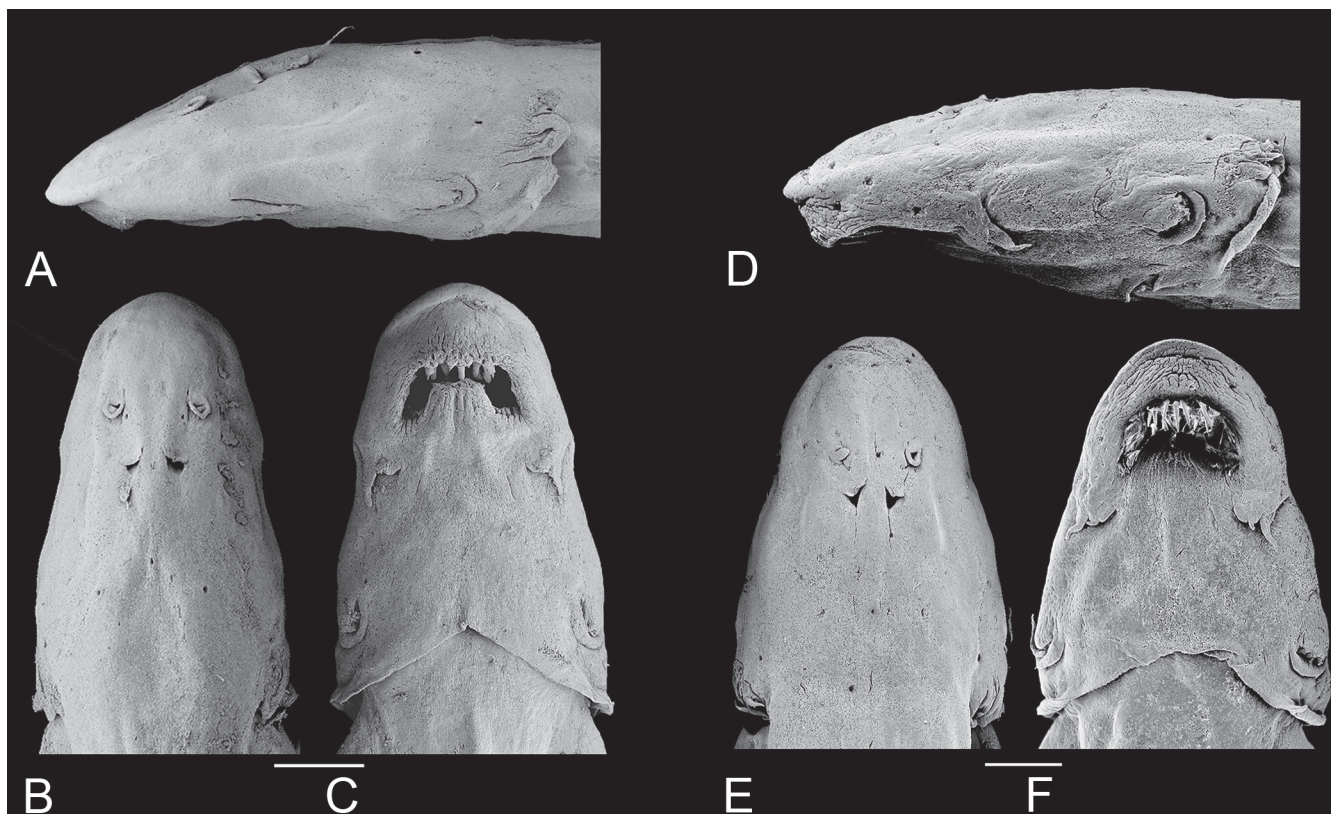


**Figure 29.** *Paracanthopoma parva,* SEM images of head. MZUSP 30400, (A) Lateral view; (B) Dorsal view; (C) Ventral view; MZUSP 74624, (D) Lateral view; (E) Dorsal view; (F) Ventral view.
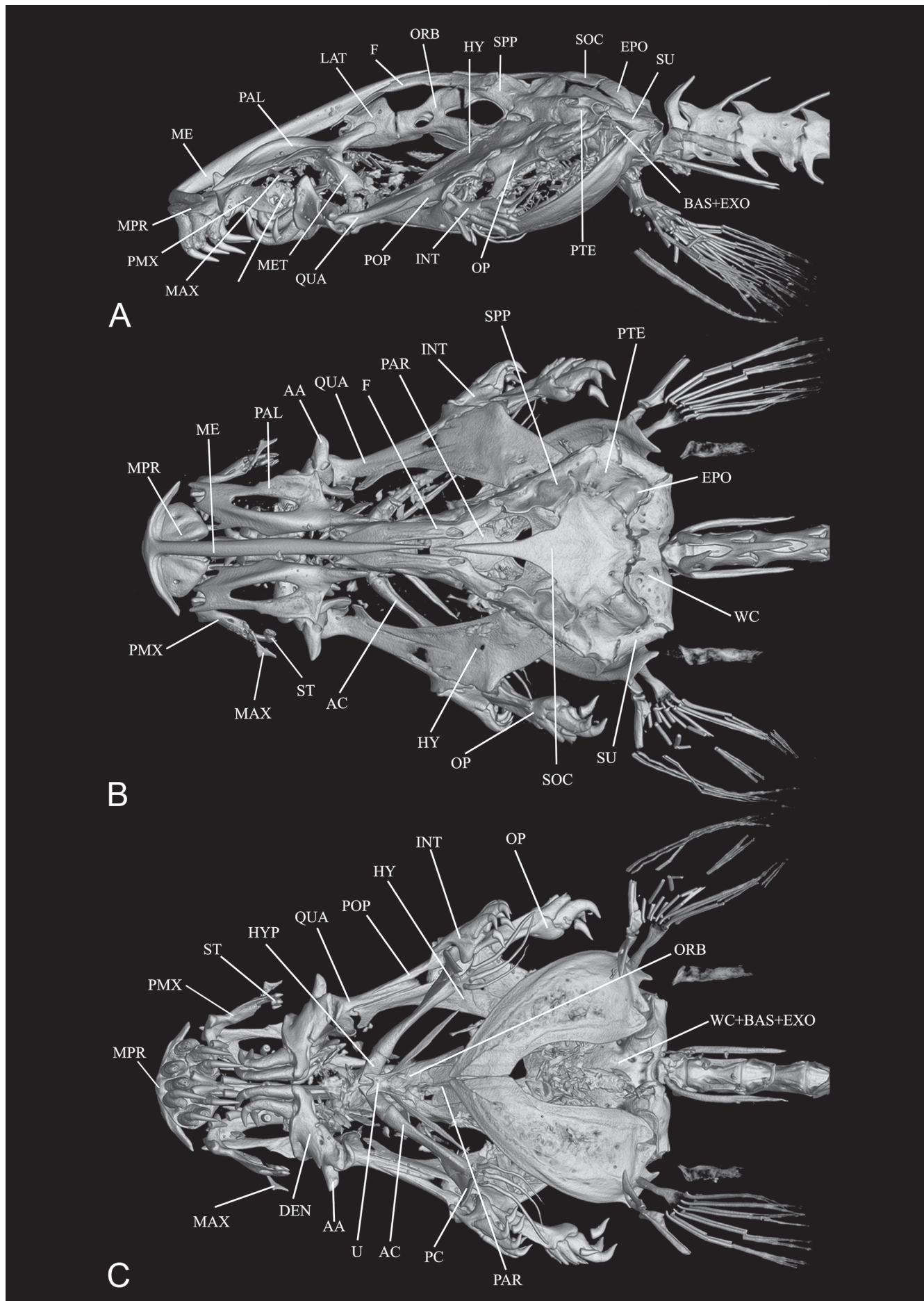
**Figure 30.** *Paracanthopoma parva,* CAS 118205, Brazil, Amazonas, upper Rio Catrimani. CT scan images of head skeleton, (A) Lateral; (B) Dorsal; (C) Ventral.

tary lobes nearly entirely fused to each other at midline, continuous with mental region posteriorly, and deeply plicate longitudinally. Jaw cleft deep and strongly directed posteriorly, approaching parallel to longitudinal axis and forming broad space separating lower jaw laterally from inner margin of upper jaw. Dentary diastema poorly differentiated, represented by small concave, sometimes angulate, area at midline, entirely absent in some specimens. Rami of mandible very close together at midline. Dentary teeth 4, closely packed at mesial end of dentary and disposed in two pairs, one dorsal and one ventral, with only latter visible in ventral view (Figs. 4H, 30). Axis of dentary teeth anteriorly-directed at base, but curved dorsolaterally distally. Branchiostegal region with large, continuous, and posteriorly concave branchiostegal velum (Fig. 29), with small median notch at midline in few specimens. Dorsal portion of branchial membrane reaching anterior margin of pectoral-fin base. Branchial membrane broadly attached to isthmus, leaving small branchial opening anterodorsally to pectoral-fin base, spanning approximately for area between ventral margin of opercular odontodophore and middepth of interopercular odontodophore. Maxillary barbel very short and proximally broad, its base flap-like, only distal portion filamentous (Fig. 29). Posterior point of is base anterior to vertical through anterior margin of eye, its tip extending posteriorly aproximately to vertical through posterior margin of eyes in lateral view. Mesial (or ventral) part of maxillary-barbel base continuous with membranous outgrowth extending posteriorly from corner of mouth. Rictal barbel small, located mesially to base of maxillary one and approximately one-third or less of its size, its base immersed in membranous expansion at corner of mouth. Rictal barbel sometimes difficult to identify among irregularities of surrounding integument folds, but its homology with trichomycterid rictal barbel evident by well-developed internal core. In some specimens, no clear external component of rictal barbel. Nasal barbel vestigially represented by posterior elongated portion of fold around anterior naris described above, with double internal elastin core.

Lateral line short and straight, curved dorsally near posterior end in some populations (*e.g.*, MZUSP 53824) its terminal pore approximately at vertical through midlength of pectoral-fin, near dorsal margin of axillary pore. Short secondary branch splitting off ventrally from anterior portion of canal, with corresponding pore opening approximately at anterior third of main canal. Single lateral-line tubule extending for more than half of sector of canal posterior to bifurcation and dorsal bending.

Pectoral fin short (56.1-70.2% HL), with i + 5 rays. Distal margin of pectoral fin gently convex, its base immediately ventral to midline of body in lateral view. Pelvic fins small, well-separated from each other at base, with i + 4 rays. Pelvic splint present. Origin of pelvics located at, or slightly anterior to, vertical through origin of dorsal-fin, entirely covering anus and extending posteriorly to almost reach origin of anal fin. Posterior margin of pelvic fin round. Dorsal fin small, triangular with broadly round apex, gently convex distal margin and ii + 6 fin rays, plus

3 to 5 procurrent ones. Few specimens with iii + 5 rays, apparently resulting from third unbranched ray failing to split, rather than actual meristic difference. Anal fin small, slightly more elongate in shape than dorsal one, with gently convex distal margin and ii + 5 fin rays, plus 3 to 5 procurrent ones. Origin of anal fin at, or slightly anterior to, vertical through end of dorsal-fin base. Anal fin normally slightly smaller than dorsal one, but opposite in some specimens. Caudal fin strongly bilobed, with equal lobes or lower lobe slightly larger than upper one. Bilobal condition of caudal fin less pronounced in small individuals, with fin practically truncate by 12 mm SL (*e.g.*, ANSP 180020). Specimens at 15 mm SL, however, already with adult bilobed condition (*e.g.*, INPA 8158). Principal caudal-fin rays 6 + 7. Procurrent caudal-fin rays 15 to 19 dorsally and 14 to 18 ventrally.

Vertebrae 35 (n = 2), 36 (n = 10), 37 (n = 31), 38 (n = 19), 39 (n = 8) or 40 (n = 1). First dorsal-fin pterygiophore subsequent to neural spine of vertebra 18 (n = 3), 19 (n = 8, holotype), or 20 (n = 5). First anal-fin pterygiophore subsequent to haemal spine of vertebra 20 (n = 2), 21 (n = 6, holotype), 22 (n = 6) or 23 (n = 2). Dorsal-fin pterygiophores 7 (n = 15). Anal-fin pterygiophores 6 (n = 15). Branchiostegal rays 3 (n = 15; 4 rays on one side of one specimen in MZUSP 30400). Type specimens have 37 and 38 vertebrae.

**Pigmentation in preservative:** Most specimens nearly entirely white (Fig. 28). Neurocranium dark with brain pigment seen by transparency. Faint dark field along lateral surface of snout, anterodorsally to maxillary barbel base. Thin streaks of dark, sometimes reduced to small spot, also along anterodorsal margin of opercular odontodophore. Irregular dark cloud vertically crossing bases of principal caudal-fin rays, sometimes extending shortly horizontally along proximal portions of middle rays. Specimens in MZUSP 109848 (Fig. 32A) have a comparatively heavy dark pigmentation unlike any other samples of the species, including (in addition to traits described above) paired series of dark spots along each side of dorsal midline (this detail is also seen in a single juvenile specimen, MZUSP 114443), intense dark fields at bases of dorsal, anal and caudal fins and distal portion of hy-
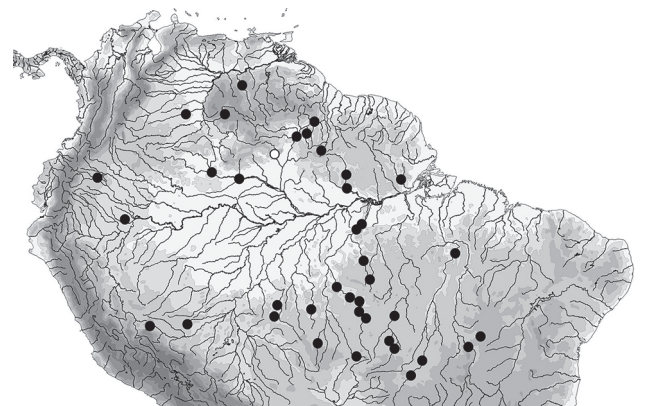


**Figure 31.** Map of northern South America showing geographical distribution of *Paracanthopoma parva*. Open symbol represents type locality. Some symbols may represent more than a single locality or lot of specimens.
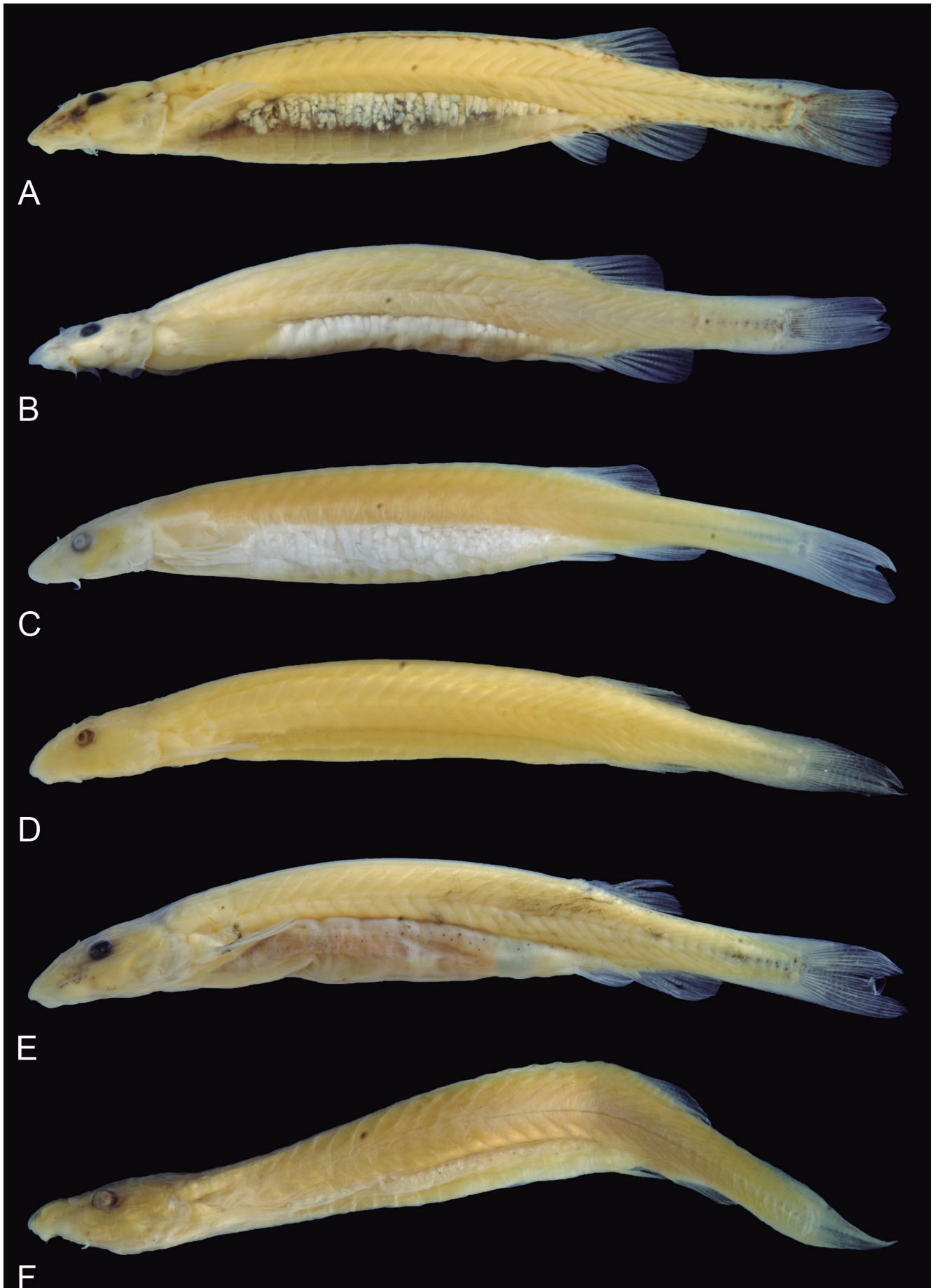
**Figure 32.** Variation in coloration, and body and head shape in *Paracanthopoma parva:* (A) MZUSP 109848 rio Juruena basin; (B) MZUSP 95662 rio Teles Pires basin; (C) MZUSP 13994 rio Machado basin; (D) MUSM 4562 rio Manu basin; (E) MPEG 3328 rio Negro basin; (F) FMNH 94767 rio Orinoco basin.

pural plate (latter two separated by narrow white band). Because those specimens have no additional co-varying characteristics which might indicate specific differentiation, they are considered as an unusual color morph of *Pc. parva*.

**Geographical distribution:** *Paracanthopoma parva* is widely distributed in the uplands of the Amazon, Essequibo and Orinoco drainages in Brazil, Colombia, Ecuador, Guyana and Peru (Fig. 31). In the Amazon, it occurs in upland sectors of most major northern and southern tributaries, but is conspicuously absent from lowland areas.

**Remarks:** *Paracanthopoma parva* is a variable species, in both details of body and head shape, and in pigmentation (Figs. 29, 32). A preliminary examination of the material available initially suggested the existence of various different species across the ample geographical range of what is here considered as *Pc. parva*. However, potentially distinguishing characteristics are of degree or proportion, rather than qualitative, and tend to vary continuously across populations, when enough representative material is available. The few discontinuities encountered are usually associated with lack of samples from intervening areas, generating suspicions about the significance of such apparent discontinuity. Obviously there is some degree of differentiation among some of the various disjunct populations of *Pc. parva,* but the level of clinal morphological variation indicates that they do not warrant recognition as separate species according to the criteria and data utilized in this work. But we do not rule out the possibility that more detailed studies, perhaps including genetic markers will find grounds for the recognition of additional species within what is here considered as *Pc. parva*.

Small specimens of *Paracanthopoma parva* (until *ca.* 14 mm SL; *e.g.,* ANSP 180020, MZUSP 95662) have a spatulate caudal peduncle, expanded dorsally and ventrally by large procurrent rays, markedly different from the narrow caudal peduncle of larger specimens. This juvenile morphology resembles the situation in species with small adult sizes, such as *Pc. irritans,* suggesting that the spatulate caudal peduncle in the latter is a paedomorphic feature. The smallest *Pc. parva* with evidence of ingested blood is a 10.5 mm SL specimen in ANSP 180020 (which also happens to be the smallest individual known of the species).

There are additional non-type specimens of *Pc. parva* collected from the same locality (upper rio Catrimany), approximate dates and collectors (Carlos Lako) as the types, namely MNRJ 4227, 3 ex (listed in Miranda-Ribeiro, 1947: 1) and CAS-SU 118205, the latter used for CT-scan imaging here (Fig. 30); the collector of the latter is listed on records as C. Laks, probably a misprint.

Henschel *et al.* (2021b) provide a redescription of *Paracanthopoma parva* based on the types and non-type specimens, along with the description of *Pc. alleynei*. The information on the types is most valuable and includes osteological data obtained with CT scan images. A lecto-type designation proposed in that paper (Henschel *et al.,* 2021b) is invalid. Giltay (1935: 1) had already designated one of the specimens as "Type" and the other as "Cotype" (and not jointly as "cotypes" as alleged in Henschel *et al.,* 2021b: 11) and this is sufficient discrimination as a holotype designation. In any event, the specimen chosen as the lectotype corresponds to the one originally labelled as "Type" by Giltay.

### *Paracanthopoma saci* Dagosta & de Pinna, 2021 (Fig. 33)

*Paracanthopoma saci* Dagosta & de Pinna, 2021 [Brazil, Mato Grosso do Sul, Alcinópolis, rio Taquarizinho (tributary to rio Taquari, rio Paraguay drainage) (18°12′14.8″S, 53°34′11.3″W)].

**Holotype:** MZUSP 125624, 19.6 mm SL, Brazil, Mato Grosso do Sul, Alcinópolis, rio Taquarizinho (tributary to rio Taquari, rio Paraguai drainage) (18°12′14.8″S, 53°34′11.3″W), alt. 363 m, col., F. Dagosta, A. Ferreira, R. Zanon, 18 Sep 2019.

**Paratypes:** MZUSP 125626, 13 ex (3 c&s), 14.5-21.8 mm SL, collected with holotype. MZUSP 125622, 2 ex, 19.5-19.9 mm SL, same locality and collectors as holotype, 17 Sep 2019. MZUSP 115585, 1 ex, 19.3 mm SL, Brazil, Mato Grosso do Sul, Alcinópolis, stream tributary to rio Taquari (rio Paraguai drainage) at dirt road between Alcinópolis and road MS-217 (18°12′16.5″S, 53°34′13.5″W), col., O.T. Oyakawa *et al.,* 26 Aug 2013.

**Diagnosis:** Distinguished from all other species of *Paracanthopoma* by the short and anteriorly-displaced opercular odontodophore, which leaves a large posterior free area of periodontodal fold surface continuous with the rest of the integument around it. As a consequence of that morphology, in dorsal view the posterior tips of the opercular odontodes do not reach the vertical through the base of the pectoral fin. Also unique in the genus is the three-rayed pelvic fin (vs. five) and the absence of an ascending process on the opercle. The presence of three teeth on the median premaxilla (vs five or more) also distinguishes *Pc. saci* from congeners (*Pc. ahriman, Pc. cangussu, Pc. capeta,* and *Pc. irritans,* all consistently with five median premaxillary teeth, often have one or two teeth in replacement, which may yield erroneous counts of three or four under superficial examination). Also distinguished from all congeners (except for extreme upper value in *Pc. cangussu*) by the long caudal peduncle (24.0-26.6% SL; vs. 14.7-24.0) and from all congeners except *Pc. satanica* by the anteriorly-located pelvic fin (prepelvic length 56.0-61.1% SL; vs. 61.6-74.4).

**Description:** Morphometric data for the holotype and paratypes are provided in Table 10. Body elongate (HL 15.1-16.1% SL). Cross-section of body as broad as deep at pectoral-fin insertion and increasingly compressed posterior to that point, tapering to caudal fin.

**Figure 33.** *Paracanthopoma saci,* holotype, MZUSP 125624, 19.6 mm SL. Brazil, Mato Grosso do Sul, Alcinópolis, Rio Taquarizinho. (A) Lateral view of body; (B) Dorsal view of head; (C) ventral view of head.

Dorsal profile of body in broad gentle arc, nearly straight, from head to origin of dorsal fin (Fig. 33). Dorsal midline with transparent fin fold anterior to dorsal fin. Dorsal and ventral profiles of caudal peduncle straight immediately posterior to ends of dorsal and anal fins, then expanded by dorsal and ventral procurrent caudal-fin rays resulting in symmetrically spatulate caudal peduncle (Fig. 33). Ventral profile of body nearly straight until pelvic-fin origin, but greatly distented in some specimens due to gut contents. Myotomes and longitudinal skeletogenous septum clearly visible through thin integument along whole body. Axillary gland large, elongate in shape, positioned dorsal to pectoral-fin base and extending posteriorly approximately to midlength of adpressed pectoral fin, its large round or oval pore located at its posterior terminus. Some specimens preserved with large amount secretion still attached to pore.

Dorsal profile of head continuous with that of dorsum. Head longer than broad (head width 83.6–100.0% HL), snout very broad, semicircular with a continuous round anterior margin (Fig. 33). Head muscles not entering skull roof. Head depressed (head depth 41.8–54.6% HL) with dorsal profile mostly continuous from nape to tip of snout. Ventral profile of head straight, flattened, though externally irregular due to integument folds. Eye medium-sized (11.3–13.6% HL), without free orbital rim, located dorsally on head and directed dorsolaterally. Integument over eye thin and transparent. Center of eye located slightly anterior to middle of HL, interorbital width equal to, or slightly larger than, longitudinal diameter of eye. Eyelens unconstricted by iris, entirely exposed on external aspect of eye. Anterior nostril small, surrounded by short tubule of integument produced posteriorly into small pointed process. Anterior internarial width slightly smaller than interorbital. Posterior naris slightly larger than anterior ones, oval (longer than broad) in shape, located close to anteromesial margin of eye. Center of posterior naris slightly anterior to transverse line through anterior margin of eyes. Posterior internarial width narrower than interorbital and approx-

imately twice as wide as anteroposterior length of one nostril.

Opercular odontodophore tiny, dorsolaterally located on head, on dorsal half of head depth in lateral view, anterodorsally to pectoral-fin base. Opercular odontodes 6, disposed in two irregular rows. Odontodes with distal portions curved medially. Opercular periodontodal fold vestigial or absent, instead fused with large well-delimited roundish area of thickened integument resembling a vastly hypertrophied periodontodal fold but being in fact a novel structure. Interopercular odontodophore min-

**Table 10.** Morphometric data of *Paracanthopoma saci.* Ranges, mean and SD include holotype. Head subunits were obtained with an ocular micrometer and therefore as projections. **Abbreviations:** min = minimum value; max = maximum value; n = number of specimens; SD = standard deviation.

| | n | holotype | min | max | mean | SD |
|---|---|---|---|---|---|---|
| Standard length (mm) | 8 | 19.1 | 15.4 | 21.1 | 18.1 | |
| **Percentages of SL** | | | | | | |
| Total length | 8 | 1.1 | 1.1 | 1.1 | 1.1 | 0.0 |
| Body depth | 8 | 13.1 | 11.7 | 15.7 | 13.9 | 1.5 |
| Caudal peduncle length | 8 | 25.1 | 24.0 | 26.6 | 25.0 | 1.0 |
| Caudal peduncle depth | 8 | 9.9 | 8.9 | 11.3 | 9.8 | 0.8 |
| Predorsal length | 8 | 68.6 | 66.5 | 69.2 | 68.1 | 0.9 |
| Preanal length | 8 | 67.5 | 65.5 | 68.8 | 67.2 | 1.1 |
| Prepelvic length | 8 | 60.2 | 56.0 | 61.1 | 59.4 | 1.5 |
| Dorsal-fin base length | 8 | 9.4 | 6.8 | 10.3 | 8.6 | 1.2 |
| Anal-fin base length | 8 | 11.0 | 7.6 | 11.0 | 9.0 | 1.1 |
| Pectoral-fin length | 8 | 11.5 | 9.7 | 12.3 | 10.8 | 0.8 |
| Head length | 8 | 15.7 | 15.1 | 16.1 | 15.6 | 0.4 |
| **Percentages of HL** | | | | | | |
| Head width | 8 | 83.6 | 83.6 | 100.0 | 89.1 | 5.1 |
| Head depth | 8 | 41.8 | 41.8 | 54.6 | 50.3 | 4.0 |
| Pectoral-fin length | 8 | 73.3 | 61.5 | 78.8 | 69.4 | 5.3 |
| Interorbital | 8 | 13.6 | 12.6 | 15.5 | 13.8 | 1.0 |
| Eye diameter | 8 | 12.7 | 11.3 | 13.6 | 12.8 | 0.7 |
| Snout length | 8 | 36.4 | 35.8 | 39.8 | 37.2 | 1.4 |
| Mouth width | 8 | 23.6 | 14.6 | 28.6 | 24.5 | 4.3 |
| Anterior internarial width | 8 | 15.5 | 14.6 | 21.8 | 17.2 | 2.5 |
| Posterior internarial width | 8 | 10.9 | 9.7 | 13.6 | 11.0 | 1.2 |

iscule, nearly invisible on surface of head, located ventrolaterally on head, horizontally aligned with origin of pectoral fin. Interopercular odontodes 4. Interopercular odontodophore closer to opercular one than to eye. Interopercular periodontodal fold absent or vestigial. Epiodontodeal velum absent.

Mouth inferior (ventral) and small, strongly flattened ventrally. Each premaxilla with one scalpelloid tooth attached to its distal tip, and one additional tooth socket with partly-formed tooth in parallel (Figs. 4I, 34). Scalpelloid teeth deeply hidden in labial tissue and difficult to expose in preserved specimens without damaging soft tissue. Conical teeth absent on premaxilla. Upper lip very broad but poorly-differentiated, continuous with ventral surface of snout. Median premaxilla miniscule, broader than long, with 3 closely-set tiny teeth (Figs. 4I, 34). Median premaxillary velum poorly-differentiated. Hypodontal pad of median premaxilla semicircular. Lower jaw narrow, composed mostly of produced dentary lobes, continuous with mental region posteriorly. Jaw cleft short, strongly directed posteriorly, but curved laterally at posterior end. Dentary diastema as deep median concavity between dentary lobes. Dentary teeth 4, large but difficult to visualize in alcoholic specimens, concentrated at mesial end of dentary and directed anteromesially, arranged in two ventral and two dorsal ones, not aligned (Figs. 4I, 34). Dentary teeth long, their axis anteriorly-directed at base, but curved dorsally or dorsolaterally at distal half. Median tooth of ventral row longer than others.

Branchiostegal velum forming large, continuous, round and posteriorly concave, free fold across whole of mental region. Dorsal portion of branchial membrane reaching and slightly overlapping anterior margin of pectoral-fin base. Branchial opening small, located anteriorly to pectoral-fin base, approximately equal to space between opercular and interopercular odontodophores. Maxillary barbel ranging from extremely short to vestigial, extending maximally for one-third distance between its base and base of interopercular odontodophore. Posterior point of its base slightly anterior to vertical through anterior margin of eye in lateral view. Rictal vestigial, reduced to small knob mesially to base of maxillary one, absent in some specimens. Nasal barbel vestigially represented by posterior elongated portion of fold around anterior naris described above.

Lateral line short, approximately half of pectoral-fin length, and straight, extending alongside dorsal margin of anterior portion of axillary gland. Terminal lateral-line pore immediately dorsal to axillary gland opening. Short secondary branch splitting off ventrally from proximal portion of main canal, with corresponding pore opening anteriorly to midlength of main canal. Single lateral-line tubule poorly calcified, extending over part of main canal immediately posterior to bifurcation.

Pectoral fin small (61.5-78.8% HL), with i + 4 rays in all specimens (except i + 3 in one side of one specimen). Pectoral-fin morphology with pronounced variation, with most specimens (n = 9, including holotype) having triangular pointed shape with first ray slightly longer than others. Some specimens (n = 5) with all rays equally long, resulting in a truncate fin profile. Two exceptional specimens in MZUSP 125626 (14.5 and 15.0 mm SL) with hypertrophied first pectoral-fin ray forming long filament. Filamentous ray corresponding to 36% SL in smaller specimen and 26% SL in larger specimen (*see* Remarks below). Pelvic fins minute, closely set together at base, with i + 2 rays (with all three rays unbranched in small specimens; one specimen with vestigial additional ray posteriorly). Pelvic splint present in single of three c& s specimens. Origin of pelvics close to origin of anal fin, well anterior to vertical through origin of dorsal-fin, extending posteriorly well beyond anus and urogenital papilla and slightly beyond origin of anal fin. Posterior margin of pelvic fin gently convex. Dorsal fin elongate, roughly triangular with roundish edge and gently convex, sinusoidal or straight distal margin. Dorsal-fin rays i + 5, ii + 5 or i + 6, plus prominent series of 5 to 8* procurrent ones. Anal fin similar in shape to dorsal fin, with i + 5 rays, plus 5 to 9 (8*) procurrent ones. Origin of anal fin at or slightly posterior to vertical through origin of dorsal-fin. Caudal fin roughly rectangular in normal preserved position but into more fan-like shape when expanded. Margin of caudal fin truncate with round edges and gently convex margin. Principal caudal-fin rays 5 + 5* or 4 + 5. Procurrent caudal-fin rays 22-29 dorsally and 20-29 ventrally.

Vertebrae 40 to 44 (42*, n = 10), with single specimen with 37. First dorsal-fin pterygiophore positioned subsequent to neural spine of vertebra 22 (n = 3). First anal-fin pterygiophore positioned subsequent to neural spine of vertebra 22 (n = 1) or 23 (n = 2). Dorsal- and anal-fin pterygiophores 6, poorly calcified or entirely cartilaginous, clearly visible only in c&s preparations. Branchiostegal rays 3.

**Pigmentation in preservative:** General aspect of fish almost entirely white. Post-orbital part of skull roof with extensive dark field formed by brain pigment seen by transparency, its anterior margin strongly concave, in continuous arc or angulate, immediately posterior to eyes. Well-defined elongate dark field extending anterior to eye, along lateral margin of olfactory capsule. In some specimens, mesial margin of olfactory capsule also with some dark pigment, but much weaker than lateral one. Dark pigment on body restricted to uniform web-like or dotted covering on dorsal part of abdominal wall and few isolated small spots along base of dorsal fin and, rarely, those of anal and caudal fins and muscular margins of caudal peduncle. Posterior portion of vertebral column with internal dark pigment on each individual vertebrae, forming series of spots visible externally by transparency along caudal peduncle (presumably more evident in life). All fins hyaline.

**Geographical distribution:** The species is so far known from a single locality in the rio Taquari system (rio Paraguay drainage) (Fig. 45). It is the only species of *Paracanthopoma* from the Paraná-Paraguay and in fact the only one from outside of the broad Amazonian drain-
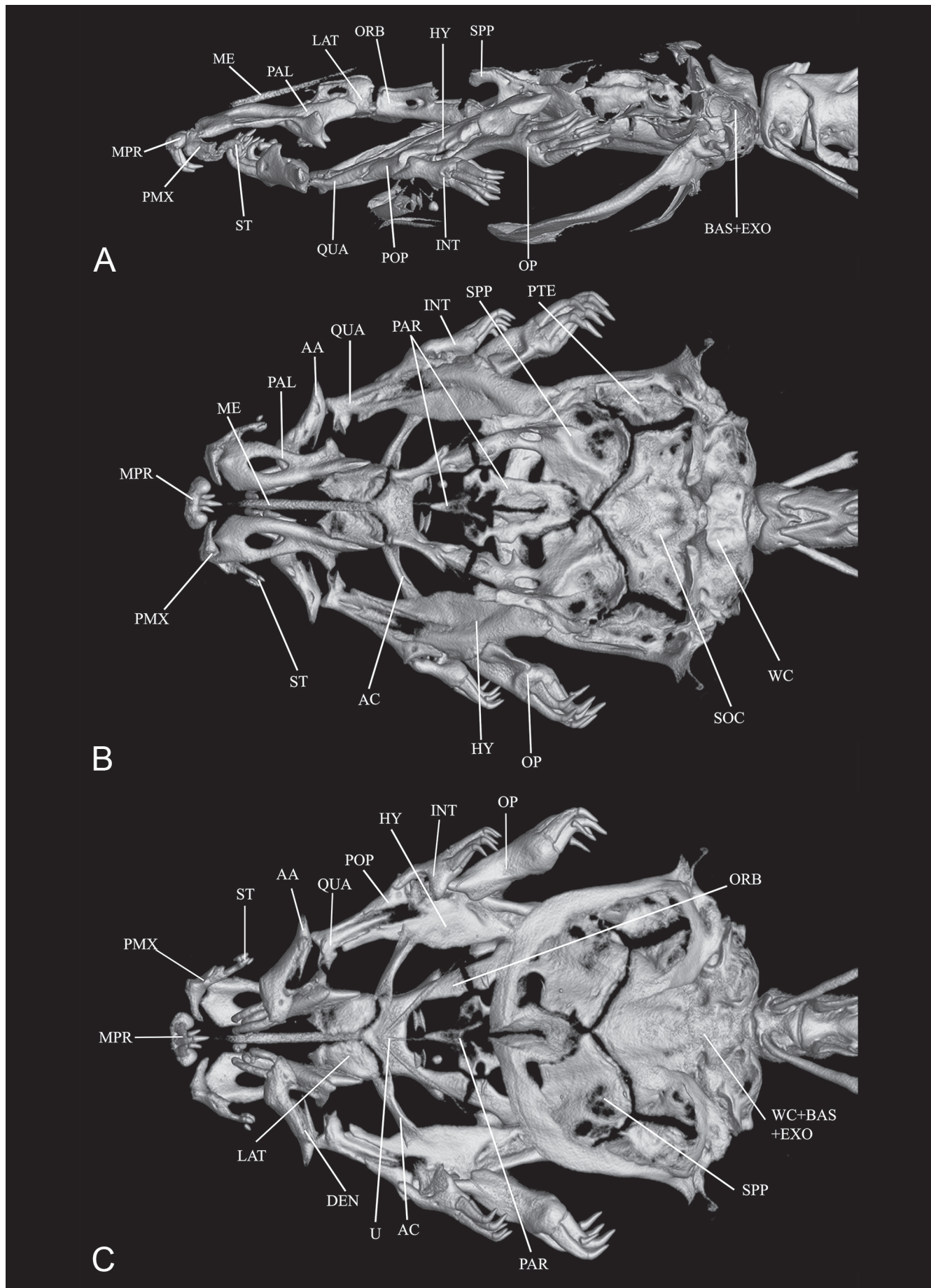
**Figure 34.** *Paracanthopoma saci,* holotype, MZUSP 125624, CT scan images of head skeleton, (A) Lateral; (B) Dorsal; (C) Ventral. Specimen poorly calcified, some structures not properly shown.

ages (Amazon, Orinoco, Essequibo and coastal Guyanan drainages). It also marks the southernmost limit of the genus.

**Ecology:** The rio Taquarizinho is *ca.* 15 m wide at the collection locality. Water is clear, slightly milky and with medium current. Specimens were collected by seining on sand banks in the middle of the river, especially in sectors shaded by riparian vegetation. There was no aquatic vegetation and depths of collection ranged from 30 to 150 cm. *Paracanthopoma saci* is sympatric with *Paravandellia oxyptera* (MZUSP 125623, 125625) with both relatively abundant at the type locality. The two species are psammophilic, but with different microhabitat preferences. *Paracanthopoma saci* favors fine sand, while *Pv. oxytera* prefers sectors with coarser granulation. Once the subtelties of their preferences are understood, it is possible to target one or the other species for collection with reasonable accuracy. Segregation is not complete however, and occasionally they were captured together in the same net (information above is based on *pers. comm.* by F. Dagosta). The abdomen is distended with blood in several specimens. Some female specimens have large eggs visible by transparency.

**Remarks:** *Paracanthopoma saci* is the only species of *Paracanthopoma* outside of the core Amazonian drainages (*see* Geographical Distribution above) and only the second species of Vandelliinae from the entire Paraná-Paraguai basin (the other being *Paravandellia oxyptera*). Other fish collected with *Pc. saci* were all typical members of the Paraná-Paraguai fish fauna, including some endemics *(e.g., Cyphocharax gillii, Steindachnerina brevipinna, Creagrutus meridionalis, Brachychalcinus retrospina, Bryconamericus exodon). Paracanthopoma saci* is obviously an outlier Amazonian component in the rio Taquari and an exception to the general composition of the Paraguai basin. Though exceptional, this situation is not unique. It has been known for a long time that the headwaters of the rio Paraguay include some odd Amazonian components, usually very restricted in distribution. Ribeiro *et al.* (2013) explains such cases as a result of events related to the formation of the Pantanal wetlands. A subsidence of the Upper Paraguai, *ca.* 2.5 mya resulted in the capture of a component of the upper rio Tapajós into the upper rio Paraguai. The ecological barrier represented by the Pantanal prevented such upper-water course, high-energy, components from spreading to the rest of the basin, thus explaining their restricted distributions. *Paracanthopoma saci* is clearly an additional element in that pattern. If such biogeographical association is correct, *Pc. saci* will be a useful marker to calibrate molecular divergence in *Paracanthopoma*.

Two paratypes of *Pc. saci* have extraordinarily elongated first pectoral-fin rays (part of MZUSP 125626, *see* Description above) (Fig. 35). This is the most extreme case of filamentous pectoral-fin ray known in Trichomycteridae. No other specimens of the species show any sign of fin elongation. The significance of this trait is difficult to interpret with the information available.

The two filamentous specimens are identical in all other relevant characteristics to other putative conspecifics, there being thus no reason to suspect that they might represent a different taxon. At 14.5 and 15.0 mm SL, those two specimens are among the smallest known of *Pc. saci*. Sexual dimorphism in pectoral-fin size and structure exists in all species of *Paravandellia* and at least one of some of *Paracanthopoma* (*Pc. irritans; see* above) with mature males having a stouter and larger pectoral fin (*see* section on Sexual Dimorphism). No such association is evident in *Pc. saci*. An alternative hypothesis of juvenile especialization is possible. The longest filament, corresponding to 36% SL, is seen in the smallest specimen. In the second specimen, only slightly larger, the filament is reduced to 26% SL. Other specimens similar in size to the latter show no sign of filament. So, if the filament is indeed a juvenile especialization, it is reduced very abruptly in the course of ontogeny (or perhaps broken off). Resolution of this question will have to await additional material and data.

The extremely reduced opercular and interopercular armatures of *Pc. saci*, a reduction reflected in their vestigial (opercular) or absent (interopercular) periodontodal folds, raises questions about the functionality of that complex in the species. One specimen in MZUSP 125626 is preserved with opercular odontodes erect, a sign that the biomechanical links usually associated with movement of the opercular odontodophore are still functional in the species. No such evidence exists for the still more reduced interopercular armature. Given that the latter is not only tiny in size in *Pc. saci* but also quite buried in integument, it is possible that it is reduced to a vestigial condition. Reductions of opercular and interopercular armature are recurrent in different lineages of sand-dwelling trichomycterids, such as psammophilic taxa in Glanapteryginae and Sarcoglanidinae. Despite such reductions, it is certain that *Pc. saci* is hematophagous like all other vandelliines, because several specimens in MZUSP 125626 have coagulated blood in their guts.

A single specimen in MBUCV-V 32270 (15.6 mm SL), Brasil, Mato Grosso, rio do Peixe, rio Negro basin, Parana-Paraguay drainage, at road to Perdigão (19°23,25'S, 54°58,79'W), col., R. Barriga *et al.,* 26 Aug 1998, probably represents *Pc. saci,* but this could not be directly verified for the present study.

### *Paracanthopoma satanica,* new species
### (Fig. 36)

**Holotype:** ANSP 178231, 25.4 mm SL, Peru, Loreto, Prov. Maynas, caño Sabalito (a terra firme stream, part of río Amazonas drainage), *ca.* 42 km south of Iquitos (04°14.743'S, 73°24.953'W), col., M. Sabaj *et al.,* 11 Aug 2001.

**Paratypes:** All collected with holotype. ANSP 189015, 10 ex, 14.4-23.1 mm SL; MZUSP 100149, 5 ex, 20.9-24.9 mm SL (2 c&s, 1 SEM); MUSM 32799, 3 ex, 15.7-22.8 mm SL.

**Figure 35.** *Paracanthopoma saci,* paratypes, MZUSP 125626, specimens with filamentous pectoral fins, 14.5 and 15.0 mm SL (*see* text, Remarks on the species).

**Diagnosis:** The presence of 13 teeth on the median premaxilla distinguishes this species from all congeners, which have either 11 or fewer, or 18 or 19 such teeth. The associated presence of seven teeth on the anterior row of the median premaxilla is equally diagnostic, and more accessible to observation than the complete count. The rectangular, broader than long, shape of the median premaxillary tooth patch (vs. roughly squarish, triangular or roundish) distinguishes the species from all congeners except *Pc. malevola*. Distinguished from the latter species by the fewer opercular and interopercular odontodes (5-6 and 4-5; vs. 11-12 and 7-8, respectively); by the more numerous vertebrae (42-43; vs. 40); by the more numerous caudal-fin procurrent rays (32 dorsally and 30-32 ventrally; vs. 19-21 dorsally and 18-20 ventrally); by the fewer median premaxillary teeth (13; vs. 18-19); by the fewer ventral principal caudal-fin rays (6 + 6; vs. 6 + 7); and by the lack of dark pigment on dorsum (or only few isolated dark spots not forming any pattern) (vs. two series of irregular dark spots alongside dorsal midline).

**Description:** Morphometric data for the holotype and paratypes are provided in Table 11. Body elongate (HL 14.8-17.0% SL). Cross-section of body broader than deep at pectoral-fin insertion and increasingly compressed posterior to that point, tapering to caudal fin. Dorsal profile of body gently convex from head to origin of dorsal fin (Fig. 36). Dorsal and ventral profiles of caudal peduncle convex along its posterior two-thirds, spatulate, expanded by procurrent caudal-fin rays. Ventral profile of body straight at pectoral-fin base and then gently convex until pelvic-fin origin, with some specimens with greatly distended abdomens due to gut contents. Myotomes and longitudinal skeletogenous septum clearly visible through thin integument along whole body. Axillary gland very large, elongate in shape, extending along limit between hypaxial musculature and abdominal cavity and protruding markedly on surface of body when full with secretion. Anterior end of gland surrounding dorsoposterior, ventral and posterior margins of muscular pectoral-fin base, as thick corselet, extending posteriorly to beyond margin of adpressed pectoral fin. Gland tapering to fine posterior tip, its large round or oval pore located at its anterior portion, approximately at vertical through middle of pectoral-fin length. Posterior portion of gland extending posteriorly from region ventral to pore, and its size evidently related to amount of secretion stored.

Dorsal profile of head continuous with that of dorsum, its origin sometimes indicated by slight constriction of anterior end of epaxial musculature. Head longer than broad (head width 69.9-80.7% HL), snout very broad, semicircular with a continuous round anterior margin (Fig. 36). Head muscles not entering skull roof.

**Table 11.** Morphometric data of *Paracanthopoma satanica*. Ranges, mean and SD include holotype. Head subunits were obtained with an ocular micrometer and therefore as projections. **Abbreviations:** min = minimum value; max = maximum value; n = number of specimens; SD = standard deviation.

| | n | holotype | min | max | mean | SD |
|---|---|---|---|---|---|---|
| Standard length (mm) | 6 | 25.4 | 15.9 | 25.4 | 21.4 | |
| **Percentages of SL** | | | | | | |
| Total length | 6 | 1.1 | 1.1 | 1.1 | 1.1 | 0.0 |
| Body depth | 6 | 11.7 | 11.3 | 16.5 | 12.8 | 1.9 |
| Caudal peduncle length | 6 | 22.4 | 22.0 | 23.3 | 22.8 | 0.5 |
| Caudal peduncle depth | 6 | 7.7 | 7.5 | 8.9 | 8.2 | 0.6 |
| Predorsal length | 6 | 69.9 | 67.9 | 72.2 | 69.8 | 1.4 |
| Preanal length | 6 | 69.9 | 67.3 | 72.2 | 69.8 | 1.5 |
| Prepelvic length | 6 | 62.2 | 60.2 | 62.4 | 61.3 | 0.9 |
| Dorsal-fin base length | 6 | 9.7 | 7.1 | 9.7 | 8.8 | 0.9 |
| Anal-fin base length | 6 | 8.2 | 8.1 | 9.0 | 8.6 | 0.4 |
| Pectoral-fin length | 6 | 10.7 | 10.7 | 12.6 | 11.4 | 0.8 |
| Head length | 6 | 14.8 | 14.8 | 17.0 | 15.9 | 0.7 |
| **Percentages of HL** | | | | | | |
| Head width | 6 | 80.7 | 69.9 | 80.7 | 74.4 | 3.8 |
| Head depth | 6 | 34.5 | 33.3 | 41.1 | 36.3 | 2.7 |
| Pectoral-fin length | 6 | 74.8 | 64.4 | 78.6 | 72.3 | 5.1 |
| Interorbital | 6 | 15.1 | 14.5 | 15.5 | 15.1 | 0.4 |
| Eye diameter | 6 | 16.0 | 14.3 | 18.1 | 15.7 | 1.3 |
| Snout length | 6 | 36.1 | 36.1 | 39.6 | 38.3 | 1.3 |
| Mouth width | 6 | 33.6 | 28.7 | 42.7 | 33.7 | 4.8 |
| Anterior internarial width | 6 | 15.1 | 12.4 | 17.8 | 14.9 | 1.9 |
| Posterior internarial width | 6 | 11.8 | 10.1 | 12.0 | 11.3 | 0.7 |

Head very depressed (head depth 33.3-41.1% HL) with dorsal profile straight and horizontal until eye, then bending ventrally, straight or gently convex, to tip of snout. Ventral profile of head straight, flattened. Eye medium-sized (14.3-18.1% HL), without free orbital rim, located dorsolaterally on head and directed dorsolaterally, with pronounced lateral component. Integument over eye thin and transparent. Eye located mostly within anterior half of HL, interorbital width approximately equal to longitudinal diameter of eye. Eyelens largely constricted by iris, with losenge-shaped pupil in specimens examined. Anterior nostril small, surrounded by short tubule of integument produced posteriorly into small pointed process (Fig. 37), with double elastin cores. Anterior internarial width approximately equal to interorbital. Posterior naris slightly larger than anterior ones, roundish or roughly triangular in shape, located close to anteromesial margin of eye and provided with anterior flap of integument (Fig. 37). Center of posterior naris approximately at transverse line through anterior margin of eyes. Posterior internarial width narrower than interorbital and three times as wide as diameter of one nostril.

Opercular odontodophore small and elongate, dorsolaterally located on head, on dorsal half of head depth in lateral view, anterodorsally to pectoral-fin base. Opercular odontodes mostly covered with integument, 5 or 6 in number, irregular and closely positioned as two or three large posterior ones and two or three smaller anterior ones. Odontode bases strongly compressed, and their main axis oriented horizontally in lateral view, with distal portions of larger posterior ones curved dorsoposteriorly. Two or three caps of replacement odontodes posteriorly to mature ones. Opercular periodontodal fold small and poorly-differentiated, extending shortly beyond tips of odontodes and mostly continuous ventrally with head integument. Interopercular odontodophore smaller than opercular one, located ventrally or ventrolaterally on head, aproximately at horizontal through origin of pectoral fin. Interopercular odontodes 4 or 5, directed posteroventrally, with tips curved dorsoposteriorly. Odontode bases strongly compressed, closely positioned in one irregular or two imbricated rows, with posterior ones largest. Interopercular odontodophore closer to opercular one than to eye. Interopercular periodontodal fold of integument poorly-differentiated, mostly continuous with head integument posteriorly. Epiodontodeal small and thick, mostly covering odontodes.

Mouth inferior (ventral), strongly flattened ventrally. Each premaxilla with one scalpelloid teeth attached to its distal tip, and one additional tooth socket, with partly formed tooth in parallel (Figs. 4J, 38). Scalpelloid teeth deeply hidden in labial tissue and difficult to expose in preserved specimens without damaging soft tissue. Conical teeth absent on premaxilla. Upper lip very broad but poorly-differentiated, continuous with ventral surface of snout. Median premaxilla broad, with 13 teeth disposed in two rows, anterior one with 7 teeth (three on each side and median one) and posterior row with 6 (three on each side, separated by gap) (Figs. 4J, 38). General shape of median premaxillary tooth patch (but not of underlying bone) roughly rectangular in ventral view in alcoholic specimens. All teeth posteriorly oblique to ventral surface of median premaxilla at base and curved further posteriorly at distal pungent portion, those on lateral edge of median premaxilla also with some lateral component. Basal portion of all median premaxillary teeth strongly compressed laterally. Five or six replacement tooth caps posterodorsally to mature dentition. Median premaxillary velum poorly-differentiated. Hypodontal pad of median premaxilla broad and rectangular, its posterior margin straight or gently convex, perpendicular to longitudinal head axis and occupying most of surface of upper jaw. Lower jaw narrow, composed mostly of roundish and mostly confluent dentary lobes, continuous with mental region posteriorly. Jaw cleft short strongly directed laterally, perpendicular to longitudinal axis. Dentary diastema reduced to small median concavity between dentary lobes. Dentary teeth 4, loosely disposed at mesial end of dentary, arranged in two ventral and two dorsal ones, not aligned so that in ventral view three teeth usually visible (Figs. 4J, 38). Dentary teeth long, their axis anteriorly-directed at base, but curved dorsally or dorsolaterally at distal half. Median tooth of ventral row longer than others.

Branchiostegal velum forming large, continuous, round and posteriorly concave, free fold across whole of mental region (Fig. 37). Dorsal portion of branchial membrane reaching and slightly overlapping anterior margin of pectoral-fin base. Branchial opening small, located anteriorly to pectoral-fin base, approximately equal to

space between opercular and interopercular odontodophores. Maxillary barbel very short, extending for half distance to base of interopercular odontodophore or less; longer in specimens 16 mm SL or under, where it can nearly reach base of interopercular odontodophore. Posterior point of its base anterior to vertical through anterior margin of eye in lateral view. Base of maxillary barbel dorsally expanded. Rictal barbel tiny, vestigial, undifferentiated externally in some specimens, located mesially to base of maxillary one. Nasal barbel vestigially represented by posterior elongated portion of fold around anterior naris described above, with double internal elastin core.

Lateral line short and straight, extending alongside dorsal margin of anterior portion of axillary gland. Terminal lateral-line pore immediately dorsal to axillary
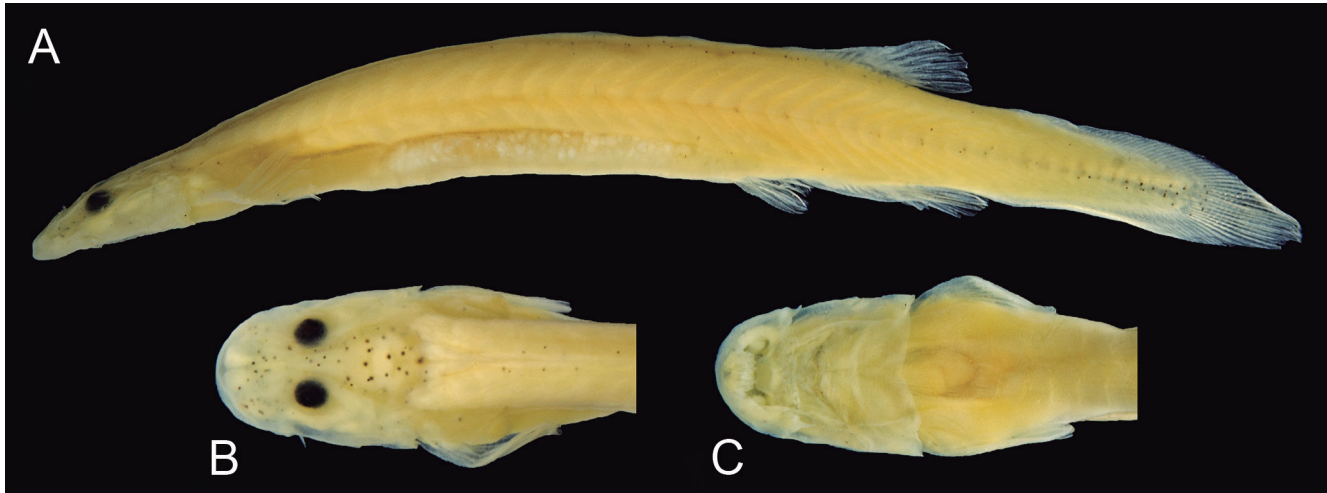


**Figure 36.** *Paracanthopoma satanica,* holotype, ANSP 178231, 25.4 mm SL. Peru, Dept. Loreto, Maynas, Caño Sabalito. (A) Lateral view of body; (B) Dorsal view of head; (C) ventral view of head.



**Figure 37.** *Paracanthopoma satanica,* paratype, ANSP 178231, SEM images of head. (A) Dorsal; (B) Ventral. Scale bar = 500 μm.
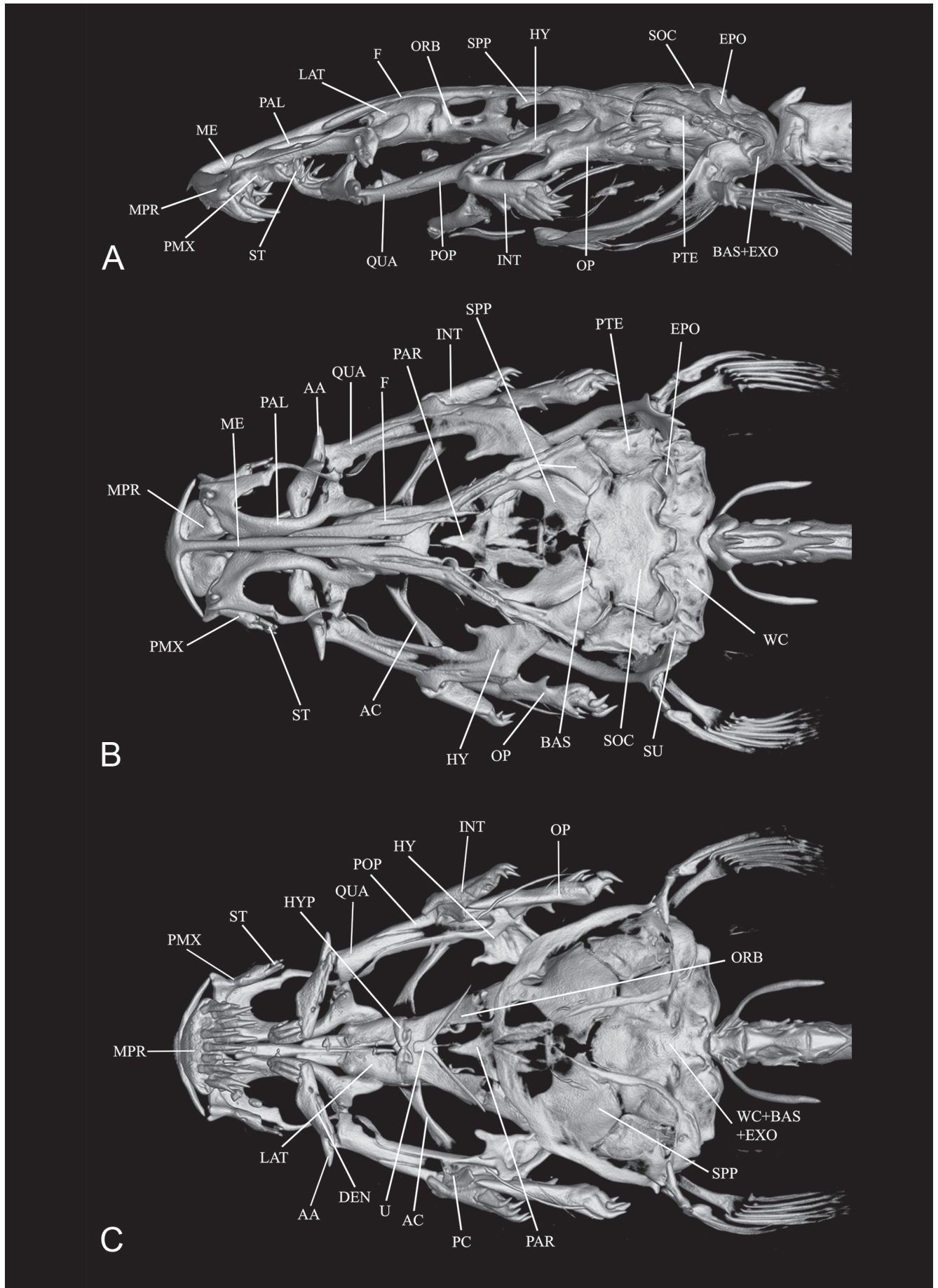
**Figure 38.** *Paracanthopoma satanica,* holotype, ANSP 178231, CT scan images of head skeleton, (A) Lateral; (B) Dorsal; (C) Ventral. Specimen poorly calcified, some structures not properly shown.

gland opening. Very short secondary branch splitting off ventrally from proximal portion of main canal, with corresponding pore opening anteriorly to midlength of main canal. Single lateral-line tubule straight, poorly calcified, extending for most of main canal posterior to bifurcation.

Pectoral fin medium-sized (64.4-78.6% HL), aproximately 75% of HL, with gently convex distal margin. First ray longer than others in few specimens. Pectoral-fin rays i + 5, its base on ventral side of body. Pelvic fin small, separated from each other at base, with i + 4 rays. Pelvic splint present. Origin of pelvics close to origin of anal fin, anterior to vertical through origin of dorsal-fin, entirely covering anus and urogenital papilla and extending posteriorly to origin of anal fin. Posterior margin of pelvic fin gently convex. Dorsal fin elongate, roughly triangular with roundish edge and gently convex distal margin. Dorsal-fin rays ii + 6, plus 5 or 6 procurrent ones. Anal fin similar in shape to dorsal fin, with ii + 5 rays, plus 6 procurrent ones. Origin of anal fin at or slightly posterior to vertical through origin of dorsal-fin. Anal fin with same size, slightly smaller or slightly larger than dorsal one. Caudal fin squarish, truncate with round edges, slightly convex in some specimens, less deep than maximum depth of caudal peduncle. Principal caudal-fin rays 5 + 6 (holotype) or 6 + 6. Procurrent caudal-fin rays 32 dorsally and 30 or 32 ventrally.

Vertebrae 42 (n = 6) or 43 (n = 1). First dorsal-fin pterygiophore subsequent to neural spine of vertebra 21 (n = 1) or 22 (n = 1). First anal-fin pterygiophore subsequent to haemal spine of vertebra 21 (n = 1) or 22 (n = 1). Dorsal-fin pterygiophores 7 (n = 1) or 8 (n = 2), when later, last element vestigial. Anal-fin pterygiophores 6 (n = 2). Branchiostegal rays 3 or 4, when later, first element vestigial.

**Pigmentation in preservative:** Body almost entirely white. Sparse isolated dark chromatophores irregularly scattered along dorsum, extending along base of dorsal fin and anterior portion of dorsal edge of caudal peduncle. Isolated dark chromatophores spread over dorsal sides of abdominal wall, exposed only in specimens with distended abdomens, otherwise hidden along limit between abdominal cavity and trunk musculature. Neurocranium with dark brain pigment forming irregular spots seen by transparency. Smaller and less dense integumentary chromatophores along margins of neurocranium, extending anteriorly between eyes and nostrils and onto dorsolateral portion of snout. Margins of snout white. Olfactory capsule outlined as dark ring. Posterior nostril always with small dark spot in its interior. Few chromatophores sometimes along dorsal margin of opercular odontodophore. Some specimens with few dark markings on anterior portion of median premaxilla in ventral view. Regular series of spots, one per vertebra, along caudal peduncle, formed mostly by internal chromatophores on individual vertebrae, visible by transparency and gradually fading anteriorly. Scattered spots across base of caudal-fin rays, sometimes forming short irregular vertical line.

**Etymology:** Satanicus is an adjective (treated as Latin) derived from the Hebrew verb satan, meaning literally "to oppose", but commonly used to refer to an enemy or the devil.

**Geographical distribution:** *Paracanthopoma satanica* is known from a single locality in a tributary to the upper Amazon drainage in Peru (Fig. 45).

**Biology:** There are three specimens in the type series with distended abdomens obviously full of coagulated blood, the smallest of which is 15.6 mm SL. Some paratypes are gravid females with the abdomen distended both by the ovaries and by blood in the gut. The eggs are yellowish in color and firm to the touch, clearly distinguishable from the white and soft adipose bodies loated nearby. In the fullest female, the egg distribution extends superficially along the lateral surface of the posterior two-thirds of the abdominal cavity, in an arrangement progressively narrower posteriorly. There are at least 50 tightly packed eggs on each side, the largest of which are approximately 0.5 mm in diameter.
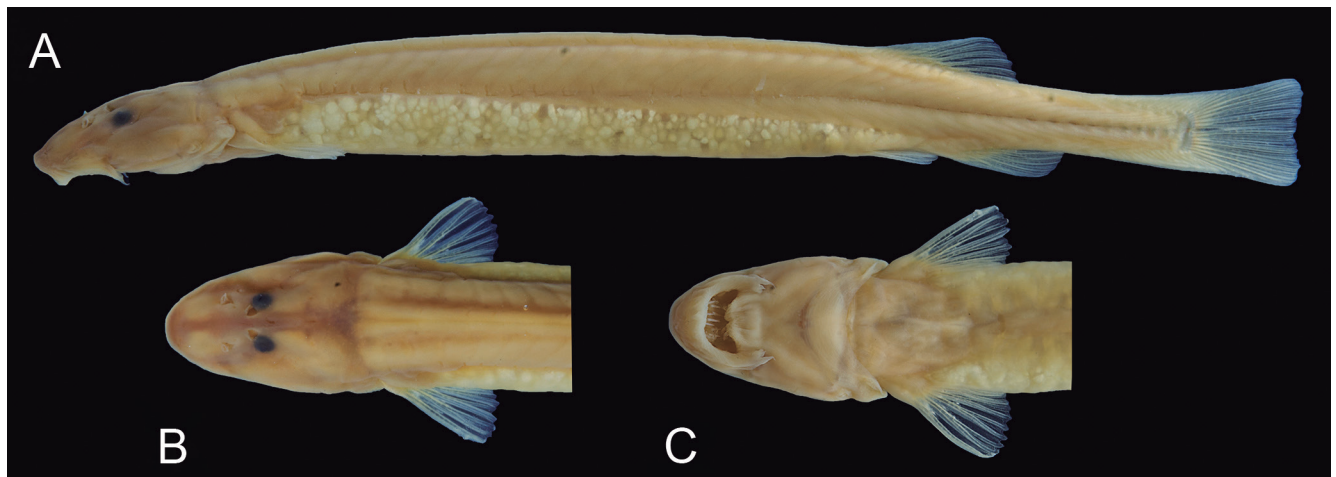
### *Paracanthopoma truculenta,* new species
### (Fig. 39)

*Paracanthopoma* sp. 1 – Wosiacki & de Pinna, 2007: 73 [catalog].

**Holotype:** MZUSP 30399, 39.7 mm SL, Rondônia, rio Madeira, Calama (08°01′42″S, 62°52′34″W), col., M. Goulding, Feb-May 1980.

**Paratypes: BRAZIL:** INPA 8188, 1 ex, 38.6 mm SL, Amazonas, rio Solimões, downstream from mouth of rio Purus (trawled at 20 m depth), col., C. Cox, J. Lundberg & L. Rapp Py-Daniel, 19 Oct 1992; INPA 16830, 1 ex, 41.4 mm SL, rio Madeira, col., M. Goulding, no date; MZUSP 30401, 6 ex, 35.1-47.1 mm SL, Brazil, Rondônia, rio Madeira at Calama (08°01′42″S, 62°52′34″W), col., M. Goulding, Feb-May 1980; MZUSP 30404, 20 ex (2 c&s), 26.5-40.6 mm SL, Rondônia, rio Madeira at Calama (08°01′42″S, 62°52′34″W), col., M. Goulding, Feb-Apr 1980; MZUSP 30409, 11 ex, 25.6-39.5 mm SL, Rondônia, rio Madeira at Calama (08°01′42″S, 62°52′34″W), col., M. Goulding, Feb-May 1980; MZUSP 30422, 13 ex, 22.3-44.4 mm SL, Rondônia, rio Madeira at Calama (08°01′42″S, 62°52′34″W), col., M. Goulding, Feb-Apr 1980; MZUSP 100750, 7 ex (1 c&s), 25.6-37.4 mm SL, Rondônia, rio Madeira at Calama (08°01′42″S, 62°52′34″W), col., M. Goulding, Feb-Apr 1980; MZUSP 103048, 10 ex, 35.5-50.7 mm, collected with holotype; **PERU:** MUSM 10849, 1 ex, 37.5 mm SL, Madre de Dios, Tambopata, río Madre de Dios, col., F. Chang, 16 May 1996; MUSM 19977, 1 ex, 41.0 mm SL, Madre de Dios, Manu, río Madre de Dios, col., M. Goulding *et al.,* 24 Aug 2001.

**Non-type material: BOLIVIA:** MZUSP 27854, 3 ex, 28.3-37.8 mm SL, Madre de Dios at Riberalta (rio Madeira drainage), col., joint expedition

**Figure 39.** *Paracanthopoma truculenta,* holotype, MZUSP 30399, 39.7 mm SL. Brazil, Rondônia, Rio Madeira, Calama. (A) Lateral view of body; (B) Dorsal view of head; (C) ventral view of head.

ORSTON-UTB, 20 May 1983; **BRAZIL:** MZUSP 30402, 3 ex, 35.9-41.0 mm SL, Rondônia, rio Madeira at Calama (08°01′42″S, 62°52′34″W), col., M. Goulding, Feb-Apr 1980; MZUSP 30403, 1 ex, 33.7 mm SL, Amazonas, rio Madeira at Aripuanã [= Novo Aripuanã] (from body of Piraíba, *Brachyplatystoma filamentosum,* 82 cm), col., M. Goulding, 11 Dec 1980; MZUSP 30410, 1 ex, 35.9 mm SL, rio Madeira, col., M. Goulding, 21 Dec 1979;

**Diagnosis:** Distinguished from all congeners by the very reduced opercular odontodophore, bearing only one or two odontodes not protruding from surface of head, sunk in small slit of integument (vs. opercular odontodes minimally four, clearly visible on surface of skin, even when small). Distinguished from all congeners, except *Pc. carrapata, Pc. daemon,* and *Pc. parva,* by the presence of nine (sometimes 10 in *Pc. daemon*) teeth on the median premaxilla (vs. 3 to 5 or 11 and more); by the presence of a single median s6 pore, visible on the middle of skull posterior to eyes (vs. paired s6 pores, distant from midline of skull), and by the supraoccipital anteriorly produced into large pointed spike (vs. either anteriorly concave or straight across skull roof). Distinguished from all congeners except *Pc. parva* and *Pc. carrapata* by the posterior margin of the anal fin well posterior to vertical through that of the dorsal fin (vs. margins of two fins approximately at same vertical or that of anal fin only slightly posterior to that of dorsal fin); and by the deeply emarginate, bilobed caudal fin (vs. truncate with round corners or only slightly concave). Distinguished from all congeners except *Pc. carrapata* by the extensive invasion of the skull roof by head musculature, with widest exposed part of neurocranium approximately equivalent to interorbital (vs. exposed part of neurocranium larger than interorbital). Further distinguished from *Pc. carrapata* by the proportionally smaller eye (9.9-13.3% HL; vs. 13.9-14.4); and the shorter head (16.5-20.0% HL; vs. 20.9-22.2).

**Description:** Morphometric data for the holotype and paratypes are provided in Table 12. Body elongate (HL 16.5-20.0% SL). Cross-section of body depressed at pectoral-fin insertion, becoming round along anterior fourth trunk and increasingly compressed posterior to that point, tapering to caudal fin. Dorsal profile of body gently convex from head to origin of dorsal fin (Fig. 39). Dorsal and ventral profiles of caudal peduncle gently convex sometmes slightly angulate at beginning of procurrent caudal-fin rays. Caudal peduncle narrow, but expanded by procurrent rays along posterior third or half. Ventral profile of body slightly swollen at cardiac region, then concave, straight or convex, depending on condition of gut content, until pelvic-fin origin. Myotomes clearly visible along whole body. Longitudinal skeletogenous septum also evident along whole of body, except anterior third of trunk in large individuals. Axillary gland short, posteriorly not reaching margin of adducted pectoral fin, not protruding markedly on surface of body and covering only very base of pectoral fin. Its large pore opening slightly anterior to midlength of pectoral fin.

Dorsal profile of head separated from that of dorsum by pronounced muscle separation. Head longer than broad (head width 55.4-66.1% HL), snout broad, parabolic with a roundish-pointed tip (Figs. 39, 40). Muscles covering most of dorsal part of head, with head width approximately 4.5 times the width of exposed skull roof in dorsal view. Exposed area proportionall larger in small specimens. Head deep for *Paracanthopoma* (head depth 20.5-32-0% HL), with convex dorsal profile, strongly curved ventrally anteriorly to eye. Eye small (9.0-13.3% HL), without free orbital rim, located dorsolaterally on head and directed dorsolaterally. Integument over eye thin, entire eyeball visible through skin. Middle of eye slightly anterior to middle of HL, interorbital width approximately 1.5 times longitudinal diameter of eye. Eyelens very large, taking most of lateral surface of eye and either entirely unconstricted by iris or constricted only marginally, with large round pupil, in specimens examined. Anterior nostril small, surrounded by short tubule of integument produced posteriorly into small pointed process (Figs. 39, 40), with double elastin cores. Anterior internarial width equal or slightly larger than interorbital. Posterior naris slightly larger than anterior ones, round, but usually with semilunar opening be-

**Table 12.** Morphometric data of *Paracanthopoma truculenta*. Ranges, mean and SD include holotype. **Abbreviations:** min = minimum value; max = maximum value; n = number of specimens; SD = standard deviation.

| | n | holotype | min | max | mean | SD |
|---|---|---|---|---|---|---|
| Standard length (mm) | 12 | 40.23 | 28.8 | 50.8 | 35.5 | |
| **Percentages of SL** | | | | | | |
| Total length | 12 | 1.1 | 1.1 | 1.1 | 1.1 | 0.0 |
| Body depth | 12 | 8.1 | 7.4 | 10.2 | 8.9 | 0.9 |
| Caudal peduncle length | 12 | 16.4 | 16.2 | 19.6 | 17.5 | 1.0 |
| Caudal peduncle depth | 12 | 5.0 | 4.5 | 5.9 | 5.4 | 0.4 |
| Predorsal length | 12 | 73.1 | 71.1 | 74.8 | 72.5 | 1.2 |
| Preanal length | 12 | 76.3 | 74.9 | 79.0 | 76.6 | 1.2 |
| Prepelvic length | 12 | 71.5 | 69.2 | 73.0 | 70.7 | 0.9 |
| Dorsal-fin base length | 12 | 6.2 | 4.7 | 8.2 | 7.6 | 1.1 |
| Anal-fin base length | 12 | 3.9 | 3.7 | 5.9 | 4.7 | 0.7 |
| Head length | 12 | 17.6 | 16.5 | 20.0 | 18.9 | 1.3 |
| **Percentages of HL** | | | | | | |
| Head width | 12 | 56.0 | 55.4 | 66.1 | 61.0 | 3.2 |
| Head depth | 12 | 27.6 | 20.5 | 32.0 | 24.9 | 3.8 |
| Interorbital | 12 | 9.2 | 9.2 | 13.2 | 11.6 | 1.2 |
| Eye diameter | 12 | 12.1 | 9.0 | 13.3 | 10.4 | 1.5 |
| Snout length | 12 | 43.0 | 38.6 | 48.8 | 44.3 | 2.6 |
| Mouth width | 12 | 35.0 | 26.7 | 45.3 | 40.3 | 5.8 |
| Anterior internarial width | 12 | 18.9 | 17.1 | 20.8 | 18.3 | 1.1 |
| Posterior internarial width | 12 | 5.5 | 5.0 | 8.5 | 6.8 | 1.0 |

cause of partial occlusion by anterior flap of integument (Figs. 39, 40). Posterior naris positioned anteromesially to eye, their middle approximately at transverse line through anterior margin of eyes. Posterior internarial width narrower than interorbital.

Opercular odontodophore tiny, laterally or slightly dorsolaterally located on head, approximately at, or slightly dorsal to, middepth of head (Figs. 39, 40). Odontodophore externally identifiable mostly by its proportionally small, oval associated periodontodeal fold. Opercular odontodes 1 or 2, closely positioned and not protruding from surface of head and sometimes entirely sunk in integument, their location in these case externally indicated by narrow horizontal slit. Main axis of opercular odontodes oriented horizontally in lateral view, with their distal portion curved dorsally. One or two caps of replacement odontodes posteromesially to mature ones. Interopercular odontodophore tiny (Figs. 39, 40), located ventrolaterally on head, at horizontal through origin of pectoral fin, with 2 or 3 odontodes closely positioned in single row, much closer to opercular odontodophore than to eye. Two or three replacement tooth caps located posteromesially to mature ones. Interopercular periodontodal fold of integument small, nearly semicircular. Epiodontodeal velum translucent, very small but proportional to size of odontodophore, entirely covering odontodes when extended.

Mouth inferior (ventral), filled in most specimens with tightly bitten chunks of meat, supposedly from host fish, often entirely hiding internal mouth morphology. Mouth very large, occupying most of anterior part of head ventrally (Figs. 39, 40). Each premaxilla with single scalpelloid teeth attached to its distal tip (visible only in skeletal preparations), but actually two tooth sockets adjacent-

ly-positioned, one of which normally vacant, corresponding to half-formed replacement tooth adjacent to mature one (Figs. 4K, 41). Normally one additional initial-stage replacement cap nearby. Mature scalpelloid tooth with distal portion disproportionately reduced and very strongly curved over rest of teeth, with pungent tip nearly adpressed to margin of basal plate. Scalpeloid teeth deeply hidden in labial tissue, its distal surface barely rupturing surface even when premaxilla forcibly abducted. Conical teeth absent in premaxilla. Upper lip thick, deeply plicate on parabucal surface. Median premaxilla very large, with 9 teeth disposed in one anterior row of four (anteriorly convex), one posterior row of four (convex posteriorly), plus single middle tooth (Figs. 4K, 41). Teeth on anterior row more or less evenly spaced, those on posterior row more widely spaced medially than laterally. All nine teeth perpendicular to median premaxilla at base, but strongly curved posteriorly at distal pungent portion, those of anterior row taller than those of posterior row. All median premaxillary teeth strongly laterally compressed basally. Numerous replacement tooth caps posterodorsally to mature dentition, creating crowded aspect at posterior limit of median premaxillary dentition. Median premaxillary dentition occupying almost all of upper jaw and most of interior of mouth. Median premaxillary velum absent. Hypodontal pad of median premaxilla thickly cushioning teeth. Lower jaw wide, with long dentary lobes nearly entirely fused to each other at midline, continuous with mental region posteriorly. Lower jaw cleft deep and strongly directed posteriorly, approaching parallel to longitudinal axis and with broad space separating it laterally from inner margin of upper jaw. Dentary diastema poorly differentiated, represented by small concave, sometimes angulate area at midline, entirely absent in some specimens. Rami of mandible very close together at midline. Dentary teeth 4 or 5 (normally 4), closely packed at mesial end of dentary (Figs. 4K, 41). When 4, teeth disposed in two pairs, one dorsal and one ventral, with only latter visible in ventral view. When five, ventral row with three and inner row with two teeth. Axis of dentary teeth anteriorly-directed at base, with distal portions curved dorsally or dorsolaterally. Branchiostegal velum forming large, continuous, round and posteriorly concave, free fold across whole of mental region (Fig. 40). Dorsal portion of branchial membrane partly covering anterior margin of pectoral-fin base. Branchial openings small, located anterodorsally to pectoral-fin base, spanning approximately for area between ventral margin of opercular odontodophore and ventral margin of interopercular odontodophore. Maxillary barbel very short and broad, its dorsal margin expanded into membranous keel, progressively larger proximally, only distal portion filamentous. Posterior point of is base anterior to vertical through anterior margin of eye in lateral view, its tip extending posteriorly approximately to vertical through middle of eyes in lateral view. Mesial (or ventral) part of maxillary-barbel base adjacent to membranous outgrowth extending posteriorly from corner of mouth. Rictal barbel small, located mesially to base of maxillary one and approximately half
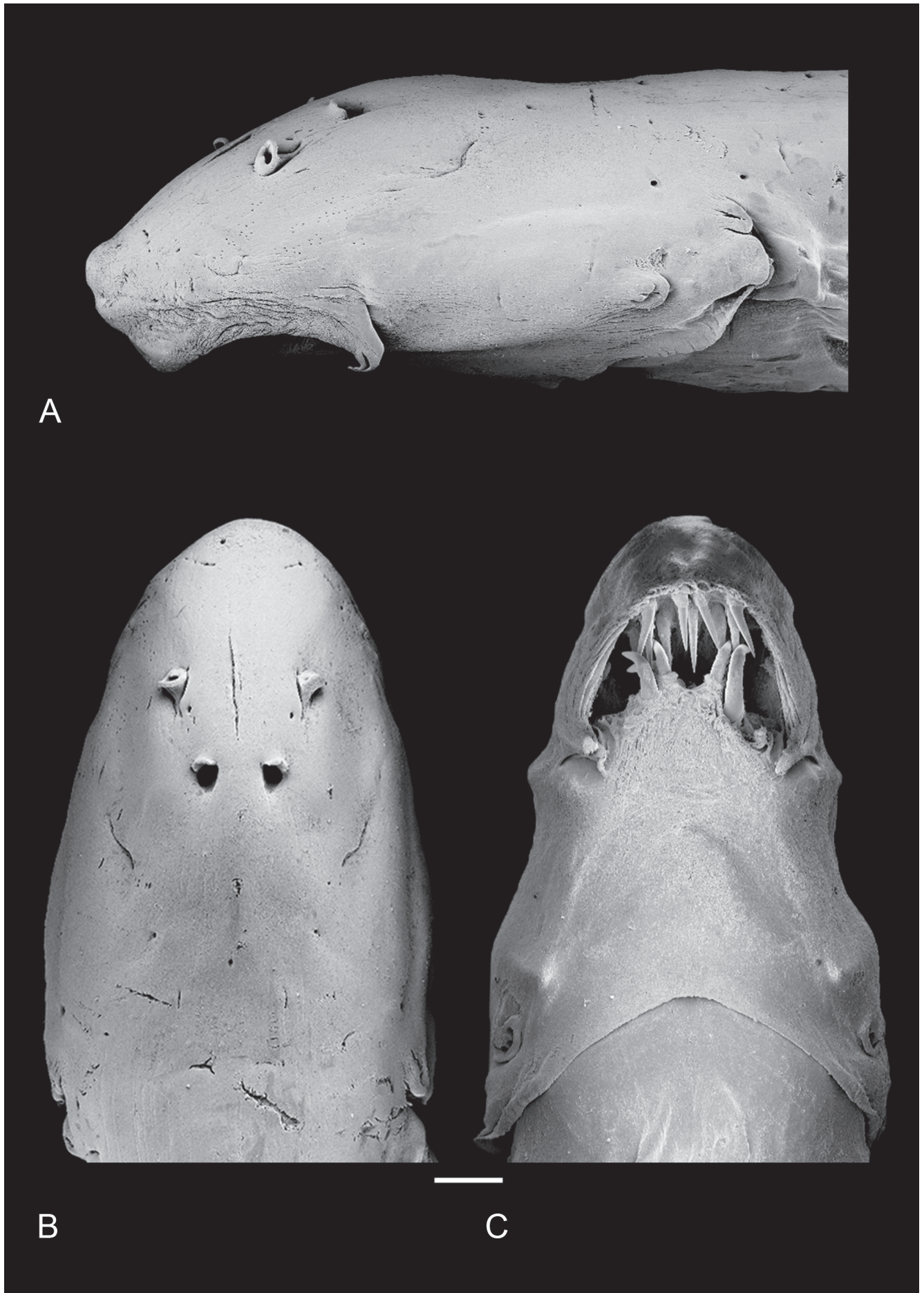
**Figure 40.** *Paracanthopoma truculenta,* paratype, MZUSP 30404, SEM images of head. (A) Lateral; (B) Dorsal; (C) Ventral. Scale bar = 500 μm.
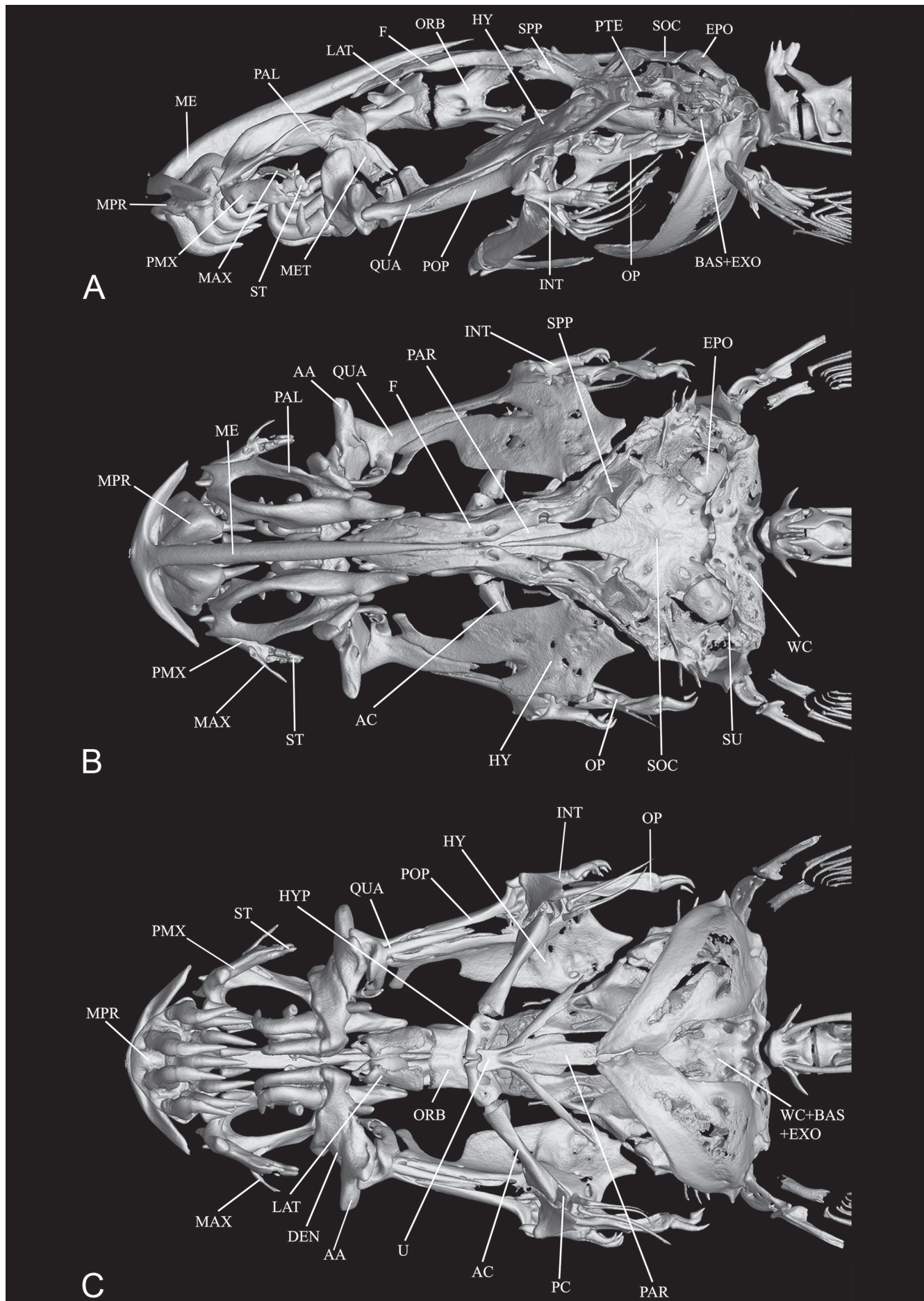
**Figure 41.** *Paracanthopoma truculenta,* holotype, MZUSP_30399, CT scan images of head skeleton, (A) Lateral; (B) Dorsal; (C) Ventral.

of its size, its base immersed in membranous expansion at corner of mouth, with well-defined membranous lobule mesially (Fig. 40). Rictal barbel sometimes difficult to identify among irregularities of surrounding integument flap, but homology with trichomycterid rictal barbel evident by well-developed internal core. Nasal barbel vestigially represented by posterior elongated portion of fold around anterior naris described above, with double internal elastin core.

Lateral line short, straight along anterior half and bent dorsally at midlength, at approximately 30° to 45°. Its terminal pore approximately at vertical through midlength of pectoral-fin, at horizontal through eye in lateral view, at or slightly posterior to vertical through posterior margin of axillary pore. Short secondary branch splitting off ventrally from anterior portion of canal, with corresponding pore opening approximately at midlength of main canal or slighly anterior to that point. Single lateral-line tubule extending for section of canal between bifurcation and dorsal bending.

Pectoral fin very short, aproximately 50% of HL or less, with i + 4 or i + 5 rays (modally i + 5; one abnormal specimen in MZUSP 30422 with i + 1 rays on left side), first one (unbranched) slightly longer than others in some specimens. Distal margin of pectoral fin gently convex, its base near ventral margin of body in lateral view, when abdomen not distended by gut contents. Pelvic fins small, well-separated from each other at base, with i + 4 rays. Pelvic splint present. Origin of pelvics located anteriorly to vertical through origin of dorsal-fin, covering anus and extending posteriorly to almost reach origin of anal fin. Posterior margin of pelvic fin round. Dorsal fin small, broadly triangular with roundish apex, with gently convex distal margin and ii + 6 fin rays, plus 4 or 5 procurrent ones. Anal fin small, slightly more elongate than dorsal one, with gently convex distal margin and ii + 5 fin rays, plus 4 or 5 procurrent ones. Origin of anal fin slightly posterior to vertical through middle of dorsal-fin base. Anal fin normally smaller than dorsal one, but opposite in some specimens. Caudal fin emarginate, with concavity more pronounced with growth. Principal caudal-fin rays 6 + 7. Procurrent caudal-fin rays 14 or 15 dorsally and 16 or 17 ventrally.

Vertebrae 37 (n = 2), 38 (n = 2), 39 (n = 8) or 40 (n = 14). First dorsal-fin pterygiophore subsequent to neural spine of vertebra 22 (n = 2) or 23 (n = 1). First anal-fin pterygiophore subsequent to haemal spine of vertebra 24 (n = 2) or 25 (n = 1). Dorsal-fin pterygiophores 7 (n = 2). Anal-fin pterygiophores 6 (n = 2). Branchiostegal rays 3 (n = 2).

**Pigmentation in preservative:** Body almost entirely white. Middorsal region of head, corresponding to narrow neurocranium, dark with brain pigment seen by transparency. Dark field anteriorly to lateral margin of eyes, extending anterolaterally to region immediately dorsal to base of maxillary barbel. Distal magin of hypural plate with narrow dark line, followed shortly posteriorly by similar but slightly wider and more irregular dark field crossing bases of principal caudal-fin rays, sometimes extending shortly horizontally along proximal portions of middle rays.

**Etymology:** From the Latin *truculentus,* meaning harsh, cruel, brutish; an allusion to the size of this species, the largest of all *Paracanthopoma*.

**Geographical distribution:** *Paracanthopoma truculenta* occurs primarily in the rio Madeira, along nearly its entire course, through upland and lowland sectors in Bolivia, Brazil and Peru (Fig. 45). A single record exists in the rio Solimões, this being the only record of any *Paracanthopoma* species in the main channel of the Amazon.

**Biology:** Surprisingly few specimens of *Paracanthopoma truculenta* have obvious remains of blood in their gut, with only one or two specimens in few lots with abdomens distended with dark coagulated blood. On the other hand, most individuals (including those distended with blood) have remains of flesh tightly held in their jaws. It seems possible that they attach to the surface of the body of their hosts by a tight bite, so firm that the removal by collectors result in tearing and removal of part of the bitten tissue. That, plus the fact that so few specimens have blood in their guts, raises the possibility that *Pc. truculenta* feeds partly from blood and other fluids taken directly from the superficial tissues of their hosts, with only occasional visits to the gill chamber for a large intake of blood. Or perhaps even that the occasional blood found comes from superficial sources as well, when the bitten spot happens to be particularly well-vascularized. The mouth morphology of *Pc. truculenta* is markedly sucker-shaped, more so than in other vandelliines, and it is possible that it can actually exert negative pressure sufficient to extract blood from systemic vascularization, and not only from major vessels. Whichever the case may be, there are indications that *Pc. truculenta* has rather especial feedings habits among vandelliines and that further study may reveal most interesting trophic adaptations in that species. *Paracanthopoma truculenta* was collected sympatrically with *Pc. carrapata* (lots MZUSP 30402 and 30404 of former and 100145 and 100143 of latter).

**Remarks:** *Paracanthopoms truculenta* is the largest species as yet known in its genus (max. 50.7 mm SL, MZUSP 103048). However, indirect evidence suggests that the species probably reaches even larger sizes. Cleared and stained large specimens show extensive cartilaginous areas in their skeleton, typical of young bony fishes. The contact area between pterotic, sphenotic and supraoccipital has a wide cartilaginous component very evident in dorsal view. Anteriorly in the skull, the median region between lateral ethmoids and posteriorly between that and the orbitosphenoids is largely cartilaginous. The entire ethmoid cartilage is still large. Finally, the anterior ceratohyal has a band of cartilage near its anterior end which is typical of long bones still undergoing linear growth. All that indicates that *Pc. truculenta* may reach a size larger still than that of the largest individuals so far captured. Why such specimens have not yet been captured, despite a relative abundance of half-grown individuals, remains to be discovered.

### *Paracanthopoma vampyra,* new species
### (Fig. 42)

**Holotype:** MZUSP 86953, 14.6 mm SL, Brazil, Amazonas, Rio Preto da Eva, Igarapé Sucuriju (trib. to rio Preto da Eva) (approx. 02°44'S, 59°33'W), col., M. de Pinna, L. Py-Daniel & L. Sousa, 14 Aug 2004.

**Paratypes: All from Brazil:** MZUSP 100137, 4 ex, 14.3-18.1 mm SL, Amazonas, Rio Preto da Eva, Igarapé Sucuriju, ao lado do Sítio Bom Jesus, estrada Francisca Mendes, km 13 (02°45'15.8"S, 59°37'29.6"W), col., O. Oyakawa *et al.,* 04 Jul 2003; MZUSP 100138, 3 ex, 20.8-22.7 mm SL, Amazonas, Rio Preto da Eva, stream tributary to rio Preto da Eva, after the Encanto da Mata beach complex (02°37'10.2"S, 59°44'30.5"W), col., MZUSP team, 09 Jul 2003; MZUSP 103049, 11 ex (2 c&s), 12.8-14.7 mm SL, collected with holotype.

**Non-type specimens: BRAZIL:** INPA 28601, 6 ex (1 c&s, 1 ex decapitated), 16.6-17.7 mm SL, Amazonas, Rio Preto da Eva, unnamed creek at km 10 of Ramal Francisca Mendes; INPA 29572, 5 ex (1 c&s) 13.1-16.0 mm SL, Pará, Porto Trombetas, Igarapé at Platô Aviso (rio Trombetas drainage); INPA 31306, 15 ex (2 c&s), 13.1-17.0 mm SL, Pará, Porto Trombetas, rio Trombetas at Araticum, col., INPA team, 10 Aug 2008; INPA 31551, 9 ex (2 c&s, 1 head SEM), 14.4-16.9 mm SL, Amazonas, Presidente Figueiredo, stream crossing "Ramal da Morena" (a local dirt road) (rio Uatumã drainage), col., INPA team, 13 Dec 2007; LIRP 7410, 3 ex, 13.4-14.6 mm SL, Roraima, Boa Vista, Igarapé Au-Au (trib. to rio Cauamá, rio Branco drainage), under bridge of road RR-205 (02°56'19"N, 61°03'03"W), col., M. Carvalho & A. Datovo, 12 Feb 2007; LIRP 12693, 26 ex, 10.3-16.9 mm SL, Roraima, Caracaraí, Igarapé Água Boa, under bridge on road BR-210 (01°57'01"N, 61°14'38"W), col., A. Datovo & M. Carvalho, 22 Feb 2007; MCP 36220, 14 ex, 11.4-16.0 mm SL, Amazonas, rio Traíra (rio Madeira drainage), *ca.* 35 km E of rio Madeira by Transamazônica road (07°35'33"S, 62°44'45"W), col., R. Reis *et al.,* 27 Jul 2004; MZUSP 105740, 2 ex, 15.0-15.3 mm SL, Pará, village of Igarapé Miri, Igarapé Macajateua (trib. to rio Moju) (01°57'51"S, 48°54'18"W), col., M.M.F. Marinho and D.A. Bastos, 09 Apr 2010; MZUSP 117521, 1 ex, 12.6 mm SL, Amazonas, Tributary of rio Aripuanã, Apuí (07°11'10.1"S, 59°50'01.4"W). **VENEZUELA:** MBUCV-V 29226, 3 ex, 16.1-20.3 mm SL, Amazonas, río Corocoro (tribut. to río Ventuari, Orinoco system), beach on río Corocoro, 30 min downstream from Yutaje (05°37'N, 66°08'W). col., S. Schaefer and S. Provenzano, 27 Apr 1999; MBUCV-V 29351, 1 ex, 18.8 mm SL, Amazonas, río Corocoro (tribut. to río Ventuari, Orinoco system), río Corocoro at campamiento Yutaje, col., S. Schaefer and F. Provenzano, 28 Apr 1999.

**Diagnosis:** Distinguished form all congeners except *Pc. alleynei* by four to six scalpelloid teeth (decreasing in size laterally) stacked in parallel at the distal end of the premaxilla (vs. scalpelloid teeth one or two, equal in size when two); by the presence of one or two conical teeth on the premaxilla (inserted basally relative to distal scalpelloid teeth) (vs. no conical teeth on premaxilla); by the long and ventrally-flat, almost spatulate, snout (vs. snout not pronouncedly spatulate); and by the presence of 11 median premaxillary teeth (vs. either three to nine or 13 and more). Distinguished from *Pc. alleynei* by the truncate or convex caudal fin (vs. bilobed or concave); by the more numerous procurrent caudal-fin rays (22 to 27 dorsal and 21 to 25 ventral) forming prominent expansions along most of caudal peduncle which as a consequence is spatulate in shape (vs. 14 to 19 procurrent rays dorsally and ventrally, forming inconspicuous expansions only on posterior half of caudal peduncle); by the pectoral fin pointedly triangular in specimens 15 mm SL or larger, with rays steeply decreasing in size posteriorly (vs. fin broadly triangular, with rays approximately with same size, or only slightly longer anteriorly); by the angulate mesethmoid cornua (vs. mostly round); by the shorter and thicker distal ramus of the premaxilla, shorter than the proximal ramus (vs. distal ramus longer than the proximal one; *cf.,* Figs. 4L, 43); by the median premaxilla broader than long (vs. as broad as long); by the shorter snout (35.3-37.6% HL, vs. 39.3-43.1); by the presence of 40-42 vertebrae (vs. 38 or 39); and by the fewer principal caudal-fin rays (5 + 6 or 6 + 6; vs 6 + 7).

**Description:** Morphometric data for the holotype and paratypes are provided in Table 13. Body moderately elongate (HL 5 to 5.3 times in SL). Cross-section of body slightly broader than deep at pectoral-fin insertion and increasingly compressed posterior to that point, tapering to caudal fin. Dorsal profile of body gently convex from head to origin of dorsal fin (Fig. 42). Dorsal and ventral profiles of caudal peduncle strongly convex posterior to dorsal and anal fins, spatulate, expanded by procurrent caudal-fin rays. Ventral profile of body straight at pectoral-fin base and then gently convex until pelvic-fin origin, with some specimens with greatly distented abdomens due to gut contents. Myotomes and longitudinal skeletogenous septum clearly visible through thin integument along whole body. Axillary gland very large, elongate in shape, protruding markedly on surface of body when full with secretion. Anterior end of gland surrounding dorsoposterior, ventral and posterior margins of muscular pectoral-fin base, as thick corselet, extending posteriorly to beyond margin of adpressed pectoral fin. Gland tapering to fine posterior tip, extending along limit between hypaxial musculature and abdominal cavity, its large round or oval pore located at its anterior portion, approximately at vertical through anterior third of pectoral- fin length. Condition of gland posterior to pore evidently related to amount of secretion stored.

Dorsal profile of head continuous with that of dorsum, its origin sometimes indicated by slight constriction of anterior end of epaxial musculature (Fig. 42). Head longer than broad, snout broad, parabolic with a continuous round anterior margin. Head muscles not entering skull roof. Head depressed (head depth approximately 58% of head width) with dorsal profile gently convex, nearly straight, to tip of snout. Ventral profile of head straight,

**Figure 42.** *Paracanthopoma vampyra,* n. sp., holotype, MZUSP 86953, 14.6 mm SL. Brazil, Amazonas, Rio Preto da Eva, Igarapé Sucuriju. (A) Lateral view of body; (B) Dorsal view of head; (C) ventral view of head.

flattened. Eye large (Fig. 42), without free orbital rim, located dorsolaterally on head and directed dorsolaterally, with pronounced lateral component. Integument over eye thin and transparent. Middle of eye slightly anterior to middle of HL, interorbital width approximately 70% of longitudinal diameter of eye. Eyelens large, constricted by iris only marginally, with large round or oval pupil, in

**Table 13.** Morphometric data of *Paracanthopoma vampyra.* Ranges, mean and SD include holotype. Head subunits were obtained with an ocular micrometer and therefore as projections. **Abbreviations:** min = minimum value; max = maximum value; n = number of specimens; SD = standard deviation.

| | n | holotype | min | max | mean | SD |
|---|---|---|---|---|---|---|
| Standard length (mm) | 6 | 15.14 | 12.8 | 22.7 | 16.7 | |
| **Percentages of SL** | | | | | | |
| Total length | 6 | 1.1 | 1.1 | 1.1 | 1.1 | 0.0 |
| Body depth | 6 | 12.1 | 11.5 | 14.2 | 12.6 | 0.9 |
| Caudal peduncle length | 6 | 20.7 | 20.1 | 21.7 | 20.8 | 0.8 |
| Caudal peduncle depth | 6 | 8.6 | 6.9 | 8.6 | 8.1 | 0.6 |
| Predorsal length | 6 | 69.0 | 69.0 | 74.2 | 71.3 | 2.3 |
| Preanal length | 6 | 69.8 | 67.9 | 73.0 | 70.7 | 1.8 |
| Prepelvic length | 6 | 62.1 | 62.1 | 64.9 | 63.9 | 1.1 |
| Dorsal-fin base length | 6 | 10.3 | 6.3 | 10.4 | 8.7 | 1.7 |
| Anal-fin base length | 6 | 9.5 | 6.3 | 9.5 | 8.1 | 1.2 |
| Pectoral-fin length | 6 | 17.2 | 12.3 | 19.3 | 15.0 | 2.8 |
| Head length | 6 | 19.0 | 19.0 | 20.2 | 19.5 | 0.5 |
| **Percentages of HL** | | | | | | |
| Head width | 6 | 65.6 | 58.3 | 70.1 | 65.2 | 4.0 |
| Head depth | 6 | 37.5 | 30.1 | 37.5 | 33.3 | 2.7 |
| Pectoral-fin length | 6 | 85.4 | 56.4 | 93.8 | 72.9 | 14.5 |
| Interorbital | 6 | 12.5 | 11.5 | 14.5 | 12.5 | 1.1 |
| Eye diameter | 6 | 15.6 | 14.5 | 16.1 | 15.4 | 0.6 |
| Snout length | 6 | 35.4 | 35.3 | 37.6 | 36.2 | 0.9 |
| Mouth width | 6 | 14.6 | 14.6 | 25.4 | 21.4 | 4.4 |
| Anterior internarial width | 6 | 16.7 | 15.6 | 17.6 | 16.5 | 0.8 |
| Posterior internarial width | 6 | 6.3 | 5.2 | 6.3 | 5.7 | 0.4 |

specimens examined. Anterior nostril small, surrounded by short tubule of integument produced posteriorly into small pointed process, with double elastin cores. Anterior internarial width slightly larger than interorbital. Posterior naris slightly larger than anterior one, roundish or triangular in shape, adjacent to mesial margin of eye and partly occluded by anterior flap of integument. Anterior margin of posterior naris posterior to transverse line through anterior margin of eyes. Posterior internarial width narrower than interorbital and slightly larger than diameter of one nostril.

Opercular odontodophore medium-sized and elongate, dorsolaterally located on head, on dorsal half of head depth in lateral view, anterodorsally to pectoral-fin base. Opercular odontodes 10 or 11, closely positioned in four irregular vertical rows of two to four. Main axis of opercular odontodes oriented horizontally in lateral view, with distal portions of larger posterior ones curved dorsoposteriorly. Two or three caps of replacement odontodes interspersed with mature ones. Opercular periodontodal fold well-differentiated but small, extending shortly beyond tips of odontodes. Interopercular odontodophore slightly larger than opercular one, located ventrolaterally on head, immediately ventral to horizontal through origin of pectoral fin, with 8 or 9 odontodes closely positioned in two irregular, partly imbricating, rows. Interopercular odontodes progressively larger posteriorly. Interopercular odontodophore approximately equidistant between opercular one and eye. Interopercular periodontodal fold of integument well-developed but narrow, roundish, extending shortly beyond tips of odontodes. Epiodontodeal velum thin and transparent, entirely covering odontodes.

Mouth inferior (ventral), strongly flattened ventrally. Each premaxilla with 4 small scalpelloid teeth attached to its distal tip and disposed in peculiar parallel and aligned arrangement, forming comb-like structure in ventral
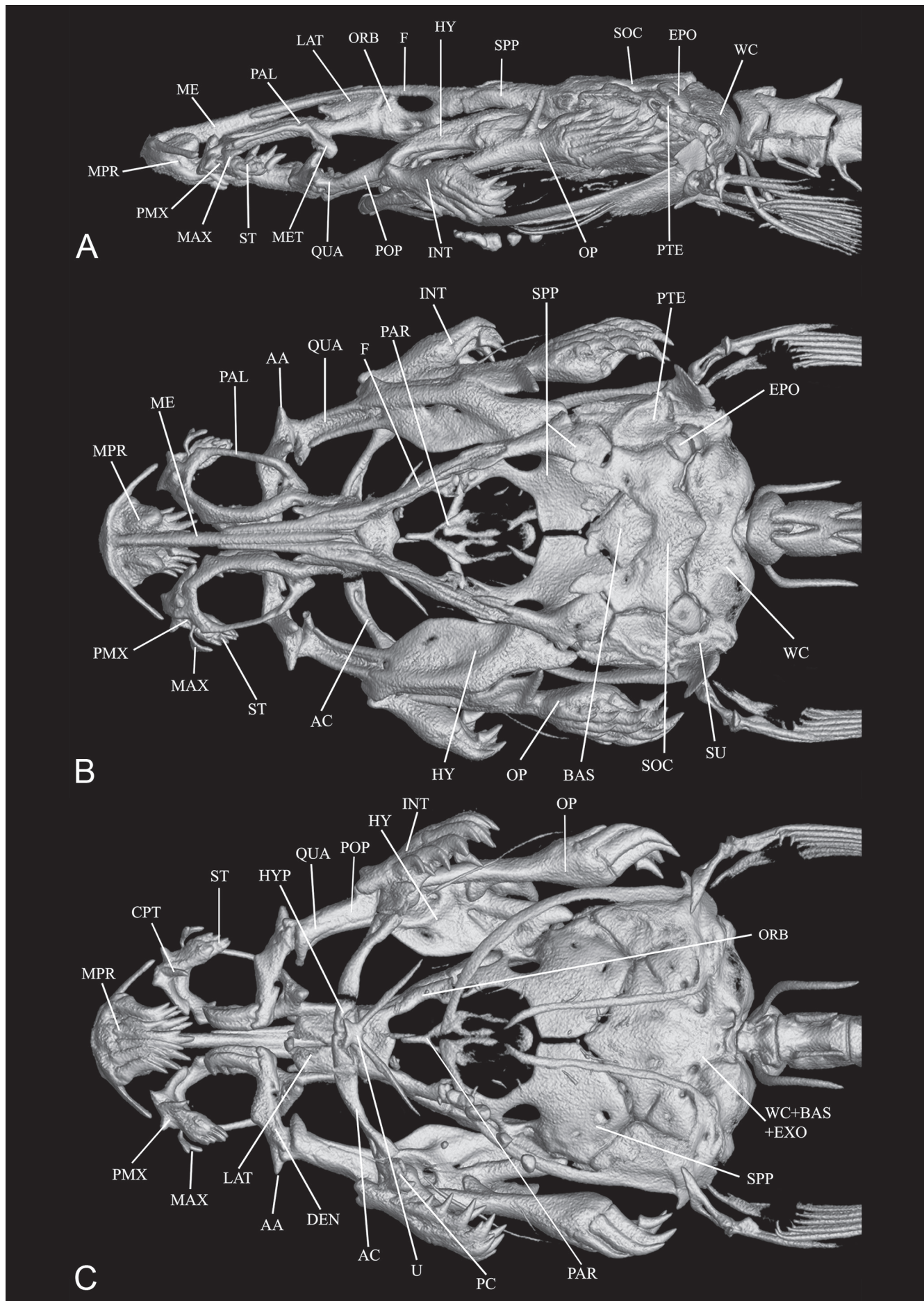
**Figure 43.** *Paracanthopoma vampyra,* holotype, MZUSP 86953, CT scan images of head skeleton, (A) Lateral; (B) Dorsal; (C) Ventral.

view of cleared and stained preparations (Figs. 4L) and CT scan images (Fig. 43). Scalpelloid teeth progressively larger mesially, deeply hidden in labial tissue and impossible to expose in preserved specimens without damaging soft tissue. One or two large conical teeth at angle at midlength of premaxilla, directed posteroventrally, with tip gently curved posteriorly (Figs. 4L, 43). Upper lip very broad, continuous with ventral surface of snout. Median premaxilla large, with 11 teeth disposed in two irregular curved rows, anterior one with three teeth on each side (separated by median gap) and posterior one with two teeth on each side and one in middle (Figs. 4L, 43). All teeth posteriorly oblique to ventral surface of median premaxilla at base and curved further posteriorly at distal pungent portion, those on lateral regions of median premaxilla also with lateral component. Basal portion of all median premaxillary teeth strongly compressed laterally. Three to five replacement tooth caps posterodorsally to mature dentition. Median premaxillary velum absent or very reduced. Hypodontal pad of median premaxilla broad, occupying most of internal surface of upper jaw. Lower jaw narrow, composed mostly of narrow and elongated dentary lobes, often adpressed at midline, round and slightly divergent anteriorly, continuous with mental region posteriorly. Jaw cleft short and strongly directed posteriorly, its lateral portion almost parallel to longitudinal axis. Dentary diastema narrow and well-defined, angulate. Dentary teeth 4, closely packed at mesial end of dentary and disposed as two ventral and two dorsal ones, not exactly aligned (Figs. 4L, 43). Dentary teeth very long, their axis anteriorly-directed at base, but strongly curved dorsally at distal half.

Branchiostegal velum forming large, continuous, round and posteriorly concave, free fold across whole of mental region. Dorsal portion of branchial membrane reaching, but not covering, anterior margin of pectoral-fin base. Branchial openings small, spanning approximately area between ventral margin of opercular odontodophore and mid-depth of interopercular oontodophore. Maxillary barbel long and thin, reaching middle of interopercular odontodophore or beyond in some specimens (shorter in some individuals, but evidently due to damage). Posterior point of its base anterior to vertical through anterior margin of eye in lateral view. Mesial (or ventral) part of maxillary-barbel base inserting directly onto corner of mouth without intervening membranous outgrowth. Rictal barbel small but well-differentiated, located mesially to base of maxillary one and approximately one-fifth of its length. Nasal barbel vestigially represented by posterior elongated portion of fold around anterior naris described above, with double internal elastin core.

Lateral line short and straight, extending alongside dorsal margin of anterior portion of axillary gland. Terminal lateral-line pore immediately dorsal to axillary gland opening. Very short secondary branch splitting off ventrally from proximal portion of main canal, with corresponding pore opening anteriorly to midlength of main canal. Single lateral-line tubule straight, poorly calcified, extending for more than half of main canal posterior to bifurcation.

In individuals 15 mm SL and larger, pectoral fin long, aproximately equal to HL, with pointed shape resulting from steep decrease in fin-ray length posteriorly. First ray extending beyond fin margin in few specimens. Margin of fin irregular at close range. In individuals smaller than 15 mm SL, pectoral fin short (approximately 70% of HL) and round, with similar-sized rays or with first slightly shorter than rest. Pectoral-fin rays i + 5, its base on ventral side of body. Pelvic fin very small, close to each other at base, with i + 4 rays. Pelvic splint present. Origin of pelvics close to origin of anal fin, well anterior to vertical through origin of dorsal-fin, entirely covering anus and urogenital papilla and extending posteriorly to origin of anal fin. Posterior margin of pelvic fin round. Dorsal fin small, elongate, roughly rectangular, with roundish edge and gently convex distal margin. Dorsal-fin rays ii + 6 or ii + 7, plus 5 procurrent ones. Anal fin small, similar in shape to dorsal fin, with ii + 5 rays, plus 4 or 5 procurrent ones. Origin of anal fin at or slightly posterior to vertical through origin of dorsal-fin. Anal fin with same size, slightly smaller or slightly larger than dorsal one. Caudal fin truncate with round edges, slightly convex in most specimens (one specimen with concave fin, apparently from damange), less deep than maximum depth of caudal peduncle. Principal caudal-fin rays 5 + 6 or 6 + 6 (one specimen with 6 + 7, seemingly due to abnormal branchimg pattern). Procurrent caudal-fin rays 22 to 27 dorsally and 21 to 25 ventrally.

Vertebrae 40 (n = 3), 41 (n = 3) or 42 (n = 2). First dorsal-fin pterygiophore subsequent to neural spine of vertebra 21 (n = 2), 22 (n = 4), or 23 (n = 2). First anal-fin pterygiophore subsequent to haemal spine of vertebra 21 (n = 1), 22 (n = 5), or 23 (n = 2). Dorsal-fin pterygiophores 7 (n = 1) or 8 (n = 7). Anal-fin pterygiophores 6 (n = 8). Branchiostegal rays 3 or 4 (5 on one side of one specimen).

**Pigmentation in preservative:** Most specimens with body almost entirely white. Posterior half of neurocranium with irregular dark brain pigment seen by transparency. Few isolated chromatophores scattered between eyes and nostrils, on opercular odontodophore and anterolateraly to eyes. Small dark spot on dorsal corner of hypural plate. Few specimens with irregular bilateral series of dark spots along dorsal midline, until dorsal fin, and sometimes an irregular row of markings along anterior half of longitudinal skeletogenous septum, until approximately vertical through middle of pelvic fin. One population (INPA 31551) with specimens particularly darkly-pigmented, following pattern above but with dark chromatophores larger and denser than in other samples, resulting in strikingly different superficial aspect.

**Etymology:** From the Slavic (treated as Latin) wampir, a blood-sucking ghost or demon, and glanis, Greek word for catfish. Used as an adjective.

**Geographical distribution:** *Paracanthopoma vampyra* is an eastern Amazon form from Brazil, so far recorded

in smaller tributaries to rio Preto da Eva, rio Uatumã, rio Trombetas and lower rio Tocantins (Fig. 45). The occurrence in the latter, rather disjunct from remaining records, indicates that the species is likely to occur more widely than so far recorded.

**Remarks:** The heavy dark pigmentation on the body of specimens in INPA 31551 distinguishes them from all other available samples of *Paracanthopoma vampyra*. In fact, they are the darkest form of any *Paracanthopoma* yet known. They also have slightly shorter snouts on average than those in other samples of *Pc. vampyra*. Such differences might at first sight be seen as indicative of a distinct species. However, closer examination does not support such conclusion. The dark markings of specimens in MZUSP 31551 actually match the pattern in other populations of *Pc. vampyra,* differing only in the number and size of dark chromatophores. Besides, specimens intermediate in pigmentation exist in some samples (*e.g.,* MZUSP 31306; *see* Fig. 44). Lot MZUSP 31306 also shows some correlation between intensity of dark pigmenta-

tion and size, with largest specimens being darkest and smallest ones almost totally white. Finally, snout length in MZUSP 31551 is only slightly shorter than, and broadly overlaps with, values in other samples of the species. Those facts, plus the lack of any additional discrete differences in internal or external anatomy which might further support specific differentiation, indicate that INPA 31551 is a populational variant of *Pc. vampyra*.

**Character evidence for recognized taxa**

In this section we provide a discussion of the evidence for the monophyletic groups relevant for the taxonomic decisions proposed in this paper, corresponding to *Paracanthopoma, Paravandellia,* and the clade composed of the two genera. The characters discussed are the basis of our nomenclatural decisions about generic allocation of species, and chosen because of their value as direct evidence of relationships. Characters are numbered sequentially across sections to facilitate future ref-
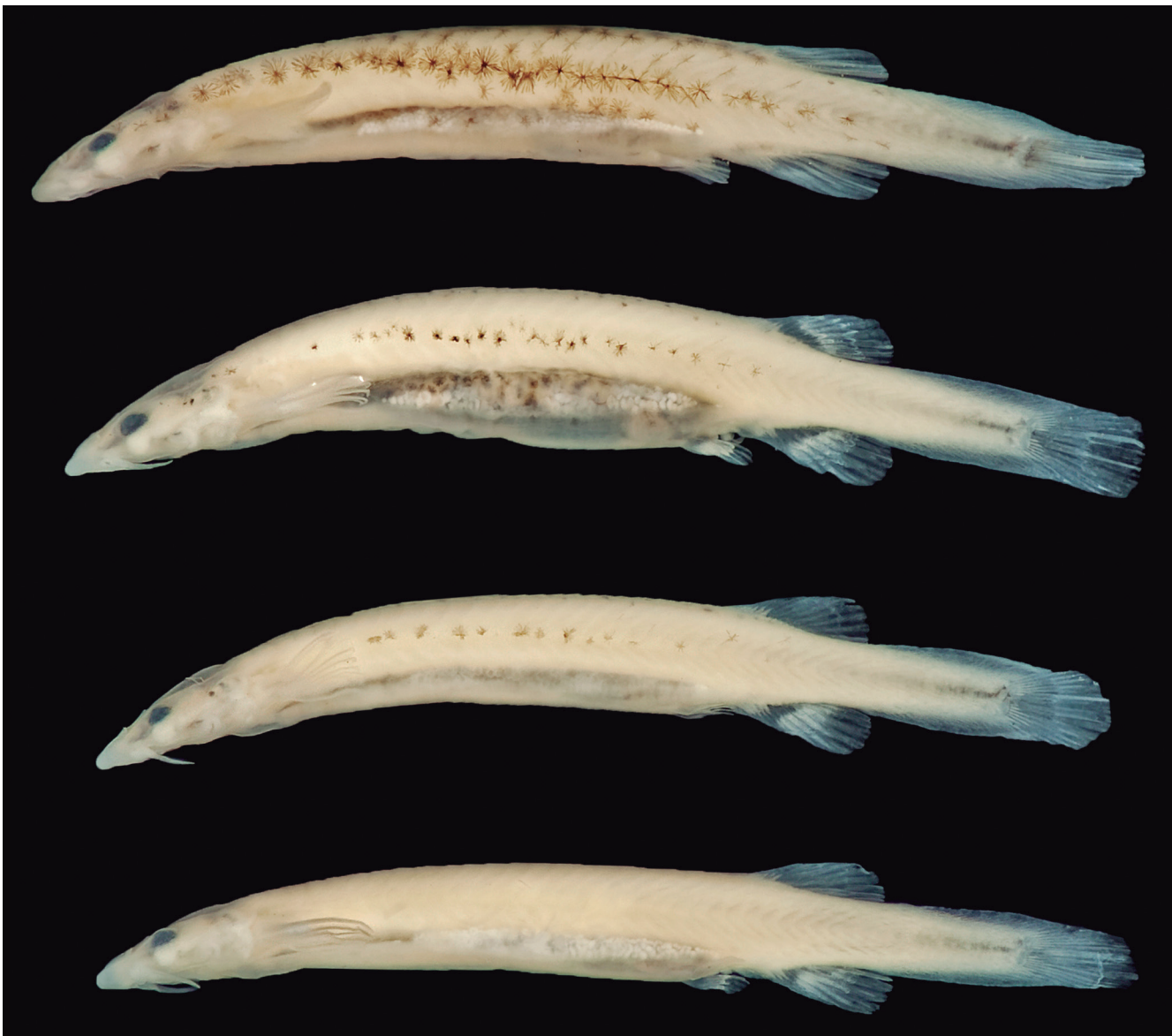


**Figure 44.** *Paracanthopoma vampyra,* INPA 31551, intraspecific variation in pigmentation pattern.
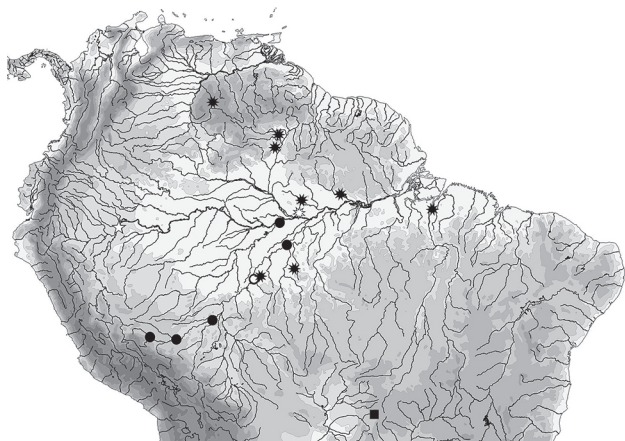
**Figure 45.** Map of northern South America showing geographical distribution of *Paracanthopoma saci* (square); *Pc. satanica* (5-tip star); *Pc. truculenta* (dot); and *Pc. vampyra* (10-tip star). Open symbols represent type localities. Some symbols may represent more than a single locality or lot of specimens.

erence. A more complete and quantitative assessment of vandelliine phylogeny will be the object of a separate paper.

### *Monophyly of* Paracanthopoma

Monophyly of *Paracanthopoma* has not been a relevant issue previously, because the genus has been monotypic for most of its history. The situation has changed drastically with the 13 species now documented. Below we provide evidence for the monophyly of *Paracanthopoma* as herein circumscribed. The evidence is straightforward, since the genus is diagnosed by numerous distinctive morphological characters unique across a wide phylogenetic spam of the family Trichomycteridae and often of Siluriformes. Suggestions of *Paracanthopoma* synapomorphies have been recently discussed in Dagosta & de Pinna (2021) and Henschel *et al.* (2021a, b). However, the most complete assessment yet done on the subject was in a phylogenetic analysis by DoNascimiento (2012), and that evidence is incorporated and discussed in this section. Some of the characters in DoNascimiento (2012) have not been included below because their significance has changed in face of the increased diversity of *Paracanthopoma*. For example, the fusion of the epioccipital with the Weberian complex (his character 96) indeed subsumes an interesting set of modification present in some species of the genus *(Pc. ahriman, Pc. cangussu, Pc. irritans, Pc. saci, Pc. vampyra),* but not others *(Pc. alleynei, Pc. capeta, Pc. carrapata, Pc. daemon, Pc. malevola, Pc. parva, Pc. satanica, Pc. truculenta).* Also, the anatomical situation across the various species seems to be more complex than simple fusion. At least in some cases *(e.g., Pc. irritans),* what happens is a loss of the epioccipital and its topological replacement with an anterodorsal laminar expansion of the Weberian capsule. One specimen of *Pc. irritans* (INPA 20529) is particularly elucidative in that regard, having on one side a tiny independent epioccipital, and on the other side no epioccipital and instead an expansion of the swimblad-

der ossification invading the corresponding position of that bone. Proper understanding of the anatomical modifications involved in this complex will require more detailed investigation and examination of developmental series of different species.

Another synapomorphy proposed for *Paracanthopoma* by DoNascimiento (2012) but not included below is the truncated proximal ends of the dorsal-and anal-fin basal radials (his characters 387 and 398). This is an interesting condition resulting from an incomplete ossification of the basal radials, which maintain a blunt cartilaginous proximal tip. In other trichomycterids and normally in catfishes and most other teleosts, the ossification of the basal radials progresses to their proximal tip, which thus end in a fine fully ossified extremity lacking any remaining cartilage. The derived, incompletely-ossified, condition applies to most species in the genus, except *Pc. alleynei* and *Pc. vampyra,* which maintain the plesiomorphic fine-pointed proximal tip of the basal radials. The apomorphic state seems to be a result of pedomorphosis, since the development of the basal radials starts as an entirely cartilaginous rod which gradually becomes ossified. The condition where there is a remaining cartilaginous tip proximally is a result of truncation in the ossification process of the structure. Curiously, this is not correlated with size, because the largest-bodied species of *Paracanthopoma,* such as *Pc. parva* and *Pc. truculenta,* have a pedomorphic truncated condition identical to that in some of the smallest, such as *Pc. irritans* and *Pc. cangussu.* Meanwhile, the two species with the fully ossified plesiomorphic state are relatively small-sized in the genus. This situation suggests that body size and pedomorphosis are decoupled within *Paracanthopoma.*

Overall, the correspondence of a monophyletic group with *Paracanthopoma* is simple. Previously described species *Pc. cangussu* and *Pc. saci* were originally correctly assigned to the genus and require no change. *Paracanthopoma alleynei* (Henschel *et al.,* 2021b), on the other hand, was originally included in *Paravandellia* and is here transferred to *Paracanthopoma* (*see* taxonomic section above). The latter species is clearly more closely related to the other species in *Paracanthopoma,* including the type species *Pc. parva,* than to any other vandelliines, including those in *Paravandellia.*

1   ***Presence of a branchiostegal velum*** – As proposed in Dagosta & de Pinna (2021: 15-16), the structure previously referred to as "free branchiostegal membrane" in *Paracanthopoma* is actually a neomorph, unique to the genus. A branchiostegal membrane (or gill membrane, or branchial membrane) is defined as the membrane lying between the opercular bones and the isthmus, supported by branchiostegal rays (McAllister, 1968: 4). Among trichomycterids, the branchiostegal membrane can be narrowly attached to the isthmus, a situation where they are united to the isthmus anteriorly at the midline only, leaving wide branchial openings. This is the condition in the entire previously considered phylogenetically basal portions of the fami-

ly, including Copionodontinae and Trichogeninae, Trichomycterinae, Sarcoglanidinae, Glanapteryginae and most Tridentinae (DoNascimiento, 2012) (the exception is *Miuroglanis,* which has an almost totally fused branchiostegal membrane). At the other extreme, the branchiostegal membranes are broadly united with the isthmus, forming a continuous integument cover over the entire gular region and leaving small branchial openings (usually between the opercle and interopercle). This is the condition in all Stegophilinae and Vandelliinae. A modification of the broadly united condition is one where the branchiostegal membranes form a free fold across the isthmus posterior to their fusion with the isthmus. This is the situation in some stegophilines *(Acanthopoma, Apomatoceros* and *Schultzichthys),* in which the free flap is clearly a portion of the membrane posterior to the fusion, because it contains embedded branchiostegal rays. In *Paracanthopoma,* the situation looks superficially similar (*e.g.,* Figs. 5, 6 and all other illustrations of ventral views of the head for species in this work, both in alcohol and SEM) but is in fact very different. The actual branchiostegal membrane in *Paracanthopoma* is nearly entirely fused to the isthmus, leaving the branchial opening reduced to a small passage limited to the region between the opercular and interopercular odontodophores as in all other vandelliines. The integument fold across the isthmus in *Paracanthopoma* is actually a different integumentary outgrowth that overlays the whole isthmal region (Dagosta & de Pinna, 2021). It contains no branchiostegal rays, which are located in the soft tissue anterior to the fusion with the isthmus. The fold forms a broad and deep integument flounce extending continuously across the isthmus, with no inbedded rays. The *Paracanthopoma* fold is probably a derivative of the branchiostegal membrane, but constitutes a set of specialization exclusive to the genus. It is therefore an especialized condition and not the widespread plesiomorphic one among lower trichomycterids. The name branchiostegal velum (Dagosta & de Pinna, 2021) has been employed to underscore its neomorphic nature, thus avoiding confusion with the actual branchiostegal membrane fold. The branchiostegal velum in *Paracanthopoma* is an easily-observable character that occurs nowhere else in Vandelliines or trichomycterids in general and has been part of the diagnosis of the genus since its establishment (Giltay, 1935). An abnormal condition of the velum has been reported in the paratype of *Pc. parva* by Henschel *et al.* (2021b: 11, fig. 3), where the membrane is narrowly fused to the midline of the gular region. This is a low-frequency variant occasionally seen in available samples and does not change the diagnostic or phylogenetic significance of the character.

**2   *Median premaxilla with dorsal bilateral flanges bracing lateral margins of mesethmoid neck:*** The median premaxilla is a structure exclusive to vandel-

liines and a majority of stegophilines. The morphology of the median premaxilla in *Paracanthopoma* is unique, and present in all species of the genus, regardless of their size and degree of development. Two traits compose the typical *Paracanthopoma* median premaxilla. The first is the presence of dorsal bilateral flanges on the dorsal surface of the bone which wrap the neck of the mesethmoid ventrolaterally (*e.g.,* Figs. 15, 17) (the second is detailed in the next character). Mechanically, the flanges partly constrain the lateral movement of the bone, guiding the slide of the median premaxilla along an anteroposterior axis. While the shape of the median premaxilla can vary widely in the genus, the flanges are always present, from those species with large hypertrophied median premaxillae (*e.g., Pc. truculenta,* Fig. 41B) to those with small and very delicate median premaxillae (*Pc. ahriman* and *Pc. saci,* Figs. 7B, 34B). *Paravandellia phaneronema* has gentle elevations in the equivalent position of its median premaxilla (Fig. 46B) which are perhaps an incipient homologous state of the flanges in *Paracanthopoma.*

**3   *Median premaxilla with well-defined median posterior recess:*** The shape and size of the median premaxilla varies widely in vandelliines and stegophilines. Its shape can be roundish, losenge-shaped or in a broad arc (as in species of *Paravandellia*). In all cases, however, the bone is a relatively simple structure with a continuous profile. Species of *Paracanthopoma* have a unique shape, with a deep recess in the posterior margin forming a median slit which results in a bilateral structure of the median premaxilla (*e.g.,* Figs. 7, 15, 19, 23, 41). The many variations of the median premaxilla make it difficult to ascertain their relative polarity, because more distant outgroups lack the bone entirely. It is plausible that the broad posterior concavity of the median premaxilla of *Paravandellia* may be a less extremely homologue of the condition in *Paracanthopoma,* and the situation in the latter genus is achieved by a narrowing of the concavity into a slit. In this case the general median premaxillary shape would be an additional synapomorphy for the two genera. Still, under such interpretation the situation in *Paracanthopoma* is a well-defined derivative state and as such also corroborating the monophyly of the genus.

**4   *Maxilla distally bifurcated:*** The maxilla in *Paracanthopoma* is distally bifurcated (*e.g.,* Figs. 10B, C, 15B, C, 19B, C, 30B, C, 43B, C). Their relative lengths may vary, ranging from equal to one of the arms being three times longer than the other. Their relative width, however, is approximately the same. In all other vandelliines and remaining trichomycterids, despite much variation of shape and length, the maxilla is distally undivided. *Paracanthopoma truculenta,* (Fig. 41B, C) while clearly having a bifurcated maxilla, displays the least extreme condition, with the bifurcation restricted to the terminal portion of the maxil-
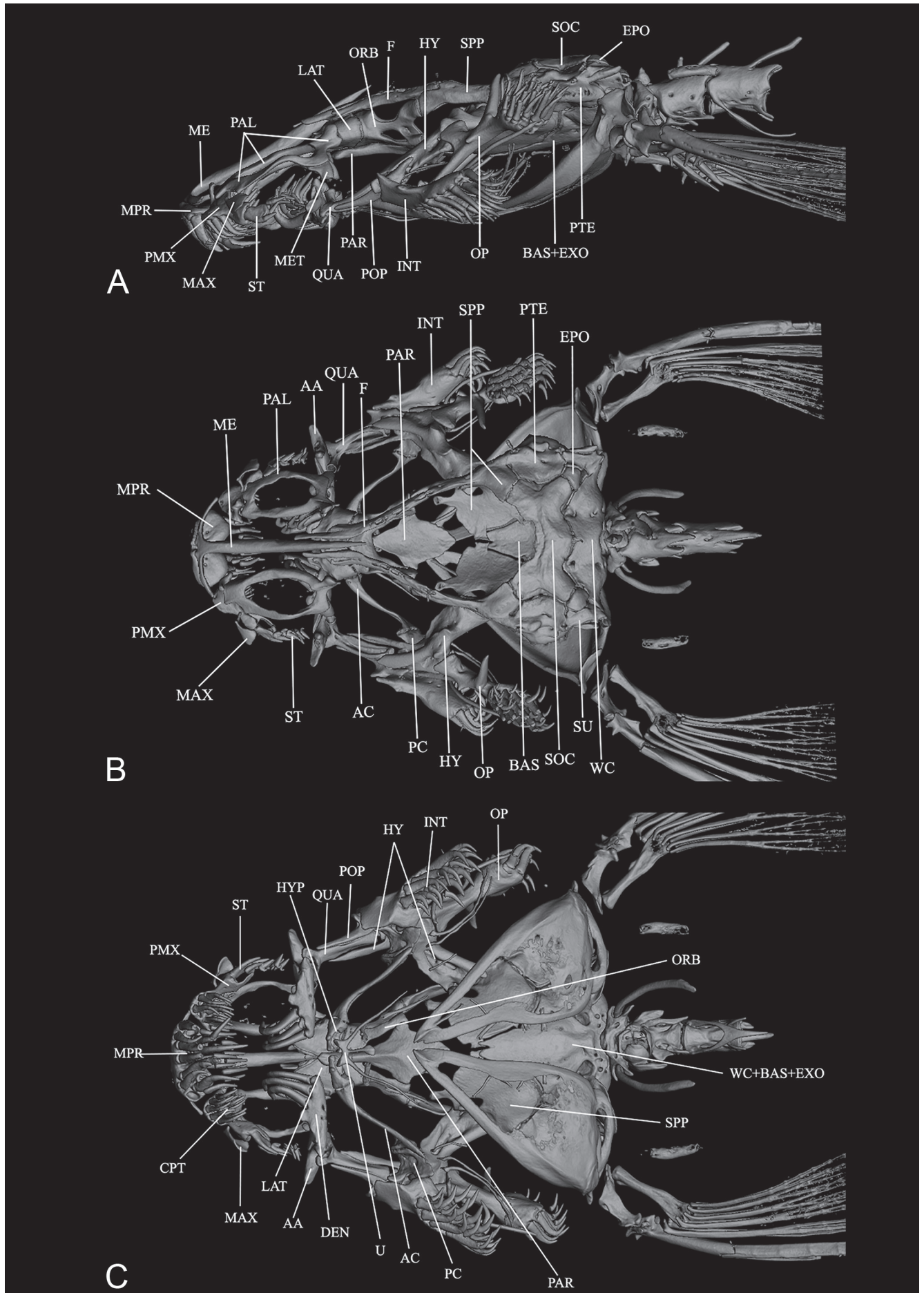
**Figure 46.** *Paravandellia phaneronema,* MCZ 35874, CT scan images of head and anterior portion of body, (A) Lateral; (B) Dorsal; (C) Ventral.

la. In *Pc. daemon,* the maxilla is reduced in overall size and modified into a rod-like small structure in two cleared and stained specimens available. In one such specimen, there is a slight distal expansion and incipient bifurcation, resembling a greatly attenuated form of the bifurcation seen in congeners. In CT images of the holotype, a bifurcation is clearly visible on the right-side maxilla (Fig. 19B, C).

5 ***Posterior articular process of palatine directed straight posteriorly, parallel to neurocranium:*** In vandelliines, the articulation between the palatine and the neurocranium is intermediated by a long process on the posterior region of the former. In *Paravandellia, Plectrochilus,* and *Vandellia,* this process is oblique relative to the longitudinal axis of the neurocranium and the actual articular surface is limited to its distal tip (*cf.,* Fig. 46). The resulting morphology is that of a stalk-like connection of the palatine with the skull. Only in *Paracanthopoma,* the posterior process is directed straight posteriorly, its mesial margin flush with that of the palatine (Figs. 7, 10, and equivalent images for other species). The articular surface of the process is thus long, extending for its entire mesial surface, which contacts an extended area of the anterior half of the lateral ethmoid.

6 ***Anterior margin of palatine with deep indentation on palatine for articulation with corresponding process of premaxilla***. As first noticed by DoNascimiento (2012), the anterior margin of the palatine in species of *Paracanthopoma* has a deep indentation, framed by a spine-like process on each side, which accommodates the ascending process of the premaxilla (*e.g.,* Figs. 10, 17, 23). The lateral spine-like process of the palatine is always larger than the mesial one, which can be attenuated in some taxa (*e.g., Pc. vampyra,* Fig. 43) but is invariably present. Such structure of the anterior margin of the palatine is unique among trichomycterids and other siluriforms. In species of *Paravandellia,* the ascending process of the premaxilla articulates ventrally with a horizontal platform on the anterior margin of the palatine. The specimen of *Pv. phaneronema* in Fig. 46 has the normal palatine condition on the left side (visible in Fig. 46B), but an abnormal morphology on the right side. Curiously, the aberrant condition, which was not seen in any other examined specimen of any *Paravandellia,* resembles somewhat the normal situation in *Paracanthopoma.*

7 ***Coronoid process formed by well-developed dentary process, with anguloarticular portion reduced or absent:*** The coronoid process of the lower jaw is plesiomorphically formed by the dentary anteriorly and the anguloarticular posteriorly. This is the condition seen in most vandelliines and other trichomycterids, and is also widespread in catfishes in general, despite much variation of detail. In *Paracanthopoma,* the coronoid process is formed mostly or entirely by the dentary. The least extreme condition is seen in

*Pc. alleynei,* where a small but clearly formed anguloarticular process is adpressed to the posterior surface of the base of the larger dentary portion of the process, and is provided with a cartilage plug. Other species with a vestigial yet identifiable anguloarticular process include *Pc. ahriman* and *Pc. satanica.* Remaining species of *Paracanthopoma* have no trace of the anguloarticular portion of the coronoid process, which is formed exclusively by the dentary. An opposite situation occurs in *Paravandellia,* where the coronoid process is formed exclusively by the anguloarticular, a condition exclusive to the genus among vandelliines (*see* below).

8 ***Absence of upper pharyngeal toothplate:*** The condition of the upper pharyngeal toothplates varies widely in parasitic catfishes and their close relatives. Taxa such as *Ochmacanthus, Pareiodon, Potamoglanis, Stegophilus,* and *Tridentopsis* have a well-developed toothplate, strongly ossified and bearing numerous functional teeth. The upper pharyngeal toothplate is reduced to a simple small toothless bone plate in *Pv. phaneronema, Vandellia, Plectrochilus,* and *Tridens.* Further reduction is seen in *Pv. oxyptera* where the plate is vestigial, represented by a small nodule of bone, sometimes asymmetrically present. Finally, total loss occurs in *Paracanthopoma* where the upper pharyngeal plate is entirely absent. Adult vandelliines always lack teeth on the upper pharyngeal toothplate. However, a juvenile of *Vandellia beccarii* (FMNH 97307) has a comparatively well-developed plate with seven or eight large conical teeth. Despite an obvious functional upper pharyngeal dentition in that specimen, the lower fifth ceratobranchial and corresponding lower dentition are entirely absent in that specimen, as in all adults of the subfamily.

9 ***Limited articulation between neural arch of complex vertebra and supraoccipital:*** In *Paracanthopoma,* the articular surface between the anterior margin of the complex centrum and the posterior margin of supraoccipital is reduced to a small cartilage-lined dorsomedian portion. This portion is differentiated as a small well-defined roughly squarish projection. In all other vandelliines and generally in trichomycterids, the articulation between the two structures comprises the entire anterior surface of the neural arch of the complex centrum. This character was first proposed as a synapomorphy for *Paracanthopoma* by DoNascimiento (2012) and is here confirmed in all currently-known species of the genus.

### ***Monophyly of* Paravandellia**

The nomenclatural history of *Paravandellia* Miranda-Ribeiro, 1912 is surprisingly complex, considering the relative simplicity of the biological situation. No less than three genera have been erected to accomodate species now in *Paravandellia: Branchioica* Eigenmann, 1917,

*Parabranchioica* Devicenzi & Vaz-Ferreira, 1939, and *Pleurophysus* Miranda-Ribeiro, 1918 all, based on species from the Paraná-Paraguay-Uruguay drainage complex. Synonymy of *Branchioica* under *Paravandellia* was suggested by Eigenmann (1918: 269 and Miles, 1943: 367) and subsequently implemented by Miranda-Ribeiro (1947), who added *Parabranchioica* as an additional synonym. The enigmatic *Pleurophysus* was identified as still another synonym of *Paravandellia* by Miranda-Ribeiro (1956: 3), a move later corroborated (de Pinna & Woiacki, 2003).

Morphological diversity in *Paravandellia* is relatively limited, despite a geographical distribution that is even broader than that of *Paracanthopoma*. There are probably a number of different taxa in the *Paravandellia,* but their differentiation is far more subtle than that among species of *Paracanthopoma*. As expected given their relative morphological uniformity, *Paravandellia* is an easily-recognizable monophyletic group. Below is a list of synapomorphies for the genus identified herein or in previous works, including the most detailed work by DoNascimiento (2012). One of the characters proposed as synapomorphic for *Paravandellia* by DoNascimiento (2012) was the insertion of the ligament between the hyomandibula and the neurocranium on the sphenotic only. In other trichomycterids the ligament inserts either on the pterotic or on the pterotic and sphenotic. While confirmed in *Paravandellia* species examined here, the condition of available material of *Paracanthopoma* did not allow reliable observation of the ligament in all species. The condition of this character in the genus, and thus its phylogenetic distribution, must await more complete data.

**10** ***Maxilla greatly expanded, plate-like:*** The maxilla in species of *Paravandellia* is markedly expanded, resembling a roundish plate covering the lateral side of the distal portion of the premaxilla (Fig. 46). This state contrasts with the normal condition in other vandelliines and remaining trichomycterids where the maxilla, despite several other variations of shape, has a longer and less expanded configuration. Among vandelliines, the only similar condition is seen in *Pl. diabolicus,* an occurrence hypothesized as convergent because of the phylogenetic distance between the two taxa (DoNascimiento, 2012; *Pl. diabolicus* is closer to a number of closely-related yet undescribed forms and *Vandellia,* than to *Paravandellia;* the latter, in turn, is closer to *Paracanthopoma*).

DoNascimiento (2012: 120, character 181) reports on the absent maxilla in two unidentified (probably undescribed) taxa of *Paravandellia,* one from the Caquetá and the other from the Orinoco, proposing this loss as a synapomorphy for cis-Andean *Paravandellia*. Material examined for this paper includes species from the Paraná-Paraguay and Amazon, all of which have maxillas with the expected morphology described above. From the Orinoco basin, of seven c&s specimens examined of *Paravandellia* sp. (FMNH 110042), two have visible max-

illas, one of which well-calcified and the other uncalcified. The bone is difficult to visualize but in the expected position flush with the dorsolateral surface of the distal portion of the premaxilla. There is clearly a trend for reduction of the maxilla in the *Paravandellia* form(s) from the Orinoco, which seems to reach total absence in some specimens. Still, the shape of the maxilla in those specimens where it is present corresponds to the shape typical for the genus.

**11** ***Anterior margin of mesethmoid with small median notch, bordered by bilateral prominences:*** The anterior margin of median portion of the mesethmoid in the majority of vandelliines and other trichomycterids is continuous, lacking pronounced relief features. In *Paravandellia,* the mesethmoid in dorsal view has a small median concavity, or notch (Fig. 46B). Laterally to the notch on each side are small prominences. This set of modifications is unique to *Paravandellia*. *Ochmacanthus* has a broad median concavity on the mesethmoid where the ascending process of the median premaxilla articulates. That concavity is a major structural feature of the mesethmoid in that genus, and not simply a disruption of the otherwise straight anterior profile. It also lacks bilateral prominences. Such anatomical differences plus the phylogenetic distance between *Ochmacanthus* and *Paravandellia* (DoNascimiento, 2012) indicate that the two states are homoplastic.

**12** ***Coronoid process of lower jaw formed exclusively by anguloarticular:*** In *Paravandellia,* the coronoid process is formed exclusively by the anguloarticular, a condition exclusive to the genus among vandelliines. The process is most prominent in *Pv. phaneronema*. In all cases, however, the process retains a cartilage lining. Other cases of a coronoid process composed only of the anguloarticular are seen in the stegophilines *Megalocentor* and *Pareiodon,* and in Tridentinae (including *Potamoglanis*) (DoNascimiento, 2012: 99, character 121). In all of the latter, the coronoid process is not well differentiated from the rest of the lower jaw, but instead continuous in a long slope with the toothed portion of the dentary, a situation is structurally different from that in *Paravandellia*. As seen above (character 2), a derived condition opposite to that in *Paravandellia* is seen in *Paracanthopoma,* where the coronoid process is formed mostly or totally by the the dentary. In vandelliines other than *Paracanthopoma* and *Paravandellia,* the process includes both anguloarticular and dentary components, as is the widespread condition in other siluriforms.

**13** ***Ventral strut of orbitosphenoid (forming ventral part of optic foramen) very narrow, curved or slanted laterally in dorsal view:*** The orbitosphenoid has much variation which is still uncharted in trichomycterids. Normally in the family, the bone is trespassed by the optic foramen, which leaves a wide bony area ventrally to it. In species of *Paravandellia,* the portion

of the orbitosphenoid ventral to the optic foramen is narrow, in the form of a bony strut slightly directed or curved laterally (Fig. 46B, C). The condition is most pronounced in *Pv. oxyptera* where the strut is very narrow, forming just a thin frame for the ventral part of the optic foramen. DoNascimiento (2012: 69, character 47) partly expressed this character as the relative size of the optic foramen, but with a different circumscription that applies also to *Vandellia.* As described here, the condition is exclusive to *Paravandellia.*

**14** ***Ventral arm of orbitosphenoid distantly connected by long stretch of cartilage to corresponding anterior arm of compound sphenotic-prootic-pterosphenoid:*** The posteroventral portion of the orbitosphenoid in species of *Paravandellia* contacts the corresponding anteroventral arm of the sphenotic-prootic-pterosphenoid by a long cartilage. The bony portions of the two bones are distant from each other (Fig. 46B, C). The plesiomorphic condition, seen in most other trichomycterids, including all other vandelliines, is to have the bony parts of the two arms closely positioned, with only a narrow intervening cartilage. As in the preceding character, here the condition in *Pv. oxyptera* is more extreme than in *Pv. phaneronema.* A similar delimitation of this character, assignable to *Paravandellia* and *Trichogenes,* was proposed by DoNascimiento (2012: 71, character 52). As defined here, it is exclusive to the latter.

**15** ***Ascending process of opercle as a simple diverging rod:*** The ascending (or dorsal) process of the opercle in trichomycterids is the main site of insertion of the dilatator and levator muscles (Datovo & Bockmann, 2010). In all species of *Paravandellia,* the ascending process of the opercle is a simple diverging rod, abruptly emerging from the dorsal surface of the opercle (Fig. 46A, B). This condition contrasts with that seen in all other vandelliines and other trichomycterids where the anterior margin of the ascending process has an oblique flange connecting it to the opercle (*e.g.,* Fig. 26A). The unique condition in *Paravandellia* is apparently caused by a loss of the bony flange seen in other taxa. The condition of this character is not comparable in taxa either lacking the ascending process of the opercle (*Pc. saci,* among vandelliines).

**16** ***Lateral surface of opercle adjacent to articulation with hyomandibula expanded to form a partial shield between the margin of the opercle and the posterior margin of the hyomandibula:*** Usually in trichomycterids and a majority of other siluriforms, the articulation between the opercle and the hyomandibula is exposed laterally. In *Paravandellia,* the opercle has a small shield-like expansion laterally protecting its articulation with the hyomandibula (Fig. 46B). The shape of the expansion differs among taxa, being anteriorly round in *Pv. phaneronema* and pointed in *Pv. oxyptera* A similar structure is seen, supposedly convergently due to phylogenetic distance among relevant taxa (*cf.,* DoNascimiento, 2012), in species of *Potamoglanis.*

**17** ***Head of urohyal with anterior processes widely spaced:*** The anterior arms of the urohyal in trichomycterids and other siluriforms are usually closely positioned, or maximally separated by a space equivalent to the length of one individual arm. This is also the condition most vandelliines. Exceptionally, species of *Paravandellia* have very broad structure of the anterior portion of the urohyal, so that the anterior arms are widely separated by a large space, equivalent to at least three times the length of one arm (Fig. 46C). This set of modifications results in a urohyal which is very typically identifiable as belonging to the genus, with no parallels among trichomycterids and clearly synapomorphic. The anterior head of the urohyal is hypertrophied relative to the rest of the bone in *Pl. diabolicus,* but the relative distance between the arms is not different from the plesiomorphic condition. This character is not comparable in taxa where the urohyal horns are vestigial (*Pc. malevola* and *Pc. satanica*) or absent (*Pc. daemon, Pc. irritans,* and *Pc. saci*), but in all such cases the narrow structure of the anterior portion of the urohyal is not physically compatible with widely spaced out processes. So, they cast little doubt on the condition as synapomorphic for *Paravandellia.*

**18** ***Fourth ceratobranchial ossification vestigial or absent:*** All vandelliines lack the fifth ceratobranchial, a synapomorphy for the subfamily with rare parallel occurrences among teleosts (Baskin 1973; de Pinna, 1998). Uniquely, species of *Paravandellia* lack also the fourth ceratobranchial. In some case (as in some specimens of *Pv. oxyptera*), the fourth ceratobranchial ossification is very reduced but still present as a small bony nodule (sometimes with a remnant proximal cartilage plug) adjacent to the lower portion of the row of gill filaments of the fourth arch. This vestigial condition is often bilaterally asymmetrical, with one of the sides sometimes reduced to a tiny ossified nodule. Despite the reduction or absence of the fourth ceratobranchial ossification, the fourth epibranchial and the respective row of gill filaments and associated soft structures of the fourth branchial arch are still present. This character was offered as a synapomorphy for *Paracanthopoma* plus *Paravandellia* by DoNascimiento (2012). However, the fourth ceratobranchial is present in all specimens examined of *Paracanthopoma* and therefore its absence is herein considered as diagnostic for *Paravandellia* only. DoNascimiento (*pers. comm.*) informs that his observations were confirmed in five specimens of *Pc. irritans* from the Orinoco (a population that may actually represent a distinct species from *Pc. irritans; see* Remarks on *Pc. irritans*). In that case, the loss of the fourth ceratobranchial in that lineage is probably homoplastic with that in *Paravandellia.*

### Monophyly of Paracanthopoma + Paravandellia

A monophyletic group composed of *Paracanthopoma* plus *Paravandellia* was originally proposed by DoNascimiento (2012). The clade is strongly corroborated by morphological evidence. It has not yet been tested by molecular data because none of the studies done so far have simultaneously included representatives of the two genera. The section below lists all characters herein identified and/or scrutinized as to their potential evidence of monophyly for the clade *Paracanthopoma* + *Paravandellia*. One of the characters proposed by DoNascimiento (2012) for this clade, the loss of the fourth ceratobranchial, is here considered as a synapomorphy for *Paravandellia* only (*see* section above on that genus).

**19 *Distribution of scalpelloid teeth restricted to distal end of premaxilla*** – Scalpelloid teeth are a highly unusual feature of Vandelliinae, present in all members of the subfamily. They have been referred to in the literature as "claw-like teeth" and consist of a combination of anatomical modifications. The tip of the teeth is scythe-like and strongly bent relative to the tooth base. Also one of the sides of the basal portion of the tooth is expanded into a large plate extending in the same direction as the distal portion. The sinusoidal jaw teeth of stegophilines and tridentines may include elements similar to those of vandelliines and in *Pareiodon* (Stegophilinae) the general morphological similarity is expressed also in an equivalent plate-like expansion. While homologies of the various modifications composing the vandelliine scalpelloid dentition to similar features in close relatives is debatable, their distribution on the premaxilla shows two well-defined conditions. In *Vandellia* and *Plectrochilus,* the scalpelloid teeth are distributed along a relatively long stretch of the ventrolateral surface of the premaxilla. In *Paracanthopoma* and *Paravandellia,* contrastingly, the scalpelloid teeth are positioned at the distal end of the premaxilla (Figs. 10B, C, 30B, C, 46B, notice that in last illustration, there are numerous partly-formed replacement teeth, but a single attached tooth). The latter condition is considered as apomorphic relative to the former because in other trichomycterids and catfishes in general, the premaxillary teeth are usually distributed along a wide portion of the premaxilla, rather than restricted to a small terminal area of the bone. The tooth distributions here considered refer only to attached teeth (*i.e.,* their sockets), not replacement tooth caps, which may be quite numerous and broadly spread out in soft tissues of the labial bursa.

**20 *Presence of large, pointed, post-articular process of anguloarticular, directed straight laterally and projecting beyond lateral limits of anterior portion of suspensorium and jaw skeleton:*** In all species of both *Paracanthopoma* and *Paravandellia,* the lower jaw has a large process directed straight laterally, projecting to or beyond the lateral limits of the suspensorium and remainder of the jaw skeleton in ven-

tral view (Figs. 7B, C, 17B, C, 46B, C). This structure is a hypertrophied dorsal post-articular process of the anguloarticular and is not homologous to the coronoid process. Despite topological relations and general position somewhat similar to the laterally-deflected coronoid process in *Plectrochilus, Vandellia, Acanthopoma* and *Ochmacanthus,* the process in *Paracanthopoma* and *Paravandellia* is a different structure, formed exclusively from anguloarticular material dorsal to its articulation with the quadrate. No part of that process is derived from coronoid process elements. Corroboration of that comes from the presence of an independent vestigial anguloarticular portion of the coronoid processes in a few taxa which also have the post-articular process (*e.g., Pc. alleynei,* Fig. 10A, B). Some variations of detail exist in the morphology of the process, *e.g.,* in *Paravandellia* the process is distally shallowly bifid (Fig. 46C), and in species of the *Pc. parva*-clade (*see* below), it is distally obliquely truncate (Figs. 17B, C, 19B, C, 30B, C, 41B, C).

**21 *Palatine ring-like, with large fenestra occupying most of its central area:*** The palatine in trichomycterids and other loricarioids is most often a continuous bone. Uniquely in *Paracanthopoma* and *Paravandellia,* the palatine ossification is composed mostly of its margins, leaving the central portion as a large well-delimited unossified fenestra (Figs. 15B, 26B, 30B, 43B, 46B). A few other vandelliines, such as some species of *Vandellia* and *Plectrochilus diabolicus,* have a fenestra on the palatine lamina. In those cases, however, the fenestra is poorly-delimited, off-center and clearly a result of gradually fading calcification. While it is possible that those conditions share homologous elements with the situation in *Paracanthopoma* and *Paravandellia,* (a view expressed in DoNascimiento, 2012: 125, character 198), the extreme condition in the latter two genera, with the fenestra being a well-delimited central feature which determines the shape and structure of the palatine, is unique. Within *Paracanthopoma* the degree of ossification varies markedly, with some species (*e.g., Pc. carrapata, Pc. parva, Pc. saci, Pc. truculenta*) having a thick-framed palatine (Figs. 17, 30, 34, 41) and others (*e.g., Pc. irritans, Pc. vampyra*) with the palatine ossification very thin, nearly thread-like (Figs. 23, 43). In all cases, however, the central fenestra is larger and more well-defined than in any other vandelliines outside of the *Paracanthopoma* + *Paravandellia* clade.

**22 *Fourth basibranchial absent:*** Among the various reductions of the branchial skeleton in vandelliines, basibranchial elements 2 and 3 are always absent (basibranchial 1 is generally absent in catfishes). Species of *Vandellia* and *Plectrochilus* retain one basibranchial element in the form of an elongated cartilage positioned between ceratobranchials 3 and 4, probably corresponding to basibranchial 4. Species of *Paravandellia* and *Paracanthopoma* exclusively share a loss of that single remaining element

(DoNascimiento, 2012) and thus lack any differentiated basibranchial elements.

**23** ***Ascending process of cleithrum absent:*** The cleithrum in trichomycterids in general has a well-defined finger-like dorsal process which forms a major component of the biomechanical link between the pectoral girdle and the skull. The process inserts dorsally into a small orifice formed between the supracleithrum, Weberian capsule and often the epioccipital. Uniquely in *Paracanthopoma* and *Paravandellia,* this process is vestigial or entirely absent (DoNascimiento, 2012). The contact between the cleithrum and the skull is instead implemented by a direct articulation with the ventral portion of the Weberian capsule and the basi-exoccipital complex. As part of such modifications, the corresponding orifice in the skull is also absent.

**24** ***Presence of an elongated cartilage-like structure horizontally between the coronoid region of the lower jaw and the premaxilla:*** DoNascimiento (2012) described a condition exclusive to *Paracanthopoma* and *Paravandellia* where the coronomeckelian cartilage of the lower jaw extends anteriorly to the posterior region of the premaxilla, adjacent to the base of the maxillary and rictal barbel cores. Our observations confirm that there is a unique alcian-blue dense structure in that shape and position in all species of those two genera. It seems, however, that the structure is contiguous but not continuous with the coronomeckelian cartilage. We are also uncertain whether it is actually constituted of cartilaginous tissue. In our specimens it seems to be composed of a bursa filled with some loose material with affinity for alcian-blue stain, superficialy similar to barbel cores. We identified a probably homologous small roundish structure close to, but independent of, the meckelian cartilage in specimens of *Vandellia* and *Plectrochilus* examined. This structure is yet poorly understood and certainly requires further anatomical and comparative study for proper description. However, its shape, size and position in *Paracanthopoma* and *Paravandellia* are indeed unique and likely represent an additional synapomorphy for the two taxa.

## DISCUSSION

### Relationships among species of *Paracanthopoma*

Species of *Paracanthopoma* can be segregated into a few well-defined subgroups based on a few clear-cut morphological characteristics. The traits for each subgroup are comparatively consistent and provide preliminary evidence of phylogenetic relationships. A test of such hypotheses requires a quantitative phylogenetic analysis of Vandelliinae which goes beyond the scope of the present work and will be the subject of a forthcoming paper. The evidence is discussed here as support for preliminary hypotheses of monophyly. Still, the value of those characters as indicative of relationships is highly consistent and as convincing as any morphological data so far used in trichomycterid phylogenetics.

The first of those clades comprises the type species of the genus, *Pc. parva,* plus *Pc. carrapata, Pc. daemon* and *Pc. truculenta.* The four species share a conspicuous supraoccipital which is anteriorly produced into a median spike-like process, the tip of which reaches beyond the epihyseal canal (Figs. 17, 19, 30, 41). The supraoccipital does not form a complete skull roof, and leaves wide spaces laterally to the anterior spike. This condition is unique among trichomycterids and other siluriforms. Other potentially apomorphic traits for the same clade include an epiphyseal canal conjoined at the midline, forming an epiphyseal commissure opening as a single median pore. The epiphyseal branch on each side exits the frontal separately and their median confluence happens entirely on soft tissue. In all other *Paracanthopoma* and other vandelliines the canals open separately as two pores. Within Trichomycteridae, a similar situation occurs in several stegophilines *(Acanthopoma, Apomatoceros, Henonemus, Megalocentor. Pareiodon,* and *Stegophilus panzeri)* and in some sarcoglanidines *(e.g., Malacoglanis* and *Sarcoglanis).* Such cases are considered as convergent due to their phylogenetic distance from the *Pc. parva* clade (DoNascimiento, 2012). Within the latter assemblage, *Pc. daemon* seems to be the sister group to a clade formed by *Pc. carrapata, Pc. parva* and *Pc. truculenta.* The latter three species share various condtions not seen in the former, such as the presence of conspicuous flange dorsally on the lateral margin of the palatine (sometimes interrupted by a V-shaped notch approximately at its mid-length) (Figs. 17, 30, 41). *Paracanthopoma carrapata, Pc. parva,* and *Pc. truculenta* are also similar in being the largest species in the genus and sharing a bilobed caudal fin, in addition to a particularly strong median premaxillary dentition. Their overall bodily robustness suggests a biology different from remaining *Paracanthopoma.* In fact, they have been observed to ride on the body of large host fishes, held fast by their jaws deep in the integument and even the musculature of the latter (*see* section on respective species above). Such behavior has not been reported for other species of the genus. *Paracanthopoma daemon* is in many respects intermediate between the robust species and remaining species in the genus, being smaller and of a more delicate constitution. While it is clearly a member of the clade, based on shared characteristics mentioned above, its phenotype shows that the increase in size, musculature and dentition is a specialization of the subclade formed by *Pc. carrapata, Pc. parva* and *Pc. truculenta,* which is seemingly associated with the exploration of a life-history markedly different from that of other *Paracanthopoma.* Specimens of *Pc. daemon* were collected from sand banks (C. Moreira, *pers. comm.*) so no information is available on their hosts or feeding/attachment strategies. More data on the biology of that rare species would be most useful in filling in informatin of the biology at a key phylogenetically-intermediate position and thus in elucidating the evolution of the peculiar adaptive path followed by the three large species.

Another *Paracanthopoma* subclade is formed by *Pc. alleynei,* and *Pc. vampyra.* Those two species are most peculiar in being the only species in the genus retaining conical teeth on the premaxilla, a trait previously considered exclusive to *Paravandellia* among vandelliines. Presence of conical premaxillary teeth is likely a plesiomorphic condition, seen also in species of *Paravandellia,* most other trichomycterids and generally in siluriforms. But those two species share other putatively apomorphic traits which indicate that they are sister groups. The most obvious and peculiar similarity is the presence of multiple (four or more) scalpelloid teeth stacked in parallel at the tip of the premaxilla (Figs. 4B, L, 10, 43). This is a unique arrangement, both in disposition and number of teeth. In all other vandelliines the scalpelloid teeth are few in number (one or two, not counting replacement ones) and positioned in offset fashion (Fig. 4A, C, D, E, F, G, H, I, J, K). *Paracanthopoma alleynei* and *Pc. vampyra* also uniquely share the presence of a secondary premaxillary process lateral to the one bearing the premaxillary-mesethmoid ligament (Figs. 10, 43). This secondary process is directed anterolaterally or laterally and is mechanically related to the connective tissue around the anterior wall of the labial bursa. The two species further share a posterior angulation of the mesethmoid cornua (Figs. 10, 43). Although many other *Paracanthopoma* and remaining vandelliines share posteriorly curved mesethmoid cornua, only in those two taxa there is an added angled bend, rather than a single continuous arc. The position of the angulation varies and can be either at approximately the middle of cornu length, as in *Pc. vampyra,* or close to its base as in *Pc. alleynei.*

A third obvious clade is the one composed of *Pc. malevola* and *Pc. satanica.* The two species share a peculiarly broad median premaxilla (Fig. 4G, J), butterfly-like in general shape (Figs. 26B, C, 38B, C), approximately twice as broad as long, resulting in a roughly rectangular patch of teeth in alcoholic specimens (Figs. 24C, 36C). They also share additional unique characteristics, such as the anterior edge of dentary expanded into a broad convex anterior lamina (Fig. 4G, J), contrasting with the mostly continuous, undifferentiated homologous portion of the dentary in congeners and most other vandelliines. A similar, probably convergent, occurrence of this state occurs in *Plectrochilus machadoi. Paracanthopoma malevola* and *Pc. satanica* also share very reduced horns of the urohyal (Figs. 26C, 38C). In vandelliines the usual condition is to have those structures well-developed and clearly differentiated (but *see* below for possible homoplastic distributions in urohyal horn development).

Three small-bodied species compose another apparent clade: *Pc. ahriman, Pc. cangussu* and *Pc. irritans.* This assemblage shares a large number of putative synapomorphies: highly asymmetric arms of the maxilla, with the posterior arm at least three times longer than the anterior one (although asymmetrical arms are not unusual in *Paracanthopoma,* with much continuous variation, in all other cases the posterior arm is at most twice as long as the anterior one); only epibranchial 3 present and fully-formed, with other epibranchial elements absent

or vestigial; and the presence of an anterior extension of the ventral part of the opercular periodontodal fold which forms a horizontal integumentary ridge between the ventral portion of the opercular and dorsal part of the interopercular odontodophores (Figs. 6A, 22A). Within that clade, *Pc. cangussu* and *Pc. irritans* are probably sister groups. They share a morphology of the basipterygium unique among trichomycterids, where the bone is narrow and anteroposteriorly elongate, with its formerly medial articular area displaced anteriorly, at the end of an anteriorly-deflected process-like modification, often representing the anteriormost part of the basipterygium. This contrasts markedly with the widespread condition where the interbasipterygial articulation is simply the mesial unmodified surfaces of each bone. The basipterygium of those two species is also unique in having a single anterior arm (likely the external one, as judging from its position on the bone), rather than two as in other *Paracanthopoma* and trichomycterids (and catfishes) in general.

Relationships of two remaining species, *Pc. capeta* and *Pc. saci,* are not as immediately obvious as previous ones, but still a few characteristics allow inferences about their probable affinities. The elongated, thread-like maxilla of *Pc. capeta* aligns it with members of the *Pc. irritans* clade, all of which share an extremely thin and long shaft of the maxilla; *Paracanthopoma saci,* on the other hand, shares with the *Pc. parva* clade a thick-walled palatine (Fig. 34) which contrasts with the delicate struts of bone which constitute the frame of the palatine in other *Parcanthopoma* and in *Paravandellia.* Also, the length of the ventral limb of the opercle is short (shorter than remainder of bone) in both *Pc. saci* (Fig. 34A) and the *Pc. parva* clade (Figs. 17A, 19A, 30A, 41A) (this condition also occurs convergently, in various degrees, in *Glanapteryx, Pv. oxyptera, Pygidianops, Typhlobelus, Vd. sanguinea,* and Tridentinae). If such evidence for the positions of *Pc. capeta* and *Pc. saci* are taken at face value, then their positions are probably as sister groups to the remainder of their respective clades, since they lack other associated synapomorphies for the clades discussed above. On the other hand, the two species share one trait unusual in the genus: their mesethmoid cornua directed straight laterally (Figs. 4D, I, 19, 34). As seen above, the widespread condition in most *Paracanthopoma* and other vandelliines is to have the cornua bent and/ or curved posteriorly. The straight condition, however, is widespread among trichomycterids, including tridentines, and therefore may represent a symplesiomorphy. No additional characters were found that might support a sister-group relationship between the two species.

The clades above are supported by convincing evidence, but are not free of homoplasy. For example, *Pc. irritans,* and *Pc. saci* entirely lack the anterior horns of the urohyal (Figs. 23C, 34C), a rare condition in trichomycterids and unique in vandelliines (condition is variable in *Pc. daemon,* with c&s specimens lacking the horns and CT specimen having them; Fig. 19C). The two species (or three, depending on resolution of ambiguous condition in *Pc. daemon*) are not closely related according to other

characters discussed above, thus that shared condition is interpreted as homoplastic. The complexity of the situation is further compounded by the reduced condition of the urohyal horns in *Pc. malevola* and *Pc. satanica* mentioned above, which can be considered as an intermediate character state. Resolution of the evolution of this and other potentially informative character must await a detailed phylogenetic analysis of Vandelliinae.

The clade formed by *Pc. alleynei* and *Pc. vampyra* lacks two derived conditions which characterize all other congeners. One of them is the presence of a few conical premaxillary teeth, discussed above. Those teeth are present (and more abundant) in species of *Paravandellia* but absent in all other *Paracanthopoma*. Such teeth are also absent in *Vandellia* and *Plectrochilus* and therefore their phylogenetic implication is somewhat ambiguous. Another is the condition of the dorsal- and anal-fin basal radials, with a complete ossification which results in a fine proximal tip lacking a cartilage (a character orginally proposed as a synapomorphy for *Paracanthopopma* by DoNascimiento (2012)). As seen above (section "Monophyly of *Paracanthopoma*") all other species of *Paracanthopoma* have an apomorphic incomplete ossification which results in a blunt, cartilage-lined, proximal tip. Although preliminary, such conditions suggest that *Pc. alleynei* and *Pc. vampyra* are probably the sister group to remaining *Paracanthopoma*.

## Sexual dimorphism in *Paravandellia* and *Paracanthopoma*

A remarkable case of secondary sexual dimorphism occurs in species of the genus *Paravandellia*. This is the first such case in Vandeliinae and only the third confimed in Trichomycteridae, the others being *Stauroglanis gouldingi* (*pers. obs.,* MP, cited in Zuanon & Sazima, 2004) and *Trichogenes claviger* (de Pinna *et al.,* 2010; *see* also de Pinna *et al.,* 2020). Males of species of *Paravandellia* have the first pectoral-fin ray markedly hypertrophied, both in length and thickness. A less pronounced increase in length occurs also in the second ray (first branched one) and this results in the fin having the shape of a long pointed triangle. Often, sexually dimorphic males are preserved with fully abducted pectoral fins, making the difference very evident in superficial examination of samples of *Pc. oxyptera* and *Pc. phaneronema*. The increase in thickness is evident in the first ray only, which can be approximately three times that of the remaining rays. An extreme case is seen in MUSM 18830, where both specimens display a particularly well-developed dimorphic fin, but with one specimen having a dramatically expanded soft tissue associated with the distal portion of the first ray, forming nearly a spatular tip. Females lack such modifications, having a normal pectoral fin where the first ray is similar in size and morphology to succeeding ones. The overall shape of the fin in females, a broad short triangle with a gently sinusoidal posterior margin, is also different from sail-like morphology of males. All such differences, in varying degrees, are also present in

all yet-undescribed species assignable to *Paravandellia* known to the authors.

The association of the different morphs with sexual dimorphism was done by directly sexing individuals available for examination, either by a small dissection or by seeing mature gonads by transparency. The hypertrophied first pectoral-fin ray is 100% correlated with males, while specimens without that trait are all females or juveniles. Thus, pectoral-fin morphology is a reliable tool for sexing adult specimens of *Pv. oxyptera* without the need for dissections. The dimorphism does not exist in small individuals. Supposedly, the modified fin ray in males develops with sexual maturity, but it may concomittantly be seasonal. In this study, the smallest male found with a clearly hypertrophied fin ray was a 17.6 mm SL in MZUSP 90600. The smallest female found with mature eggs was 23 mm SL. Some samples include specimens which cannot be sexed with certainty, despite a broad size range (*e.g.,* MZUSP 102421, with 32 ex, 17.5-21.0 mm SL, where only three males could definitely be sexed, the smallest 18.7 mm SL). The sex ratio in species of *Paravandellia* is approximately 50% in samples available: *Pc. oxyptera* MZUSP 83703, 8 ex (5 males, 3 females); NUP 312, 7 ex (2 males, 5 females); MZUSP 92973, 11 ex (6 males, 5 females); *Pv. phaneronema* ICN-MHN 16131, 47 ex (25 males, 22 females). The large lot of *Pv. phaneronema* from the Magdalena (ICN-MHN 16131) confirmed the sexual dimorphism by direct external visualization of mature gonads in most specimens and dissection of two specimens (now cleared and stained; Fig. 47). On the other hand, *Pv. phaneronema* from the upper Cauca are represented by limited material. One paratype of the species (MCZ 35874) has a mature male morphology, with a hypertrophied first pectoral-fin ray. No eggs can be seen by transparency in that specimen, and no dissection was attempted. Another similar-sized paratype (USNM 120141) is definitely a female, with eggs seen by transparency inside the abdominal cavity. This specimen has a female-pattern pectoral fin.

The shape of the male morph pectoral fin of *Paravandellia* has been recorded in the literature, which occasionally described a pectoral fin typical of the male pattern without attributing to it any especial significance or considered it as a species-specific trait. This was the case in Miles' (1943) decision to recognize two separate species of *Paravandellia* in the Cauca/Magdalena system. *Branchioica magdalenae* was reported by Miles as differing from *B. phaneronema,* among other traits, by the first pectoral-fin ray not markedly thicker than remaining rays. Specimens available to Miles from the upper Cauca were large and supposedly mature. They may have been all males, simply by chance, and therefore uniformly displayed the striking dimorphic first pectoral-fin ray (extant types are all dimorphic males). Specimens from the Magdalena, on the other hand, were smaller, supposedly immature, and thus with a normal pectoral-fin ray regardless of sex. A simple sampling artifact might explain why the different pectoral-fin morphologies (which are indeed striking) at first appealed to Miles as indicative of taxonomic differentiation. Later, the same au-
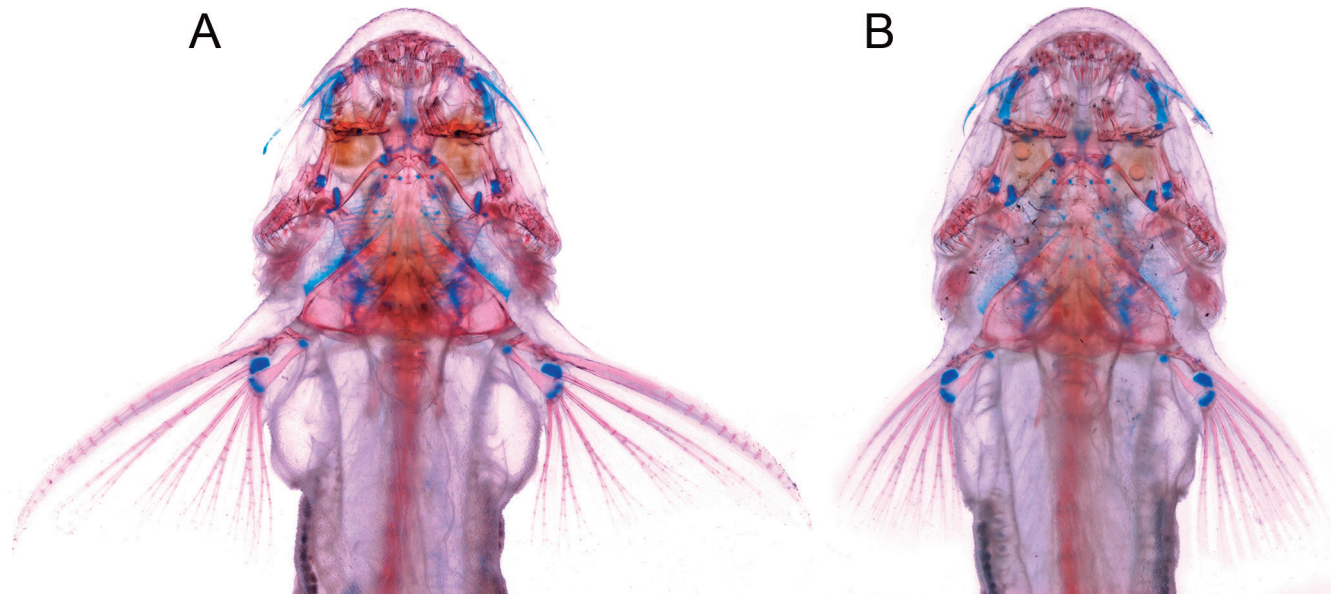
**Figure 47.** *Paravandellia phaneronema,* ICN 16131, cleared and stained specimens, head, pectoral fins, and anterior part of body, ventral views. (A) Male; (B) Female.

thor concluded that the species differentiation was not warranted and synonymized the two taxa (Miles, 1971), a hypothesis subsequently corroborated (Dahl, 1971, Román-Valencia, 1998).

The sexual dimorphism identified in species of *Paravandellia* might seem at first as a clear-cut synapomorphy for the genus. However, there are observations of possibly similar situations in some *Paracanthopoma* which cast doubt on such interpretation. A sample of *Pc. irritans* (MBUCV-V 17853) from río Orinoco includes at least 3 mature females with large ova, all of which with a small round pectoral fin. Four other specimens have longer and more pointed pectoral fins, with a small filament in the first ray, all of which lack any sign of ova and seem to be males (but testicles not directly examined). This suggests that *Pc. irritans* has a form of sexual dimorphism similar to that of a few other congeners and *Paravandellia* spp., though in a less extreme form (the same observation was recorded in DoNascimiento 2012: 207: character 432 and we thank Carlos Nascimiento for calling attention to this lot and its potential significance). No other samples of the species have clear evidence of sexual dimorphism, although mature individuals are available in some. It is possible that the pectoral-fin dimorphism is ephemeral and reversible in some *Paracanthopoma,* and therefore rarely captured in samples. While the dimorphism is certainly present and confirmed in all species of *Paravandellia,* equivalent knowledge is sketchy in *Paracanthopoma* and more data and study are necessary. It is possible that pectoral-fin sexual dimorphism is a synapomorphy for the two genera, with cases of reversal, but current knowledge does not allow a full understanding of its phylogenetic distribution.

## Natural history

The members of the subfamily Vandelliinae include the only exclusively hematophagous adult ver-

tebrates besides three species of desmodontine bats (Phyllostomidae) and 18 blood-feeding species of lampreys (Petromyzontiformes). All species of Vandelliinae are presumed hematophagous, although not all of them have been studied as to their feeding habits, especially considering that several are known from very few or single specimens. Still, museum specimens with blood in their guts are known for a vast majority of vandelliine species and no item other than blood has ever been reported for any specimen belonging to the subfamily (chironomid larvae were reported in the gut of two specimens of *Pc. cangussu* by Henschel *et al.,* 2021a: 6, but interpreted as likely an accidental ingestion during capture, a view followed here). Considering further that all vandelliines share mouth parts highly specialized for blood-feeding it is warranted to generalize hematophagy to the entire group. It is also certain that they are obligate blood feeders, at least as adults. The ten species herein described, plus other ten so far known in other genera, make Vandelliinae the largest radiation of hematophagous vertebrates.

Although often referred to as "parasitic", the feeding mode of Vandelliinae does not confortably fit some of the more strict definitions of parasitism. For example, they do not require the bodies of their hosts in order to complete their life cycle and are not permanently associated with individual hosts, but rather may move from host to host for intermittent meals. Also, vandelliines feed on their hosts for a short periods of time. This has led to some different designations for their trophic mode, *e.g.,* semi-parasitism (Machado & Sazima, 1983). As understood today, this feeding strategy is a subset of parasitism called micropredation (Lafferty & Kuris, 2002), defined as the situation where a parasite attacks multiple hosts sequentially in the course of its life, is only temporarily in contact with any individual host (from seconds to days) and does not necessarily decrease its fitness. Also, the various sequential hosts can belong to different species (Poulin & Randrawa, 2015). In terms of ecologi-

cal strategy, this mode of feeding is supposed to spread the decrease in host fitness throughout various individuals, thus scattering the individual damage and not decreasing their numerical availability by parasite-induced death (Lafferty & Kuris, 2002). Micropredation is the kind of parasitism also typical of many other animals, such as most leeches and various dipterans, in addition to vampire bats and some lampreys as mentioned above.

Reports of *Paracanthopoma* feeding habits are few, and the most detailed published information comes from Zuanon & Sazima (2005). The authors report specimens of *Paracanthopoma* sp. (then suspected to be representatives of a new species but actually a variant form of *Pc. parva*) clinging to the flesh at the bases of pectoral, dorsal and caudal fins of a large captured individual of *Zungaro zungaro* (Pimelodidae). The parasites were attached by their jaws, with their snouts buried to eye level in the thick skin of the host. Numerous small round wounds in various degrees of healing were also visible. The half-empty guts of the *Paracanthopoma* specimens led authors to conclude that they were not feeding while attached to the body of the host. By comparison with other gill-feeding vandelliines, the authors concluded that the parasites probably fed in the gills and subsequently left the branchial chamber and attached to their preferred spots on the body. This second stage in their association with the host would then be a case of phoresis, with the micropredator taking a ride in the much larger host catfish. The host fish thus offered not only nutrition, but also energy-efficient dispersal and protection from predators. The chain of inferences from the observations in Zuanon & Sazima (2005) are plausible and await confirmation from direct natural history observations, with one exception. The authors considered it as unlikely that the parasite feeds while attached to the body of the host. The reasons for that are related to the limited systemic blood circulation in the superficial tissues of fish in general and the fact that *Vandellia* species are not capable of active oral suction, instead relying on the pressure of the host's major blood vessels to drink blood (*see* paragraph above). But there are reasons to consider that *Pc. parva* may be markedly different in those regards. Morphological evidence suggests that *Pc. parva* is probably capable of a more active oral sucking action than *Vandellia.* Its mouth morphology is strongly sucker-like, with thick flattened lips forming a nearly continuous fleshy rim encircling the entire perimeter of the mouth. The surface of the lips are even provided with integumentary plicae typical of sucker mouths in other fishes. Therefore, although systemic blood circulation is indeed rather limited in superficial tissues of fish, *Pc. parva* may be able to suck some amount of blood and other bodily fluids while attached to superficial soft tissues of the host. Parasitic species of lampreys certainly get enough nutrition from surface tissues of their fish prey with their sucker mouths and associated dentition. Blood flow is certainly not as plentiful as in major branchial vessels, but may still be significant if the parasite stays attached long enough. A similar sucker-like mouth morphology is seen also in *Pc. carrapata* and an even more extreme con-

dition in *Pc. truculenta,* close relatives of *Pc. parva.* Many preserved specimens of *Pc. truculenta* have chunks of flesh in their jaws. Those are presumably from the body of the host, onto which they were attached so tightly that their forceful removal by the collector tore off the piece of flesh in their jaws. But this mode of feeding is particular to the large species of *Paracanthopoma (Pc. carrapata, Pc. parva, Pc. truculenta),* and wide variation of feeding behavior is expected among the many other species in the genus. The powerful mouth morphology of those three large species is provided with thick jaw bones, heavy jaw musculature and formidable tooth armature. This situation is very different from that of smaller species such as *Pc. cangussu, Pc. capeta, Pc. irritans,* and *Pc. saci.* In the latter forms the entire jaw apparatus is extremely delicate, with thin bones and few and fine median premaxillary teeth. Also differently from their large relatives, their lips do not form an obvious sucking apparatus. All that suggests a feeding strategy very different from that of their robust relatives. Given their small size and slight oral constitution, they probably rely on approaching their prey in inconspicuous manner, feeding unobstrusively on delicate blood vessels of the gills and then leaving unnoticed. The peculiar swimming mode of some of the small species, which minimizes body undulations (*see* below), is perhaps also an adaptation related to that strategy. Of course, between the stout species on the one hand and the delicate ones at the other, there are alternative or intermediate morphologies of a number of other species *(e.g., Pc. alleynei, Pc. malevola, Pc. satanica, Pc. vampyra).* All this suggests an extraordinarily diverse set of feeding adaptations which are yet entirely uncharted.

Some direct observations on the behavior of *Paracanthopoma parva* were kindly provided by Humberto Mendes and Ricardo M.C. Castro. The specimens were collected attached to the bodies of *Pseudoplatystoma* sp. (Pimelodidae), caught by trotline, and did not let go of their hosts during capture and transportation. A specimen of *Paracanthopoma* was left in place as the host was moved into a tank. It remained attached to the same spot on the larger fish for nine hours, and only left when forced to do so by the collector, who in the process was bitten in the hand by the fish. Sites of attachment near the caudal and anal fin of the host fish were clear as red wounds. Several of the available preserved specimens of *Paracanthopoma* were collected from the body of larger fish. In that, they differ from other vandelliines, which attach to their hosts only during feeding in the gill chamber, leaving their victims as soon as their needs are satisfied. Indirect evidence seems to suggest that species of *Paracanthopoma* have a closer association with their hosts than other parasitic catfish. Preserved specimens of *Pc. truculenta,* the largest species in the genus, nearly always have chunks of flesh clutched in their teeth. That seems to be a result of their jaw grip being so firm and unyielding on the host that tearing of host tissue ensues upon forceful removal by collectors. It may even be possible that they attach semi-permanently to the body of a host, occasionally leaving their anchoring spot and entering the gill chamber only to feed, sub-

sequently reattaching to the body surface. But also possible is that they feed on juices directly from the bitten tissues on the surface of the body, therefore never letting go of their bite on the body of the host, and not entering the branchial cavity. The wide range of variation in mouth morphology in the various species of *Paracanthopoma* also suggests that more than one strategy exists in the genus. If long-term attachment is demonstrated for any species of *Paracanthopoma,* that will be the only case of true (*i.e.,* permanent) parasitic vertebrate known. In any case, it seems likely that the habits of the heavy-dentition and heavy-muscled species of *Paracanthopoma,* such as *Pc. carrapata, Pc. parva,* and especially *Pc. truculenta,* may be markedly different from those of the more delicate forms, such as *Pc. capeta, Pc. irritans,* and *Pc. vampyra.* Unfortunately, nearly nothing is yet known about the habits in the latter group. One of the authors (MP) maintained a single specimen of *Pc. vampyra* in aquarium for some weeks. Most of the time the fish was buried in fine sand (taken from its habitat). During its brief periods of swimming, its propelling was done mostly or entirely by means of its fast-beating caudal peduncle, with the rest of the body remaining relatively stiff. This resulted in a swift yet remarkably stable mode of motion, with the fish swimming at steady speed, *ca.* 1 cm above the substrate, in a convoluted path, making abrupt deliberate turns as if scanning the surroundings before disappearing again into the sand. It was never observed to attempt feeding on potential prey in the same tank.

So far, there has been no indication of host specificity for vandelliines, which have been collected from widely diverging orders of fishes, including both chondrichthyans and osteichthyans. There are records of *Paracanthopoma* (probably *Pc. alleynei* or some related form) found in the gill chamber of freshwater stingrays (Potamotrygonidae, *Potamotrygon scobina;* Lasso *et al.,* 2015). *Paracanthopoma alleynei* has also been recorded from the gills of *Brachyplatystoma vailantii* Valenciennes 1840 and of *Doras micropoeus* Eigenmann 1912 (Schmidt, 1993; Henschel *et al.,* 2021b). Information associated with collection data include a few additional host records for species of the genus. *Paracanthopoma capeta* was collected in association with *Phractocephalus hemioliopterus* (Siluriformes, Pimelodidae) and *Pc. truculenta* from *Brachyplatystoma filamentosum* (MZUSP 30403) (Siluriformes, Pimelodidae). *Paracanthopoma parva* has been recorded from at least five different hosts belonging to two orders and three families: *Rhaphiodon vulpinus* (MZUSP 53824) (Characiformes, Cynodontidae), *Brycon* sp. (MZUSP 101366) (Characiformes, Bryconidae), *Brachyplatystoma filamentosum* (MZUSP 13994, MZUSP 30397, MZUSP 30400, MZUSP 30407, MZUSP 15715-23), *Pseudoplatystoma* sp. (MZUSP 101366) and *Zungaro zungaro* (Zuanon & Sazima, 2005) (Siluriformes, Pimelodidae). Some vandelliines have evidence of ingested blood from a very small size. The smallest specimen of *Pc. parva,* a large-size species, with evidence of ingested blood is 16.1 mm SL (MZUSP 114443). On the other hand, a small-size species, *Pc. irritans* has an 8.4 mm SL specimen (MZUSP 87049) as

the smallest vandelliine yet found with evidence of ingested blood.

Several localities are inhabited by more than one vandelliine species, often by several. It is reasonable to expect that, while not strict specificity, at least some form of host preference exists in nature, but this has yet to be supported by data. Specimens of *Paravandellia* sp. (MZUSP 100135) and the much smaller *Paracanthopoma irritans* (MZUSP 100136) were observed and collected at night, while swimming on the surface in open waters of the rio Trombetas (A.C. Lima, *pers. comm.*) and in the río Orinoco (C. DoNascimiento, *pers. comm.*). The record number of different vandelliines at the same place is a locality in the rio Curisevo (rio Xingu drainage), with a total of seven sympatric species (*Pc. irritans* MZUSP 87049, *Pc. parva* MZUSP 87048), plus five undescribed species of *Vandellia,* at least four of which are locally abundant. This indicates a heavy load of haematophagy on local fish hosts. Considering the wide range of mouth morphologies, body sizes and shapes among those species, it is likely that some degree of microhabitat- and host-segregation exists. Again, there are no hard data to test this idea, which remains a most promising area for future research.

Little is known about reproductive biology in Vandelliinae. For several decades, the only observation yet published of any relevance to the subject was by Miranda-Ribeiro (1912: 30; a fact also noted by Spotte, 2002: 57), who reported full ovaries in his 94 mm examined specimen of *V. cirrhosa* (caught in December; locality unspecified, but possibly near Manaus). For this study, a number of specimens with mature ovaries were found in different species of *Paracanthopoma*. The holotype of *Pc. satanica* is a particularly elucidative specimen, because its transparent abdomen is distended by gut contents, displaying side by side the eggs and the superficial adipose bodies with which they might otherwise be mistaken, against a dark background of coagulated blood. The eggs extend along the ventral margin of the hypaxial musculature for the posterior 60% of the abdominal cavity, their arrangement gradually narrower posteriorly. On superficial counting, they seem to be at least 50 on each side, possibly much more. The white and opaque adipose bodies partly overlap with the gonads posteriorly, but cephalad they diverge ventrally towards the middle of the abdominal wall, away from the ventral margin of hypaxial muscles. The lot MZUSP 96052 includes six female specimens of *Pc. irritans* with large mature eggs visible externally, one of which is 13.0 mm SL, the smallest vandelliine yet with evidence of sexual maturity.

Nothing is yet known about the digestive physiology of vandelliines. Hematophagous animals must have specific means of dealing with large and potentially toxic amounts of iron in vertebrate blood, because excess iron has been known for a long time to cause oxydizing damage to DNA and proteins (Fenton, 1894; Andrews, 2000). Considering the large volume of blood ingested in a single feeding episode, evident in many specimens of vandelliine species, it is expected that some form of iron binding or other biochemical pathway also exists

in vandelliines that allows them to cope with potentially hazardous iron levels. Likewise, some form of obtaining B vitamins is probable, because low levels of that nutrient in vertebrate blood is a challenge faced by exclusively hematophagous species (Wigglesworth, 1939). In some cases such deficiency is supplemented by vitamin-B producing symbiotic bacteria (Manzano-Marín *et al.,* 2015; Zepeda-Mendoza *et al.,* 2018). Vandelliines are also expected to have some kind of anticoagulant, because many blood-feeding animals have such secretions that aid in feeding and/or digestion. When gorged with blood, vandelliines specimens often regurgitate some blood upon capture. The blood is fluid immediately upon regurgitation, but partly coagulates once outside of the fish. This may indicate that some form of anticoagulant exists, but again no investigation has been done on the subject. Vandelliine physiology is a promising area of research and one which will certainly bring fascinating discoveries.

# REFERENCES

Andrews, N.C. 2000. Iron Metabolism: Iron Deficiency and Iron Overload. *Annual Review of Genomics and Human Genetics,* 1: 75-98.

Arratia, G. 1990. Development and diversity of the suspensorium of Trichomycterids and comparison with Loricarioids (Teleostei, Siluriformes). *Journal of Morphology,* 205(2): 193-218.

Arratia, G. & Schultze, H.-P. 1990. The urohyal: development and homology within osteichthyans. *Journal of Morphology,* 203(3): 247-282. https://doi.org/10.1002/jmor.1052030302.

Arratia, G. & Schultze, H.-P. 1991. Palatoquadrate and its ossifications: Development and homology within osteichthyans. *Journal of Morphology,* 208: 1-81. https://doi.org/10.1002/jmor.1052080102.

Baskin, J.N. 1973. *Structure and relationships of the Trichomycteridae.* Ph.D. Thesis, City University of New York, New York.

Briggs, J.C. 1955. A monograph of the clingfishes (Order Xenopterygii). *Stanford Ichthyological Bulletin,* 6: 1-224.

Burgess, W.E. 1989. *An atlas of freshwater and marine catfishes.* A preliminary survey of the Siluriformes. Neptune City, T.F.H. Publications, Inc.

Conway, K.W.; Stewart, A.L. & Summers, A.P. 2018. A new genus and species of clingfish from the Rangitāhua Kermadec Islands of New Zealand (Teleostei, Gobiesocidae). *ZooKeys,* 786: 75-104. https://doi.org/10.3897/zookeys.786.28539.

Costa, W.J.E.M. & Bockmann, F.A. 1994. A new genus and species of Sarcoglanidinae (Siluriformes: Trichomycteridae) from southeastern Brazil, with a re-examination of subfamilial phylogeny. *Journal of Natural History,* 28(3): 715-730.

Dagosta, F.C.P. & de Pinna, M. 2017. Biogeography of Amazonian fishes: deconstructing river basins as biogeographic units. *Neotropical Ichthyology,* 15: 1-24.

Dagosta, F.C.P. & de Pinna, M. 2019. The fishes of the Amazon: distribution and biogeographical patterns, with a comprehensive list of species. *Bulletin of the American Museum of Natural History,* 431(13): 1-163.

Dagosta, F.C.P. & de Pinna, M. 2021. Two new catfish species of typically Amazonian lineages in the Upper Rio Paraguay (Aspredinidae: Hoplomyzontinae and Trichomycteridae: Vandelliinae), with a biogeographic discussion. *Papéis Avulsos de Zoologia,* 61(47): e20216147.

Dahl, G. 1971. *Los peces del norte de Colombia.* Inderena, Bogotá, 391pp.

Datovo, A. & Bockmann, F.A. 2010. Dorsolateral head muscles of the catfish families Nematogenyidae and Trichomycteridae (Siluriformes: Loricarioidei): Comparative anatomy and phylogenetic analysis. *Neotropical Ichthyology,* 8(2): 193-246.

DoNascimiento, C. 2012. *Sistemática y relaciones filogenéticas de la subfamilia de bagres parasitos Stegophilinae (Siluriformes: Trichomycteridae).* Doctoral Thesis, Universidad Central de Venezuela, Facultad de Ciencias, Postgrado en Zoologia, Caracas.

Eigenmann, C.H. 1918. The Pygidiidae, a family of South American catfishes. *Memoirs of the Carnegie Museum,* 7: 260-373.

Eschmeyer, W.N. 1990. *Catalogue of the genera of Recent fishes.* California Academy of Sciences, San Francisco. v + 697 pp.

Eschmeyer, W.N. 1998. (Ed.). *Catalog of fishes.* San Francisco, California Academy of Sciences. 2905p.

Eschmeyer, W.N.; Ferraris, C.J.; Hoang, M. & Long, D. 1998. Species of fishes. *In:* Eschmeyer, W.N. (Ed.). *Catalog of fishes.* San Francisco, California Academy of Sciences. p. 25-1820.

Fenton, H.J.H. 1894. Oxidation of tartaric acid in presence of iron. *Journal of the Chemical Society, Transactions,* 65: 899-910.

Fernández, L. & Schaefer, S.A. 2009. Relationships among neotropical candirus (Trichomycteridae, Siluriformes) and the evolution of parasitism based on analysis of mitochondrial and nuclear gene sequences. *Molecular Phylogenetics and Evolution,* 52(2): 416-123.

Ferraris, C.J. 2007. Checklist of catfishes, recent and fossil (Osteichthyes: Siluriformes) and catalogue of siluriform primary types. *Zootaxa,* 1418: 1-628.

Ferreira, E.; Zuanon, J.; Forsberg, B.; Goulding, M. & Briglia-Ferreira, S.R. 2007. *Rio Branco: peixes, ecologia e conservação de Roraima.* Manaus, Amazon Conservation Association, Instituto Nacional de Pesquisas da Amazônia and Sociedade Civil Mamirauá. 201 p.

Fink, S.V. & Fink, W.L. 1981. Interrelationships of the ostariophysan fishes (Teleostei). *Zoological Journal of the Linnean Society,* 72(4): 297-353. https://doi.org/10.1111/j.1096-3642.1981.tb01575.x.

Giltay, L. 1935. Notes ichthyologiques. X – Description d'une espèce nouvelle de Trichomycteridae. *Mededeelingen van het Koninklijk Natuurhistorisch Museum van België,* 11: 1-3.

Gosline, W.A. 1945. Catálogo dos Nematognatos de água doce da América do Sul e Central. *Boletim do Museu Nacional, Zoologia,* 33: 1-138.

Gudger, E.W. 1930. *The Candirú.* New York, Paul B. Hoeber. xvii + 120p.

Henschel, E.; Katz, A.M. & Costa, W.J.E.M. 2021a A new candiru of the genus *Paracanthopoma* (Siluriformes: Trichomycteridae) from the Araguaia River basin, central Brazil. *Journal of Fish Biology,* 99(6): 1990-1997. https://doi.org/10.1111/jfb.14906.

Henschel, E.; Bernt, M.J.; Baskin, J.N.; Schmidt, R.E. & Lujan, N.K. 2021b. Osteology-focused redescription and description of the blood-feeding candirus *Paracanthopoma parva* and *Paravandellia alleynei* sp. n. (Trichomycteridae: Vandelliinae). *Journal of Fish Biology,* 100(1): 161-174. https://doi.org/10.1111/jfb.14930.

Kubicek, K.M. 2022. Developmental osteology of *Ictalurus punctatus* and *Noturus gyrinus* (Siluriformes: Ictaluridae) with a discussion of siluriform bone homologies. *Vertebrate Zoology,* 72: 661-727. https://doi.org/10.3897/vz.72.e85144.

Lafferty, K.D. & Kuris, A.M. 2002. Trophic strategies, animal diversity and body size. *TREE – Trends in Ecology and Evolution,* 17(11): 507-513.

Lasso, C.A.; DoNascimiento, C.; Morales-Betancourt, M.A. & Lasso-Alcalá, O.M. 2015. Parasitism of freshwater stingrays (Potamotrygonidae) by hematophagous catfishes (Vandelliinae). *Ichthyological Exploration of Freshwaters,* 26: 83-86.

Lundberg, J.G. 1975. Homologies of the upper shoulder girdle and temporal region bones in catfishes (Order Siluriformes), with comments on the skull of the Helogeneidae. *Copeia,* 1975: 66-74. https://doi.org/10.2307/1442407.

Lundberg, J.G. & Baskin, J.N. 1969. The caudal skeleton of the Catfishes, order Siluriformes. *American Museum Novitates,* 2398: 1-49.

Machado, F.A. & Sazima, I. 1983. Comportamento alimentar do peixe hematófago *Branchioica bertonii* (Siluriformes, Trichomycteridae). *Ciência e Cultura,* 35(3): 344-348.

Manzano-Marín, A.; Oceguera-Figueroa, A.; Latorre, A.; Jiménez-García, L.F. & Moya, A. 2015. Solving a bloody mess: B-Vitamin independent metabolic convergence among gammaproteobacterial obligate endosymbionts from blood-feeding Arthropods and the Leech *Haementeria officinalis. Genome biology and evolution,* 7(10): 2871-2884. https://doi.org/10.1093/gbe/evv188.

McAllister, D.E. 1968. Evolution of branchiostegals and classification of teleostome fishes. *Bulletin of the National Museum of Canada,* 221: 1-237.

Miles, C. 1943. *Estudio economico y ecologico de los peces de agua dulce del Valle del Cauca.* Cali, Publicaciones de la Secretaria de Agricultura y Fomento del Departamento de Valle del Cauca. 99p.

Miles, C. 1971. *Los peces del Río Magdalena.* Ibagué, U.T. Ediciones. 213p.

Miranda-Ribeiro, A. de. 1912. Loricariidae, Callichthyidae, Doradidae e Trichomycteridae. *In: Publicações da Comissão de Linhas Telegraphicas Estrategicas de Matto-Grosso ao Amazonas.* Annexo no. 5: 1-31.

Miranda-Ribeiro, A. de. 1917. De Scleracanthis Fluvio "Solimões" anno MCMVIII a cl. F. Machado da Silva duce brasiliense invenis et in Museo Urbis "Rio de Janeiro" servatis. *Revista da Sociedade Brasileira de Sciencias,* 1: 49-52.

Miranda-Ribeiro, P. de. 1947. Notas para o estudo dos Pygidiidae brasileiros (Pisces-Pygidiidae-Vandelliinae), II. *Boletin do Museu Nacional,* 78: 1-8.

Miranda-Ribeiro, P. de. 1956. Notas para o estudo dos Pygidiidae brasileiros V (Pisces-Pygidiidae). *Boletin do Museu Nacional,* 142: 1-6.

Myers, G.S. 1944. Two extraordinary new blind nematognath fishes from the Rio Negro, representing a new subfamily of the Pygidiidae, with a rearrangement of the genera of the family, and illustrations of some previously described genera and species from Venezuela and Brazil. *Proceeding of the California Academy of Sciences,* 23: 591-602.

Nelson, G. 1973. Relationships of clupeomorphs, with remarks on the structure of the lower jaw in fishes. *Zoological Journal of Linnean Society,* 53(1): 333-349.

Nelson, G. & Platnick, N. 1981. *Systematics and biogeography, cladistics and vicariance.* New York, Columbia University Press.

Nixon, K.C. & Wheeler, Q.D. 1990. An amplification of the phylogenetic species concept. *Cladistics,* 6(3): 211-223.

Ochoa, L.E.; Roxo, F.F.; DoNascimiento, C.; Sabaj, M.H.; Datovo, A.; Alfaro, M. & Oliveira, C. 2017. Multilocus analysis of the catfish family Trichomycteridae (Teleostei: Ostariophysi: Siluriformes) supporting a monophyletic Trichomycterinae. *Molecular Phylogenetics and Evolution,* 115: 71-81.

Ochoa, L.E.; Datovo, A.; DoNascimiento, C.; Roxo, F.F.; Sabaj, M.H.; Chang, J.; Melo, B.F.; Silva, G.S.C.; Foresti, F.; Alfaro, M. & Oliveira, C. 2020. Phylogenomic analysis of trichomycterid catfishes (Teleostei: Siluriformes) inferred from ultraconserved elements. *Nature Scientific Reports,* 10: 2697. https://doi.org/10.1038/s41598-020-59519-w.

Patterson, C. 1975. The braincase of pholidophorid and leptolepid fishes, with a review of the actinopterygian braincase. *Philosophical Transactions of the Royal Society B: Biological Sciences,* 269(899): 275-579.

de Pinna, M.C.C. 1998. Phylogenetic relationships of Neotropical Siluriformes (Teleostei: Ostariophysi): historical overview and synthesis of hypotheses. *In:* Malabarba L.R.; Reis R.E.; Vari R.P.; Lucena Z.M. & Lucena C.A.S. (Eds.). *Phylogeny and Classification of Neotropical Fishes.* Porto Alegre, Edipucrs. p. 279-330.

de Pinna, M.C.C. 1999. Species concepts and phylogenetics. *Reviews in Fish Biology and Fisheries,* 9(4): 353-373.

de Pinna, M.C.C. 2016. The dawn of phylogenetic research on neotropical fishes: a commentary and introduction to Baskin (1973), with an overview of past progress on trichomycterid phylogenetics. *Neotropical Ichthyology,* 14: e150127, 20166.

de Pinna, M.C.C. & Wosiacki, W.B. 2003. Family Trichomycteridae (pencil or parasitic catfishes). *In:* Reis, R.E.; Kullander, S.O. & Ferraris, C.J. (Eds.). *Check list of the freshwater fishes of South and Central America.* Porto Alegre, EDIPUCRS. p. 270-290.

de Pinna, M.C.C.; Helmer, J.L.; Britski, H.A. & Nunes, L.R. 2010. A new species of *Trichogenes* from the rio Itapemirim drainage, southeastern Brazil, with comments on the monophyly of the genus (Siluriformes: Trichomycteridae). *Neotropical Ichthyology,* 8(4): 707-717.

de Pinna, M.C.C.; Reis, V.J.C. & Britski, H.A. 2020. A new species of *Trichogenes* (Siluriformes, Trichomycteridae), with a discussion on the homologies of the anterior orbital bones in trichomycterids and other loricarioids. *American Museum Novitates,* 3951: 1-27p.

Poulin, R. & Randhawa, H.S. 2015. Evolution of parasitism along convergent lines: from ecology to genomics. *Parasitology,* 142: 6-15.

Reis, V. & de Pinna, M.C.C. 2022. Diversity and systematics of *Trichomycterus* Valenciennes 1832 (Siluriformes: Trichomycteridae) in the Rio Doce Basin: iterating DNA, phylogeny and classical taxonomy. *Zoological Journal of the Linnean Society,* 2022: 1-98. https://doi.org/10.1093/zoolinnean/zlac018.

Ribeiro, A.C.; Jacob, R.M.; Silva, R.R.S.R.; Lima, F.C.T.; Ferreira, D.C.; Ferreira, K.M.; Mariguela, T.C.; Pereira, L.H.G. & Oliveira, C. 2013. Distributions and phylogeographic data of rheophilic freshwater fishes provide evidences on the geographic extension of a central-brazilian amazonian palaeoplateau in the area of the present day Pantanal Wetland. *Neotropical Ichthyology,* 11(2): 319-326.

Román-Valencia, C. 1998. Redescripción de *Branchioica phaneronema* Miles (Pisces: Trichomycteridae) de la Cuenca del río Magdalena, Colombia. *Revista de la Academia Colombiana de Ciencias,* 17: 299-303.

Rosen, D.E. 1978. Vicariant patterns and historical explanation in biogeography. *Systematic Zoology,* 27(2): 159-188.

Rosen, D.E. 1979. Fishes from the uplands and intermontane basins of Guatemala: revisionary studies and comparative geography. *Bulletin of the American Museum of Natural History,* 162(5): 267-376.

Sabaj, M.H. 2020. Codes for Natural History Collections in Ichthyology and Herpetology. *Copeia,* 108: 593-669. https://doi.org/10.1643/ASIHCODONS2020.

Schmidt, R.E. 1993. Relationships and notes on the biology of *Paracanthopoma parva* (Pisces: Trichomycteridae). *Ichthyological Explorations of Freshwaters,* 4(2): 185-191.

Schultze, H.P. & Arratia, G. 1989. The composition of the caudal skeleton of teleosts (Actinopterygil: Osteichthyes). *Zoological Journal of the Linnean Society,* 97(3): 189-231.

Shelden, F.F. 1937. Osteology, myology and probable evolution of the nematognath pelvic girdle. *Annals of the New York Academy of Sciences,* 37: 1-96.

Slobodian, V. & Pastana, M.N. 2018. with Description of a new *Pimelodella* (Siluriformes: Heptapteridae) species a discussion on the upper pectoral girdle homology of Siluriformes. *Journal of Fish Biology,* 93(5): 901-916. https://doi.org/10.1111/jfb.13795.

Song, J. & Parenti, L.R. 1995. Clearing and staining whole fish specimens for simultaneous demonstration of bone, cartilage and nerves. *Copeia,* 1995(1): 114-118.

Spotte, S. 2002. *Candiru – Life and legend of the bloodsucking catfishes.* Berkeley, Creative Arts Book Company.

Taylor, R. & Van Dyke, C.C. 1985. Revised procedures for staining and clearing small fishes and other vertebrates for bone and cartilage study. *Cybium,* 9(2): 107-119.

Tchernavin, V.V. 1944. A revision of some Trichomycterinae based on material preserved in the British Museum (Natural History). *Proceeding of the Zoological Society of London,* 114(1-2): 234-275.

Walschaerts, L. 1987. Catalogue des types de poissons recents de l'Institut Royal des Sciences naturelles de Belgique. *Documents de Travail,* 40: 1-67.

Weitzman, S.H. 1962. The osteology of *Brycon* meeki, a generalized characid fish, with an osteological definition of the family. *Stanford Ichthyological Bulletin,* 8: 1-77.

Weitzman, S.H. 1974. Osteology and evolutionary relationships of the Sternoptychidae, with a new classification of stomiatoid families. *Bulletin of the American Museum of Natural History,* 153(3): 327-478.

Wigglesworth, V.B. 1939. *The principles of insect physiology.* Methuen, London.

Winterbottom, R. 1974. A descriptive synonymy of the striated muscles of the Teleostei. *Proceedings of the Academy of Natural Sciences of Philadelphia,* 125(12): 225-317.

Wosiacki, W.B. & de Pinna, M.C.C. 2007. Família Trichomycteridae: Vandelliinae. p. 73. *In:* Buckup, P.A.; Menezes, N.A. & Ghazzi, M.S. (Eds.). *Catálogo das espécies de peixes de água doce do Brasil.* Rio de Janeiro, Museu Nacional. 195p.

Zepeda-Mendoza, M.L.; Xiong, Z.; Escalera-Zamudio, M.; Runge, A.K.; Thézé, J.; Streicker, D.; Frank, H.K.; Loza-Rubio, E.; Liu, S.; Ryder, O.A.; Castruita, J.A.S.; Katzourakis, A.; Pacheco, G.; Taboada, B.; Löber, U.; Pybus, O.G.; Li, Y.; Rojas-Anaya, E.; Bohmann, K.; Baez, A.C.; Arias, C.F.; Liu, S.; Greenwood, A.D.; Bertelsen, M.F.; White, N.E.; Bunce, M.; Zhang, G.; Sicheritz-Pontén, T. & Gilbert, M.P.T. 2018. Hologenomic adaptations underlying the evolution of sanguivory in the common vampire bat. *Nature Ecology & Evolution,* 2(4): 659-668. https://doi.org/10.1038/s41559-018-0476-8.

Zuanon, J. & Sazima, I. 2004. Natural history of *Stauroglanis gouldingi* (Siluriformes: Trichomycteridae), a miniature sand-dwelling candiru from central Amazonia streamlets. *Ichthyological Exploratioon of Freshwaters,* 15(3): 201-208.

Zuanon, J. & Sazima, I. 2005. Free meals on long-distance cruisers: the vampire fish rides giant catfishes in the Amazon. *Biota Neotropica,* 5(1): 109-114.